Optimization Problems in Wireless Sensor and Passive Optical Networks

by

Ji Li

Submitted in total fulfilment of
the requirements for the degree of

Doctor of Philosophy

Department of Electrical and Electronic Engineering
The University of Melbourne
Australia

2008

The University of Melbourne
Australia

Abstract

Optimization Problems in Wireless Sensor and Passive Optical Networks

by Ji Li

In this thesis, we optimize network design and planning for the contemporary and future generation networks. In particular, we are interested in optimal resource placement, which is critical for cost-effective network deployment and performance improvement. The thesis investigates three problems.

The first problem focuses on the virtual backbone in a randomly deployed Wireless Sensor Network (WSN). We aim to find a minimum size virtual backbone, which plays an important role in efficient broadcasting and energy-conserving routing. It is equivalent to the NP-hard problem of finding the minimum connected dominating set (MCDS), in a graph corresponding to the network topology. We numerically evaluate the distribution of the virtual backbone cardinality, and its mean, for a dense single-dimensional sensor network. For a two-dimensional scenario, we develop an efficient distributed algorithm, called Incremental Coverage Algorithm (INCOA), to determine the virtual backbone in dense sensor networks. INCOA is scalable to large dense sensor networks due to its low time complexity. We also numerically estimate the expectation of the virtual backbone cardinality, which can serve as a benchmark to evaluate the routing algorithms for wireless networks, in terms of the minimum number of relays.

Secondly, as WSNs are required to be connected, and minimum consumption of resources is a common consideration for practical design, we evaluate the minimum number of sensors required to maintain the network connectivity with a certain probability. We specifically consider a network with sensors deployed targeting at predetermined positions but with random perturbation. We conduct extensive simulations, and use curve fitting as a tool to obtain empirical formulae based on the simulation results. We also consider the dual problem, evaluating the probability of connectivity in a given network with a certain number of nodes. The tolerable perturbation on the node positions to ensure a given probability of connectivity is also estimated.

In the last part of the thesis, we look into the optimal deployment of greenfield Passive Optical Network (PON). We minimize the total deployment cost, which is important to network operators. As the optimization problem was shown to be NP-hard, we develop an efficient heuristic, Recursive Association and Relocation Algorithm (RARA), to solve the problem. The study also exploits the concept of cable conduit sharing to further reduce the deployment cost. Finally, for a large PON deployment scenario with hundreds or even thousands of users, we also propose a disintegration scheme to solve the cost minimization problem. By dividing a large planning scenario into several small scenarios, and then solving the small ones independently, we can significantly improve the computational efficiency without degrading the planning performance much.

This is to certify that

(i) the thesis comprises only my original work,

(ii) due acknowledgement has been made in the text to all other material used,

(iii) the thesis is less than 100,000 words in length, exclusive of table, maps, bibliographies, appendices and footnotes.

Acknowledgments

I would like to take this opportunity to express my gratitude to all those who have given me advice, help and support throughout my work. Foremost among these are my supervisors Professor Moshe Zukerman and Dr. Lachlan L. H. Andrew. Moshe opens the door to research for me, and generously provides his encouragement for me whenever I feel depressed. Lachlan shows me the pleasure of research, and his geniuty, and preciseness influence the way I look at the world.

I also would like to thank my collaborateurs Dr. Chuan Heng Foh, Dr. Gangxiang Shen and Professor Macel F. Neuts. I did enjoy the collaboration with them.

Special thanks to Dr. Gangxiang Shen who partially took the responsibility as my supervisor, in the second half of my candidature, when Moshe and Lachlan were away from the University.

I am pleased to acknowledge the support of the Australian Research Council (ARC) and ARC Special Research Centre for Ultra-Broadband Information Networks (CUBIN).

I feel grateful to my colleagues Liang Chen, Wei Chen, Jun Guo, Malka Halgamuge, Yuanyuan He and her husband Yongfeng Zheng, Chaofeng Li, Chi Li, Feng Li, Mei Li, Boon Ng, Taka Sakurai, Feng Shu, Thaya Thanabalasingham, Dongxia Xu, Yizhuo Yang, and Andrew Zalesky.

I want to thank my parents Hanqi and Liusheng, my sister Zheng and my brother in law Jianhua for inspiring and encouraging me continuously during this work. My little niece Chenjun (little fish) brought me a lot of fun at the end of the candidature.

I am indebted to my parents in law Qingkui and Rihong, my sisters in law Liling, Leilei, and Yuling, and my brothers in law Bob, Shiyi, and Xiangsheng. I also wish to thank my nephews John, Tiantian, and my nieces Jessica and Qinqin for the happiness they brought to me.

Finally, my gratitude goes to the most important person of my life, my wife Jinling. Without her love, support and encouragement during all the tough time we spent together, this work cannot be possible.

TO THE MEMORY OF MY GRANDPARENTS.

Contents

List of Figures

List of Tables

List of Algorithms

Chapter 1

Introduction

This thesis investigates optimization problems for design and planning of Wireless Sensor Networks (WSNs) and Passive Optical Networks (PONs). The objective is to save overall deployment and operation costs, and to improve system performance. Three specific problems are studied. These problems focus on finding optimal positions for resource placement and arrangement in a geometric plane.

The first research problem is to find a minimum relay set in a random Wireless Sensor Network, which is equivalent to finding a Minimum Connected Dominating Set (MCDS) in a graph corresponding to the network topology. This problem is of interest since MCDS plays an important role in achieving efficient broadcasting, and energy-conserving routing. The second problem focuses on computing the minimum number of sensors to achieve a certain level of connectivity in a random WSN. This problem is called the connectivity problem, which is also important as full connectivity is critical for a WSN to successfully operate. We aim to provide connectivity with minimum resources, i.e., minimum number of nodes. In addition, we evaluate the probability of sensor network connectivity with a given number of sensor nodes, and estimate the tolerable node position perturbation to maintain a required level of connectivity. The last problem, optimal Passive Optical Network planning for greenfield network deployment, concentrates on minimizing the total deployment cost of PON systems, subject to a variety of PON system constraints, such as maximal transmission distance, maximal differential distance, and maximal split ratio. This problem is of importance for network operators and service providers when widely deploying PON systems as the next generation broadband access networks.

We study these three problems through a variety of methodologies including probability modelling, asymptotic analysis, graph theory, computer simulation, and optimization techniques.

The rest of this chapter is organized as follows. Section 1.1 gives a brief introduction

to WSNs and PONs, and addresses the motivations for this research. Next, the structure and the main contributions of the thesis are described in Section 1.2.

1.1 Overview and Motivation

1.1.1 Wireless Sensor Networks

Sensor networks have a long history, which can be initially traced back as far as the 1950's. It is recognized that the first obvious sensor network is the Sound Surveillance System (SOSUS) [52] [218]. The SOSUS was made up of an array of acoustic sensors that were interconnected by wired cables and were deployed by the US in deep ocean basin during the Cold War to detect and track Soviet submarines. Another conventional example of sensor networks is a networked air defence radars system. In its early stage, development of sensor networks was mainly driven by military usage, in which sensor nodes were wired together to provide battlefield surveillance.

Evolution of technologies has driven sensor networks away from its original appearance. With the emergence of integrated sensors embedded with wireless capability, most of current sensor networks compose a collection of wirelessly-interconnected sensors, of which each is embedded with sensing, computing and communication components. These sensors can observe and respond to phenomena in the physical environment [7]. This type of sensor networks are referred to as wireless sensor networks. Because of low power consumption and low cost of these wireless sensors, large scale and self-organized sensor networks are possible. They provide flexibility in deployment and maintenance, exploit the ability of wireless networks to be deployed in highly dynamic environments and hence enable sensor networks to be potentially used in various military and civilian applications. These applications include, but are not limited to, security surveillance (e.g., alert to terrorist threats [213]), environment monitoring [156], habitat monitoring [152], hazard and disaster monitoring and relief operations, health fields applications [200], and home applications (e.g., smart environment) [7]. The wireless communication techniques in WSNs can be either ad hoc (multi-hop), or single-hop wireless transmission [207]. Though the latter is popular in short-range applications, such as smart homes, the former, ad hoc technique, attracts more interests due to its high flexibility and capability of supporting long-range, large scale, and highly distributed applications. In particular, in this thesis, we only focus on wireless sensor networks adopting ad hoc transmission.

WSNs posses many advantages, such as high reliability, event driven operations, flexibility of deployment, self-adjustment and ease of maintenance [213]. Typical tasks of WSNs include information gathering, processing and dissemination, which require sensors to be embedded with four components, including sensing, processing, power supply units, and transceiver [7]. These components enable sensor networks to gather information from environments, to perform data processing and to transmit processed data to information collection nodes via wireless ad hoc communications.

In design and implementation of WSNs, many system parameters need to be optimized. Firstly, a WSN is expected to have a long life span. However, as a WSN may be deployed in an inaccessible terrain, and contains a tremendous number of sensor nodes, it is often difficult to replace or recharge their batteries, if it is not impossible. Thus, energy conservation is critical for WSNs, both for each sensor node and the entire network level operations. Various approaches were proposed to save energy consumption for sensor networks. For example, for the network level operations such as routing, if only a small fraction of sensors are involved in the routing process, the rest of the sensors can be turned off to save energy. This scheme is supported by the hardware and software advances that leverage the capability of temporarily shutting down those sensors that are not involved in any network operations. For instance, Rockwell's WINS sensor nodes can achieve a factor of ten power reduction when shutting down the radio transceiver, compared to those active nodes (with transceivers on) in idle state [185]. However, a prerequisite for this type of energy saving scheme is that the WSNs must still provide all the required functions even with those nodes turned off. Thus, there raises an important research problem, what is the maximum number of sensors that can be turned off, while the whole WSN is still functional. This problem is equivalent to minimizing the total number of active nodes, subject to ordinary operations of the system. In this thesis, we consider to find such a minimum set of active sensors and their positions, such that proper routing operations can still be facilitated. The selected sensors will function as backbone relay nodes to data communications within the whole sensor network.

Secondly, in a WSN, after collecting information from the environment, sensors need to transmit aggregated data to gateways or information collection nodes. It is important to ensure that every sensor can communicate with the gateways. Due to the ad hoc communication features of WSNs, a sufficient condition for reliable information transmission is the full connectivity of the network, which is defined as the fact that every pair of nodes

can communicate with each other, either directly or via intermediate relay nodes. Due to the large number of sensors in a WSN, the total cost could be high for the whole network, though the cost of each individual sensor is low. Thus in addition to minimizing the number of active nodes, finding the minimum number of required nodes in a WSN so as to achieve network connectivity is another important problem. We investigate this problem for a special type of networks, in which all the sensors are deployed randomly around some targeting nodes.

A commonly used model for wireless network is the unit disk graph [54] model. A unit disk graph is defined as a graph such that there exists an edge between any two vertices with distance no more than one unit length. If the radio transmission range is set to be one unit length, we can develop the corresponding unit disk graph for a wireless network, in which each node in the network is represented by a vertex in the corresponding unit disk graph, and an edge connects any two nodes if their distance is no more than the radio range.

The usage of unit disk graph to model a wireless network is based on the following two assumptions

- All the sensors are equipped with omnidirectional antennas, and the propagation model is the free space propagation.
- The radio transmission range is isotropic for each sensor, and all the sensors have an identical radio range.

The second assumption is a direct result of the first assumption. With these assumptions, the radio transmission range of all the sensors can be abstracted as circles with identical radius centered at the sensors. Though in practice, the transmission area of each sensor, the so called footprint, is amorphous due to the random fluctuation of the wireless channel, the systematic approaches of system design and the scalability planning for future service provisioning do require to represent the radio coverage by a regular shape, and circle is a nature choice [186]. Moreover, recent study [30] in percolation theory also reveals that circular discs are the hardest shape to connect together, which states that more irregular radiation patterns require lower nodal density to form an unbounded connected network. Thus the results obtained by using circular radiation pattern are generally applicable to practical situations if more irregular shapes are used.

Throughout this thesis, unless otherwise specified, we adopt unit disk graph to model WSNs. Also, the terms sensor, node, and vertex are used interchangeably.

1.1.2 Passive Optical Networks

Passive Optical Networks (PONs) [69] [136] are growing to be a popular technology for the future generation access networks. Its advantages are potentially low cost, high bandwidth, scalability and ease of upgrade. It can cater to the requriement of the emerging bandwidth-intensive applications such as IPTV, Video-on-Demand (VoD), and 3D online gaming. Current major PON technologies can be classified into Ethernet Passive Optical Networks (EPON) [115] [136] and Gigabit-capable Passive Optical Networks (GPON) [120] [121]. The former is based on Ethernet technology, which can provide up to 1 Gb/s capacity in both upstream and downstream directions, and cover up to 20 km transmission distance, while GPON, evolving from ATM PON (APON) technology, can carry up to 2.5 Gb/s capacity and cover up to 60 km transmission distance.

Because of the point-to-multipoint architecture, it is important to optimally design and plan for PON system deployment. As the costs of land trenching and laying fibres are high, which generally dominate the overall cost of the whole deployment, minimizing the total trenching distance for laying fibres is often considered as a key optimization objective for cost minimization PON deployment. With this motivation, one of our research problems in this thesis focuses on optimally finding the total number of PON and the geometric positions of PON splitters, and ONU-splitter association patterns, to serve a given set of ONUs, such that the total cost is minimal.

1.2 Thesis Outline and Contributions

The rest of the thesis is organized as follows.

Chapter 2: Background and Literature Review. This chapter surveys wireless sensor network technologies, and reviews the related work for the connectivity problem and the MCDS problem in WSNs.

Chapter 3: Minimum Connected Dominating Sets in 1-D Dense Wireless Sensor Networks. This chapter models the set of active nodes (the relay set) in WSNs by a connected

dominating set, and tries to minimize its cardinality to obtain a minimum-sized backbone in one-dimensional dense networks. We propose approaches to compute the statistics of the cardinality of the relay set numerically, by using a "modified transmission range" approach.

Chapter 4: Minimum Connected Dominating Sets in 2-D Dense Wireless Sensor Networks. This chapter considers the minimum-sized backbone in a more practical two-dimensional scenario. Based on the asymptotic results given by existing literature, we develop an efficient algorithm to approximate the MCDS in two-dimensional dense networks. We also develop an approach to estimate the expected value of the cardinality of the MCDS in 2-D dense networks without computing the MCDS explicitly.

Chapter 5: Connectivity in a Class of Wireless Networks. This chapter provides a sensor deployment model, which is different from existing models. Similar to that in Chapter 4, we also assume that relays are randomly distributed around targeted locations in this chapter. However, this chapter considers a 1-D network. The positions of all the sensor nodes are assumed to follow non-identical Gaussian or Laplace distributions, with identical variances, in one-dimensional space. Curve fitting is the major tool to apply in this chapter. By using curve fitting and surface fitting, we obtain empirical formulae to compute the minimum number of nodes required to achieve a certain probability of connectivity. We also evaluate the connectivity probability for a network with a given number of nodes, and estimate the tolerable variance of node positions such that the network is still connected with a required probability.

Chapter 6: Background for Passive Optical Networks. This chapter gives background information for the PON technologies, and discusses existing research work for optimal deployment of PON systems.

Chapter 7: Cost Minimization Planning for Greenfield Passive Optical Networks. This chapter looks into the cost minimization problem for PON system deployment. We take into account several PON system parameters, such as maximal transmission distance, maximal differential distance and maximal split ratio, and develop an efficient algorithm, called Recursive Association and Relocation Algorithm (RARA) to solve this problem.

We also evaluate the benefits of cable conduit sharing, and demonstrate how a disintegration scheme can help to improve the computation efficiency of the optimization.

Chapter 8: Concluding Remarks. This chapter summarizes the main results in this thesis, and describes the potential directions for the future research.

There are four main contributions in this thesis. First, we develop new approaches to evaluate the cardinality of the MCDS in 1-D dense random WSNs probabilistically. The approaches not only evaluate the expectation of the cardinality of the MCDS but also approximate its distribution numerically. The results provide an evaluation scheme for routing algorithms, in terms of the number of relays needed.

Secondly, for 2-D random WSNs, by applying probability modelling, we develop an efficient algorithm, the Incremental Coverage Algorithm (INCOA), to compute the dominating set that is, with high probability, a good connected dominating set, in dense networks. We also propose an approximation to evaluate the expectation of the cardinality of the MCDS in dense networks.

Thirdly, we introduce a network model in 1-D space, in which nodes are not purely randomly deployed but have intended positions to be placed, nonetheless with random perturbation. We use curve fitting and surface fitting approaches to obtain empirical formulae, which can compute the number of nodes required to achieve a certain probability of connectivity. Different distributions for node deployment are compared.

Finally, for the optimal PON deployment, we develop an efficient recursive algorithm, called RARA, to minimize the total deployment cost. The algorithm further exploits the Minimum Spanning Tree (MST) concept to share the cable conduit, in order to further reduce the cost. To improve computation efficiency, we also propose a disintegration scheme to efficiently solve large scale PON deployment problem.

All the contributions of this thesis have been fully or partially presented in the following papers.

Journal Paper

1. J. Li, L. L. H. Andrew, C. H. Foh, M. Zukerman, and M. F. Neuts, "Meeting Connectivity Requirements in a Wireless Multihop Network", *IEEE COMMUNICATIONS LETTERS*, Vol. 10, No. 1, Jan, 2006.

2. J. Li, G. Shen, "Cost Minimization Planning for Greenfield Passive Optical Networks", accepted to be published in *IEEE/OSA Journal of Optical Communications and Networking.*

3. J. Li, L. L. H. Andrew, C. H. Foh, M. Zukerman, and Hsiao-Hwa Chen, "Connectivity, Coverage and Placement in Wireless Sensor Networks", accepted to be published in *WIRELESS SENSOR TECHNOLOGIES AND APPLICATIONS* (Special Issue).

4. J. Li, L. L. H. Andrew, C. H. Foh, and M. Zukerman, "Minimum Connected Dominating Sets in Two-Dimensional Dense Wireless Networks", In preparation to submit.

Conference Paper

1. J. Li, C. H. Foh, L. L. H. Andrew, and M. Zukerman, "Sizes of Minimum Connected Dominating Sets of a Class of Wireless Sensor Networks", In Proceedings of *IEEE International Conference on Communications 2008 (ICC08), May, 2008, Beijing, China.*

2. J. Li, G. Shen, "Cost Minimization Planning for Passive Optical Networks", In Proceedings of the *OFC/NFOEC*, Feb, 2008, San Diego, California.

Chapter 2

Background and Literature Review

The first part of the thesis is concerned with connectivity, either of the sensors themselves or a small relay set.

This chapter provides an overview of wireless sensor networks (WSNs), and discusses existing work that focused on the connectivity issues in WSNs. In particular, we are interested in maintaining connected WSNs and their connectivity related characteristics, as well as the construction of a small connected relay set in WSNs. We aim to review the extensive existing results related to these topics, in order to identify our contributions presented in this thesis.

Section 2.1 gives a general introduction to WSNs and discusses their fundamental aspects, and hence provides the background of the areas covered in the first part of the thesis. The existing work on network connectivity is reviewed in Section 2.2. It first reviews the prior results for connectivity studies in wireless ad hoc networks and WSNs (Subsection 2.2.1). That provides backgrounds for our contribution described in Chapter 3 to 5. Then it considers the construction of a small connected relay set, such that the packet delivery can be achieved by forwarding packets using only sensors in the relay set (Subsection 2.2.2). Chapter 3 and 4 in the thesis focus on the problem of small relay set construction, and the evaluation of statistics of that relay set. After that, Subsection 2.2.3 covers the optimal placement of sensor nodes, which has a fundamental impact on the connectivity and other operational requirements of WSNs. Finally, we discuss some other connectivity related issues, including percolation theory, imperfect wireless channels, and mobility of nodes, in Subsection 2.2.4. Section 2.3 summarizes this chapter.

2.1 Wireless Sensor Networks

Sensor networks are useful for observing the physical world [70], hence they provide a bridge between environments and the digital data world. A sensor network is a collec-

tion of networked sensors that can collect information from the environments they are embedded in, perform information processing, and transmit processed data [8].

Although sensor networks were wired in the early stages, recent technology advances enabled the integration of sensor devices and wireless communication equipment. This integration drives the sensor networks to wireless sensor networks, in which sensor nodes can communicate wirelessly in an ad hoc fashion, without the support of fixed infrastructure [165]. This evolution motivates the research on both technologies and applications of sensor networks, which may potentially revolutionize our lives in the future. (See Chong and Kumar [52] for a detailed discussion of the history and evolution of sensor networks.)

Potential applications of WSNs include, but are not limited to, health applications [11], agricultural monitoring [35], environment monitoring [39], habitat monitoring [41] [152], smart home applications [226], and structure health monitoring [227]. For a more comprehensive list of WSN applications, see Sohraby [207]. Inspired by the wide range of applications, it was predicted in 2004 that more than 500 million sensor nodes will be deployed for WSN applications, which will create an over $7 billion market by 2010 [104]. In this section, we review some introductory and survey work, and provide a general background for WSNs.

Both Pottie and Kaiser [181], and Akyildiz *et al.* [8] gave detailed introductions to WSNs. Pottie and Kaiser [181] mainly discussed the hardware aspects and physical principles of WSNs through an example of security applications. Sensing propagation law, communication constraints, hardware energy consumption, signal processing architecture, WSN network architectures, and sensor node architectures were also described in [181]. The authors claimed that distributed arrangement of sensors is essential for accurately sensing multiple targets. This result is one of the major driving forces of WSNs. It was also shown that for ad hoc communications, radios consume similar amount of power for transmitting and receiving, which take much more power than data processing. These facts indicate that the radio transceivers should be turned off as much of the time as possible. Moreover, in terms of data transmission, processed and aggregated data are preferred rather than transmission of raw data in order to reduce the volume of transmitted information, as communications dominate the energy consumption compared with processing.

In contrast, Akyildiz *et al.* [8] focused on the layering architecture of WSNs, based on

the TCP/IP protocol stack. WSNs were studied from the application areas to the system architectures. Research efforts and unsolved problems for each specific layer were also highlighted. It was identified that the main factors influencing sensor networks include (1) fault tolerance and reliability, (2) scalability, (3) costs of production, (4) hardware, (5) topology, (6) transmission, and (7) energy management. Sensor nodes are prone to failure as they are often deployed in harsh environments. Hence reliability is important for sensor networks to provide continuous services in the presence of individual sensor failure. Scalability is another important issue for the WSN design, as sensor networks may contain a large number of densely deployed sensors, and protocols need to be well-scaled. The dense sensor deployment that leads to the mass production of sensors also require the cost for each sensor to be cheap. Nowadays, an individual sensor is desirable to cost less than $1. With these low-cost sensors, several constraints on the hardware design are imposed, such as physical volume, energy consumption, radio transmission, data processing, sensing, and so on. Therefore, the hardware design is forced to provide high capability while meeting all the constraints. In addition to that, sensor networks should be able to adapt to topology changes, and be self-manageable, in order to save maintenance costs, as sensors are not reliable and sensor networks are often deployed in inaccessible terrains. The harsh environments in which WSNs are deployed also prevent sensor batteries from being replaced, or it is very expensive to do so. Thus WSNs should operate in an energy efficient manner to reduce the power consumption and enable the networks to have long life span.

Tubaishat *et al.* [213] also gave an overview of WSNs. The authors discussed the potential applications and main challenges of WSNs. These challenges included frequent topology changes, limited sensor capabilities (power, computation, communications, and memory), failure-prone sensors, lack of global ID's for each individual sensor, scalability in network layer and data link layer, efficient deployment schemes, and dynamic environment constraints. (Also see Haenggi [94] for a comprehensive discussion of open research issues for WSNs.) Tubaishat *et al.* also compared the data-centric and address-centric querying schemes. With the former, the data collection centres send queries to specific regions, and wait for answers from sensors with required data, while in the address-centric scheme, each sensor owns a unique ID, and data queries are sent to specific nodes identified by their IDs. It is clear that data-centric is preferred as assigning unique ID to a massive number of sensors is costly. The authors also pointed out that the overall

communication architecture prefers clustering structure. However, in terms of the end-to-end communication, it is achieved via ad hoc communications. Therefore, WSNs can be considered as an application of mobile ad hoc networks (MANETs).

WSNs and MANETs share some common features. The most important feature is that they both involve in wireless multi-hop communications, i.e., each terminal can function as a router for data forwarding. In spite of the similarity, WSNs have some unique characteristics compared to MANETs. For instance, sensors in WSNs have much more strict energy consumption constraints while terminals in general MANETs often have continuous power supply. Moreover, WSNs contain many more nodes (possibly by several orders of magnitude) than that of MANETs. However, at the end-to-end communication level, we do not distinguish these two types of networks, as they both exploit wireless multi-hop communications.

A typical wireless-enabled sensor node may contain four components, they are sensing unit, processing unit, wireless transceiver, and power supply unit [8]. The logical architecture of a wireless sensor node is shown in Fig. 2.1. A sensor node contains one or more sensing units, which are necessary for information collection. Multiple sensing units are needed if we are interested in various information. The sensing units pass the collected information to the data processing unit, in which some simple signal processing, such as data aggregation, is performed. The processing unit also controls the sensor, and coordinates the functions of different units. The sensor transmits processed data to other sensors or data sinks via its wireless transceiver. Note that application-specific sensors may also contain additional components, such as actuators or mobilizers. They are in general, however, not considered as parts of sensors because they are not common components of a typical sensor. All these components rely on the energy supplied by the power supply unit.

As in most cases sensor nodes are generally batteries powered, they have limited energy resources, which leads to short radio transmission ranges. On the other hand, sensor nodes which collect information from embedded environments are required to report the occurrence of events to data collection centres. Therefore, the communications in a WSN are often conducted in an ad hoc fashion, which leverage the connectivity of the network as an intrinsic requirement. In addition to the considerations of network connectivity, WSNs also need to perform efficient routing as multi-hop communications are involved. Since MANETs and WSNs often have very limited, or even no fixed infrastructures, the

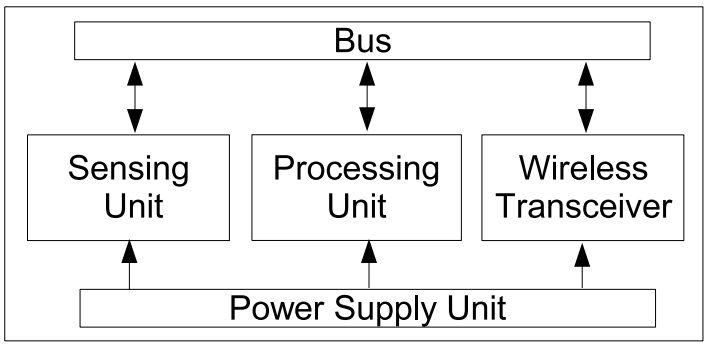

Figure 2.1: The logical architecture of a sensor node.

routing process in such networks is often complicated, and generates a large amount of overheads, due to the broadcasting nature of the wireless communications. Thus it is helpful to find a small set of sensor nodes, and the routing is restricted to perform in these nodes. Furthermore, this node set can help to resolve the broadcast storm problem [169], which is often caused by the blind flooding [107]. To successfully accomplish these tasks, it is essential to ensure that nodes in the selected set are connected to each other, either directly or in an ad hoc fashion via other nodes in the set. As this node set forms a virtual infrastructure for the network, it is often called a virtual backbone.

In the next section, we discuss the connectivity issues. We first review the existing studies of connectivity for MANETs and WSNs. Related terminologies are explained in this section. We discuss algorithms that create a virtual backbone by connecting nodes in a special set. Also, we provide a taxonomy for a type of schemes exploiting graph theoretical concepts for virtual backbone construction, and survey algorithms falling in each categories. A section discussing the node placement problem which affects the network connectivity is followed. Finally, we discuss some other issues, including the percolation theory, the impacts of the imperfection of wireless channels and node mobility, on the connectivity of networks. We aim to provide backgrounds to and position our work presented in Chapter 3- 5.

2.2 Network Connectivity

Connectivity is critical for WSNs, as information collected needs to be sent to data collection or processing centres. This transmission is conducted through ad hoc communica-

tions, which require network connectivity as a mandated criterion. The connectivity of a WSN is usually defined based on a graph associated with that WSN.

A WSN or a wireless ad hoc network is often represented by a graph, in which vertices correspond to the communication nodes in the wireless network, and an undirected edge between a pair of vertices indicates that the corresponding nodes can communicate directly. Edges of the graph are undirected because all the nodes in the WSN are assumed to have homogeneous transmission range. With this graph representation, a network is called connected if its associated graph is connected. A graph G is connected if and only if there exists a path between any pair of its vertices [62]. A connected network implies that any pair of nodes can communicate with each other, possibly through multiple hops by using relay nodes. More strict definitions of connectivity exist, such as 2-connectivity and 3-connectivity, which have similar meanings as in the graph theory, i.e., there exist two or three disjoint paths between any pair of nodes, for 2-connectivity or 3-connectivity, respectively. Though the two and three connectivity provide better fault-tolerance, we do not emphasize them. Our studies focus on the single connectivity as we would like to analyse the necessary conditions for the communication between arbitrary pair of nodes.

It is clear that the connectivity of a WSN is related to the positions of nodes, and those positions are heavily affected by the sensor deployment. In general, there are two types of approaches to deploy sensors in a WSN, the deterministic deployment, i.e., sensors are placed exactly on pre-engineered positions, and the random deployment, i.e., nodes are deployed on random positions. For the deterministic deployment, networks are carefully planned, and nodes are placed on desired positions. Therefore, it is not difficult to achieve network connectivity, if specifications of nodes are known. Although the deterministic deployment has such an advantage, in order to reduce installation costs, there are also requirements for applying random deployment to deploy large WSNs which contains very large numbers of nodes. Nodes may be dispersed by a moving vehicle or artillery shell [8]. Therefore, sensors often have nondeterministic positions, and the analysis of connectivity of such a type of networks involves proper modelling of random networks.

Communication networks are often modelled as random graphs. Mathematically, a random graph is a graph that is generated by some stochastic process [29]. The theory of random graphs began with Erdős and Rényi's pioneer work [71] [72] in the late 1950s and early 1960s. It was originally derived as a tool of proof in the combinatorial mathematics. However, it is now widely accepted as a modelling method in communications [14] [68]

[83], social studies [117] [167], biology [199], and so on. Almost at the same time, Gilbert [80], Austin *et al.* [15], and Ford and Uhlenbeck [77] also studied the statistical aspects of graphs independently. However, unlike Erdős and Rényi, they used enumeration methods, which are essentially deterministic, to estimate exact values of graph properties, while Erdős and Rényi studied the distributions of graph properties. Thereby, Erdős and Rényi are often credited with the foundation of the theory of random graphs.

One type of the most extensively studied random graphs are Erdős-Rényi graphs. An Erdős-Rényi graph $G(n, p)$ is a graph with n vertices, and each of the C_n^2 possible edges exists independently with a probability p. As Erdős-Rényi graphs assign randomness to edges, i.e., there is a link between each pair of nodes with certain probability, it is not an ideal model to describe real networks with geometric properties, in which distance between nodes is an important parameter to affect the existence of communication links. For example, if the distance between two nodes is too long such that setup a direct link is too expensive, or impossible, no direct communication exists between these two nodes. Hence there are no edges between those nodes. Moreover, as discussed by Chlamtac and Faraó [51], Erdős-Rényi graphs do not consider correlations between different links. Therefore, we need new methods to model networks with randomness.

A spontaneous candidate for random network modelling is the so called *Random Geometric Graphs* [177]. With node set V, a *geometric graph* $G = (V, r)$ is equivalent to a graph $G_1 = (V, E)$, in which V is the vertices set, and $E = \{(u, v) | \forall u, v \in V, \|u - v\| \leq r\}$. If the nodes in V are uniformly independent and identically distributed (i.i.d.) in the metric space, G is called a random geometric graph. Hence random geometric graphs are useful to model wireless ad hoc networks if all the nodes are i.i.d. and uniformly distributed.

For a WSN with sensors randomly deployed according to arbitrary probability distributions in the Euclidean space, the associated unit disk graph is a graph that abstracts each sensor as a vertex, and an edge exists for two vertices with the Euclidean distance between them less than the unit distance r, i.e., transmission range r. As the position of each node is random, the distance between an arbitrary pair of nodes is also random. Therefore, this type of unit disk graph can be considered as a random graph. A random unit disk graph boils down to a random geometric graph if all the sensors are i.i.d. and uniformly distributed.

2.2.1 Connectivity in Wireless Ad Hoc and Sensor Networks

It is recognized that Erdős-Rényi random graphs are not suitable to model wireless multi-hop networks, mainly due to their incapability of describing the distance-dependent characteristics. To resolve this problem, Gilbert [81] proposed a model called *Random Plane Networks*, and indicated its usage in the connectivity studies of packet radio networks. This model virtually abstracts a network as a graph by taking the same idea as unit disk graph model. Gilbert used this model to analyse networks deployed in an infinite plane, on which stations are distributed according to a Poisson point process with density λ. This type of models were also used to study the spread of contagious disease [81].

Literature on connectivity of random WSNs in general falls into two types. On the one hand, given a random WSN with n nodes, the minimum transmission range for each node so as to ensure a certain level of connectivity probability is of interest. On the other hand, for n random nodes each with an assigned radio transmission range, the probability of connectivity is an important metric to evaluate the performance of WSNs.

Santi *et al.* [197] studied the minimum transmission range $r_{\min}$ that can maintain the connectivity in a homogeneous wireless network, in which all the nodes have an identical transmission range. It was shown that in a 1-dimensional network with n nodes uniformly distributed in an interval $[0, d]$, the network is connected if and only if the product of r and d is on the order of at least $d \log d$. A particular transmission range assignment scheme was thereby proposed to provide asymptotic almost sure connectivity. Related to this problem, topology control is another important problem. It is the coordination of the decisions about the transmission ranges of all the nodes so as to generate a network with some desired properties, such as network connectivity [194]. The topology control problem arises because an ad hoc network contains many nodes geometrically distributed without fixed infrastructures, and all these nodes share common wireless medium. The lack of central infrastructures indicates that ad hoc networks do not have a fixed topology. However, such a fix topology is desirable to implement routing protocols. On the other hand, in a wireless network, in order to maintain connectivity, it is expected to have long transmission range for each node so that they can communicate with other nodes. Nonetheless, a long transmission range results in a high nodal degree, which in turn causes high interferences and reduces the network throughput. Much work has been conducted to explore the tradeoff by finding the optimal nodal degree for ad hoc

networks.

The study of the optimal nodal degree problem can be traced back to the classic work [133] presented in 1978 by Kleinrock and Silvester. By maximizing one hop progress of packet transmission in the direction from a source to a destination, Kleinrock and Silvester [133] showed that in a packet radio network with Poisson distributed terminals and slotted ALOHA [187] MAC scheme, the optimal homogeneous transmission range that maximizes the network throughput leads to an average of six neighbors for each node. Takagi and Kleinrock revised the result, and gave a new optimal nodal degree eight [210]. Other nodal degrees were also obtained under different transmission protocols and inhomogeneous transmission ranges [97] [109] [210]. However, the connectivity of networks was implicitly assumed in the previously mentioned work, and this assumption is only valid for small size networks. Philips *et al.* [179] proved that with a constant average nodal degree, a sufficiently large network is almost surely disconnected. Ni and Chandler [168] showed the similar results based on simulations. As nodes in an ad hoc network may have homogeneous or inhomogeneous transmission ranges, research on the connectivity problem focused on two directions.

For networks in which all nodes have a homogeneous transmission range, Philips *et al.* [179] conjectured that the transmission range should grow logarithmically in order to maintain the asymptotic network connectivity. Piret [180] studied the same problem for one-dimensional networks, in which the conjecture in [179] does not hold. Therefore, it was postulated that the conjecture does not hold for two-dimensional networks as well. However, in contrast to Piret's postulation, Gupta and Kumar [91] showed that for n nodes uniformly i.i.d. in a disk of area A, with the particular radio transmission range $r(n) = \sqrt{(A(\log n + \gamma_n))/(\pi n)}$, the network is asymptotically connected if and only if $\gamma_n \rightarrow +\infty$, such a finding is similar to the conjecture claimed by Philips *et al.* [179]. Penrose [176] showed that if all nodes have homogeneous transmission range, the minimum radio range for achieving k-connectivity is asymptotically equivalent to the minimum radio range for achieving k nodal degree as n goes to infinity. Analytically, Bettstetter [21] applied Penrose's result to obtain a suitable radio range r, which ensures that a network with a given node density λ is asymptotically almost surely k-connected.

If each node adjusts its transmission power independently, there have inhomogeneous transmission ranges. Much research has been conducted for this situation. Xue and Kumar [228] showed that if inhomogeneous range assignment is allowed, each node in a

random network with n uniformly distributed nodes should connect to $\Theta(\log n)$ nearest neighbors so as to maintain the asymptotic connectivity. They further showed that the constant in the asymptotic relationship is greater than 0.074 and less than 5.1774, i.e., the network is almost surely disconnected if the asymptotic nodal degree $k < 0.074 \log(n)$, and the network is almost surely connected if $k > 5.1774 \log(n)$. The value of the critical constant still remains an open problem. However, in [228] it was conjectured the value may be close to one. By applying Xue and Kumar's results [228], Blough *et al.* [27] developed a topology control mechanism that generates a network topology by connecting each node to its k-nearest neighbors. The value of k that can provide high probability of connectivity was estimated. Other work that finds the radio transmission ranges can be found in [20], [191], [193], [196], and [214].

In the design and planning of a WSN, given the radio transmission range of each node, it is important to know that what is the necessary number of nodes required to ensure the a required probability of connectivity. Given r, Santi and Blough [195] studied the minimum number of nodes that ensures a 1-D network connected with a high probability. In [21], Bettstetter found the necessary number of nodes required to maintain a k-connected network for a particular transmission range r.

Estimating the probability of network connectivity for given network parameters, such as transmission range r and number of nodes n, is essential to network performance evaluation. Foh and Lee [75] enhanced the results in [195] by providing a closed form formula to compute the probability that two nodes with distance d is connected through n additional random nodes in a 1-D WSN. In [60], [85], and [86], a different setting is considered. They studied the probability that n nodes are connected in a 1-D interval, without two additional nodes on the borders of the interval. Bettstetter [21] studied the relationship between the probability of connectivity and the probability that there are no isolated nodes in a network with homogeneous transmission range. As no isolated nodes is a necessary (but not sufficient) condition for the network to be connected, its probability forms an upper bound for the probability of connectivity, while the corresponding critical transmission range when there are no isolated nodes forms a lower bound for that of a connected network. With similar rationale, it was shown that the probability that the network has a minimum nodal degree k is a tight upper bound for the probability that the network is k-connected. The author of [21] also discussed how to avoid border effects. See [24] and [25] for detailed discussions on border effects.

Simply maintaining the connectivity of a WSN is not sufficient for data dissemination. Routing issue should also be considered. Due to the large amount of sensors in WSNs, designing scalable and energy-efficient routing protocols is one of the major challenges for WSNs. One available solution is to perform routing through a set of nodes, so called a virtual backbone. A good virtual backbone can simplify the routing process and reduce the overall network energy consumption. The argument that virtual backbone routing can save energy is supported by two reasons. First, as only nodes in the virtual backbone forward packets, the network can turn off as many non-backbone nodes as possible to reduce power consumption. Second, sensor nodes support in-network processing and data aggregation. Performing these types of operations within virtual backbone nodes can eliminate redundant data and relax the packet transmission burden, which leads to energy saving.

For a given WSN, we always wish to find a minimum number of nodes as a virtual backbone. This number is an important performance metric to evaluate routing algorithms, in terms of the minimum number of relays required to achieve successful packet delivery through the network. The successful packet delivery requires the connectivity among the nodes in the virtual backbone.

In the next subsection we first introduces cluster-based routing, which groups nodes according to their geometric positions, and selects a head node for each group (i.e., cluster). All the cluster heads form a virtual backbone. We also discuss a graph theoretical concept, Minimum Connected Dominating Sets (MCDS), which can effectively model a small connected relay set. We also cover the state-of-the-arts algorithms for MCDS construction, which can be used to facilitate the utilization of infrastructure-based or virtual backbone based routing algorithms.

2.2.2 Virtual Backbone and Minimum Connected Dominating Set

Routing is challenging for WSNs. This is because wireless ad hoc communications suffer limited bandwidth, stringent energy constraints, and multi-hop communications. Special characteristics of WSNs such as multicasting transmission, a large amount of sensors, and so forth, also introduce difficulties into routing. Conventional routing schemes in wired networks, such as distance vector routing [105] or link state routing [164] that periodically perform routing information updates require all the nodes to participate in. They are not effective for wireless ad hoc networks due to the high computational complexity and the

large amount of control overhead.

It is commonly believed that clustering is an effective way to achieve efficient routing for WSNs [207] [213]. It can reduce the communication overhead, and simplify routing and management operations in densely deployed WSNs. Under clustering routing, the whole WSN is partitioned into several clusters of which each contains nodes in proximity. In each cluster, there is a cluster head. Inter-cluster communications can only occur between cluster heads, hence nodes in different clusters must connect to their cluster heads first if they need to communicate with each other. Examples of cluster-based routing schemes include, but are not limited to, LEACH [106], HCR [111], CBRP [126], and CEDAR [205]. CEDAR and CBRP are general cluster-based routing algorithms for wireless ad hoc networks, while LEACH is specialized for WSNs, and HCR is an extension of LEACH. Other cluster-based routing algorithms for WSNs include TEEN [153] and APTEEN [154].

The usage of cluster-based routing in WSNs is also motivated by the intrinsic requirements of in-network processing and data aggregation to reduce energy consumption, as such operations can be spontaneously performed at cluster head nodes. It should be noted that once the clusters are formed in a WSN, traditional proactive routing schemes such as distance vector routing and link state routing, as well as reactive routing approaches such as DSR [127] and AODV [178] can be used among those cluster head nodes, either for routing information update or for data delivery.

Indeed, cluster-based routing is a special example of backbone-based routing [58], if nodes in a backbone are considered as cluster heads. Since a backbone is not a fixed infrastructure in the context of WSNs, it is called a "virtual" backbone. A virtual backbone in a WSN is a set of nodes that are connected together, and routing operations are restricted to those nodes in the backbone. Therefore, to ensure its communications to other nodes, each sensor should connect to at least one node in the virtual backbone in a single hop, while virtual backbone nodes can communicate with each other via multi-hop paths. It is clear that the nodes in the virtual backbone need to maintain the connectivity among each others. A virtual backbone also has other functions, such as route maintenance, transmission scheduling, and broadcasting [216].

A virtual backbone of a WSN can be modelled by a **C**onnected **D**ominating **S**et (CDS) in a graph representing the WSN, such as a geometric graph and unit disk graph as mentioned in Section 2.2. For a graph $G = (V, E)$, in which V is the set of vertices with

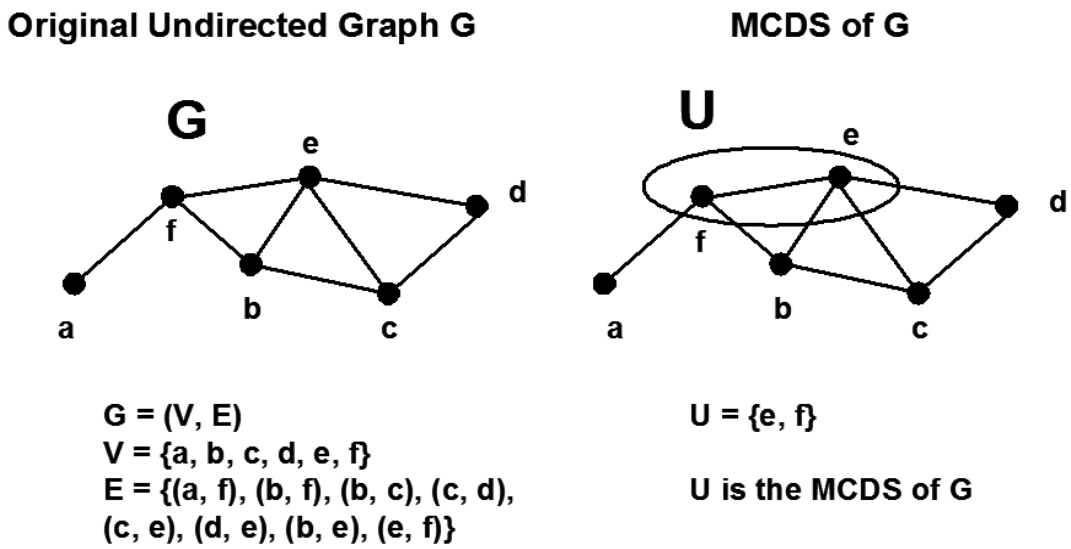

Figure 2.2: An example of Minimum Connected Dominating Set

cardinality n, and E is the set of edges, a dominating set (DS) is defined as a subset of V, such that any vertex in V is either an element of the DS or has at least one neighbour in the DS. If G is connected and such a dominating set is connected, i.e., any arbitrary pair of vertices in the DS are connected with each other, it is called a connected dominating set (CDS). A graph can have multiple DS and CDS. The CDS that has the smallest cardinality is named a **M**inimum **C**onnected **D**ominating **S**et (MCDS). Just like CDS, MCDS may not be unique. We call the cardinality of the MCDS *domination number* throughout this thesis. Fig. 2.2 illustrates the concept of MCDS by a simple example. A network is modelled as a connected graph $G = (V, E)$, in which $V = \{a, b, c, d, e, f\}$ is the set of vertices, representing all the nodes in the network, while an edge between two vertices in the graph stands for the existence of a direct connection between the corresponding sensor nodes, and the edges set $E = \{(a, f), (b, f), (b, c), (c, d), (c, e), (d, e), (b, e)(e, f)\}$ is the collection of all the connections. According to the previous definition, the MCDS of G in Fig. 2.2 is a subset U of vertices set V, which comprises vertices e and f, i.e., $U = \{e, f\}$. The domination number of U is two. Since we model WSNs by graph models, connected dominating set in the corresponding graphs can form the virtual backbone for the WSNs. Also, if we can find the MCDS in the graphs, we can construct a virtual backbone with the least number of nodes.

Unfortunately, finding a MCDS in a given connected graph is not always as easy as the previous example in practical situations. This problem is known to be NP-hard [78]. The research activities on MCDS problem mainly focus on providing approxima-

tion algorithms, which achieve near MCDS construction. Existing algorithms constructing MCDS can be classified into three categories, including constructive, pruning-based and multipoint-relay-based algorithms. Constructive algorithms approximate the MCDS in a graph by gradually adding nodes to a candidate set. In contrast, pruning-based algorithms begin with taking a large candidate set, then detect and remove redundant nodes to eventually obtain a small CDS. The last type, multipoint-relay-based algorithms, allows each node to determine its smallest one-hop message relay set, and all nodes selected as relay nodes for a particular message relaying form a CDS.

For all these three types of algorithms, the connectivity among the relay nodes need to be considered. A common approach used by constructive algorithms is to select a **M**aximal **I**ndependent **S**et (MIS) first, and then by using some additional nodes to provide connectivity among nodes in the MIS. Algorithms in this class are generally differentiated according to the approaches to produce the MIS and find the additional nodes. An independent set (IS) of a graph $G = (V, E)$ is defined as a subset $\overline{V} \subseteq V$, such that there is no edge between any two vertices in $\overline{V}$, i.e., $\forall\ u, v \in \overline{V}$, $(u, v) \notin E$. An independent set that is not a proper subset of any other independent set is called a maximal independent set. Note the difference between maximal independent set and maximum independent set. The latter is defined as the independent set with the largest cardinality. While construction of a maximal independent set can be solved in polynomial time by greedy algorithms, finding the maximum independent sets is NP-complete [78]. In contrast to constructive algorithms, pruning-based algorithms generate a large CDS first, and then remove redundant nodes while keeping the connectivity among the remaining nodes in the CDS. In terms of the multipoint-relay-based algorithms, the connectivity of the constructed dominating set is guaranteed in the selection of multipoint relay nodes. Our algorithm described in Chapter 4 can be classified as a constructive algorithm without using MIS.

These three types of algorithms are described in more detail in the following subsection. Typical examples of each type are also discussed, hence this subsection provides the motivations of our research problems and anchor the work in Chapter 3 and Chapter 4.

Constructive Algorithms

In Guha and Khuller's seminal paper [89], they first showed that a β algorithm to approximate MCDS corresponds to a 2β approximation for another NP-hard problem, travelling

tourist problem, and then proposed two polynomial time heuristics for the MCDS problem. These two algorithms have approximation factors of $2(H(\Delta)+1)$ and $H(\Delta)+2$, respectively, in which Δ is the maximum nodal degree and H is the harmonic function [87].

The first algorithm approximates the MCDS by creating a tree T incrementally by greedy criteria. All the non-leaf nodes of T form the approximate MCDS, which is indeed a CDS. Nodes have three states, which are black, grey and white. Black nodes are nodes in the final CDS, so called dominators. Grey nodes are candidates of dominators, and white nodes are those nodes not yet in T. Initially, all the nodes are white nodes, and the algorithm finds out the node with maximum degree of white neighbors, marks it black, and marks all its white neighbors grey. The algorithm then iteratively marks the grey node or the pair of connected grey nodes that have maximum white neighbors to black, and update those white neighbors to grey state. The set of black nodes in the final result is the CDS.

To develop the second algorithm, Guha and Khuller introduced a new concept called *piece*, which is defined as either a connected black component, or a white node. The second algorithm selects nodes with maximum degree of *pieces* as dominators until there are no white nodes. It then connects all the dominators by constructing a Steiner tree.

Both of the algorithms are not localized as they need global information to select the nodes with maximum degree of white neighbors or *pieces*. Das and Bharghavan [58] proposed to construct a virtual backbone in a wireless ad hoc network by using its MCDS, and developed a distributed implementation of Guha and Khuller's algorithm. Das and Bharghavan's distributed algorithm is also non-localized, as it is based on a centralized algorithm. A distributed algorithm is called localized if each node decides on its own behavior based on only the information from nodes within a limited hop distance, e.g., one or two hops. With localized algorithms, topology changes in part of the network can be isolated, and may not affect the rest of the network. In contrast, a non-localized algorithm requires nodes to know global knowledge of the network to perform correct operations [40].

Alzoubi and Wan [9] developed a distributed heuristic to compute the MCDS for a wireless ad hoc network. The algorithm is non-localized as it involves the construction of a spanning tree. Indeed, this algorithm follows the same idea as the second algorithm of Guha and Khuller. It selects a dominating set first, and then connects nodes in the

dominating set by choosing some additional nodes as connectors. The selection of the dominating set is based on the construction of a maximal independent set (MIS), and the connection step is completed by selecting some additional nodes to form a spanning tree. The authors provided performance bounds by applying the property that a node in a unit disk graph cannot have more than five independent neighbors [155]. If n is the number of vertices for the whole network, the algorithm has time complexity of $O(n)$, and message complexity of $O(n \log(n))$, while providing a constant approximation factor. This algorithm is non-localized as it needs a leader node to generate a rooted tree. To overcome this drawback, Alzoubi *et al.* [10] proposed another algorithm, which generates MIS based on multiple leaders, and hence it is localized. The algorithm obtains a CDS with cardinality at most $192 \cdot |OPT| + 48$, in which $|OPT|$ is for the cardinality of the MCDS. The main drawback of this algorithm is the low efficiency of the connector selection procedure. Other work based on computing and connecting a MIS include [36], [38], [172], and references therein.

Pruning-Based Algorithms

Besides constructive algorithms, there also exist other algorithms which are based on pruning procedures to approximate MCDS. As indicated by its name, a pruning-based algorithm gradually reduces a candidate CDS according to some greedy criteria, and the left-over set after the reduction is the approximated MCDS.

Wu and Li [223] proposed a localized algorithm to construct a CDS in a network. This algorithm consists of two steps. In the first step, each node in the network gets information of its two-hop neighbors via the exchange of beacons. Every node that has two neighbors that are not within the radio range r of each other marks itself as a dominator. The second step is a pruning process, which takes out some redundant nodes from the dominator set generated in the first step. There exist two rules to reduce the size of the CDS generated in the first step. A node u can be removed from the CDS if its closed neighborhood is a subset of that of another node v in the CDS, or the open neighborhood of u is a subset of the union of the open neighborhood of another two nodes v and w, which are in the CDS. The open neighborhood of a node u is defined as the set of all the nodes that direct link to u. The closed neighborhood of u is the union of its open neighborhood and u. Wu *et al.* [222] also extended this algorithm to take energy property of all the nodes into account to make the algorithm energy aware. For an arbitrary node u, an attribute

$el(u)$, which indicates the remaining energy level of u, is considered when the pruning process is performed. Nodes with lower energy level are preferred to be removed.

Another algorithm that uses pruning process is by Butenko *et al.* [37]. This algorithm takes the entire set of nodes V as the initial candidate CDS, and then iteratively removes nodes greedily. In order to determine whether a node can be removed from the current CDS, the connectivity of the remaining nodes is tested. The node can be removed only if the remaining candidate CDS is still connected. This algorithm has high message complexity due to the operations of connectivity tests, especially for large dense networks. However, simulation results show that the performance in terms of the domination number is comparative to existing algorithms. Sanchis [192] also discusses similar approach in the construction of dominating sets.

Multipoint Relaying (MPR) in CDS Construction

Multipoint relaying is a technique that is widely used for flooding in wireless ad hoc networks. In multipoint relaying, each node u in the network selects a subset of its first-hop neighbors, named multipoint relay set (MRS), which are responsible for forwarding packets from node u to u's two hop neighbors. Only nodes in the MRS of u can forward packets sent by u. Qayyum *et al.* [183] showed that finding a minimum size MRS in a network is NP-Complete. The MRS of a node u forms a local dominating set, which dominates nodes within two hops distance from u. Although MRS do not directly generate a global CDS, they can be extended to do so.

Note that in [183], node u and its MRS only form local CDS. However, some algorithms approximate MCDS for the whole network based on MRS. Adjih *et al.* [6] developed a source-independent MPR algorithm, called MPR-CDS algorithm, to construct a global CDS based on the MPR approach. The algorithm assumes that each node in a connected network has a unique ID. The global CDS is constructed based on the ID of nodes, according to the following criteria. A node u is added into the CDS if it has the smallest ID among all its first-hop neighbors, or it is a member of the MRS of its neighbor with the smallest ID. The time complexity is shown to be $O(\Delta^2)$, while the message complexity is $O(n)$. However, as pointed out by Wu [221], the CDS generated by MPR-CDS can be inefficient as the nodes selected by the first criterion may not be necessary. This is because the first criterion only select CDS nodes based on their IDs. Hence for certain network topologies, nodes chosen by the first criterion are redundant. Therefore, Wu [221] devel-

oped *enhanced MPR* (EMPR) algorithm by enhancing the MPR-CDS in both smallest ID nodes selection and original MPR selection. However, due to these two enhancements, the EMPR suffers potentially high computation complexity. Other MPR-based CDS construction heuristics include Chen *et al.* [48], Wu *et al.* [220], [224], and others. For a comprehensive survey about multipoint-relay-based broadcast schemes, see Ou *et al.* [171], which includes, but are not limited to, multipoint-relay-based CDS construction. Note that all the discussions of MCDS are based on the fact that the network is connected. When dealing with a disconnected network, we can only find CDSs of each connected part of the network.

2.2.3 Placement of Nodes

The placement of nodes largely influences the operations and performance of WSNs, as sensor nodes deployed need to observe events that are interested in, and transmit the information to data collection centres. Moreover, sensor placement also affects the resource management in WSNs [61]. According to the roles that the deployed nodes play, node placement can be classified into placement of ordinary nodes, and placement of relay nodes, respectively. The former focus on the deployment of normal sensors, while the latter places a special type of nodes, which are responsible for forwarding packets. We survey these two types of placement next.

Placement of Ordinary Nodes

The foremost step needs to be done for a WSN to perform its designed functions is deploying all the sensor nodes to form a WSN. To ensure that the WSN can operate properly, sensor placement scheme needs to be carefully determined. There are two types of sensor deployment methodologies, random deployment and deterministic deployment, e.g., sensors are thrown in mass on random positions and placed exactly on carefully engineered positions [8]. For instance, to apply the random placement, we can drop all the sensors from a vehicle in batch, thereby reducing the labour cost of the deployment. However, this approach brings randomness in the positions of sensors, and the randomness may degrade the network performance. The other option is to cautiously plan sensor deployment, for which sensor nodes are dropped exactly on predetermined positions, either manually or by machines. The usage of deterministic deployment may be constrained by harsh environments that the WSNs embedded in and the large amount

of sensor nodes.

Most of existing literature in the field focuses on determining the "optimal" deterministic placement pattern. The optimality is defined on different context according to the applications and goals of the WSNs.

A natural objective for the optimal sensor placement is to minimize the number of required sensors needed, subject to the constraint that the whole sensing field is monitored by the deployed sensors. It is equivalent to finding the minimum number of nodes, such that every position in the sensing field is within the sensing coverage by at least one node. One method to solve this problem is to model it as the art gallery problem [170], which aims to find the minimum set of locations for security guards inside a polygonal art gallery, such that the boundary of the entire gallery is visible by at least one of the security guards. Gonzólez-Banos [84] proposes a randomized algorithm to solve art gallery problem to find locations for sensor nodes. However, in art gallery problem, all security guards are assumed to have infinite vision, if there is no obstacles. This assumption does not hold for WSNs since sensor nodes have limited sensing range. Zhang and Hou [230] proved that arranging sensors at the centres of regular hexagons is optimal for a WSN with a large sensor field, given that all the sensor nodes have identical limited sensing range. Indeed, this problem was well-studied in mathematics community, see Kershner [130].

The above work on the node placement only considers the coverage constraints that the WSN needs to be able to observe any positions within the sensor field. They did not include the discussion about the connectivity, or they implicitly assumed that the WSN formed by the obtained pattern was connected, regardless the transmission range. Nevertheless, this assumption may not be true. To find the optimal node placement pattern subject to the coverage and the connectivity constraints, Biagioni and Sasaki [26] modelled the problem as an optimization problem that minimizes the number of required sensor nodes, under the constraints that any position of the sensor field is under surveillance of at least one node and all nodes are connected. However, the authors did not solve the problem optimally. They only studied a wide range of regular sensor network deployment patterns. These patterns include circular, and star topologies, as well as grid topologies, such as triangular, square and hexagonal grids. Iyengar *et al.* [125] proved that a strip-based pattern is nearly optimal for large networks in two-dimensional space. Bai *et al.* [16] extended the work in [125] by proving that this strip-based pattern is the

asymptotic optimal pattern for an infinite network. A slight modification of the asymptotic optimal strip-based pattern, which is optimal to achieve coverage and 2-connectivity was also proposed in [16]. Very recently, Bai *et al.* [17] published new results, which proposed optimal sensor placement patterns to achieve coverage and k-connectivity ($k \leq 6$). Note that k- connectivity can provide fault tolerance. Above work assumed that the WSN was deployed in an open area, without obstacles such as buildings or stationary. In contrast, Wang *et al.* [217] developed a general sensors deployment scheme, which can efficiently determine sensor positions for arbitrary sensing field, probably with obstacles.

In addition to minimize the total number of sensor nodes, there also exist other objectives when considering the optimal sensor placement. Khan [131] studied the node placement problem in a grid sensor field. The problem was formulated as an optimization problem aiming to minimize the distance between sensors, subject to the constraints that all the n sensors (n is given) have to be placed on grid points, and all the grid points have to be sensed by some sensors. Other work adopting grid-based deployment include Chakrabarty *et al.* [43], and Lin *et al.* [147]. Chakrabarty *et al.* [43] tried to find the node placement scheme that minimizes the cost of sensors to meet the complete coverage constraints. Lin *et al.* [147] developed an algorithm to solve the sensor placement problem on a grid field. Each grid point was coded according to the coverage relationship to sensors. The algorithm aimed to find the set of grid points that can minimize the maximum coding distance between any pair of grid points, subject to the cost limitation.

Above mentioned work were based on deterministic sensor placement. However, for a large scale WSN, random placement strategy is perhaps a more attractive option. Therefore, it is necessary to establish proper models to describe the random deployment. Ishizuka and Adia [118] proposed three types of random placement models. They are *Simple Diffusion*, *Constant Placement*, and *R-random Placement*. *Simple diffusion* assumes that node positions follow identical Gaussian distribution, while *Constant Placement* considers each node uniformly distributed in the sensor field. The last model, *R-random Placement* assumes that sensors are uniformly distributed in terms of the network radius and angular direction from the sensor field centre, which could represent a data collection point. The authors studied the fault-tolerance and sensing coverage through simulations, and suggested that the *R-random Placement* to be the best candidate for random node placement. See Leoncini *et al.* [144] for a different setting of random placement.

Although there exist different types of models to formulate different random deploy-

ment strategies, the most widely-used model for the positions of sensors in a randomly deployed WSN is the uniform distribution model (i.e., Constant Placement). However, the validity of the assumption that nodes are randomly and uniformly distributed is difficult to be verified, and is left as an open research problem, though some partial results exist in literature. Blough *et al.* [28] studied the spatial distribution of nodes in a wireless ad hoc network. Given the initial distribution of nodes is uniform distribution, and all the nodes move according to the random waypoint model, it is shown by simulations that the common assumption that nodes are distributed according to a uniform distribution holds if all the nodes move for a large number of steps of Brownian-like motion, which represents unintentional movement. Even though the results gave some insights into the spatial distribution of nodes locations, they did not investigate other initial distributions. Moreover, they did not justify the selection of the initial distribution. On the other hand, Miller [161] showed that as long as all the nodes have identical distribution, the choice of the initial distribution is not critical. This result holds at least for uniform and Gaussian distribution.

Placement of Relay Nodes

In a WSN, if a small set of special nodes, whose main function is packet forwarding, are deployed, the management and network operations in the WSN can be potentially simplified drastically. These nodes are called relay nodes, and have attracted flourishing interests [49] [102] [173] [212] [231]. A fundamental problem arises when establish such a network is how to efficiently deploy those relay nodes to achieve required grade of service, while meeting the system constraints. This subsection covers this general topic.

Relay node placement problem can be categorized into either single-tiered or two-tiered, according to the data forwarding schemes the WSNs adopted. If both of relay nodes and ordinary sensor nodes can forward packets, this is single-tiered relay node placement. In contrast, in a WSN with two-tiered relay node placement, only relay nodes participate in the packet forwarding. We survey the prior work related to these two types of relay placement. In the following discussion, the transmission ranges for relays and ordinary sensors are denoted R and r, respectively.

Cheng *et al.* [49] developed algorithms to place minimum number of relay nodes and maintain the connectivity of a WSN, under the assumption that $R = r$, i.e., all relays and ordinary sensors have identical transmission range. Single-tiered situation was con-

sidered. The problem was modelled by the *Steiner Minimum Tree with Minimum Number of Steiner Points and Bounded Edge Length (SMT-MSP)* problem, which was arisen in the study of amplifier deployment in optical networks, and was proved to be NP-hard [148]. To resolve the SMT-MST problem, Lin and Xue's [148] developed a 5-approximation minimum spanning tree based algorithm, while Cheng *et al.* [49] proposed a 3-approximation algorithm and a randomized 2.5-approximation algorithm based on Lin and Xue's algorithm. Chen *et al.* [47] also proposed a 3-approximation algorithm, and they further prove that Lin and Xue's algorithm has an approximation ratio 4. In order to provide fault-tolerance, Kashyap *et al.* [129] studied how to place minimum number of relays such that the resulted WSN is 2-connected, when relay nodes and ordinary sensor nodes have identical transmission range, i.e., $R = r$. Recently, Zhang *et al.* [231] improved Kashyap *et al.* [129]'s results by developing algorithms to compute the optimal node placement for networks to achieve 2-connectivity, under the more general condition that R is no less than r. These algorithms aimed to minimize the number of relay nodes while providing fault-tolerance.

In contrast to previously mentioned work, Pan *et al.* [173] focused on the two-tiered situation, in which only relay nodes can perform the packet forwarding. [102] and [212] also studied the optimal two-tiered relay placement, but for a i.i.d. uniformly distributed sensor network when there exists certain relationship between the transmission range of relay nodes and ordinary nodes, i.e., $R \geq 4r$. Lloyd and Xue [149] improved [49] and [102] by developing algorithms to find optimal placement of relay nodes for more general relationship between R and r ($R \geq r$), under single-tiered and two-tiered infrastructure, respectively.

All the above work assume that relay nodes can be placed on anywhere, this is called unconstrained relay node placement. However, practical considerations such as interferences or forbidden regions prevent relay nodes from being placed on certain positions. This is known as constrained relay node placement problem. A recently published work [163] discusses this problem and proposed approximate algorithms to resolve it. Srinivas and Modiano [208] considered a different model, which place a fixed number of relays to optimize the network throughput.

It should be noted that for two-tiered relay node placement, the deployed relays form a connected dominating set of the resulting WSN (i.e., including both the relays and ordinary sensor).

2.2.4 Other Connectivity Related Work

Percolation Theory and Partial Connectivity

Percolation theory plays an important role in the investigation for connectivity of wireless ad hoc networks, and provides insights to understand their intrinsic characteristics. As such, it can be a complementary approach to the empirical method taken in Chapter 5. This section gives an introduction to percolation theory, and reviews some existing work related to the network connectivity studies. We aim to provide background information and to put Chapter 5 in context.

The notion of percolation was developed by Broadbent [32], Broadbent and Hammersley [33], and Hammersley [101] to mathematically model the phenomena of fluid flowing through random porous materials, e.g., water soaking a sponge. In the percolation model, the randomness of the porous materials lies in the fact that the paths fluid can get through are random. An important characteristic of percolation models is that there exists a phase transition. For the parameters related to the system, there is a critical value that enables a phase transition, e.g., if the density of holes in the sponge exceeds that value, water may get through, otherwise the sponge only gets wet in the surface.

Mathematically, percolation theory studies infinite random graphs, which contain a set of infinite number of vertices V spreading over an infinite plane. Correspondingly, percolation theory in wireless ad hoc networking areas focuses on the connectivity of infinite networks, which contain infinite number of nodes that are distributed on an infinite plane. In particular, we are concerning the formation of an infinite connected component. Therefore, it is the partial connectivity rather than the full connectivity that we are interested in. An infinite connected component is a collection of vertices, which is an infinite subset V_1 of V, and there is at least one path between an arbitrary pair of nodes in V_1. An infinite connected component corresponds to a communication network of infinite nodes spread over a large geographic plane. Therefore, the existence of an infinite connected component implies the capability of long distance communication via multi-hop links.

There are three types of percolation, namely, bond, site and continuum percolation. The first two types, bond and site percolation, are lattice based discrete percolation models. The last model, continuum percolation, studies the percolation phenomenon in a continuous space. A lattice is essentially a graph, in which vertices are arranged according to some regular grid patterns, and there are edges between adjacent vertices. For example,

in a rectangle lattice, vertices are aligned with rectangle grid patterns, in which vertices in the same row have identical vertical coordinates, and nodes in the same column have the same horizontal coordinates, if the lattice is equipped with rectangle coordinate system. There exists an edge between each pair of adjacent vertices for a lattice. A bond percolation model is defined for an infinite lattice. Each node sits on a corner of the lattice, and each edge (so called a bond in the context of lattice percolation) is randomly remained with probability p, or be removed with probability $(1-p)$ [88]. We call a remained bond an open edge, and a removed bond a closed edge. An open edge indicates that the two end nodes of the edge can communicate directly, while a closed edge blocks the communication. It is shown that there is a critical value of p, p_0, such that an unbounded connected component is formed, if each bond is kept with identical probability that is more than p_0. Site percolation takes the similar idea with the bond percolation, except that each node has probability p to be opened, and $(1-p)$ to be closed, while all edges are open with probability one.

In contrast, continuum percolation, which was firstly studied by Gilbert [81], assumes that nodes are distributed following a homogeneous Poisson point process of intensity λ, rather than be placed at lattice points. Note that nodes in continuum percolation can distribute according to more general stationary and ergodic point processes other than Poisson processes. However, continuum percolation with Poisson process is more intensively studied due to its tractability. If a link exists between any two nodes with distance less than a constant r, this model is named a *boolean model*, in the context of percolation theory. It is essentially unit disk model. There also exist other models in continuum percolation, such as *random connection model* [158]. In a random connection model, the probability that there exists a link between two nodes a and b is determined by a certain function of the distance between a and b. Continuum percolation is widely applied in the study of network connectivity (e.g., [64] [65] [66] [67]) as it imposes less constraints on the positions of nodes, compared to bond and site percolation models.

Gilbert [81] was the first to introduce the concept of continuum percolation. He indicated its usage in multi-hop communications in his seminal work [81]. It investigated $\mathrm{P}(n)$, the probability that there exists a connected component containing n nodes, in particular, as n goes to infinity, which is the probability to form an infinite connected component. It was expressed as a function of average nodal degree E, i.e., $E = \lambda\pi r^2$. It was shown that there is a critical value E_c of E, such that an infinite connected component is

only possible when $E > E_c$. Although the exact value of E_c was not known, [81] showed that $1.75 \leq E_c \leq 17.4$. Philips *et al.* [179] improved the results by providing a tighter bound of E_c as $2.195 < E_c < 10.526$. Besides the analytical approaches to evaluate E_c, numerical methods [184] were also used to obtain the bounds for E_c. These results gave us some necessary conditions to construct a connected network in a large plane. As percolation theory focuses on the infinite networks and studies the existence probability of an infinite connected component, the connectivity it emphasized is indeed partial connectivity rather than full connectivity. However, it is shown that the partial connectivity converges to the full connectivity as the network intensity increases.

Gilbert's work only gave necessary conditions for connectivity of large scale networks, it does not reveal how the number of nodes in the connected component, n, affects the probability of connectivity. Philips *et al.* [179] applied the Poisson boolean model to a wireless packet radio network within a finite area A and extended Gilbert's results by studying the relationship between A and the average nodal degree E to ensure the network connectivity. It is proved that for any $\epsilon > 0$, with transmission range r given by $r = \sqrt{(1-\epsilon)\log A/\pi\lambda}$, the limiting property of network $\lim_{A\to\infty} \mathrm{P}(connected) = 0$. It is also conjectured that given $r = \sqrt{(1+\epsilon)\log A/\pi\lambda}$, $\epsilon > 0$, the network is almost surely connected. This conjecture suggests that to obtain almost surely connectivity, the expected number of nodes within transmission range of an arbitrary node should grow logarithmically with network area. Piret [180] proves that this conjecture does not hold for one-dimensional networks. Nevertheless, the conjecture coincides with the results in [228], except that [228] states that ϵ cannot be an arbitrary number.

The above discussion assumed the boolean model (i.e., unit disk model). This model results in a circular radio transmission range for each node. However, the wireless propagation in the practical situation yields irregular shapes other than circle. Interestingly, it was shown by Booth *et al.* [30] that this irregularity enables the network to percolate in a lower density if the footprint of each node is convex, which indicates that sufficient conditions for connectivity obtained by boolean models hold in general for unreliable and non-rotational symmetric wireless channels. However, for networks that each node produces arbitrary footprint, the connectivity is still an open problem.

One of the main drawbacks of boolean model is that it does not consider the interferences, though dense networks produce strong interferences. To take the interferences into account, Dousse *et al.* [64] used another model named signal-to-interference-plus-noise-

ratio (SINR) model, in which two nodes are connected if SINR between the transmitter and receiver exceeds a certain threshold. As signal strength is considered in this model, the connectivity of the network depends on the selection of the attenuation function. It was proved that percolation occurs for SINR model in a similar way as in the boolean model. It was also shown that the commonly used power law attenuation function results in symmetry properties, and attenuation functions with finite support can also achieve percolation. The authors showed that an efficient CDMA system with small orthogonality factors can improve the connectivity. However, due to the difficulty to design efficient CDMA codes to achieve a small orthogonality factor, a simple TDMA scheme was proposed, which also percolate.

Network capacity or throughput is an important constraint when considering the connectivity of ad hoc networks. In a wireless ad hoc network, the increase of the transmission power could increase the transmission distance of each node, which leads to the increased probability of network connectivity. However, the large power results in severe interferences within the network, which reduces the network capacity and degrades the performance of decoding at receivers. On the other hand, short transmission range, which comes from small transmission power, can limit the interferences, but the connectivity cannot be guaranteed. Therefore, it is worthy to analyse the trade-off between connectivity and network capacity. Motivated by this counteracting effect, there exists a third model, which studies the connectivity from information theoretic point of view [65], in addition to the boolean and SINR models.

In this model, it is declared that two nodes connect to each other if and only if they can communicate with a predefined minimum data rate. Thus this model gives more flexibility about the transmission schemes as it does not assume any particular relay scheme. Note that this model boils down to SINR model if all signals are Gaussian. It was shown in [65] that as the number of nodes goes to infinity, if partial connectivity is allowed, an arbitrary pair of nodes in the connected component formed by the percolation phenomena can communicate with each other with a certain rate if all other nodes are potential relays. It was also shown that if we want to impose a required data rate for possible transmission as the number of nodes goes to infinity, a fraction of nodes, which is a function of the required data rate, are automatically disconnected. Note the coincidence between this result and the results shown by Gupta and Kumar [92], which stated that under the constraint of the full connectivity, the throughput of each node eventually vanishes as

the number of nodes goes to infinity. Therefore, the network capacity does not scale up linearly with the number of nodes, hence this implies that base stations are required. To investigate the relationship between connectivity and capacity, Dousse and Thiran [66] proved that the attenuation function is one of the major factors affecting the properties of dense ad hoc networks. Under the assumption of power law attenuation, the network connectivity probability becomes higher as the increase of nodes density, even though the interference also increases. The increase of network total capacity is bounded by $\sqrt{n}$. However, the total network capacity keeps constant with bounded attenuation functions, and the network maintains connectivity at the expense of capacity. See Xin and Srikant [225] for another treatment of connectivity via information theoretic viewpoint, without using percolation theory.

The above work is based on the pure ad hoc networks. In addition to that, hybrid networks also attract research efforts, due to the existence of infrastructures of base stations, and the requirements to improve network capacity, as implied in [92]. A hybrid network contains not only peer terminals, but also some base stations, which can communicate to terminals via single or multi hops. Percolation in a hybrid network was also studied. Booth *et al.* [31] studied algorithms to place base stations to cover Poisson distributed nodes. Dousse *et al.* [67] studied the impact of base stations on the connectivity in two-dimensional sparse networks. It was shown that base stations help increasing the network connectivity significantly, when the node density in one dimension is much higher than the density in the other dimension. The authors explained the phenomenon by percolation theory. More theoretical analysis about percolation can be found in [100] and [160].

Impact of Imperfect Channels

Interferences, which are mainly consisting of *adjacent channel interference* and *co-channel interference*, in wireless environments are considered as one of the major factors that affect performance of wireless networks [186]. Adjacent channel interference refers to unwanted signals from other frequency channels which are nearby to the frequency that is being used, while co-channel interference is defined as the unwanted signals generated by other transmission system which is using the same frequency bands [206]. Note that ideally, the adjacent channel interferences are eliminated in a CDMA system. It is clear that interferences largely affect the decoding performance at the receiver side. Therefore,

it is important to deal with interferences when considering the connectivity of WSNs. However, not much work have been done in this area. An example of such work is Dousse *et al.* [64], which studied the connectivity of ad hoc networks suffering interferences, as discussed in the subsection on the percolation theory.

Besides interferences, shadowing effect is another major factor to affect the transmission in wireless environments. The widely accepted model to describe shadowing effect is the log-normal shadowing, which applies the log-normal distribution to model the signal level for an arbitrary value of transmitter-receiver distance [186]. In [234], it was shown that the optimal transmission range should be selected such that the average number of nodes closer to the transmitter than the receiver to be $\phi(G/b)^{2/\zeta}$, where ϕ is a constant depending on the physical systems, G represents the spread spectrum processing gain, b is the threshold for the outage SNR and ζ accounts for the power loss factor.

Bettstetter and Hartmann [23] studied the probability that a single node is isolated under log-normal shadow fading environment with Poisson distributed nodes. A tight bound for the Poisson density to achieve a highly connected subnetwork is derived. It was shown that the fading would influence the connectivity significantly. Because the shadowing effect introduces randomness into the signal attenuation, the transmission range of each node would vary and some links may exist to farther nodes, while there may be no links to closer nodes, hence homogeneous transmission range assignment does not work here.

Networks with Mobile Nodes

Aforementioned results are all based on stationary networks, in which all the nodes are static, i.e., once sensors are deployed, they no longer move. However, there exists another important practical scenario that sensors do not stay at the positions they are initially placed, and they move as time evolves. For example, sensors deployed to monitor animal habitats may move around as target animals wander, or sensors equipped in human bodies to monitor the health parameters of patients in hospital may be mobile, as the patients move around. Some direct communication links may be lost while some other new links become available during the movements of nodes, i.e., node mobility may affect the connectivity of a network. Under those situations, it is important to study the impacts of node mobility to ensure that a WSN with mobile nodes can function properly. Many research efforts have been devoted into this area.

Bettstetter [22] derived a formula to obtain the minimum transmission range $r_{\min}$ so that a 2-D ad hoc network with n mobile nodes, which are doing random waypoint movement, has high probability to be connected, i.e., connected with probability greater than 99 percent. Average nodal degree during the movement was computed, as well as the distribution of the distance between nodes. Random waypoint scheme is generally used to model intentional movements, as it is defined as every node moves to randomly selected position in the geographical space with some velocity (either constant or random). Once a node reaches the destination position, it stays there for a pre-defined period of time t_p, and then repeat the above procedure. Similar to [22], Foh *et al.* [76] studied the connectivity of ad hoc network with random waypoint movement, but for one-dimensional networks. Santi and Blough [195] also investigated random waypoint scheme for 2-D networks, however, via the simulation studies. In addition to random waypoint scheme, drunkard-like movement is also widely applied to model motion of nodes as it can describe non-intentional movements.

It was shown in [195] that if the number of static nodes in a network is around half or more of the total number of nodes, the network can be considered stationary from the connectivity viewpoint. Therefore, a certain number of fixed nodes can largely improve the probability of connectivity in a sparse ad hoc network. Note that this result agrees to that in [67], which stated that base stations in planar network significantly improve the connectivity if the network has unbalanced nodes densities, i.e., there is much more nodes in one dimension than in the other dimension.

For a detailed taxonomy of mobility models of nodes for sensor networks, see Zheng *et al.* [233], in which mobility models were divided into three categories, *Trace Based Model, Constrained Topology Based Model, and Statistical Model*, respectively, according to the degree of randomness.

2.3 Summary

Wireless Sensor Networks have potential to revolutionize our everyday life, as they provide a flexible approach for us to observe the surrounding environments, and response to the occurred events. Battery-powered tiny sensor nodes, embedded with sensing, processing, and communication capabilities, which are wirelessly networked together via multi-hop communication, leverage the opportunities for WSNs to find applications in

wide areas. Along with the opportunities, there are also challenges and requirements for the successful deployment and operations of WSNs.

Connectivity is one of the stringent requirements for a WSN to function properly, because sensors need to transmit data to information collecting points. Most of the previous work about wireless network connectivity is based on a simple assumption that all the nodes follow i.i.d uniform distribution. This model is widely accepted as it is analytically tractable. Others (see [161] for an example) assume that all nodes follow identical Gaussian distribution. The uniform distributed sensors assumption stands for the situation that all sensors are deployed in a purely random manner, while the identical Gaussian distributed nodes represent the circumstance that all the nodes are targeting to a single position. These assumptions may not hold in practice. Hence new models need to be introduced to reflect more practical situations.

As we aim to provide high performance, we would like to impose some control schemes into the pure random deployment, or to consider some randomness in the deterministic placement. Thereby, in Chapter 5, we consider a different situation that all the nodes follow non-identical distributions, such that nodes are targeted at some expected positions but with i.i.d. random errors. Connectivity study for this network is more complex than that of the previous models, since nodes follows non-identical distributions.

In addition to the connectivity of ordinary sensors in WSNs, we also consider to perform routing and data forwarding within a small set of connected relay nodes. Obtaining such a set can be modelled as finding an Minimum Connected Dominating Set in a graph corresponding to the network. An Minimum Connected Dominating Set can effectively function as a virtual backbone in a WSN, and the virtual backbone would simplify the routing process and reduce the communication overheads, hence it can help to reduce the total network energy consumption. Moreover, if we can identify an MCDS in a WSN, the cardinality of the MCDS works as a performance metric to evaluate existing routing algorithms. However, as finding an MCDS is an NP-complete problem, only approximations and heuristics exist to approximate the solution. Current algorithms are too computationally costly to be used in large scale sensor networks. Hence new approaches that are simple and efficient are desirable.

In Chapter 3 of this thesis, we evaluate the domination number for a class of random WSNs probabilistically, without explicitly obtaining an MCDS. In Chapter 4, we propose a simple algorithm, which can approximate an MCDS for dense networks efficiently.

Chapter 3

Minimum Connected Dominating Sets in 1-D Dense Wireless Sensor Networks

As mentioned in the last chapter, a small relay set in WSNs can improve the efficiency of network operations such as flooding, network management, and routing. It can also help to reduce network energy consumption. Having some knowledge about the cardinality of the minimum relay set is important to evaluate algorithms to construct such a set. In this chapter, we evaluate the cardinality of the minimum relay set probabilistically for a single-dimensional random network.

3.1 Introduction

To prolong network lifetime, energy conservation is a major concern for wireless sensor networks due to the difficulty of battery replacement [7]. It is generally believed that sending data through many short hops is more energy-efficient than using a smaller number of longer hops in wireless environment [188], mainly because of the power law attenuation in received power as the single hop transmission distance increases.

However, this assumption may not hold as the local oscillators and bias circuitry dominate the energy consumption in practical power amplifier [93]. Moreover, for short distance transmission, the power consumption of the receiver can often exceeds that of the transmitter [185]. Hence only taking transmission power into account and assuming the reduction of transmission energy leads to a proportional reduction of total energy consumption may not be appropriate. This argument is supported by experiment results [95]. More importantly, considering a sensor network in which all sensor nodes operate in two modes, *Active* and *Sleep*, those sensor nodes that are not involved in any activities can be turned off. Many small hops result in more active nodes hence consuming more energy. The fewer nodes participate in routing, the fewer nodes need to be active thus saving energy and prolonging the overall network lifetime. Therefore, keeping the

number of nodes involved in routing small is important to achieve energy conservation. Recent research such as Haenggi and Puccinelli [95] also reveals that using a small number of long hop is a competitive alternative to adopting many short hops in routing, if network capacity, end-to-end delay, energy consumption and efficiency are all considered.

In order to ensure that the sensor network operates properly, the active nodes need to be connected to perform the data dissemination, and information collected by any node should be able to be sent to at least one active node. Therefore, to minimize the number of active nodes subject to the above constraints, it is equivalent to minimizing the Connected Dominating Set in the associated graph of the sensor network. This problem is known as Minimum Connected Dominating Set (MCDS) problem. The concepts of Dominating Set (DS), Connected Dominating Set (CDS), and Minimum Connected Dominating Set (MCDS) are given in Chapter 2. Finding the Minimum Connected Dominating Set (MCDS) in a connected graph is known to be NP-hard [78].

Existing work related to the utilization of connected dominating set in ad hoc network routing include [58], [132], [222] and references therein, just to name some. Das and Bharghavan [58] imposed the first effect to construct a minimum size virtual backbone in wireless ad hoc networks to disseminate routing information by proposing a distributed algorithm to compute the MCDS in ad hoc networks. The algorithm first selects some nodes based on their nodal degrees, and then uses a minimum spanning tree algorithm to select the necessary connecting nodes to ensure the dominating set computed is connected. Unlike [58], which restricted the CDS to routing information exchange only, Wu *et al.* [222] proposed algorithm to approximate the MCDS, which not only involved in routing information relay, but is also responsible for data forwarding. Therefore, nodes in the obtained MCDS also called gateways. Kim *et al.* [132] proposed two protocols to construct small CDS. The construction procedure not only considers the topology of the network but also takes the energy level at each node into account. Therefore, the protocols can dynamically adapt to the network energy level. In contrast with previous work, we do not aim to provide algorithms to obtain the sub-optimal CDS for a given network instance. Instead of computing the MCDS explicitly, we derive statistics of the cardinality of the MCDS. We consider a single-dimensional stochastic network in this chapter.

It should be noted that one-dimensional (1-D) sensor networks are practically important in reality. For example, there have been proposals for networking cars on main roads

[110] [166] for purposes such as reporting traffic disruptions. Drivers can learn information about congestion and traffic accidents via wireless sensors equipped on their cars. In particular, such information can be acquired by drivers that are far away from the problem sites by repeated relaying through sensors on other cars. Thus drivers can select alternative routes in advance in order to avoid further congesting the road. Another example is the sensors networks monitoring rivers, or deployed along a mountain ridge, which can also be approximated as 1-D networks. Indeed, as shown by Fig. 3.1, if the magnitude of one dimension is much less than that of the other dimension, and it is also much less than the transmission range, a two-dimensional network can be approximated by an one-dimensional network. More importantly, recent research shows that the optimal node placement pattern to achieve both coverage and connectivity in 2-D networks is a strip-based pattern [16], which implies that single dimension results are useful when considering the MCDS asymptotically in 2-D networks.

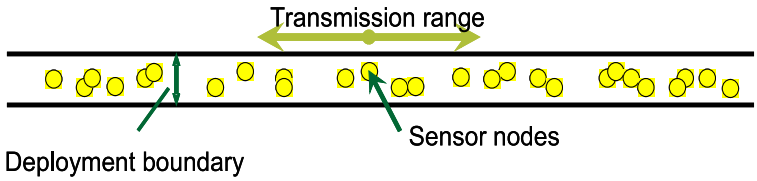

Figure 3.1: Approximation of one-dimensional networks.

To explain why we are interested in a random network, there are several underlying arguments to support it. Indeed, wireless sensor networks are often deployed in inaccessible terrain with a large number of sensor nodes, which prevent them from being placed deterministically. In addition to that, assuming random nodes also models the compulsory randomness in the precise deployment where the available mounting points to deploy (e.g., suitable trees, accessible buildings) sensors are often random. Therefore, random deployment is a widely accepted sensor network implementation scheme and results in the deployed network to pose stochastic characteristics.

Our main contributions are new approaches to computing the distribution and the mean of cardinality of the MCDS, which is not only applicable for 1-D network, but also can be generalized to more practical 2-D cases, as shown in Chapter 4. These results are important because they can be adopted to evaluate the performance of sensor network routing protocols in terms of the least number of nodes involved in routing. Therefore,

they also allude the critical performance measure, network lifetime, in sensor networks.

The rest of this chapter is organized as follow. In Section 3.2, we define our problem and notation first, and then introduce a 1-D network model. We provide simple approaches to obtain the mean of the MCDS cardinality in Section 3.3. A numerical method for the distribution of that cardinality is proposed in Section 3.4. Simulation and numerical results in Section 3.5 show the validity of our assumptions and the effectiveness of our evaluation approaches. Conclusion is drawn in Section 3.6.

3.2 Problem Statement and Network Model

We assume that sensor nodes are randomly and uniformly distributed within an interval in one-dimensional space. A uniform random distribution of sensor nodes is a widely applied assumption, mainly because of its tractability. In fact, there is no unified node distribution pattern due to the variety of sensor network applications and different deployment schemes. However, uniform sensor distribution is an ideal scenario, in which every point in the network has equal probability to be equipped with a sensor node. In addition, uniform distribution can be considered as the steady state of nodes distribution if nodes can move randomly [28]. We study the minimum cardinality of the CDS of this one-dimensional network, which is also the necessary number of nodes involved in the Route Request (RREQ) broadcasting in routing to achieve complete RREQ delivery in the entire network. RREQ is usually used in reactive routing protocols such as DSR [127] for route setup.

In the network we are considering, let the coordinates of the n sensors be $X_1 \leq X_2 \cdots \leq X_n$. The MCDS in a 1-D topology can be found using **greedy** routing. Greedy routing is defined as a routing scheme in which every node involved in data transmission forwards packets to the neighbour that is closest to the destination [209]. In 1-D networks, the resulting hops will have longest length in the direction toward the destination among all possible hops, and so we also call greedy routing *longest hop* routing in this chapter.

This chapter uses the following notation, illustrated in Fig. 3.2

- n — total number of nodes in the network.
- d — total network distance, which is the length of the interval in which all sensor nodes are uniformly distributed.

- r — radio transmission range, which is identical for all the sensor nodes.
- N_{CDS} — the cardinality of a particular CDS.
- N — $\min_{CDS's}(N_{CDS})$.
- $\mathrm{P}(N)$ — probability mass function of N. We will denote $\mathrm{P}_n(N = k)$ as the probability that N takes a particular value k. It is also a function of n.
- C, $\overline{\mathrm{C}}$ — C denotes the event that the network is connected, i.e., there exists at least one path between any pair of sensor nodes; and $\overline{\mathrm{C}}$ is the complement event of C, i.e., network is disconnected.
- L — the network span, $L = X_n - X_1$.
- $F_L(\cdot)$, $F_L(l|\mathrm{C})$ — cumulative distribution function (CDF) of L and the CDF of L conditioning on the network connectivity.
- $f_L(\cdot)$ — probability density function (pdf) of L.
- W_i — the length of the i^{th} hop in greedy routing, in which $i = 1, 2, ..., N + 1$.
- T_i — the residual of i^{th} hop, i.e., $T_i = r - W_i$.
- D_k — sum of the lengths of the first k hops, $D_k = \sum_{i=1}^{k} W_i$.

Variables N, L, W_i, T_i are all random, and are dependent on the random placement of sensors.

We also adopt the commonly used assumption that direct links only exist between any two nodes with straight distance no more than a predefined threshold r, which is the radio transmission range [50] [67] [92]. This may not be the case in some practical situations. However, in addition to its analytical tractability, this model implies a bound if we select r as the smallest value of transmission range. This model is also justified in Chapter 2. Without loss of generality, we normalized all the distance parameters with transmission radius r, therefore, $r = 1$. Therefore, we are virtually applying an unit disk graph to model the network.

We consider networks with a large number of nodes. This ensures that the network is connected with high probability. As it is meaningless to discuss the number of relays if the network is disconnected, a small value of n is not of our interest. In a collation

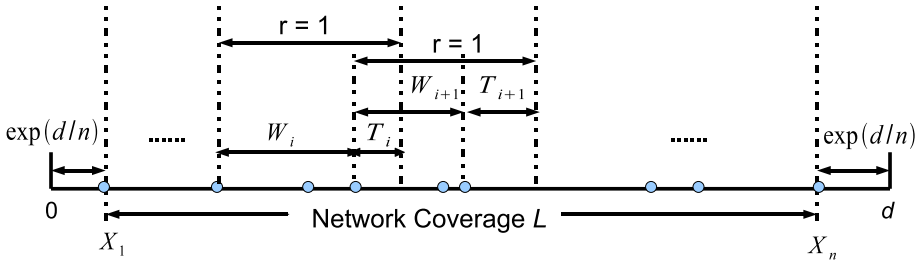

Figure 3.2: Network Model for Poisson Approximation

of n points which are i.i.d. uniformly distributed on $[0, d]$, the spacing between pairs of adjacent points multiplied by n tend to i.i.d. exponential random variables with mean d as $n \to \infty$ [73]. Thus, we model the sensor locations as a 1-D Poisson process. Cheng and Robertazzi [50] studied the expected number of relays in the first connected component in a 1-D Poisson distributed network with infinite length. Our work differs from it as we assume the network with finite length d is connected and obtain the cardinality of the MCDS. As n is large, W_i's, for $i = 1, 2, \ldots, N$ are considered to be approximately i.i.d. random variables. Furthermore, each individual W is approximately independent of N. These approximations are supported by simulation results in Section 3.5, which shows the consolidation of our approximations.

As the following analysis are based on the Poisson approximation, our results will not only apply to uniformly distributed network with large value of n, but are also applicable to networks with all nodes forming a Poisson process, which increases the applicability of our results.

3.3 Mean Number of Relays

In order to evaluate the performance of a given routing protocol in terms of the necessary number of relays to be involved, N, we derive its expectation directly, and its distribution is computed numerically in Section 3.4.

In a system of many nodes that provides a connected network, after each hop there is usually another node "near" the transmission range, and so all hops are only slightly below r. Moreover, these hop lengths are approximately independent. (In the Poisson limit, the length $r - W_{i-1}$ is an exponential random variable truncated by W_i, with the dependence between W_i and W_{i-1} only through this truncation.) Thus, a very coarse estimate is

$$\begin{aligned} E[N] &\approx E[L|\mathrm{C}]/E[W] \\ &\approx E[L]/r. \end{aligned} \tag{3.1}$$

The rest of this section quantifies how much below r the average hop is, refining the second approximation above, and obtains $E[N]$ by studying $E[L|\mathrm{C}]$ and $E[W]$. We first derive the distribution and density functions of the network span (network coverage) L via two different approaches, Poisson approximation and Order Statistics, respectively. Although the Order Statistics approach gives the exact distribution of L while the Poisson approximation is only an approximation, the Poisson approximation shows good agreement with the exact result when the network is dense. More importantly, the Poisson approximation gives insights into the impact of connectivity on the network span under asymptotic situations.

3.3.1 Distribution of Network Span - Poisson Approximation

To quantify the probabilistic properties of L, we introduce the following lemma first.

Lemma 3.3.1. *Consider sensor nodes randomly deployed on a line, forming a Poisson point process with parameter λ. Let n be the number of nodes falling in $[0, d]$. The expected value of the network coverage L, as λ approaches infinity is:*

$$E[L] = d - \frac{2}{\lambda} + O(e^{-\lambda d}), \quad \lambda \to \infty. \tag{3.2}$$

Proof. Let $Z_0 = X_1$ and $Z_n = d - X_n$. Note that they are *truncated* exponentials [1], with

[1] Indeed, in addition to $Z_0 \leq d$ and $Z_n \leq d$, there is still a joint truncation $Z_0 + Z_n \leq d$. However, we ignore the joint truncation as it occurs with very small probability to violate that truncation.

pdf

$$f_Z(x) = \frac{\lambda \exp(-\lambda x)}{1 - \exp(-\lambda d)}, \qquad x \in [0, d]$$

and 0 otherwise, and hence Z_0 and Z_n have mean

$$\begin{aligned} E[Z] &= \frac{e^{\lambda d} - \lambda d - 1}{\lambda(e^{\lambda d} - 1)} \\ &= \frac{1}{\lambda} - \frac{d}{e^{\lambda d} - 1} \\ &= \frac{1}{\lambda} + O(e^{-\lambda d}) \end{aligned} \tag{3.3}$$

for large λ and fixed d. Combining eq. (3.3) with the fact that the network coverage is $L = d - (Z_0 + Z_n)$ gives eq. (3.2). □

Equation (3.2) shows that as λ goes to infinity, $E[L] \approx d - 2/\lambda$, since L is approximately the difference between d and the sum of two exponential random variables each with mean approximately $1/\lambda$. Indeed, if we approximate Z_0 and Z_n as i.i.d. exponential RV's, the probability density function of their sum is the convolution of each individual pdf. As $L = d - (X_1 + X_n)$, which means that L is approximately a linear function of the sum of two i.i.d. exponential RV's. Hence we can approximate the pdf and the CDF of the network coverage L, $f_L(l)$ and $F_L(l)$ as:

$$f_L(l) = \lambda^2(d - l)e^{-\lambda(d-l)}, \qquad l \in [0, d], \tag{3.4}$$

and

$$F_L(l) = e^{-\lambda(d-l)}(1 + \lambda(d - l)), \qquad l \in [0, d]. \tag{3.5}$$

respectively.

The following lemma shows that $E[L|\mathrm{C}]$ is a good approximation to $E[L]$ for dense networks; both of them tend to d, but the difference between $E[L|\mathrm{C}]$ and $E[L]$ is much smaller than the difference between either of them and d.

Lemma 3.3.2. *Consider sensor nodes randomly distributed on a line according to a Poisson point process with parameter λ. Nodes within the required network terrain, which is an interval $[0, d]$, form a sensor network. As λ goes to infinity, the cumulative distribution function of the network coverage, L, and the cumulative distribution function of L conditioned on the network being*

connected satisfy

$$\begin{aligned} F_L(l|\mathrm{C}) - F_L(l) &= O(e^{-\lambda r/2}) \\ &= o(1/\lambda), \quad \lambda \to \infty. \end{aligned} \tag{3.6}$$

In particular, the expectation of L and conditional expectation of L given the connectivity of the network satisfy

$$E[L|\mathrm{C}] - E[L] = o(d - E[L]), \quad \lambda \to \infty. \tag{3.7}$$

Proof. To show eq. (3.6), note that

$$\begin{aligned} & F_L(l|\mathrm{C}) - F_L(l) \\ = \; & F_L(l|\mathrm{C})\mathrm{P}(\mathrm{C}) + F_L(l|\mathrm{C})\mathrm{P}(\overline{\mathrm{C}}) - \left[F_L(l|\mathrm{C})\mathrm{P}(\mathrm{C}) + F_L(l|\overline{\mathrm{C}})\mathrm{P}(\overline{\mathrm{C}})\right] \\ = \; & \left[F_L(l|\mathrm{C}) - F_L(l|\overline{\mathrm{C}})\right]\mathrm{P}(\overline{\mathrm{C}}). \end{aligned} \tag{3.8}$$

The factor in brackets is bounded above by $1 = O(1)$. To bound $\overline{\mathrm{C}}$, partition $[0, d]$ into $2d/r$ intervals, each of length at most $r/2$. A sufficient condition for the network to be connected is that each interval has at least one node, which occurs with probability at least $(1 - e^{-\lambda r/2})^{2d/r}$. Thus $\mathrm{P}(\overline{\mathrm{C}}) = O(e^{-\lambda r/2})$ for large λ and fixed r, d.

Equation (3.7) is proved in a similar way

$$\begin{aligned} & E[\,l|\mathrm{C}] - E\,[\,l\,] \\ = \; & E[\,l|\mathrm{C}]\mathrm{P}(\mathrm{C}) + E[\,l|\mathrm{C}]\mathrm{P}(\overline{\mathrm{C}}) - \left[E[\,l|\mathrm{C}]\mathrm{P}(\mathrm{C}) + E[\,l|\overline{\mathrm{C}}]\mathrm{P}(\overline{\mathrm{C}})\right] \\ = \; & \left[E[\,l|\mathrm{C}] - E[\,l|\overline{\mathrm{C}}]\right]\mathrm{P}(\overline{\mathrm{C}}). \end{aligned} \tag{3.9}$$

The term within brackets is bounded by a constant, hence it is $O(1)$, and $\mathrm{P}(\overline{\mathrm{C}}) = O(e^{-\lambda r/2})$ from previous result. Also, note that $d - E[L] = 2/\lambda + o(1/\lambda)$ from Lemma 3.3.1, giving eq. (3.7). □

3.3.2 Distribution of Network Span - Order Statistics Approach

We can also derive the pdf of L explicitly via order statistics approach. As all the sensor nodes are i.i.d. uniformly distributed in the interval $[0, d]$, and $L = X_n - X_1$. Therefore, the joint pdf of X_1 and X_n, $f_{X_1,X_n}(x, y)$, is given by

$$f_{X_1,X_n}(x,y) = n(n-1)\left(\frac{y-x}{d}\right)^{n-2}\left(\frac{1}{d}\right)^2, \quad 0 \le x \le y \le d. \tag{3.10}$$

In fact, the event that X_1 and X_n fall into infinitesimal intervals $x < X_1 < x + \mathrm{d}x$ and $y < X_n < y + \mathrm{d}y$ simultaneously is equivalent to the event that $n-2$ nodes fall into the interval $[x, y]$, while there are $(n)_n$, which is the permutation number of 2 out of n, choices to form X_1 and X_n.

Substituting X_1 by $X_n - L$ in eq. (3.10) and integrating it over X_n from l to d yields the pdf of L, which is

$$\begin{aligned} f_L(l) &= \int_l^d f_{X_1,X_n}(y-l,y)\mathrm{d}y \\ &= \int_l^d n(n-1)\left(\frac{l}{d}\right)^{n-2}\left(\frac{1}{d}\right)^2 \mathrm{d}y \\ &= n(n-1)\left(1-\frac{l}{d}\right)\left(\frac{l}{d}\right)^{n-2}\left(\frac{1}{d}\right), \end{aligned} \tag{3.11}$$

for $0 \le l \le d$. The integration limits are determined as X_n must be larger than L but less than d.

The CDF of L can be derived from eq. (3.11) as

$$F_L(l) = n\left(\frac{l}{d}\right)^{n-1} - (n-1)\left(\frac{l}{d}\right)^n, \quad \text{if } 0 \le l \le d. \tag{3.12}$$

With density function (3.11) of L, the expectation of L can be easily obtained, which is

$$\begin{aligned} E[L] &= \int_0^d t f_L(t)\mathrm{d}t \\ &= \left[n-1-\frac{n(n-1)}{n+1}\right]d \\ &= \frac{n-1}{n+1}d \end{aligned} \tag{3.13}$$

3.3.3 Properties of Hop Length

The number of relays, or the number of hops, is not only affected by the network span, but is also influenced by the hop length W. This section drives the distribution of W's. We consider a sensor network with sensor nodes forming a Poisson point process with parameter λ on a line. Let W_0 be equal in distribution to the random hop length in the

longest hop routing scheme, for any but the last hop. The CDF and pdf of W_0 can be approximated by

$$F_{W_0}(t) \approx 1 - \frac{1 - \exp\left[-\lambda(r-t)\right]}{1 - \exp(-\lambda r)}, \quad 0 < t \leq r, \tag{3.14}$$

and

$$f_{W_0}(t) \approx \frac{\lambda \exp\left[-\lambda(r-t)\right]}{1 - \exp(-\lambda r)}, \quad 0 < t \leq r, \tag{3.15}$$

respectively.

The expectation of W_0 is:

$$\begin{aligned} E[W_0] &\approx \frac{1}{1 - \exp(-\lambda r)} \left[r - \frac{1}{\lambda} + \frac{1}{\lambda} \exp(-\lambda r) \right] \\ &= \frac{r}{1 - \exp(-\lambda r)} - \frac{1}{\lambda}. \end{aligned} \tag{3.16}$$

Equation (3.14) is only strictly true for the first hop W_1, which is proved in [108]. In fact, for other hops W_i, $i = 2, 3, \ldots, N$, the distribution of $r - W_{i-1}$ is truncated by W_i. However, this dependence is negligible for large n (i.e., large λ). Therefore, in a Poisson point process with large λ, we consider the i^{th} hop, where $i \leq N$, the distance between the next hop relay to the transmission range limit, denoted by $T_i = r - W_i$, has an exponential distribution with parameter λ, except that, T_i is less than or equal to the transmission range r, thus it follows a truncated exponential distribution, with the cumulative distribution function

$$F_T(t) \approx \frac{1 - \exp(-\lambda t)}{1 - \exp(-\lambda r)}, \quad 0 < t \leq r \tag{3.17}$$

which leads to eqs. (3.14) and (3.15), hence eq. (3.16) follows.

For $r \ll N/\lambda$, the expected length of the last hop is half the expected length of the other hops, since the destination will be approximately uniformly distributed within the maximum possible range of the last hop. Thus

$$E\left[NW_0 + W_0/2\right] \approx E\left[L\right]. \tag{3.18}$$

Lemma 3.3.2 implies that it is reasonable and accurate to replace $E[L|\mathrm{C}]$ with $E[L]$ when compute the $E[N]$ via eq. (3.1) for dense networks. The basic idea of above lemmas is as follows. A dense network in which nodes follow a Poisson process is highly likely to be connected. So we can use the network span $X_{(n)} - X_{(1)}$, to approximate the coverage of a connected network, $E[L]$ can serve as an accurate approximation of $E[L|\mathrm{C}]$. Therefore, combining eq. (3.18) with eqs. (3.2) and (3.16) gives

$$E[N] \approx \frac{d - 2/\lambda + 2\exp(-\lambda)/\lambda}{r/\left[1 - \exp(-\lambda)\right] - 1/\lambda} - \frac{1}{2} \tag{3.19}$$

$$\approx \frac{d - 2/\lambda}{r - 1/\lambda} - \frac{1}{2}. \tag{3.20}$$

neglecting terms of $O(e^{-\lambda})$.

3.4 Distribution of Relay Number

In this section, we propose an approach to compute the distribution of N numerically. In order to derive the distribution of N, we have the following proposition, which is a straightforward result of the law of total probability.

Proposition 3.4.1. *Consider sensor nodes randomly deployed according to Poisson process with parameter λ in 1-D space, forming a connected sensor network. Let n be the Poisson distributed number of nodes in the network terrain $[0, d]$. The probability mass function of the cardinality of the MCDS of this network, $P(N = k - 1)$, is given by:*

$$\mathrm{P}(N = k - 1) = \int_0^d \mathrm{P}(N = k - 1 | L = l) f_L(l)\, dl. \tag{3.21}$$

The following proposition derives the probability that $N = k - 1$ given that the network coverage is l, $\mathrm{P}(N = k - 1 | L = l)$.

Proposition 3.4.2. *In 1-D space, if all nodes are randomly deployed forming a Poisson process with parameter λ and the resulting network is connected, then the conditional probability that the cardinality of the MCDS is $k - 1$, given the network coverage l, is*

$$\mathrm{P}(N = k - 1 | L = l) = \mathrm{P}(D_{k-1} < l) - \mathrm{P}(D_k < l), \quad 0 < l < d \tag{3.22}$$

where $D_k = \sum_{i=1}^{k} W_i$, is the sum of length of the first k hops.

Proposition 3.4.2 follows because the event $D_{k-1} < l$ is equivalent to the union of two mutually exclusive events: $D_k < l$, or $D_{k-1} < l$ while $D_k \geq l$.

We can approximately compute $\mathrm{P}(D_{k-1} < l)$ by numerical inversion of Laplace transform, as $D_k = \sum_{i=1}^{k} W_i$, and W_i's can be approximated by i.i.d. RV's with pdf given by eq. (3.15).

The Laplace transform of (3.15) for $r = 1$ is

$$\mathcal{L}(f_W(t)) = \frac{\lambda \exp(-\lambda)}{1 - \exp(-\lambda)} \left[\frac{\exp(\lambda - s) - 1}{\lambda - s} \right]. \tag{3.23}$$

As the pdf of D_k is a k fold convolution of $f_W(t)$, by transform method, we can obtain the Laplace transform of pdf of D_{k-1}, which denote as $\mathcal{L}(D_{k-1})$ to be given by

$$\mathcal{L}(D_{k-1}) \quad = \quad \left[\frac{\lambda \exp(-\lambda)}{1 - \exp(-\lambda)} \right]^{k-1} \left[\frac{\exp(\lambda - s) - 1}{\lambda - s} \right]^{k-1}. \tag{3.24}$$

Numerical inversion of (3.24) yields the pdf of D_{k-1} and D_k, denote as $f_{D_{k-1}}(x)$ and $f_{D_k}(x)$, which lead to $\mathrm{P}(D_{k-1} < l)$ and $\mathrm{P}(D_k < l)$ where the probability that $D_{k-1} = l$ and $D_k = l$ are ignored as they are zero for continuously distributed nodes.

Combine eqs. (3.4), (3.22) and (3.24), by (3.21), we can numerical compute the probability mass function of N.

For networks with uniformly distributed nodes, if n is large, we adopt Poisson approximation yielding $n \approx E(n) = \lambda d$, which enables the above approach to compute the distribution of N.

3.5 Numerical Results and Model Validation

To verify our preliminary assumptions that $W's$ are approximately independent of each other in dense sensor network, as well as are independent of N, we conduct 10^5 Monte Carlo simulation for $n = 25, 30, ..., 500$, in a network with all nodes uniformly distributed within $[0, 12]$ and $r = 1$. For each network instance, we obtain the values of $W's$ and N, and compute their Correlation Coefficients (CC)

Although Chi-square test is a more general methodology to test the independence of random variables, we compute the correlation coefficients to demonstrate the independence, mainly because the dependence between W_{i-1} and W_i only through the truncation

of W_i to T_{i-1}, which leads to the negative correlation between W_{i-1} and W_i. Correlation coefficients between different $W's$, and between $W's$ and N are computed. Results are shown in Fig. 3.3 and Fig. 3.4. It is clear in Fig. 3.3 that the correlation coefficients between different $W's$ become closer to zero as the number of nodes n increases as we expected. The dotted line shows that the correlation coefficient between the length of first hop W_1 and the length of the last hop W_{last} is small when n is small, which is different from other curves. This comes from the border effect of W_{last}. The standard deviation of W_{last} could be large when n is small, results in a small correlation coefficient. In Fig. 3.4, as we expected, N and $W's$ pose negative correlation and the correlation coefficients approach zero as n increasing. The magnitude of the correlation coefficient between N and W_3 (shown with triangles) starts with a small value when n is small, increases with n when n is not too large, and then approaches zero as n becomes large. This phenomenon can be explained by the following argument. When n is small, the correlation between $W's$ and N is high, however, the variances of $W's$ and N are also large, which produce a relative small correlation coefficient. As n increasing, strong correlation between $W's$ and N still exists, while the variances of $W's$ and N become small, which generate large correlation coefficients. As n keep increasing larger and larger, variances of $W's$ and N, and dependence between them are very small, stated by small values of correlation coefficients, in terms of magnitude. So our assumptions are valid for large n.

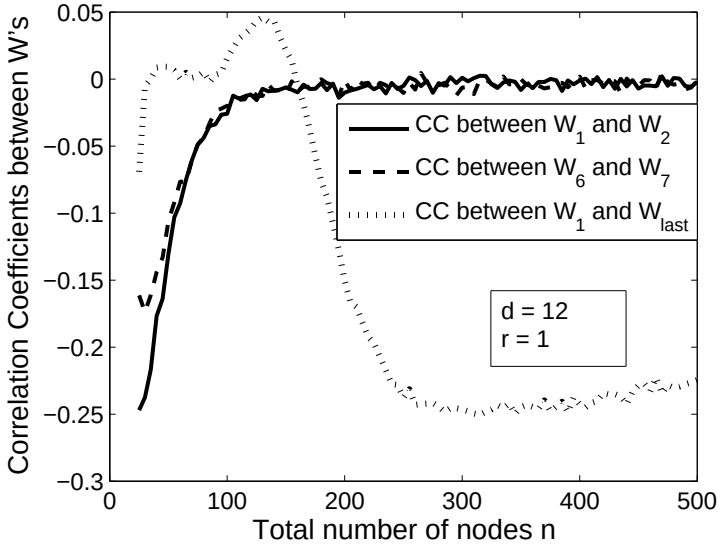

Figure 3.3: Simulation results for Correlation Coefficients (CC) between W's

To show Lemma 3.3.2, and verify eq. (3.12), Fig. 3.5 and Fig. 3.6 demonstrate the

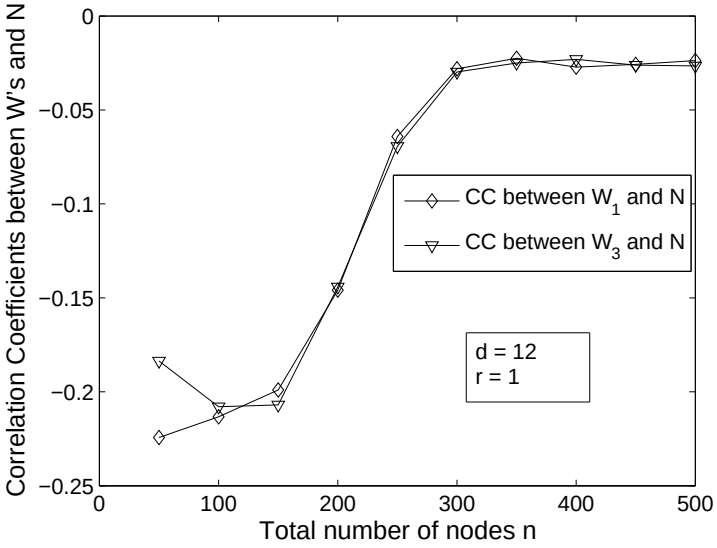

Figure 3.4: Simulation results for Correlation Coefficients (CC) between W's and N

comparison of CDF of the network coverage given by eq. (3.5) and eq. (3.12), and the network coverage conditioning on the network connectivity obtained by simulations, for a network that all nodes are uniformly distributed within interval $[0, 12]$, other parameters are indicated in the graph. Solid lines in the graphs represent the analytical CDF obtain from eqs. (3.5) and (3.12), while the markers demonstrate the simulation results. We can see from the figure that for a network with normalized total distance $d = 12$, both eq. (3.5) and eq. (3.12) demonstrate good agreement with simulation results when the number of nodes n is high, which is as expected. Moreover, both Fig. 3.5 and Fig. 3.6 show that for large n and same values of CDF, the difference between argument of CDF, which is the network span, is less than one radio-range. The observation reveals that the distribution of N is highly concentrated on its expected value, and is not so important in practice. Thus the more interesting case is the MCDS in two dimensional networks, which is the topic of the next chapter.

Furthermore, Fig. 3.7 compares the CDF of L obtained from eq. (3.12) and (3.5). Notice that eq. (3.12) gives us the exact solution of F_L, we can see that eq. (3.5) over-estimates the CDF of L. This is because the derivation of (3.5) approximate two truncated exponential RV's X_1 and $d - X_n$ by exponential RV's on infinite support. However, as shown in Fig. 3.7, the difference can be ignored. This also consistent with our theory since the Poisson Approximation is only valid when n is large. We also verify eq. (3.14), by measuring the CDF of the lengthes of the first hop W_1 and the seventh hop W_7, as examples, in networks

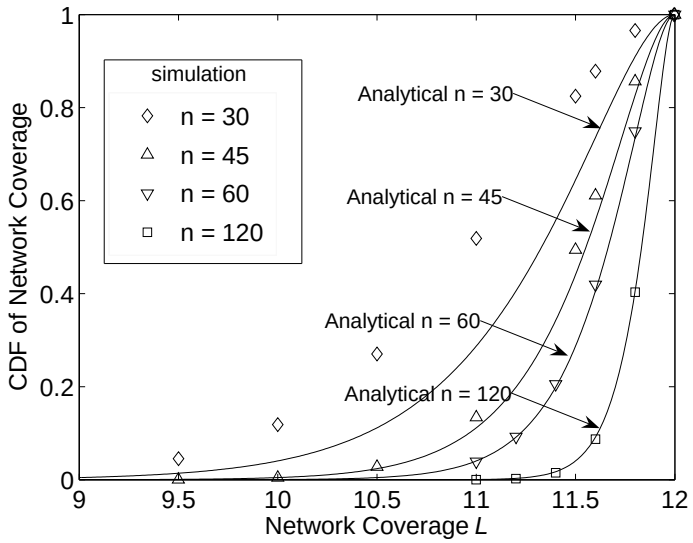

Figure 3.5: Comparison of analytical (equation (3.5)) and simulation results for CDF of the network coverage

with same total distance and transmission range, but $n = 90$ and $n = 60$ respectively. It can be seen that eq. (3.14) predicts W_i with reasonable accuracy in probabilistic sense, as shown in Fig. 3.8 and 3.9.

The algorithm to do the numerical inversion of (3.24) is based on Abate's algorithm [4], which is essentially a Fourier-series method, and the discretization error is bounded by $\frac{\exp(-8\ln(10))}{1-\exp(-8\ln(10))} \approx 10^{-8}$ according to the parameters we selected in the algorithm.

To demonstrate the accuracy of our approaches to obtain the mean and the pmf of N, we do 10^6 Monte Carlo simulation for $d = 12$, $n = 60, 100, 140, 180, 200$, obtain the expected value of minimum number of relays nodes that maintain the whole network coverage, comparing with the analytical results calculated by eq. (3.20). It can be seen that good agreement is achieved between simulation and analytical results, from Fig. 3.10.

As the number of nodes n goes large, it is with increasing probability that the minimum number of nodes equal to the ceiling of d/r, i.e., $E[N] \to \lceil d/r \rceil$ as $n \to \infty$, as the example obtained from simulation shown in Fig. 3.10. In Fig. 3.11, we compare the simulation results of probability mass function of N and the analytical result given by eq. (3.21). For $n = 90$, $d = 12$ and $r = 1$, 10^5 monte carlo simulations yield the empirical pmf of N. Filled circles represent analytical results while empty circles for simulation results. This example illustrates that our approach provides an acceptable accuracy level.

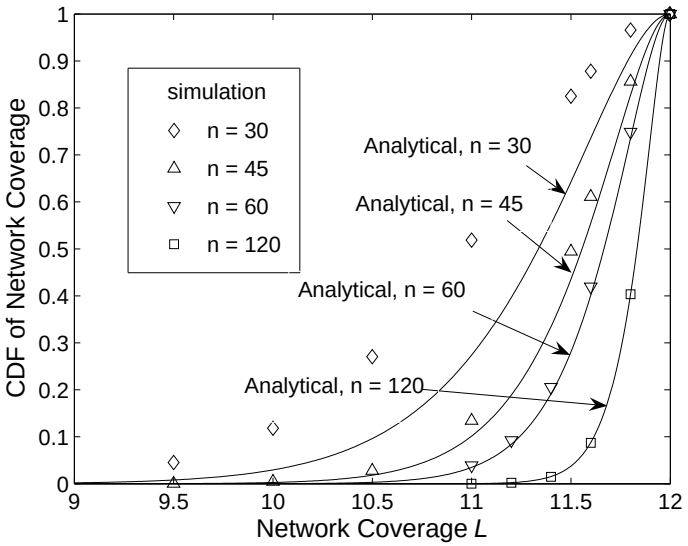

Figure 3.6: Comparison of analytical (eq. (3.12)) and simulation results for CDF of the network coverage

3.6 Conclusion and Discussion

In this chapter, we have shown that for a one-dimensional sensor network with n i.i.d. uniformly distributed nodes, the cardinality N of the MCDS can be evaluated probabilistically. We have derived its expectation, $E[N]$, and computed its distribution, numerically. The expectation and the distribution obtained imply important measures to evaluate existing and potential ad hoc network routing protocols, especially for strictly energy constrained sensor networks.

The classic result that a point process with all n points i.i.d. uniformly distributed can be well approximated by a Poisson process as n goes large was adopted, which enabled our results to be valid for networks with nodes have either uniform or Poisson distributions. The approaches used in this chapter were based on the evaluation of the margin between the ideal hop length and the actual hop length of each hop. This is possible because a one-dimensional network only requires a route that forms a line. However, for more practical two-dimensional networks, our approaches require to be modified in order to evaluate the cardinality of the MCDS, since there may be multiple routes among a pair of source-destination nodes.

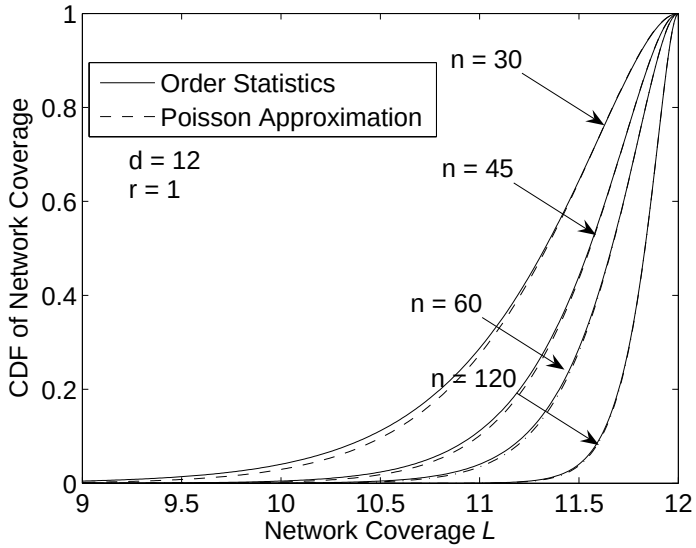

Figure 3.7: Comparison of F_L obtained from Poisson Approximation and Order Statistics

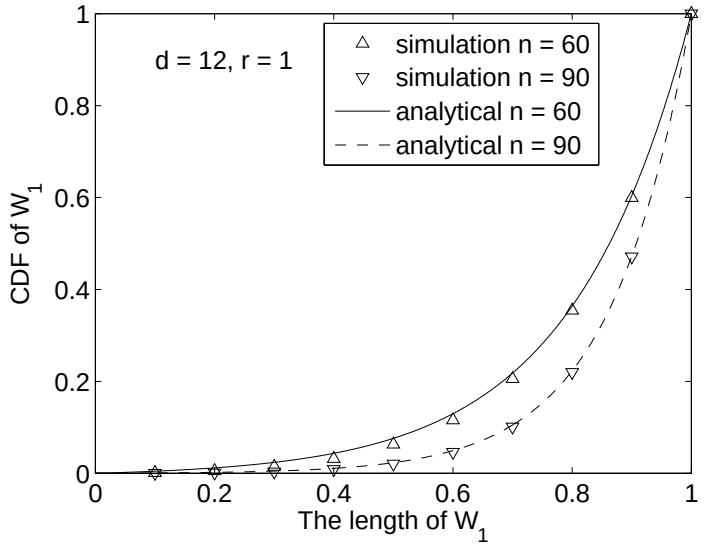

Figure 3.8: CDF of length of the first hop W_1

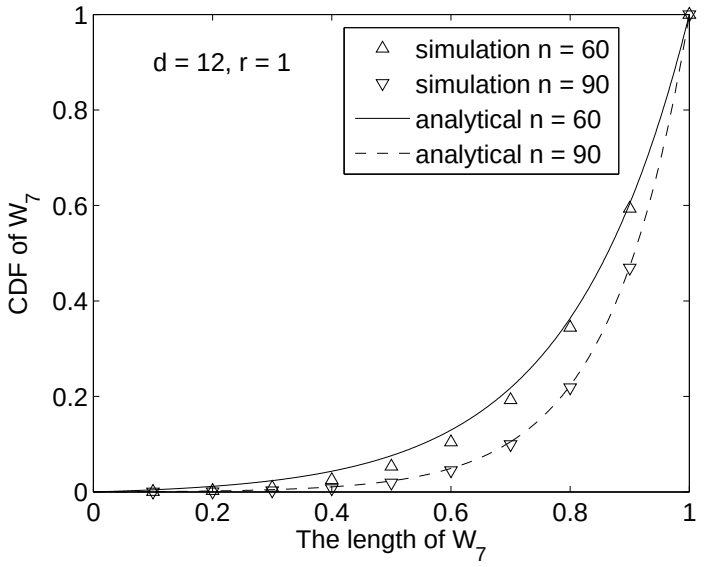

Figure 3.9: CDF of length of the 7th hop W_7

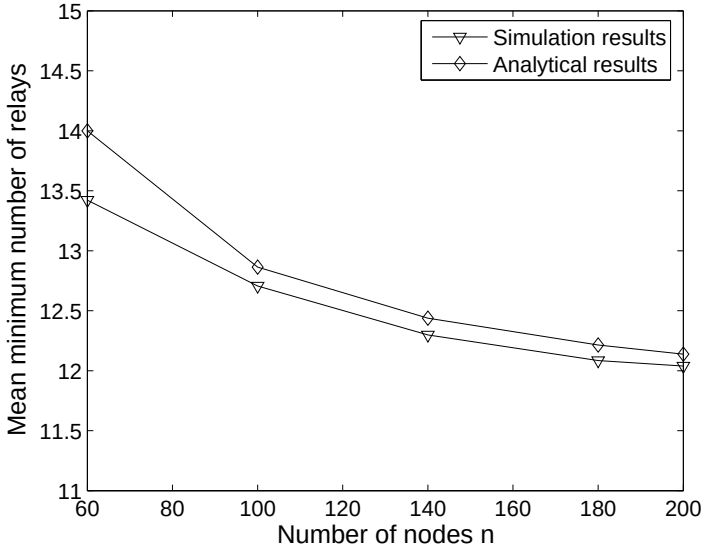

Figure 3.10: Comparison of analytical and simulation results for expected minimum number of relays

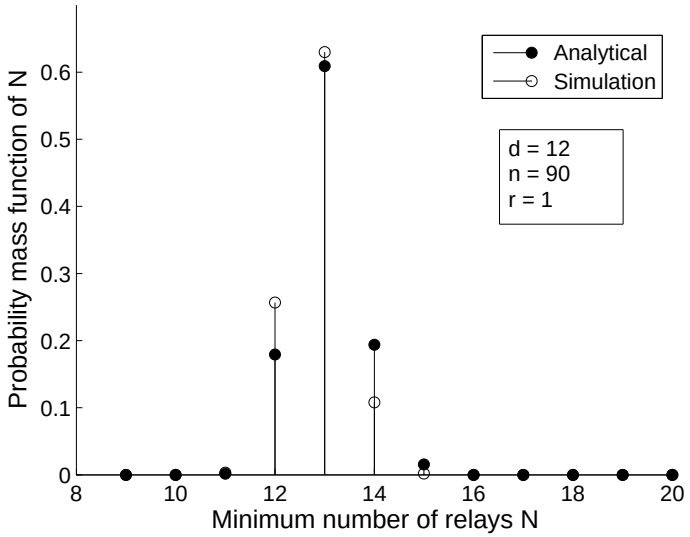

Figure 3.11: Probability mass function of N

Chapter 4

Minimum Connected Dominating Sets in 2-D Dense Wireless Sensor Networks

4.1 Introduction

In Chapter 3, we investigated statistics of the cardinality, N, of the MCDS for one-dimensional dense sensor networks. In this chapter, we extend this, and evaluate the cardinality of the MCDS in two-dimensional dense networks. Based on our evaluation approaches, we also propose a new algorithm, the Incremental Coverage Algorithm (INCOA), to construct small sub-optimal dominating sets to approximate small CDS. Dense networks are of interest because the sensing radius r_s of each node could be much smaller than the communication range r [1] [2] [3], which results in a high nodal degree for a sensor network.

The MCDS plays an important role in facilitating efficient network operations, because performing data aggregation at nodes in the MCDS and restricting packet relaying to only those nodes in the MCDS can reduce the traffic when broadcasting is initiated. This also enables us to turn off as many inactive nodes as possible, hence reducing the energy consumption. Under this situation, the MCDS is essentially a virtual backbone in the networks, and this virtual backbone can greatly reduce the network traffic. It is clear that light traffic results in less congestion, especially in dense networks, and consequently, less energy consumption.

In addition to the consideration of energy saving, reducing the number of active nodes for relaying is also a requirement of improving the throughput of the network, as the transmission of multiple sensor nodes in dense networks can lead to severe interference. Therefore, establishing a virtual backbone, which contains a small set of nodes that are in active mode, is an attractive solution for multi-hop routing in sensor networks.

Constructing the MCDS for a network is an effective approach to establishing such a virtual backbone. As computing the MCDS in a given network is known to be NP-

hard [78], only heuristics, which construct a sub-optimal CDS, are efficient for general networks. Existing heuristic algorithms include Alzoubi, Wan and Frieder [10], Butenko *et al.* [37], Das and Bharghavan [58], Guha and Khuller [89], Ou *et al.* [172], Sanchis [192], Wu and Li [223], and the references therein. A brief introduction to these algorithms is given in Chapter 2.

Most existing CDS construction algorithms are specifically designed for ad hoc networks, and hence they are not scalable for sensor networks, which may contain hundreds or even thousands of sensor nodes. One such an example is a sensor network for military surveillance. Since this network needs to provide a high level robustness and fault tolerance [207], it may contain a large number of sensors. Constructing virtual backbones in such networks could be very complicated, in terms of both time complexity and message complexity. In this chapter, we also propose a new algorithm, which can efficiently construct a dominating set to approximate a small connected dominating set in dense networks.

This chapter is organized as follows. In Section 4.2, we review some existing work related to the asymptotically optimal results for the MCDS problem. A formal statement of our research problem is given in Section 4.3. We evaluate the expectation of the cardinality of the MCDS in Section 4.4, and propose our algorithm in Section 4.5. Numerical and simulation results are shown in Section 4.6. We conclude this chapter in Section 4.7.

4.2 Background and Related Work

In this chapter, we are considering a network in which every single point in the sensing field is within the connectivity range of some relay nodes. Therefore, we define a finite dense sensor network as a finite network in which the spacing between sensor nodes is very much less than the transmission range.

One related problem is the integrated consideration of network connectivity and sensing coverage, the so called connectivity-coverage problem [215]. This problem arises because in sensor networks, it is desirable that events should be detected wherever they occur as long as it is within the sensing field, while at the same time, the network should be connected such that the occurrences of events can be reported to control centres. Hence any location where events may occur should be within the sensing range of some sensors, and sensors should be able to communicate with each other. The connectivity-coverage

problem aims to arrange the minimum number of sensors such that these two requirements can be satisfied simultaneously.

The connectivity-coverage problem is still an open problem for general networks. However, some understandings and the asymptotically optimal result, which solved the connectivity-coverage problem for a network in an infinite plane, were obtained. Wang *et al.* [215] proposed the concept of connectivity-coverage, and analysed the relationship between connectivity and coverage. They proved that a network is connected whenever its sensing field is fully covered, if the transmission range r is at least twice of the sensing range r_s, i.e., $r \geq 2r_s$. A coverage configuration algorithm was proposed which can provide a different degree of coverage for networks with $r \geq 2r_s$. That is, each point can be ensured to be covered by multiple sensors. Zhang and Hou [230] proved the same result for the relationship between r and r_s with a different approach. They also reproved Kershner's classical result [130] that the optimal pattern in terms of the number of nodes to achieve full coverage under asymptotic scenario is placing sensors on the vertices of an equilateral triangular lattice by minimizing the overlapped sensing area. The approach is different from that in [130], in which geometric analysis was adopted. For the case $r = r_s$, Iyengar, Kar and Banerjee [125] showed that a strip-based deployment pattern is near optimal for an infinite network, but without a rigorous proof. Iyengar *et al.*'s asymptotically optimal layout is shown in Fig 4.1. Sensors are deployed in equally spaced horizontal strips. In each strip, adjacent sensors have spacing r between them. Adjacent strips are a distance $(1 + \sqrt{3}/2)r$ apart. One vertical rib of sensors is used to connect sensors in different strips. Bai *et al.* [16] improved Iyengar *et al.*'s results by proving that the strip-based deployment pattern is asymptotically optimal, not only when $r = r_s$, but also for $r \leq \sqrt{3}r_s$. Furthermore, they also proved the optimality of a slightly different strip-based layout, which can achieve full coverage and 2-connectivity, for an arbitrary ratio of r/r_s. This deployment layout could be advantageous to the network reliability.

The connectivity-coverage problem is related to our 2-D MCDS problem in the following sense. For the MCDS problem, we aim to minimize the size of the virtual backbone, subject to the constraint that all the nodes are within the transmission range r of at least one node in the backbone. For an asymptotically dense network, the constraint becomes that every point in the sensing field is within the distance r of some nodes in the backbone, so that events which occur there can be reported to at least one relay node. As relay nodes in the backbone are connected, eventually these events can be reported to

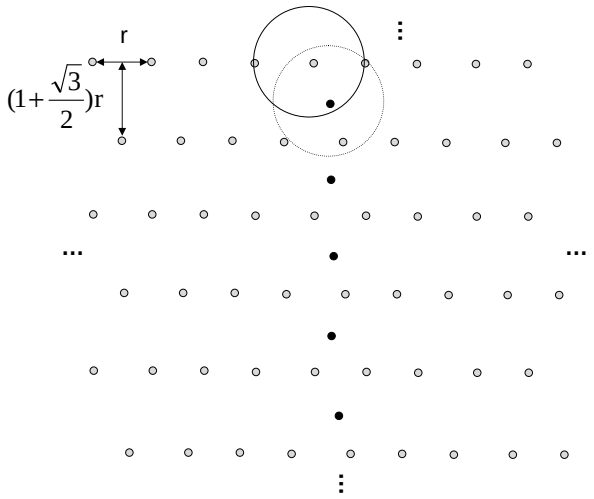

Figure 4.1: Asymptotically optimal pattern for achieving both connectivity and coverage, $r = r_s$

data collection centres. Therefore, the backbone itself is a connected sensor network that can be reached from arbitrary points in the sensing field. Hence, solving the minimum virtual backbone problem for an asymptotically dense network is mathematically equivalent to solving the asymptotic coverage-connectivity problem with $r_s = r$, which also tries to minimize the set of nodes that are connected while every point within the sensing field is under surveillance. The deployment pattern for this asymptotically optimal solution is shown in Fig. 4.1. According to our previous discussion, if there are sensor nodes on those positions in Fig. 4.1, those sensors form the MCDS under the asymptotic scenario. Hence we call those positions asymptotically optimal positions. Under this pattern, the optimal sensor node density (in the context of connectivity-coverage problem), λ_o, is given by [125]

$$\lambda_o = \frac{1}{(\frac{\pi}{3} + \frac{\sqrt{3}}{2})r^2} \approx \frac{1}{1.914r^2}. \tag{4.1}$$

Note that the sensor nodes in the context of connectivity-coverage problem correspond to the relays for the MCDS problem.

Although this asymptotically optimal solution for the MCDS problem is known, it cannot be applied to practical problems directly. In a realistic situation, sensor networks always contain a finite number of sensor nodes within a finite area. Furthermore, the probability that there exists a sensor node on an arbitrary point is zero for a network that is randomly deployed, no matter how dense it is. Thus the real interesting problem is: what is the cardinality of the MCDS in a large, finitely dense sensor network? How can

we find such an MCDS efficiently? We aim to answer the questions in this chapter.

4.3 Problem Description

We define our network model first. We consider a random network in a $d \times d$ square area. There are n sensor nodes, which are i.i.d. uniformly distributed in this network area, each with isotropic transmission range r. We assume d is large compared to r. We also assume that the average nodal degree $\pi r^2(n/d^2)$ is large. Therefore, the network scenario we are investigating is a large dense sensor network. We aim to obtain the expectation of the cardinality of the MCDS, $E[N]$, for this network. We are also interested in developing efficient algorithms to construct the MCDS for such a network.

As we study dense networks, by similar reasons for 1-D scenario, we approximate the spatial point process formed by the positions of all the sensor nodes by a spatial Poisson point process, with intensity $\lambda = n/d^2$. We also normalized all the distance parameters by the transmission range r, which leads to $r = 1$. From now on, all distance-related parameters, e.g., λ and d, are normalized. With the above setting, $\pi\lambda$ represents the average nodal degree, which is the average number of nodes within the radio range of a single node.

As mentioned before, under the asymptotic situation, one MCDS is a set of nodes that are aligned as the strip-based pattern. However, in practical situations, the probability of having a node on each asymptotically optimal position is zero. We can select the nodes that are closest to each asymptotically optimal position as relay nodes. However, they may not form a CDS. Nodes in the relay set may not connect to each other, or some ordinary nodes may not be able to connect to any relay. Hence we may need extra nodes in addition to that relay set.

4.4 Problem Formulation

To obtain the MCDS by exploiting the asymptotically optimal solution, we adopt a modified spacing approach, which tries to find the MCDS according to the strip-based pattern, but with a different spacing parameter. We described the approach as follows. In the asymptotically optimal pattern, the ideal spacing parameter is r for nodes in a common horizontal strip, and $(1 + \sqrt{3}/2)r$ for two adjacent horizontal strips. However, the strip-

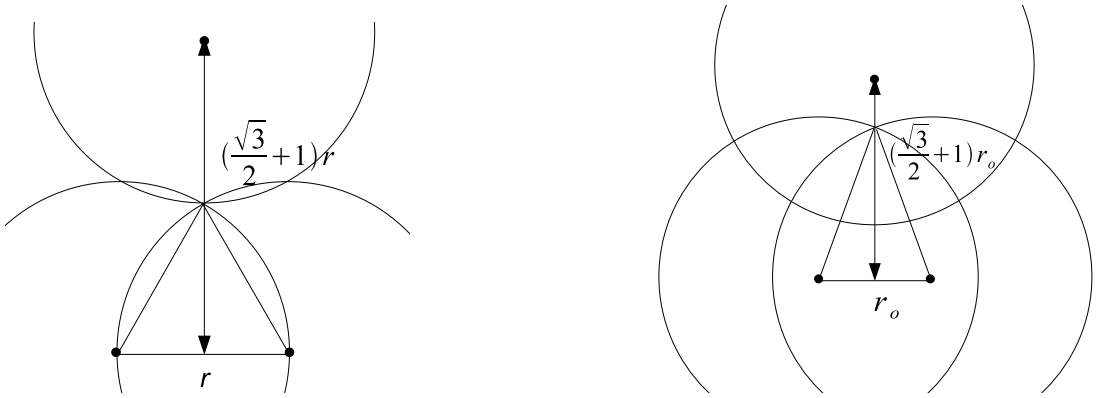

(a) Asymptotic optimal pattern (b) Modified spacing pattern

Figure 4.2: Three node pattern

based asymptotic pattern is only applied to an infinitely dense network. For a finitely dense network, we try to utilize a modified value $r_o < r$, which gives a margin to tolerate the randomness in the nodes positions, such that the relay set produced can form a CDS, though they may not exactly be on the positions expected.

We demonstrate our approach through a three node example in Fig. 4.2. In this illustration, we only show three nodes which are adjacent to each other in adjacent horizontal strips. Figure 4.2(a) is the asymptotically optimal pattern in which the spacing between consecutive relays in a horizontal strip is r, and the distance between two adjacent horizontal strips is $(\frac{\sqrt{3}}{2}+1)r$. Figure 4.2(b) shows the modified spacing pattern in which r is replaced by r_o.

We define some terminology first. We call the positions in the asymptotically optimal pattern the *asymptotically optimal positions*. According to some rules (discussed later), the asymptotically optimal pattern can be transformed and hence applied to finite networks by using the modified spacing parameter r_o. We call the expected position of relays in this finite transformation of the asymptotically optimal pattern the *nominal position* of relays. Each nominal position corresponds to a relay, which is the closest node to that nominal position, so called a *nominal relay*. We denote the number of nominal relays by N_1. Note that nominal relays will not generally be exactly at nominal positions. We call the position of nominal relays the *actual position*. In Fig. 4.2(b), we can see that there is an intersection or an overlapping area among the three discs representing the transmission coverage of each node. If such an intersection does not exist, for a given set of three *actual positions*,

there is a gap between the three transmission ranges and nodes within that gap cannot connect to those three nominal relays. Under that situation, we need an additional relay, called a *filling relay*, wherever the transmission areas of the three actual relays do not have an intersection. We denote the number of filling relays by N_2. Hence the cardinality of the CDS, N_{CDS} is approximately the sum of N_1 and N_2, i.e., $N_{CDS} \approx N_1 + N_2$. We want to find the particular r_o, denoted by r_{om}, such that the expected value of N_{CDS} is minimized. Therefore, our problem can be mathematically formulated as the following optimization problem

Objective:

$$\min_{r_o} \quad E\left[N_{CDS}\right] \approx E\left[N_1\right] + E\left[N_2\right], \tag{4.2}$$

given r, n and d. With the normalization of $r = 1$, both N_1 and N_2 are functions of r_o.

The following section proposes an approximation to compute the optimal solution of (4.2), $r_{om} = \arg\min E[N_{CDS}]$.

4.4.1 Approximation of the Cardinality of the MCDS

As mentioned in the previous section, the asymptotically optimal pattern is only applied to an infinitely dense network. We need to do some transformation of the asymptotically optimal pattern, such that it can be applied to a finite dense network. We describe the rules of the transformation as follows.

In a square network with a $d \times d$ sensing field, as the network is finite, in order to cover the upper-left corner of the sensing field, there should be a relay on the position that has distance r_o to the upper-left corner. We let the nominal position of this relay on the location that has distance r_o to the upper-left corner, and the angles between the segment line connecting the upper-left corner and the nominal position to both the vertical and the horizontal edges to be 45 degree, as shown in Fig. 4.3. The black dot in Fig. 4.3 is the nominal position. Once we have this first nominal position, the nominal positions for the rest of nominal relays can be determined according to the modified asymptotically optimal pattern, in which adjacent nodes in a single horizontal strip have distance r_o, and adjacent horizontal strips have distance $(1 + \sqrt{3}/2)r_o$.

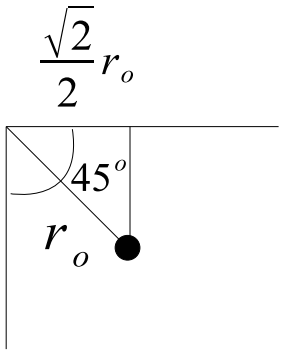

Figure 4.3: Illustration of the nominal position of the upper-left relay.

4.4.2 Expected Number of Nominal Relays

In order to solve (4.2), we first express $E[N_1]$ as a function of r_o. For a $d \times d$ network, given d and r_o, N_1 is deterministic, and is independent of λ. Hence we have $E[N_1] = N_1$. We call a horizontal strip of nodes a row. Denote the number of rows by $\mathbf{H}$, and the number of nominal positions in the vertical rib by Δ_1. Geometrical analysis yields N_1 approximately

$$N_1 \approx \left[\frac{d - r_o/\sqrt{2}}{r_o}\right] \times \mathbf{H} + \Delta_1. \tag{4.3}$$

Equation (4.3) can be explained as follows. Since the network area is finite, relays are expected to be on the nominal positions whose pattern was described in the previous section. The nominal position of the upper-left relay is shown in Fig. 4.3. As the nominal positions are expected to align every r_o in a row, and the network edge length is d, we have approximately $(d - r_o/\sqrt{2})/r_o$ nominal relays in a row, if we ignore the edge effect and the fact that we can only have integer number of relays. The set of nominal relays also contains Δ_1 relays in the vertical rib.

We now find $\mathbf{H}$ as a function of d and r_o. Since the distance between adjacent horizontal strips is $(\frac{\sqrt{3}}{2} + 1)r_o$ in the nominal situation, the number of rows depends on whether the transmission range of the sensors in the last row can cover the bottom edge. However, we ignore this fact, and approximate $\mathbf{H}$ by adding an additional row, which also provides a conservative estimation of $\mathbf{H}$. This leads $\left[\frac{d-r_o/\sqrt{2}}{r_o}\right] \times \mathbf{H}$ to be an approximation of the

total number of relays in all the horizontal strips. The $\mathbf{H}$ in eq. (4.3) is approximated by

$$\begin{aligned} \mathbf{H} &\approx \left[\frac{d - r_o/\sqrt{2}}{\left(\frac{\sqrt{3}}{2} + 1\right) r_o} \right] + 1 \\ &= \left[\frac{2d/r_o - \sqrt{2}}{\sqrt{3} + 2} \right] + 1. \end{aligned} \tag{4.4}$$

The Δ_1 is the number of nodes in the vertical rib, and it is slightly less than the number of rows. If we need an additional row of relays to cover the bottom edge of the network, we need a relay corresponding to each row, except for the last two row, in the vertical rib, i.e., $\Delta_1 = \mathbf{H} - 2$, otherwise we need a relay for each row except the last row in the vertical rib, i.e., $\Delta_1 = \mathbf{H} - 1$. As we always add an additional row at the bottom of the sensing field, we have $\Delta_1 = \mathbf{H} - 2$. So Δ_1 is given by

$$\begin{aligned} \Delta_1 &\approx \mathbf{H} - 2 \\ &= \left[\frac{2d/r_o - \sqrt{2}}{\sqrt{3} + 2} \right] - 1, \end{aligned} \tag{4.5}$$

Note that N_1 should be an integer. However, in this section, we ignore the integer effect by smoothing it to a real number. More accurate analysis of N_1 is given in Appendix A.

4.4.3 Expected Number of Filling Relays

The number of filling relays, N_2, is also a random variable. In order to evaluate its expectation, we investigate the three node pattern, which is shown in Fig. 4.2(b). In the graph, the overlapping area between the transmission range of these three nodes guarantees that nodes between these three nodes can communicate with them. Hence we do not need a filling relay for the three node pattern if there is overlapping, otherwise a filling relay needs to be added. Let B_i denote the event that the i^{th} set of three discs representing the transmission range of the three nodes do not overlap, which is equivalent to the event that we need an extra relay for this three node pattern.

Define

$$\mathbf{I}_{B_i}(x) = \begin{cases} 1, & x \in B_i \\ 0, & \text{otherwise,} \end{cases} \tag{4.6}$$

which is the indicator function of event B_i, i.e., $\mathbf{I}_{B_i}$ equals to 1 if and only if event B_i occurs. The expected number of filling relays for the i^{th} set of three node pattern is $E[\mathbf{I}_{B_i}]$. Thus if we can compute the number of three node patterns, denoted by N_3, we can evaluate the expected number of extra filling relays required, for a given network and given r_o, which is

$$E[N_2] = E\left[\sum_{i=1}^{N_3} \mathbf{I}_{B_i}\right] = N_3 E\left[\mathbf{I}_{B_1}\right]. \tag{4.7}$$

Note that N_3 is a function of d and r_o.

When d is large,

$$N_3 \approx N_1. \tag{4.8}$$

This is because for a large network, corresponding to each node in the network, there exists a three node pattern, as can be seen in Fig. 4.1. This approximation becomes tight when both d and λ approach infinity. Therefore, eq. (4.7) becomes

$$E[N_2] \approx N_1 E\left[\mathbf{I}_B\right]. \tag{4.9}$$

A more accurate evaluation of N_3 is given in Appendix A.

4.4.4 Expected Number of Filling Relays for a Three Node Pattern

As $\mathbf{I}_B$ is the indicator function of the event that we need a filling relay for a three node pattern, its expectation, which is the expected number of filling relays needed, equals to the probability that the underlying event occurs. It is

$$E\left[\mathbf{I}_{B_i}\right] = \mathrm{P}(B_i). \tag{4.10}$$

Exact computation of $\mathrm{P}(B)$ is difficult, as nodes can be on arbitrary positions around the nominal positions and the overlapping area is not a polygon. However, we can evaluate $\mathrm{P}(B)$ through an approximation.

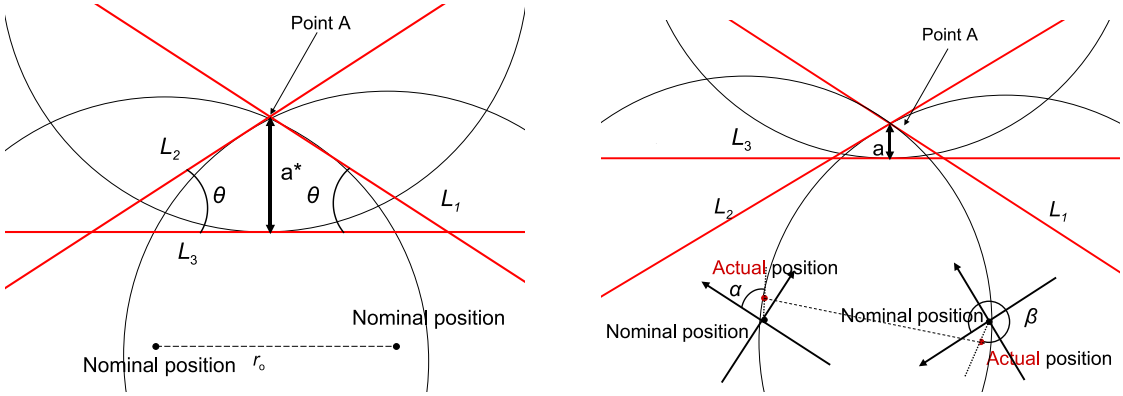

(a) Illustration of nominal positions

(b) Illustration of actual positions

Figure 4.4: Three node pattern to compute $E[I_B]$

To obtain the probability $\mathrm{P}(B)$ that we need an extra relay node for a three node pattern, we approximate the boundaries of the overlapping area of the three transmission range discs by straight line segments. This idea is shown in Fig. 4.4. Figure 4.4(a) shows the ideal situation, in which nodes locate exactly on the nominal positions. If there are three nodes exactly located on the nominal positions in the three node pattern, the discs representing the radio range overlap as shown in Fig. 4.4(a). The intersection point for the two lower discs is denoted by A. The two straight lines L_1 and L_2 for the two lower discs are the tangent lines at the intersection point A, for lower left and lower right transmission range discs, respectively. The third line L_3 is the horizontal tangent line of the upper disc. Hence the overlapping area of transmission ranges of these three nodes can be approximated by the triangle circumscribed by L_1, L_2 and L_3. We also denote by variable **a** the distance between L_3 and A. It takes the particular value $\mathbf{a}^*$ (discussed later) for the ideal situation, i.e., when nodes locate on the nominal positions.

For a random network, the ideal situation occurs with probability zero, hence we cannot find nodes exactly located on those nominal positions, if nodes are randomly distributed according to uniform distribution. If we select the nearest node to each nominal position to be the nominal relay corresponding to that nominal position, we can have the actual nominal relay pattern, actual pattern in short, as the example shown in Fig. 4.4(b).

As can be seen in Fig. 4.4(b), the actual relays do not locate on the nominal positions. Thus, the position of A is random, which results in **a** being a random variable as well. The positions of L_1, L_2 and L_3 are also random. If **a** is less than zero, L_1, L_2 and L_3 do not

overlap, and we need an extra filling relay node. By this setting, we assume that the two lower nodes are always connected, which is a reasonable assumption for dense network. We propose a scheme to approximate the probability that $\mathbf{a} < 0$ in the rest of this section.

Let $\mathbf{a}^*$ be the particular value of $\mathbf{a}$ for the ideal nominal pattern. Based on simple geometric manipulation, $\mathbf{a}^*$ is given by

$$\begin{aligned} \mathbf{a}^* &= \sqrt{r^2 - \frac{r_o^2}{4}} - (r_o + \frac{\sqrt{3}}{2} r_o - r) \\ &= \sqrt{1 - \frac{r_o^2}{4}} - (1 + \frac{\sqrt{3}}{2}) r_o + 1. \end{aligned} \tag{4.11}$$

Note that $\mathbf{a}^* = \mathbf{0}$ if $r_o = r\ (= 1)$. We can compute the increment of $\mathbf{a}$ for the actual pattern compared to the ideal nominal pattern. Denote this increment $\Delta\mathbf{a}$, and it can take negative values. Therefore, for the actual pattern, $\mathbf{a} = \mathbf{a}^* + \Delta\mathbf{a}$, and $\mathbf{a} < 0$ is equivalent to

$$\mathbf{a}^* + \mathbf{\Delta a} < \mathbf{0}. \tag{4.12}$$

We are aiming to express $\Delta\mathbf{a}$ as a function of modified spacing r_o.

In Fig. 4.4(b), consider the lower left disc. If the line connecting the actual position and the nominal position of the relay is parallel to the tangent line L_1 in the nominal pattern, and the distance between the nominal and actual position is small, we can approximately consider that the tangent line L_1 in the actual pattern coincides with the L_1 in the nominal pattern. We construct an orthogonal coordinate system for the lower left node in the actual pattern. The origin is the nominal position. The axis of the first dimension is parallel to L_1 with the positive direction pointing to the upper left corner, and the axis of the second dimension is orthogonal to L_1, with the positive direction pointing to the upper right corner, as shown in Fig. 4.4(b). With these configurations, we can approximately consider that the offset of the position of the lower left relay affects A and $\mathbf{a}$ only via its projection onto the second dimension of the coordinates system, scaled by the cosine of the angle θ between L_1 and L_3 under the nominal pattern. This approximation is valid when the offset is small, i.e., dense network cases. The details are as follows.

Denote the distance from an arbitrary point to its nearest Poisson point of a Poisson

process with intensity λ by R. So R is a random variable with distribution function [190]

$$F_R(x) = 1 - \exp\left(-\lambda x^2 \pi\right), \qquad x \geq 0, \tag{4.13}$$

and its pdf is given by

$$f_R(x) = 2\lambda\pi x \exp\left(-\lambda x^2 \pi\right), \qquad x \geq 0. \tag{4.14}$$

Let R_1 be the distance from the nominal position of the lower left node to its nearest Poisson point, which is the actual position of the nominal relay. The distribution of R_1 is given by eq. (4.13). Let α be the angle between the line connecting the actual position and the nominal position and the axis of the first dimension, as shown in Fig. 4.4(b). The distribution of α is uniform within the interval $(0, 2\pi]$. The projection of R_1 onto the axis of the second dimension is consequently $R_1 \sin\alpha$. Similarly, we define R_2, β and R_3, γ for the lower right node and the upper node. By symmetry, the angle between L_2 and L_3 in the nominal pattern is also θ. Hence $\Delta\mathbf{a}$ can be expressed by

$$\Delta\mathbf{a} = -\left(\cos\theta(R_1 \sin\alpha + R_2 \sin\beta) + R_3 \sin\gamma\right). \tag{4.15}$$

$\cos\theta$ is the weight factor of the offset of the actual positions of the lower two nodes on $\mathbf{a}$. A simple geometric argument yields the value of $\cos\theta$ as

$$\begin{aligned} \cos\theta &= \frac{\sqrt{r^2 - \frac{r_o^2}{4}}}{r} \\ &= \sqrt{1 - \frac{r_o^2}{4}}. \end{aligned} \tag{4.16}$$

The second equality comes from the fact that $r = 1$. Based on above discussion, the event that we need an extra relay for these three nodes is equivalent to the event that $\Delta\mathbf{a} + \mathbf{a}^* < 0$, which is

$$\left(\sqrt{1 - \frac{r_o^2}{4}} - (1 + \frac{\sqrt{3}}{2})r_o + 1\right) - \left(\sqrt{1 - \frac{r_o^2}{4}}(R_1 \sin\alpha + R_2 \sin\beta) + R_3 \sin\gamma\right) < 0. \tag{4.17}$$

We know that $E[\mathbf{I}_B] = \mathrm{P}(B)$, which is the probability of the underly event that enables the occurrence of (4.17). This probability can be evaluated either analytically or by Monte

Carlo methods, as shown in the following two subsections.

4.4.5 Analytical Approach

To evaluate the probability of (4.17), let $Y = \sin\alpha$. Its pdf f_Y is the common density function that $\sin\alpha$, $\sin\beta$ and $\sin\gamma$ follow. By the similar reasoning as shown in [175], f_Y is given by

$$f_Y(y) = \frac{1}{\pi\sqrt{1-y^2}}, \qquad -1 < y < 1. \tag{4.18}$$

Let $Z = R_1 \sin\alpha$, and denote the density function of Z by f_Z. The analytical formula of f_Z is given by eq. (B.2) in Appendix B. The $R_2 \sin\beta$ and $R_3 \sin\gamma$ follow the same distribution. This leads to the density of $R_1 \sin\alpha + R_2 \sin\beta$ as a two fold convolution of f_Z, denote it by f_{Z*Z}.

Therefore, the density of $\Delta\mathbf{a}$, whose expression is given by eq. (4.15) is

$$f_{\Delta\mathbf{a}}(y) = \int_{-\infty}^{\infty} \frac{1}{\cos\theta} f_{Z*Z}\left(\frac{-x'}{\cos\theta}\right) f_Z(y - x')\mathrm{d}x'. \tag{4.19}$$

and we have

$$\mathrm{P}(B) = \int_{-\infty}^{-\mathbf{a}^*} f_{\Delta\mathbf{a}}(y)\mathrm{d}y. \tag{4.20}$$

in which $\mathbf{a}^*$ is given by eq. (4.11).

The exact expression of eq. (4.20) is given in Appendix B. Due to its complexity, we develop a Monte Carlo method to compute this probability.

4.4.6 Monte Carlo Method

For a given r_o and other system parameters such as n and d, we generate 10^6 random samples of R_1, R_2, R_3, α, β and γ, according to their distributions. The frequency that (4.17) occurs approaches its probability as the number of samples increases, which enables us to approximate $\mathrm{P}(B)$ by this frequency. With this Monte Carlo method, we propose a heuristic algorithm to evaluate the r_{om} that yields an good approximation of the optimal N_{CDS}.

4.4.7 Heuristic for r_{om}

We aim to find the optimal solution r_{om} of r_o, such that the expected value of N_{CDS}, $E[N_{CDS}]$, is minimized. As $N_{CDS} \approx N_1 + N_2$, we have

$$\begin{aligned} E[N_{CDS}] &\approx N_1 + N_3 E[\mathbf{I}_B] \\ &\approx N_1 + N_1 \mathrm{P}(B). \end{aligned} \tag{4.21}$$

in which N_1 is given by eq. (4.3), which is a decreasing function of r_o, and N_3 is approximated by N_1, while $\mathrm{P}(B)$ is an increasing function of r_o, which can be computed by Monte Carlo method mentioned in Section 4.4.6. Therefore, we can find a particular r_o, r_{om} such that (4.21) is minimized. We propose a heuristic to compute that r_{om}. This heuristic adopts the Monte Carlo approach to evaluate $\mathrm{P}(B)$ for a given r_o, and then by applying Golden Section Search [219] to compute the r_{om} such that $E[N_{CDS}]$ is minimized. The formal statement of the algorithm is shown in Algorithm 1.

Algorithm 1 Heuristic for r_o

Input: Total number of nodes n; the normalized network edge length d; $m = (\sqrt{5}-1)/2$; error threshold ϵ; the potential range of r_o, $r_o \in [r_{start}, r_{end}]$.
Output: r_{om}, such that $E[N_{CDS}]$ is minimized.

$r_s = r_{start}$, $r_e = r_{end}$.
$r_1 \leftarrow r_e - m(r_e - r_s)$, compute $E[N_{CDS}(r_1)]$ by eq. (4.21).
$r_2 \leftarrow r_s + m(r_e - r_s)$, compute $E[N_{CDS}(r_2)]$ by eq. (4.21).
while $|r_e - r_s| > \epsilon$ **do**
  if $E[N_{CDS}(r_1)] > E[N_{CDS}(r_2)]$ **then**
    $r_s \leftarrow r_1$.
    $r_1 \leftarrow r_2$.
    $E[N_{CDS}(r_1)] \leftarrow E[N_{CDS}(r_2)]$.
    $r_2 \leftarrow r_s + m(r_e - r_s)$.
    compute $E[N_{CDS}(r_2)]$.
  else
    $r_e \leftarrow r_2$.
    $r_2 \leftarrow r_1$.
    $E[N_{CDS}(r_2)] \leftarrow E[N_{CDS}(r_1)]$.
    $r_1 \leftarrow r_e - m(r_e - r_s)$.
    compute $E[N_{CDS}(r_1)]$.
return $r_{om} \leftarrow \frac{r_1 + r_2}{2}$.

To successfully execute this algorithm, we need to know the total number of nodes n, the normalized network edge length d, and λ is computed as n/d^2. As we adopt Golden

Section Search in this algorithm, the computation procedure is iterative, and we need an error threshold ϵ as the stoping criterion. The parameter m is set to $(\sqrt{5}-1)/2 \approx 0.618$, corresponding to the name Golden Section Search, which is the search interval reduction factor for each round of iteration. We also need to know the potential range of r_o, which is within the interval $[r_{start}, r_{end}]$. As the network is normalized to the transmission range r, r_{end} could take the value of one, and r_{start} could be a value close to 0.5. In fact, we could do some pre-evaluation to reduce the possible range of r_o. The output of the algorithm is the r_{om}, such that the $E[N_{CDS}]$ takes a value that is close to the minimum. In line 3, 10 and 16 of Algorithm 1, $E[N_{CDS}]$ is computed according to eq. (4.21), in which N_1 is given by eq. (4.3), and N_3 is approximated by N_1. The $E[\mathbf{I}_B]$ is obtained by the Monte Carlo approach described before. The algorithm reduces the search interval iteratively according to the Golden ratio, until the length of the search interval $|r_e - r_s|$ is less than a pre-defined threshold ϵ. The algorithm outputs the median of the two end points.

The underlying reasoning of the above approach is as follows. We only investigate three node patterns. The overlap between these three transmission range discs guarantees that we do not need an extra relay for these three nodes. Thus we want to evaluate the probability that the transmission range of these three nodes do not overlap each other, indicating that we need an extra relay node. Hence if we know the number of three nodes pattern, we can compute the expected number of additional filling relays required. By this model, we implicitly assume that the two lower nodes are always connected. This is a reasonable assumption if the network is dense.

4.5 An Algorithm to Construct an MCDS

In this section, we propose a new algorithm, Incremental Coverage Algorithm (INCOA), to approximate an MCDS in connected dense networks by exploiting the above approach. This algorithm first computes the optimal r_{om} according to Algorithm 1, then uses this r_{om} to compute the nominal relay positions with the optimal strip-based pattern. With these positions, the algorithm finds the nominal relays, and finally, computes the filling relays, such that all sensor nodes can be reached by at least one relay. The generated MCDS can be used in flooding to greatly reduce the retransmission.

We first propose the centralized version of INCOA and then develop its distributed version.

4.5.1 A Centralized Algorithm INCOA to Compute an MCDS

First, consider a centralized algorithm, the Incremental Coverage Algorithm (INCOA), which is shown in Algorithm 2.

Algorithm 2 Incremental Coverage Algorithm (INCOA)

Input: A set of nodes T, all nodes know their positions; total number of nodes n; network edge length d.
Output: $T_1 \subset T$, and T_1 is a dominating set.

```
1: T1 ← ∅
2: Compute the optimal spacing r_om according to Algorithm 1.
3: Compute the nominal positions according to r_om and the strip-based pattern. Those
   positions are indexed by set Q.
4: for all i ∈ Q do
5:    Select the nearest node of nominal position i as the nominal relay i.
6:    T1 ← T1 ∪ nominal relay i
7: while The set of uncovered nodes, T2, has cardinality |T2| > 0 do
8:    Select a node j from covered nodes that can cover the largest number of uncovered
      nodes.
9:    T2 ← T2 \ j.
10:   T1 ← T1 ∪ node j
11: return T1
```

In this algorithm, with the computed r_{om}, we can manipulate the nominal positions, and find the nominal relays, which are the closest node to each nominal position. The algorithm also selects some additional nodes as filling relays by greedy criteria to cover those nodes that cannot be connected by any nominal relay.

Note that in this algorithm, the connectivity of the selected nodes is not guaranteed. If those relays are not connected, we can have an additional step to Algorithm 2 to select some connecting relays to maintain the connectivity. However, this will not affect the cardinality of the selected relay set much.

Another solution to the connectivity of the relay set is selecting a set of candidate nodes for a nominal position, and by selecting different nodes in each candidate set to be the nominal relay, we can establish connectivity gradually. This solution will be left as future work.

4.5.2 Distributed Version of INCOA

As it is desirable to use distributed algorithms and protocols in a practical sensor network environment, we propose a distributed version of INCOA. To develop the distributed algorithm, we make following assumptions first.

- The networks we are considering are connected, as the connected dominating set is not well-defined in an unconnected network.
- There is a MAC layer protocol that manages the point-to-point links, such that there are no errors, acknowledgements and retransmissions in the network layer. The MAC layer protocol could be either a random access scheme, such as IEEE 802.11 [112], 802.15.3 [113], or 802.15.4 [114], or an access scheme based on scheduling, such as TDMA or CDMA [182].
- Each node has a unique ID.
- All nodes know their own positions, either via GPS or some other localization techniques.
- All the links are bi-directional.
- There is synchronization among all the nodes, either via GPS or other techniques.
- Nodes are stationary, i.e., nodes do not move once deployed.

We then define four states for nodes.

- White node (initial state)
- Dominatee
- Nominal Dominator
- Filling Dominator

The algorithm can be divided into two steps

- Nominal Dominator selection
- Filling Dominator selection

Initially, all nodes are white nodes. A white node u periodically broadcasts a "Hello" message (with time interval $t(r)$), which contains its own ID and the ID of the node which is known by u to have the shortest distance to the nominal positions corresponding to u. The corresponding distance is also contained in the "Hello" message. After the nominal dominator selection step, some nodes become nominal dominators, and the rest of

nodes become dominatees if they are within the transmission range of some nominal dominators, otherwise they are still white nodes. The second step, filling dominator selection, selects filling dominators from dominatees, to provide connectivity to those white nodes which are not able to be reached by any nominal dominator. The union of nominal dominators and filling dominators is the dominating set we obtained to approximate the MCDS.

We assume all nodes know their own positions, the network edge length d, and the optimal spacing r_{om} computed by Algorithm 1. We also assume that each node has the knowledge of all the nominal positions, which can be computed by using the r_{om} and d. Therefore, each node knows to which nominal position it belongs, and is aware of the distance, R_d, between its own position and the nominal position(s) it belongs to. As we have assumed that all nodes are synchronized, we assume that there is a start time 0, which is common to all the nodes to begin the operations of the distributed algorithm. In addition, we define a common function t for all the nodes, which returns a value of time, $t(R_d)$, that is proportional to the distance R_d. A longer R_d results in larger $t(R_d)$. The value of $t(R_d)$ is used by each white node to schedule the broadcasting of the first "Hello" message. We also assume that the messages transmitted by a node u can be immediately received by all of u's one-hop neighbours.

In the following description, all the R_d are referred to the R_d of local nodes. Initially (at time 0), all the white nodes schedule a broadcast of a "Hello" message, T, which will be transmitted at time $t(R_d)$. Note that the values of $t(R_d)$ are different for different nodes, as they have different distances between their own positions and the nominal positions they belong to. Corresponding to each nominal position, every node u has a pair of local parameters (y_1, y_2), in which y_1 is the known smallest R_d to that nominal position, and y_2 is the corresponding ID of the node with the smallest R_d. Initially, y_1 of a node u is set to the R_d value of u, and y_2 is the ID of u. Upon receiving a "Hello" message, each node updates its local parameter pair (y_1, y_2). The "Hello" message contains the (y_1, y_2) pair of the sender. After a time $2t(r)$, all the nodes within the radius r of a nominal position will realize who has the shortest distance to the nominal position. This node sends a "dominator claim" message at time $2t(r) + t(R_d)$ to state the fact that it is a nominal dominator. All nodes that can receive a "dominator claim" message sets themselves as a dominatee. At the same time, all white nodes initiate a "request to be covered" message, which will be sent at a time $2t(r) + t(R_d)$. However, if a white node receives a "domina-

tor claim" message before the scheduled time, the "request to be covered" message will be cancelled. Therefore, after a time $3t(r)$, all the dominatee will have the information about all its uncovered white neighbours. Each dominatee then schedule a message to broadcast how many white neighbours it has at a time $3t(r) + t(R_d)$. After a time $4t(r)$, all the dominatee will know which neighbour dominatee has the largest number of white neighbours, and this dominatee set itself as a filling dominator. The dominatee with smaller ID will be selected if there is a tie. This dominatee schedules a "dominator claim" message, which is going to be sent immediately after it becomes a filling dominator (i.e., at time $4t(r)$). All the white nodes receiving this message set themselves as dominatees. The uncovered white nodes will keep sending "request to be covered" messages at time $gt(r) + t(R_d)$, in which g is any even number. As each time, a dominatee with highest degree of white neighbours will be selected as a filling dominator, and all the uncovered white neighbours of that filling dominator will become dominatees, the total number of uncovered white nodes will keep decreasing, and eventually all the uncovered white nodes will become dominatees.

The operations of this distributed algorithms are as follows.

Distributed version of $INCOA$

State space S = {**White Node, Nominal Dominator, Filling Dominator, Dominatee**}
$S_{INITIAL}$ **=** {**White Node**}
$S_{TERMINAL}$ **=** {**Nominal Dominator, Filling Dominator, Dominatee**}.

WHITE NODE

- At time 0, a white node u initializes its local parameter y_1 to be the R_d of u, and y_2 to be the ID of u.
- Upon receiving a "Hello" message, a white node u performs the following operations. If *Incoming* y_1 $<$ *local* y_1, then *local* y_1 = *Incoming* y_1, and *local* y_2 = *Incoming* y_2.
- A white node u sends a "Hello" message if the time is $t(R_d)$, and re-sends it every $t(r)$, if the time is less than $2t(r)$.

- A white node u set itself to "nominal dominator", if the time is $2t(r)$, and its local y_1 and y_2 indicate it has the shortest distance to the nominal position.
- A white node u set itself to "dominatee" if it receives a "dominator claim" from its neighbour.
- A white node u sends a "request to be covered" message if the time is $gt(r) + t(R_d)$, in which g is an arbitrary even number.

NOMINAL DOMINATOR

- A nominal dominator v sends a "dominator claim" message at time $2t(r) + t(R_d)$.

DOMINATEE

For a dominatee w,

1: Initialize $wnc \leftarrow 0$
2: **if** receiving a "request to be covered" message **then**
3: $wnc = wnc + 1$.
4: **while** $wnc > 0$ at time $qt(r)$ ($q \geq 3$, q is odd) **do**
5: At time $qt(r) + t(R_d)$, $q \geq 3$ and q is odd, a dominatee w broadcasts how many white neighbours it has (the value of wnc).
6: At time $(q+1)t(r)$, $q \geq 3$ and q is odd, a dominatee w changes its state to filling dominator if it has the highest value of of wnc, among all its dominatee neighbours.
7: At time $(q+1)t(r)$, $q \geq 3$ and q is odd, a dominatee w resets its local white neighbour counter to zero, if w does not become a dominatee.
8: **if** receiving a "request to be covered" message **then**
9: $wnc = wnc + 1$.

FILLING DOMINATOR

- A filling dominator m sends a "dominator claim" message immediately after it becomes a filling dominator.

The state transition diagram of nodes in the distributed INCOA is shown in Fig. 4.5.

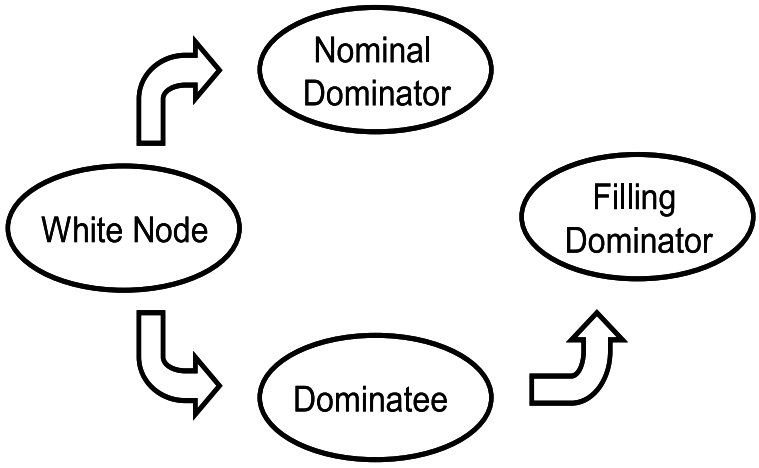

Figure 4.5: The state transition diagram of nodes in the distributed INCOA

4.6 Model Validation and Numerical Results

4.6.1 Algorithm Comparison and Mean of the MCDS Cardinality

To verify our approaches, we consider a network scenario with $d = 10$, for total number of nodes $n = 1000, 2000, ..., 5000$, i.e., $\lambda = 10, 20, ..., 50$. We generate 500 connected network instances, with all the nodes i.i.d. uniformly distributed in the $d \times d$ network area. We compute r_{om} for each value of n. With these r_{om}, we compute the number of relays needed numerically according to the Monte Carlo approach mentioned above, we then run the INCOA algorithm and obtain the number of relays needed. The results are compared with the results obtained by Butenko *et al.*'s algorithm [36], and also the number of nominal relays. All the comparisons are based on the average number of relays over 500 network instances. The results are shown in Fig. 4.6. The analytical results in the figure are obtained through eq. (4.21), in which $\mathrm{P}(B)$ is computed through the Monte Carlo method described before, and N_1 is computed by substituting the r_{om} for r_o in eq. (4.3).

As shown by the example in Fig. 4.6, the average number of relays obtained by INCOA is less than that computed by Butenko's algorithm, when λ is larger than about 20 (for this example), which is expected as INCOA works for dense networks.

It can also be seen that the analytical results for the expectation of the cardinality of the CDS obtained by Algorithm 1 and Monte Carlo approach are close to those computed by INCOA. More importantly, these two values both approach the number of nominal re-

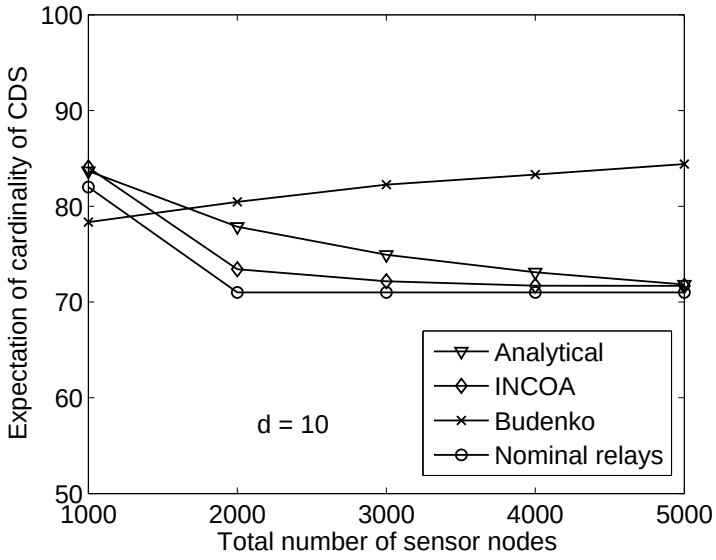

Figure 4.6: Expectation of minimum number of relays.

lays, when the network density becomes large. The number of nominal relays is obtained by eq. (A.1). This result is not surprising as the higher network density indicates a higher probability that we can find nodes in the vicinity of nominal positions, hence a lower probability to need extra relays. In the figure, it is also shown that the analytical results are larger than those obtained by INCOA, this is because we take approximation to compute N_1, which ignores the integer round-off effects, hence are larger than the true value of N_1, when we compute the analytical results. It is noted that the number of nominal relays is a decreasing step function taking integer values, which means that with the increase of λ, hence the increasing of r_{om}, the number of nominal relays keeps constant until r_{om} reaching a value that makes the number of nominal relays in each horizontal strip decreases by 1. This is also the edge effect caused by finite networks.

4.6.2 Probability of Requiring a Filling Relay

In this subsection, we demonstrate some results of the probability of requiring a filling relay for a three node pattern, $\mathrm{P}(B)$, obtained from our approximation using intersecting hyperplanes and simulations of actual discs. The aim is to verify our approach, and gain a clear understanding of it.

We compare the approximation and simulation results of $\mathrm{P}(B)$ for $\lambda = 100$ and 20, and $r_o = 0.7, 0.75, ..., 1$. We generate 10^5 random samples for each of R_1, R_2, R_3, α, β and γ according to their distributions. The results are shown in Fig. 4.7. The probability

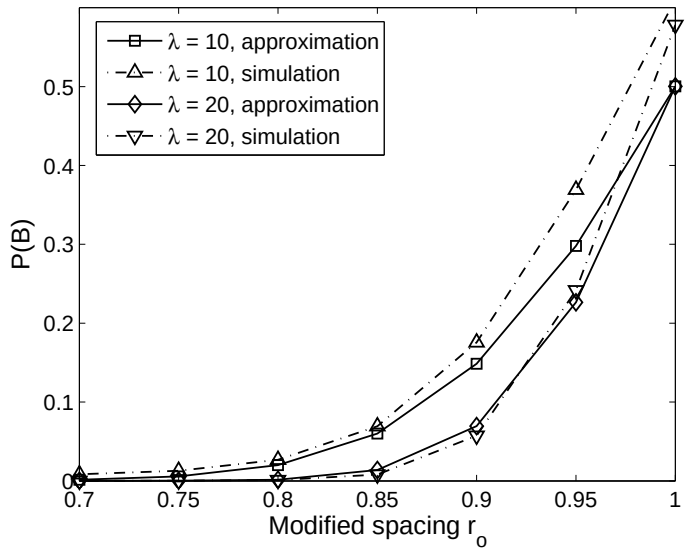

Figure 4.7: Probability of requiring a filling relay for a three node pattern.

$E[\mathbf{I}_B] = \mathrm{P}(B)$ is a function of only r_o and the network density λ, independent of the network edge length d.

As shown in Fig. 4.7, the results obtained from the approximation and simulation match well. Our approach is a good approximation when λ is large. It should be noted that in general, the curves of actual discs (simulation results) should be above the approximation results, as we approximate the intersection area by a triangle that has a larger area than the actual intersection area. However, as can be seen from the curves for the case that $\lambda = 20$, the approximation results may exceed the simulation results, especially for some r_o that are not too large. This is because we assume that L_1 and L_2 have constant slopes, which is not exactly. In particular, for a small r_o, the relative offset of the actual position of relays has a larger impact, and the constant slope assumption also has a larger impact. Hence we have the results.

Note that I_B is a Bernoulli random variable. The variance of a single sample is $\mathrm{P}(B)(1-\mathrm{P}(B))$. So the variance of $\mathrm{P}(B)$ is approximately $\mathrm{P}(B)(1-\mathrm{P}(B))/10^5$, by taking the square root, we can have the standard deviation of $\mathrm{P}(B)$. Following this approach, the standard deviations of $\mathrm{P}(B)$ for $\lambda = 10$, $r_o = 0.7, 0.75, ..., 1$ are estimated as: 0.0003, 0.0004, 0.0005, 0.0008, 0.0012, 0.0015, 0.0015. The standard deviation of $\mathrm{P}(B)$ for $\lambda = 20$ are estimated as: 0.00003, 0.000046, 0.000106, 0.000284, 0.000735, 0.00135, 0.00156. It is clear that for a larger λ, $\mathrm{P}(B)$ has a smaller variation.

It is interesting to see that for different values of λ, our approximation predicts that

$P(B) = 0.5$, when $r_o = r = 1$. In fact, **a** equals to zero when $r_o = r = 1$, which means that the overlapping triangle of three radio transmission discs reduces to a single point. However, the actual positions of those three nodes vary from the nominal positions, and only the directions of the offsets affect the value of **a**, if the directions make the size of the triangle bigger, then no filling relay is needed, but if the directions make it smaller, then a filling relay is necessary, no matter how small the change is. The value of λ does not affect the directions, it only influences the values. The directions of the offsets are affected by α, β and γ, which are uniformly distributed. For $r_o = r = 1$, the intersection area of the ideal reduces to a single point A^*, if those three nodes are exactly on the nominal positions. However, the actual positions of those three nodes have random perturbations. The distance between each actual position to A^* is i.i.d., so we have equal opportunity to have a positive or negative intersection area.

4.6.3 Relaxation for the Number of Nominal Relays

We approximate N_1 in Subsection 4.4.2, and give a more accurate evaluation in Appendix A. In fact, N_1 is an integer given d and r_o, as shown by eq. (A.1) in Appendix A. However, to simplify the calculation, we relax eq. (A.1) by removing the rounding operation, as shown in eq. (4.3).

To show the impact of this relaxation, we compute N_1 by eq. (A.1) and eq. (4.3), for $d = 10$ and 50, with $r_o = 0.7, 0.71, ..., 1$. The results are shown in Figs. 4.8 and 4.9.

Both Figs. 4.8 and 4.9 show that the values of N_1 obtained by relaxed approximation are close to the more accurate results obtained by taking integer rounding. The relative errors of N_1 between the relaxation version and the integer version is shown in Fig. 4.10. Its maximal value is around 15% for $d = 10$, and 3% for $d = 50$. The fluctuations in the curves are because the actual N_1 are taking integer values, and are not a strictly decreasing function. More importantly, the relative error of N_1 is a decreasing function of d, as shown in Fig. 4.11. The curve in Fig. 4.11 shows the maximal relative error for $d = 10, 20, ..., 50$. It is clear that the relative error decreases as d increases. Therefore, our relaxation is more accurate for a large network.

4.6.4 Impact of Network Density on the Modified Spacing

It is expected that for a given network, with the increase of network density λ, the r_{om} computed by Algorithm 1 also increases, because denser networks give a higher proba-

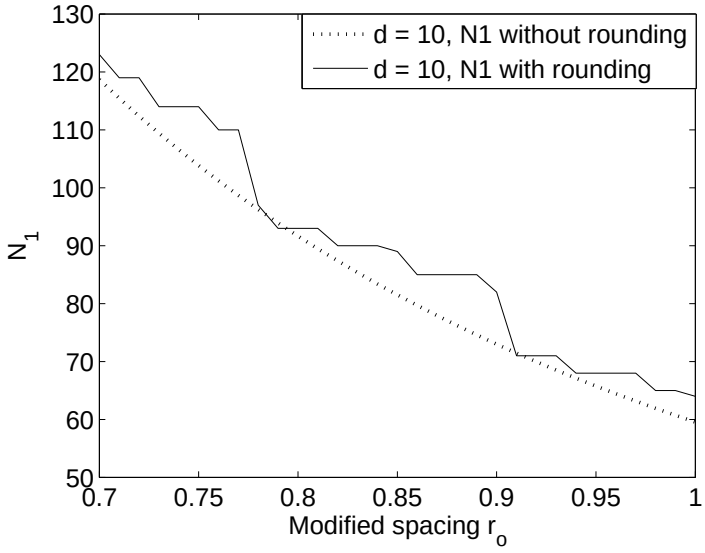

Figure 4.8: N_1 vs. r_o, $d = 10$.

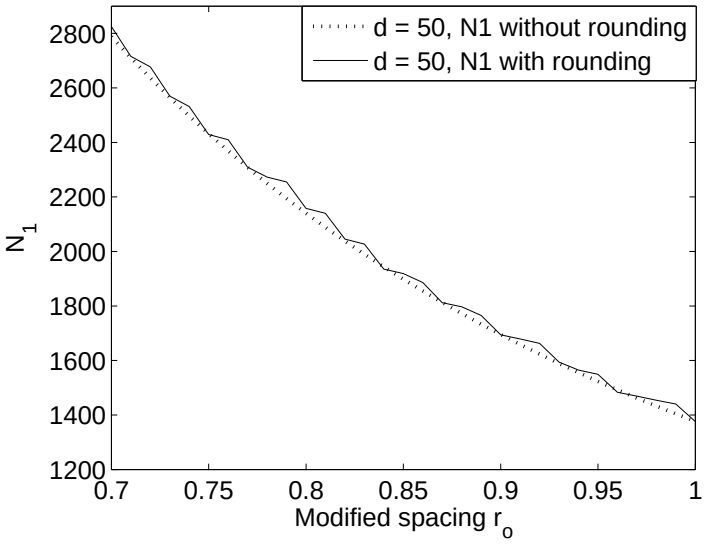

Figure 4.9: N_1 vs. r_o, $d = 50$.

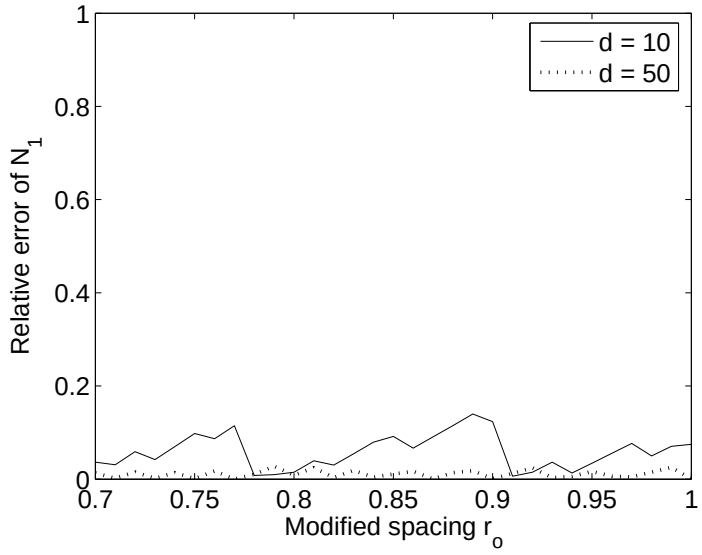

Figure 4.10: Relative error of N_1.

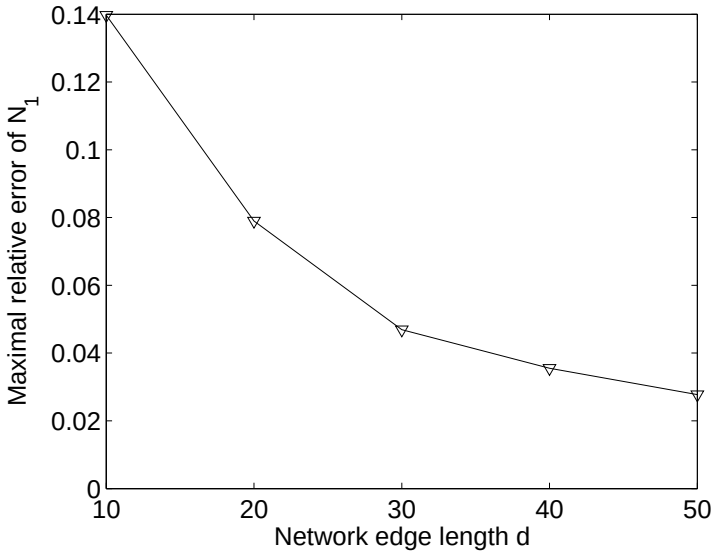

Figure 4.11: Maximal relative error of N_1 vs. network side length d.

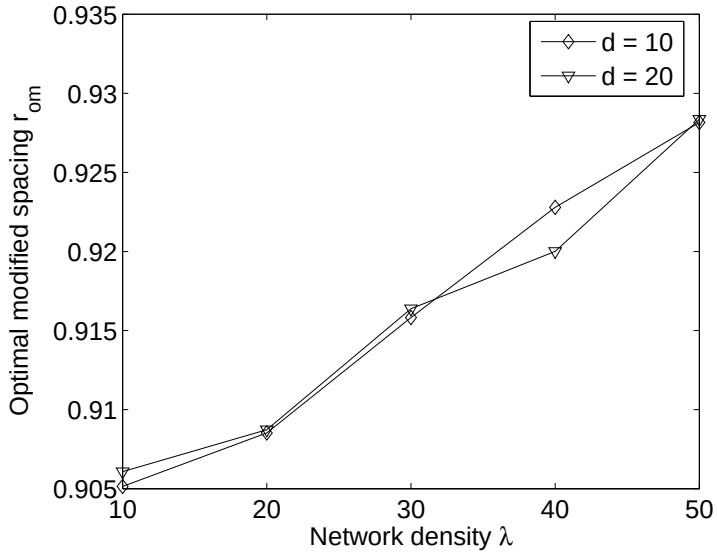

Figure 4.12: Optimal modified spacing, r_{om} vs. network density λ, $d = 10$.

bility that there exist nodes in the vicinity of those nominal positions. This can be verified by Fig. 4.12, which shows that for networks with $d = 10$ and 20, $\lambda = 10, 20, ..., 50$, the optimal modified spacing r_{om} increases with λ.

4.6.5 Total Number of Relays

Fig. 4.13 show the values of $E[N]$ computed by (4.2), for $d = 10$, $\lambda = 10$ and 20, respectively.

We can see that for a fixed d and λ, the expected number of relays, $E[N]$, is a convex function, which enables us to find its minimum by using Golden Section Search method. In Fig. 4.13, the values of $E[N]$ are equal for small r_o and for $r_o = 1$, independent of λ. This is because for small r_o, $E[N_2] = 0$, and N_1 is deterministic, independent of λ; while $r_o = 1$ indicates that $P(B) = 0.5$, which is also independent of λ, as shown in Fig. 4.7.

We use Fig. 4.14 to compare the $E[N]$ computed without the rounding operation and with the rounding operation, and show the effectiveness of our approximation. The figure shows that the $E[N]$ obtained by using different N_1 and N_3, for a network with $d = 10$ and network density $\lambda = 10$. It can be seen that the more accurate $E[N]$, which takes N_1 as eq. (A.1) is not a convex function of r_o, hence the Golden Section Search method is not guaranteed to find the optimal value of r_o. The figure also shows that the $E[N]$ obtained by eq. (A.1) fluctuates with r_o. This is because N_1 given by eq. (A.1) is influenced by the edge effects. This problem can be solved by either using the relaxation method in

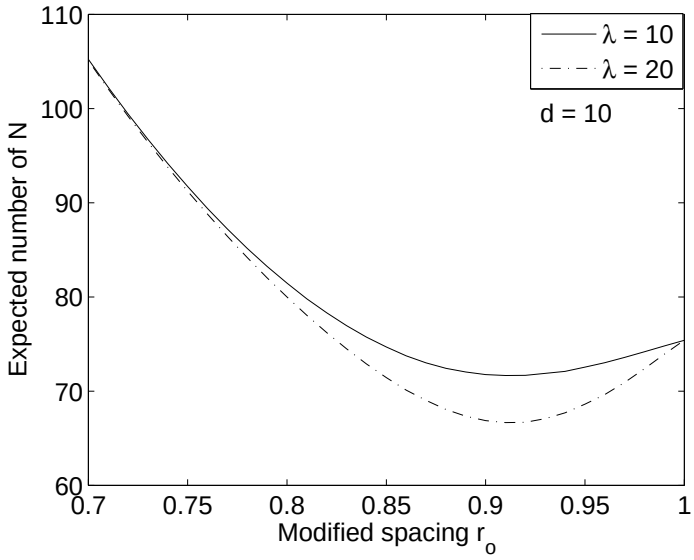

Figure 4.13: Expected number of relays, $E[N]$, $d = 10$.

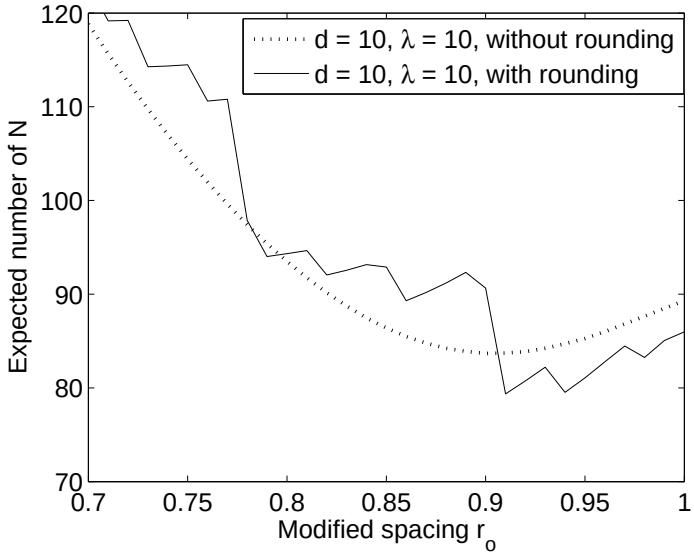

Figure 4.14: Comparison of expected number of relays, $E[N]$, with and without rounding operations.

which the integer round-off effects are ignored (this approach has been adopted in this chapter), or applying curve fitting approach to the curve of eq. (A.1) to smooth the results. However, the latter solution may not be able to produce a general formula to apply to the whole range of system parameters. Therefore, we need to repeat the fitting approach for each set of system parameters.

4.7 Conclusion

In this chapter, we have developed a new algorithm, the Incremental Coverage Algorithm (INCOA), and its distributed version, which can efficiently generate a dominating set that maintains a high probability of network connectivity, in a large and dense sensor network. The cardinality of the generated dominating set is close to that of the MCDS. The accuracy of our algorithm increases with the network size and network density.

We have also proposed a new approach to numerically evaluate the cardinality of the MCDS for 2-D large dense sensor networks. The approach is an extension of the asymptotically optimal result which is only applicable to infinite networks. Our approach computes the expectation of cardinality of the MCDS numerically by using a Monte Carlo method. The value obtained through our approach can be useful for evaluation of routing protocols and algorithms to generate the MCDS, specifically for dense networks.

Chapter 5

Connectivity of a Class of Wireless Sensor Networks

In Chapter 3 and 4, we studied a small connected relay set for dense WSNs. In this chapter, we focus on the connectivity of the sensors themselves for low-density networks, rather than a virtual backbone. In addition, in Chapter 4, we studied relays which are randomly located around some nominal positions. In contrast, we investigate network connectivity with sensors are randomly located around some nominal positions in this chapter. We assume that all sensors have their own target positions, and they attempt to locate on the target positions so as to provide optimal performance. However, due to the constraints of deployment, they may not be able to be placed on the target positions, hence position randomness is introduced.

5.1 Introduction and Background

In a WSN, sensor nodes are often highly resources constrained, with limited computation, memory, energy and communication capabilities. These limitations prevent the sensors from communicating over a single hop as in cellular networks. Therefore, WSNs require multi-hop communication as a spontaneous choice for data dissemination. Maintaining connectivity in such a network is vital, since direct communications between two nodes may not exist. This chapter focuses on this fundamental problem, i.e., connectivity, of random WSNs.

As pointed out in Chapter 2, positions of nodes in a WSN are random in many cases due to the batch deployment or the environmental constraints of the WSN. The randomness imposes the requirement of probabilistic measures to analyse the connectivity of WSNs, i.e., the connectivity is studied in probabilistic sense. Although the randomness is often unavoidable, it is not desirable to deploy sensor nodes in a purely random manner without any control mechanism, as such a kind of deployment may not be cost-effective. In contrast to the purely random deployment, a better way to deploy sensors is to place sensors targeting some carefully pre-engineered locations, which results in a low-density

WSN. For example, this may arise if nodes are dropped at equal intervals from a vehicle (either airborne or terrestrial) travelling at a constant speed. The network setting could also arise when untrained volunteers are asked to place sensors at a height y above the ground (for good radio propagation), and every x metres (x and y can be arbitrary values which are determined by the network design specification). Since there may not be suitable mounting points exactly every x metres, randomness could exist in the exact sensor locations. This motivates us to propose a new network model.

We consider stationary networks, in which all nodes are static. In particular, we focus on one-dimensional space, in which stationary nodes are randomly deployed according to non-identical probability distributions, which have identical variances. Mathematically, we consider the scenario that the positions of n nodes form a one-dimensional point process. These n points are randomly distributed with deterministic and equally spaced mean locations. That is, for n sensors, there are n target locations that are equally spaced with one for each sensor. Each sensor is deployed randomly according to a distribution function, which has an expectation equal to the corresponding target location. The offset in the sensor locations is i.i.d. For such a network, we aim to evaluate its connectivity probability. We also would like to estimate the number of nodes required, and evaluate the tolerable randomness of the node placement, to maintain a certain probability of connectivity.

Extensive research has been dedicated to the connectivity study of wireless multi-hop networks. Gupta and Kumar [92] used connectivity requirements to bound the capacity of wireless networks. Bettstetter [21] investigated the number of nodes required to maintain k-connectivity in a certain area. Foh *et al.* [75] derived formulae to compute the probability of connectivity for a network with uniformly distributed sensors in one-dimensional space. Other work that studied network connectivity includes [27], [45] and [66]. These studies all assumed that the positions of all the nodes are randomly distributed according to identical distributions, usually a uniform distribution, whereas in this chapter we are considering a different setting.

The rest of the chapter is organized as follows. Section 5.2 introduces our research problems and the model applied. Section 5.3 gives a brief introduction to curve fitting, which is a major tool used in this chapter. Section 5.4 develops an empirical approach that can evaluate the network connectivity probability, as well as compute the number of nodes required to achieve a desired probability of connectivity. We consider special and

extreme cases that are not covered by the empirical approach in Section 5.5. In Section 5.6, a similar empirical approach is adopted to investigate networks with nodes distributed according to a different distribution. We develop an algorithm in Section 5.7, aiming to provide a conservative estimate of the necessary number of nodes required to provide a certain level of connectivity. We conclude this chapter in Section 5.8.

5.2 Problem Statement and Model Description

We aim to establish a finite linear sensor network, and maintain the connectivity between nodes fixed at the edges of the network via n additional randomly deployed intermediate nodes. Note that in a linear network, connectivity between the two nodes located at the edges of the network indicates the connectivity between any pair of sensor nodes. The network setting could also represent the scenario that a data collection point sits on the edge of the network, and we aim to establish the connectivity between the farthermost sensor and the data collection point. We assume that all the sensors have identical transmission radius r, and the unit disk model is applied.

Fig. 5.1 shows a sample network. We consider a one-dimensional coordinate system with the source at the origin and the destination at the position with coordinate d. Without loss of generality, all spatial variables are scaled such that $d = 1$. The location of the i^{th} intermediate node is assumed to follow a double sided distribution F with mean $\mu_i = i/(n+1)$, and identical variance σ^2. Note that μ_i is the nominal position (target position) for the i^{th} node, and σ stands for the position offset. The numerical labels in Fig. 5.1 stand for the target position of sensors, and the spike curves above the coordinate axis represent that F are Gaussian distributions. In this chapter, we consider two scenarios, where F are Gaussian distributions and Laplacian distributions.

Let C denote the event that the network is connected. We are interested in answering three problems. First, given node transmission radius r, the number of nodes n, and the measure of sensor placement dispersion σ, what is the probability $\mathrm{P}(\mathrm{C})_{n,r,\sigma}$ that the network is connected? The second problem is how many nodes does the network need to achieve a required probability of connectivity $\mathrm{P}_{\text{target}}$, for given r and σ. Mathematically, it

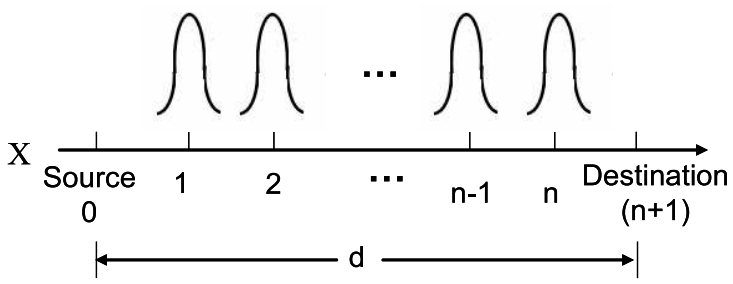

Figure 5.1: Sensor placement model

is equivalent to the optimization problem

$$\begin{aligned} &\textbf{objective:} \quad \min \quad n \\ &\textbf{subject to:} \quad \mathrm{P(C)}_{n,r,\sigma} \geq \mathrm{P}_{\text{target}}. \end{aligned} \tag{5.1}$$

Notice that $\mathrm{P(C)}_{n,r,\sigma}$ is an increasing function of n, since with more nodes, it has higher opportunity to find a relay within the transmission range of a node. Therefore, finding the minimal n is equivalent to finding the n such that $\mathrm{P(C)}_{n,r,\sigma}$ is minimal. The third problem that we are interested in is to find the dispersion σ for positions of nodes, such that $\mathrm{P(C)}_{n,r,\sigma} \geq \mathrm{P}_{\text{target}}$, for given n and transmission radius r. This problem is important when we need to select proper node deployment schemes.

Let x_i, $i = 1, ..., n$ denote the location of the i^{th} intermediate sensor, which represent the coordinates of those sensor nodes in a 1-D coordinate system. Note that the locations of the sensors may not be in the same order as they are dropped due to the randomness in their positions. That is, we may have $x_i \geq x_{i+1}$ for some i. Let $x_{(1)} \leq x_{(2)} \leq ... \leq x_{(n)}$ be a relabelling of the node positions in increasing order based on their physical locations. With this model, the question of whether the network is connected is mathematically equivalent to testing the hypothesis that all physically consecutive sensors are within a certain distance from each other. This gives a sufficient statistic, the maximum distance between two physically consecutive nodes. Its probability distribution is crucial to the application of that hypothesis test or equivalently to the network connectivity probability. This distribution is easily described in terms of the underlying event in the experiment sample space, but the analytic expression involves a complicated n-fold integral which defies explicit evaluation, especially for large n. Therefore, we use empirical approaches, which apply curve fitting, to answer the first two questions for this model. The next

section gives background of curve fitting.

5.3 Background of Curve Fitting

In science and engineering, we are often required to estimate and predict the behaviour of certain systems based on partially available information [44]. Moreover, real systems are often continuous, while measuring can only be done in discrete manner, which also requires us to evaluate system states other than those discrete points in which measurements are taken. To achieve these goals, we may express empirical data based on models of mathematical equations. Finding proper values for parameters of those equations is known as curve fitting.

The goal of curve fitting is to find the values of parameters for the mathematical models that most closely match the measured data. Simply speaking, curve fitting is seeking function parameters such that for certain values of independent variables, the dependent variables obtained from the function match the measured data, which can be obtained from experiments, simulations, or observation. The name curve fitting comes from the fact that if the function has only one independent variable, the given data set is often plotted as a curve on a two-dimensional plane. We are aiming to find the best curve that can not only approximate existing data values but also give reasonable prediction for those data points without measurements.

Complete curve fitting procedure comprises of two steps. First, selection of a proper model, i.e., a reasonable function, to fit the empirical data; and the second, determining the values of parameters in the function selected in step one, such that the function with these parameter values can best approximate the measured data. The model selection may or may not be dependent on the physical properties of the systems. In terms of the curve with the best values of parameters for a given model, it is the curve with parameters that minimize the deviation between the measured data and the expected value predicted by the function for the same measured points. The matching between the measured values and the computed values of the dependent variables can be either with or without errors.

Depending on the sizes of errors associated with the measured data, curve fitting can be divided into two general categories. The first class is regression, which is often applied when the measured data contains significant errors. As the values of measured

total number of nodes	average received packets per node (packets/s)
57	0.74
60	1.06
64	0.85
68	0.81
72	1.41
78	1.34
82	1.41
87	1.20
90	1.62
95	1.30
96	2.01

Table 5.1: Average received packets per node and the total number of nodes.

data are not accurate, we are more interested in the general trend of the data rather than the values at exact data points. Thus the curve is derived to match the overall behaviour trend of the whole set of available data points. On the other hand, if the existing data set is known to be very accurate, the second class of curve fitting can be applied, which fits a curve that matches the values of existing data points exactly. For the second type of fitting, the estimation of values within the range of a discrete set of known data points is called as interpolation, while the process to evaluate the function values of new data points outside the range of the known discrete data set is called extrapolation.

Regression can be further divided into linear and nonlinear regression, depending on whether the function is restricted to be linear combination of parameters to be estimated. Note that when the selected model only has one independent variable, the linear regression produces a function that is not only linear with regard to the parameters, but also linear to the independent variable. So the curve is a straight line for linear regression. Exact fitting can also be classified as either linear or nonlinear, depending on whether the selected function is linear to the independent variable or not. We illustrate these concepts by an artificial example of a WSN. In the example, we assume that experimental data, which measures the average received packets per node within one second under light random traffic load condition is obtained, for each value of total number of nodes in the WSN.

Table 5.1 shows the correspondence between the average received packets per node and the total number of nodes in the WSN. To derive the functional relationship between these two data sets, we do curve fitting.

The plot of the original data set is shown in Fig. 5.2(a), and the result of linear re-

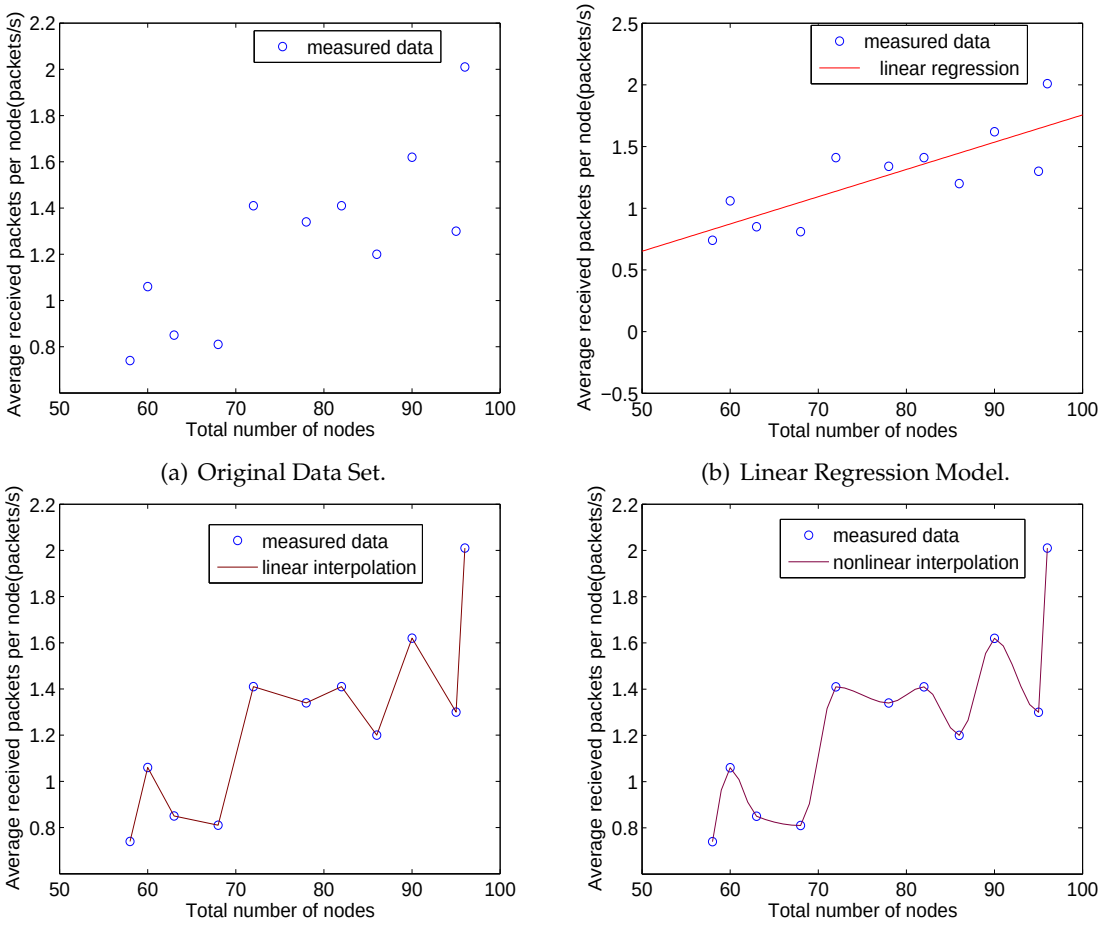

Figure 5.2: An illustration of different types of curve fitting.

gression is shown in Fig. 5.2(b). It is clear that regression only interprets the overall trend of the data, but without going through exactly those measured data points. The curve obtained by linear interpolation is shown in Fig. 5.2(c). A straight line segment that connects two concatenated data points form the linear function to approximate the data between these two points. If the data set contains more than two points, the curve obtained by linear interpolation is piecewise linear. Figure 5.2(d) demonstrates the result of nonlinear interpolation for the same set of data. As its name suggests, the curve connecting two consecutive data points need not be a straight line. Note that curves obtained through fitting may not be unique. It depends on the mathematical model selected to fit the measured data.

Exact fitting requires that the measured data contains no errors, which is a stringent condition. This constraint restricts the utilization of exact fitting and causes the wide usage of regression. In regression analysis, in order to derive the best parameter values for

the model, we need some functions of model parameters that can measure the closeness between the measured data and the model predicted values. The best curve is then obtained by minimizing this function with respect to the parameters. This function is called the test-of-fit function. Commonly used test-of-fit functions include least square function and Chi-square function. Basically, these two types of functions are similar. They all consider the aggregate effects of errors between each measured data point and the model predicted data value. As we are interested in the magnitudes of the errors, all errors are squared, and then are summed up. The difference is that Chi-square function is defined as a weighted difference between the observed data and the expected data. Another widely used method to compute the best curve is maximum likelihood estimation, which is the computation of the parameters that have the largest probability to generate the observed data. This method is mainly used to fit measured data to known probability distribution functions. Other estimation methods for regression analysis include Quasi-likelihood estimation, LAM estimator, L_1-norm minimization, robust estimation, and Bayesian estimation. See Seber and Wild [201] for a detailed discussion of these methods. In general, to assess the fitting results, a quantitative value named *goodness of fit* is applied. It is the fraction of the total discrepancy of the measured data with respect to the model. The smaller the value is, the better the fit.

Curve fitting that uses data obtained from experiments or simulation is a very common technique in many fields of science and engineering. Typical applications can be found in [44]. However, it is not pervasively applied in the study of networking. One existing work of the application of curve fitting in network research is the OSPF performance analysis by Cui *et al.* [57]. Tang *et al.* [211] also exploit curve fitting to study the connectivity of ad hoc networks by using Monte Carlo simulation to determine the probability of connectivity empirically. Nonetheless, the network scenarios they considered contain uniformly distributed nodes, which is different from our setting. In this chapter, we use curve fitting as a major tool to analyse the connectivity of the aforementioned network model.

5.4 Empirical Approach

In this section, we develop an empirical approach to evaluate the probability of connectivity for a given network, and conversely, to determine the number of nodes required to

maintain a certain level of connectivity. The results obtained from this approach can be applied to network design and provisioning.

As the maximum distance between two physically consecutive nodes corresponds to a sufficient statistic for the network connectivity, we investigate the network connectivity by estimating the distribution of this sufficient statistic. The estimation is readily performed by simulating a large number of n-tuples of sensor locations. We can empirically investigate the probability of connectivity by fitting a curve to the Cumulative Distribution Function (CDF) of the maximum distance between consecutive nodes. The parameters of this curve are again expressed as empirical functions of the problem parameters, by surface fitting.

5.4.1 Empirical Analysis

To investigate the probability of connectivity for a given network, we study the CDF of the maximum distance between physically consecutive sensors $\max_i(x_{(i+1)} - x_{(i)})$ by simulation. For a given sensor network, let $r_m = \max_i(x_{(i+1)} - x_{(i)})$. Note that the probability of connectivity is a function of the transmission range r, total number of nodes n, and the standard deviation σ of the distributions of node positions. The network is connected if and only if $r_m \leq r$. We have

$$\mathrm{P(C)}_{n,r,\sigma} = \mathrm{P}(r_m \leq r). \tag{5.2}$$

On the other hand, let n^* be the solution of optimization problem (5.1), which is the minimal value of n that satisfies the constraint: $\mathrm{P(C)}_{n,r,\sigma} \geq \mathrm{P}_{\text{target}}$, i.e., n^* is the smallest number of sensors required for our one-dimensional network to be connected with a prespecified probability $\mathrm{P}_{\text{target}}$. We also aim to find a good approximation for n^*.

To achieve these two goals, we empirically obtain the CDF of r_m parameterized by n and σ in two steps: 1) for many pairs (n, σ) the CDF of r_m is modelled by a parametric distribution; 2) the parameters of these distributions are expressed as functions of n and σ which leads to an approximate CDF of r_m that is applicable to a wide range of n and σ. The procedure is explained as follows.

5.4.2 Step 1: CDF Fitting of r_m

We consider $38 \times 26 = 988$ pairs (n, σ) with n = 10, 20, ..., 190, 200, 300, ... 2000 (38 values); σ = 0.005, 0.010, ..., 0.045, 0.05, 0.10,..., 0.85 (26 values). For each of these (n, σ) pairs we obtained 10^6 values of r_m by Monte Carlo simulation yielding an empirical CDF. The distribution function we select to fit is Log-Logistic distribution [135]

$$\mathrm{P}(r_m \leq x) = \frac{1}{1 + \exp\left[-(\log x - \alpha)/\beta\right]}. \tag{5.3}$$

The method to fit the Log-Logistic distribution function is the maximum likelihood estimation [135] [103]. For each pair of (n, σ), we can obtain a pair of parameters α and β after fitting.

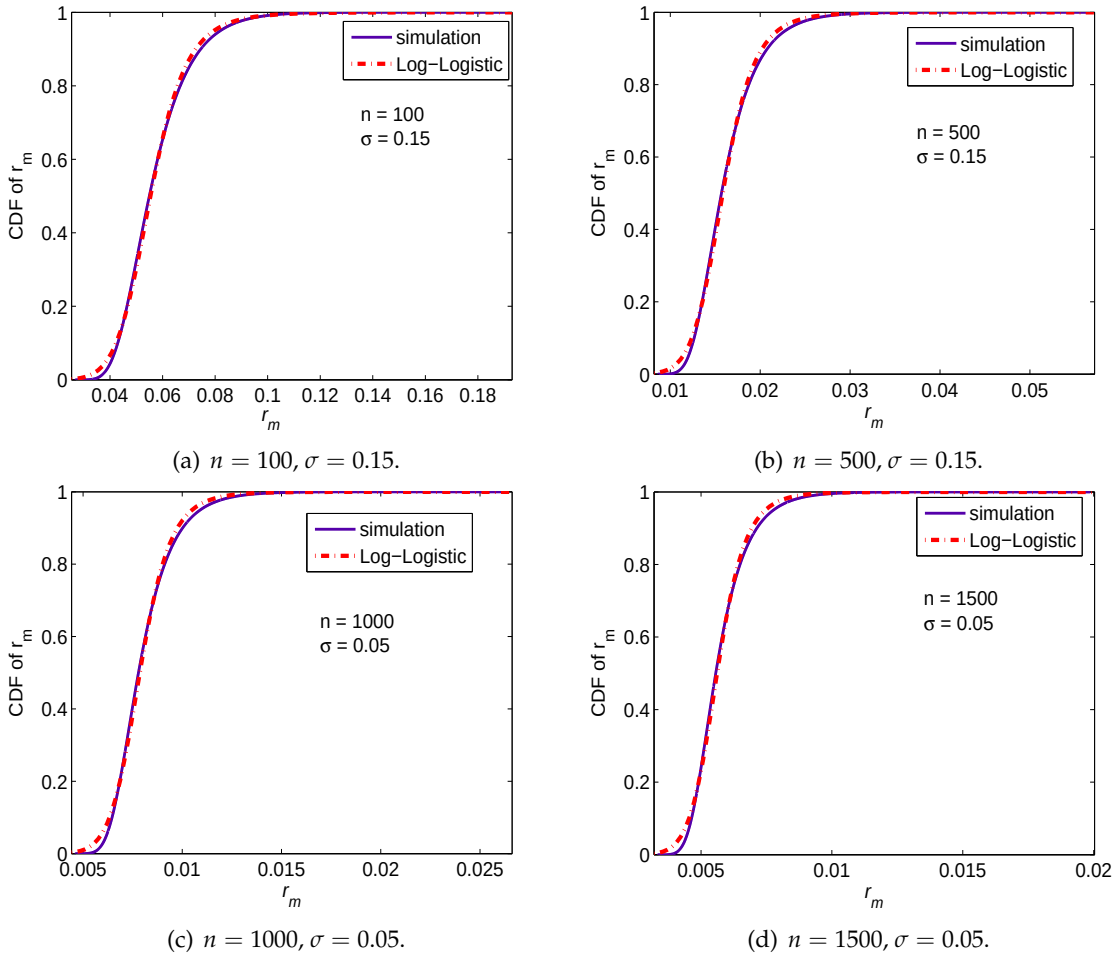

(a) $n = 100, \sigma = 0.15$. (b) $n = 500, \sigma = 0.15$.

(c) $n = 1000, \sigma = 0.05$. (d) $n = 1500, \sigma = 0.05$.

Figure 5.3: Illustrations of fitting of Log-Logistic distribution function to the CDF of r_m.

Fig. 5.3 shows some examples of the fitting results for the CDF of r_m. The four subfigures compare the empirical CDF of r_m obtained from simulations and the CDF of Log-

Logistic distribution after fitting the simulation data. The four different scenarios shown are (a) $(n = 100, \sigma = 0.15)$, (b) $(n = 500, \sigma = 0.15)$, (c) $(n = 1000, \sigma = 0.05)$, and (d) $(n = 1500, \sigma = 0.05)$, respectively. As shown by these examples, the empirical CDFs are well approximated by Log-Logistic distributions.

5.4.3 Step 2: Meta Fitting of Parameters of Log-Logistic Distribution

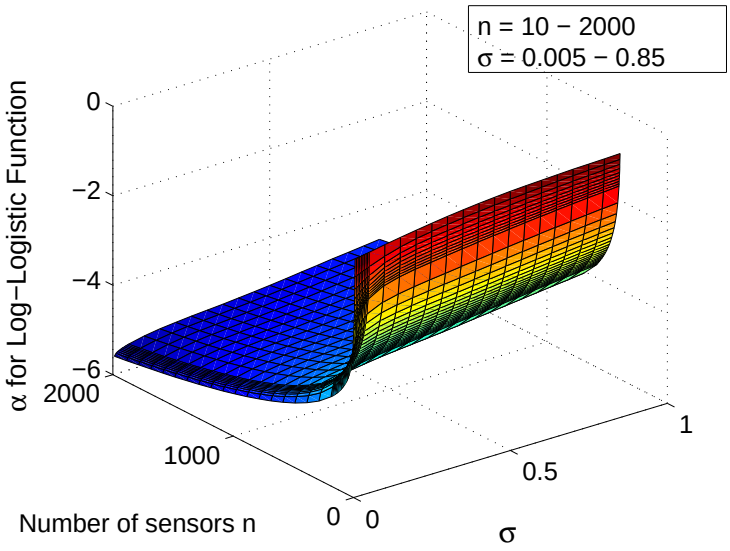

Figure 5.4: α as a function of σ and n

For each pair of (n, σ), we can obtain a pair of parameters α and β. Hence α and β are also functions of system parameter n and σ.

For all the α and β obtained after fitting the CDF of r_m, they are modelled as functions of the parameters (n, σ). Fitting is again applied to find the appropriate functions, such that we can express the probability of connectivity as a function of n, r, and σ, which also enables us to estimate the n^* numerically.

The graphs that illustrated α and β, obtained from the fitting of the CDF of r_m, as functions of n and σ are plotted in Figs. 5.4 and 5.5. As can be seen from these graphs, the surfaces of α and β have irregular shapes and no simple curves are found which fit these surfaces well for all n and σ. In particular, there are difficulties in cases of small values of n and σ which will be treated separately in the next section.

When $n \geq 10$ and $\sigma \geq 0.005$, the surface can be well approximated by piecewise

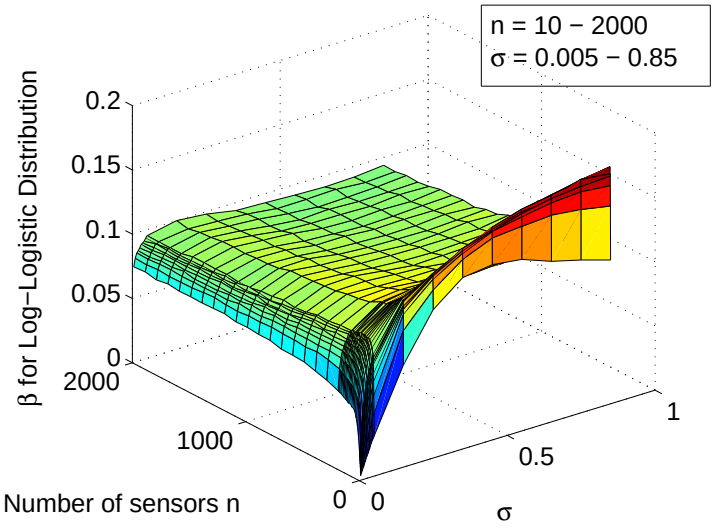

Figure 5.5: β as a function of σ and n

functions, with boundaries at $n = 200$ and $\sigma = 0.1$.[1] The four pieces are denoted xy, where $x = 0$ if $n < 200$ and $x = 1$ otherwise, and $y = 0$ if $\sigma < 0.1$ and $y = 1$ otherwise. Then, α and β are given by:

$$\alpha = \begin{cases} a_{11} + a_{12}\log n + a_{13}/\sqrt{\sigma}, & \text{in piece 00} \\ a_{21} + a_{22}\log n + a_{23}\sigma, & \text{in piece 01} \\ a_{31} + a_{32}\log n + a_{33}(\log\sigma)^2, & \text{in piece 10} \\ a_{41} + a_{42}\log n + a_{43}\sigma, & \text{in piece 11} \end{cases} \tag{5.4}$$

where a_{ij} are the elements of:

$$A = \begin{bmatrix} -0.05395 & -0.59031 & -0.06547 \\ 0.19443 & -0.69949 & 0.81407 \\ 0.70759 & -0.78886 & -0.01237 \\ 0.87847 & -0.82842 & 0.76975 \end{bmatrix},$$

[1] Because of the difficulties to predict the form of these functions, we utilize a software TableCurve 3D to accomplish this task. The best function is selected from more than 50,000 available functions.

and

$$\beta = \begin{cases} b_{11} + b_{12}\log n/n + b_{13}\sqrt{\sigma}\log\sigma, & \text{in pieces 00} \\ 1/(b_{21} + b_{22}(\log n)^2 + b_{23}\log\sigma), & \text{in pieces 01} \\ 1/(b_{31} + b_{32}\sqrt{n}\log n + b_{33}/\sqrt{\sigma}), & \text{in pieces 10} \\ b_{41} + b_{42}\log n + b_{43}\sigma^2\log\sigma, & \text{in pieces 11} \end{cases} \tag{5.5}$$

where b_{ij} are the element of matrix B given by:

$$B = \begin{bmatrix} -0.00732 & -0.12021 & -0.17869 \\ 5.11980 & 0.08831 & -0.71657 \\ 7.95398 & 0.00239 & 0.38936 \\ 0.18681 & -0.01173 & 0.02877 \end{bmatrix}.$$

From (5.4) and (5.5), we can calculate α and β, and substitute them into (5.3), giving

$$\mathrm{P}(r_m \leq r)_{n,\sigma} = \frac{1}{1 + \exp\left[-\frac{\log r - \alpha(n,\sigma)}{\beta(n,\sigma)}\right]} \equiv f(n, r, \sigma) \tag{5.6}$$

in which we define a function f of n, r, and σ by the CDF of Log-Logistic distribution and the fitting results of α and β. Indeed, f is the estimated probability of connectivity for given transmission radius r, number of nodes n, and node dispersion measure σ.

On the other hand, for given r, σ, and pre-specified $\mathrm{P}_{\text{target}}$, by letting $f(n, r, \sigma) = \mathrm{P}_{\text{target}}$, we can solve n from (5.6) numerically, yielding an approximation n_1 of n^*. In Fig. 5.6, we show an example, which compares the n_1 obtained by eq. (5.6), and n^* obtained by simulation, for $\sigma = 0, 0.01, 0.015, ..., 0.1$, $r = 0.1$, and $\mathrm{P}_{\text{target}} = 99\%$, to demonstrates that our approach gives a very accurate result in terms of n^*. It can be seen that n_1 and n^* match well. The results also indicate that even for small values of σ, i.e, small randomness in sensors locations, we have a large increment of n^* compared with $\sigma = 0$, the case that sensors are placed on the optimized locations precisely. This result confirms our motivation to introduce control mechanism in node placement rather than purely random node deployment.

To illustrate our approach, we consider σ = 0.004, 0.008, ..., 0.04; r = 0.002, 0.008, 0.014,..., 0.038. We compute n_1 by solving the equation $f(n, r, \sigma) = \mathrm{P}_{\text{target}}$ for n. For each n_1 obtained, we conduct Monte Carlo simulation using the corresponding r and σ

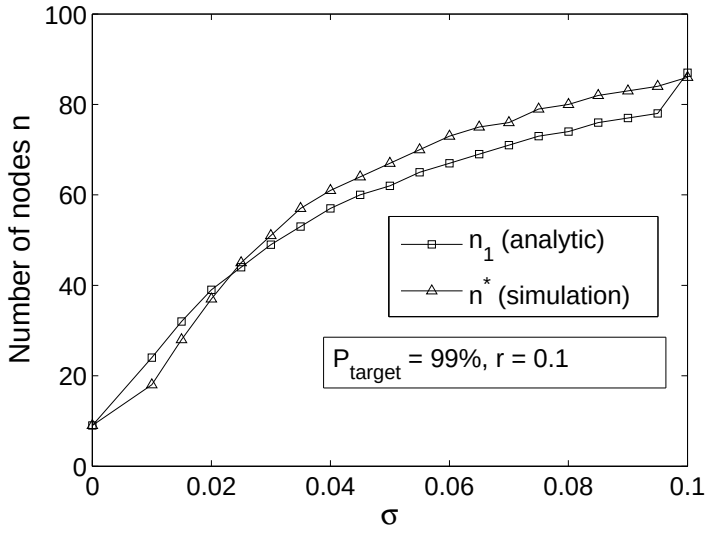

Figure 5.6: Analytical and simulation results for n.

to evaluate the probability of connectivity. Figure 5.7 demonstrates the intervals representing the range between the 5th percentile and the 95th percentile for $P_{target} = 0.91$, 0.94, 0.96, 0.98, 0.992, 0.995, and 0.998. The graph is plotted based on log scale. We set $P(C) = 1 - 10^{-6}$ if there is no disconnection in 10^5 samples. It is clear in Fig. 5.7 that our approach approximates the n^* accurately by n_1. However, as shown by the example, n_1 may be less than n^*, and it may not actually give connectivity with probability P_{target}.

5.4.4 Complementary Cases

As discussed in Subsection 5.4.3, there are difficulties in applying our fitting procedure to the cases of small n and σ. However, it is not difficult to obtain a very accurate approximation of n^* from simulation, when n^* is small, i.e., $n^* < 10$. So we only consider some important situations when σ is small in this subsection. We define $n_{\text{optimal}} = d/r - 1$, which is the necessary number of nodes to maintain connectivity when all the nodes are precisely placed on target positions.

Small σ, constant r: The smaller the σ is, the more precise are the locations of the sensors. If $\sigma = 0$, $n^* = n_{\text{optimal}}$. If $\sigma > 0$, but close to zero, adding a few relays to the value of $d/r - 1$ provides a good approximation for n^*. An approximation is given in the next section to obtain the n^* under small σ situations.

Small r, constant σ/r and $d = 1$: Interestingly, this case is equivalent to the case where r and σ are fixed and d increases to infinity. In Fig. 5.8, we present simulation

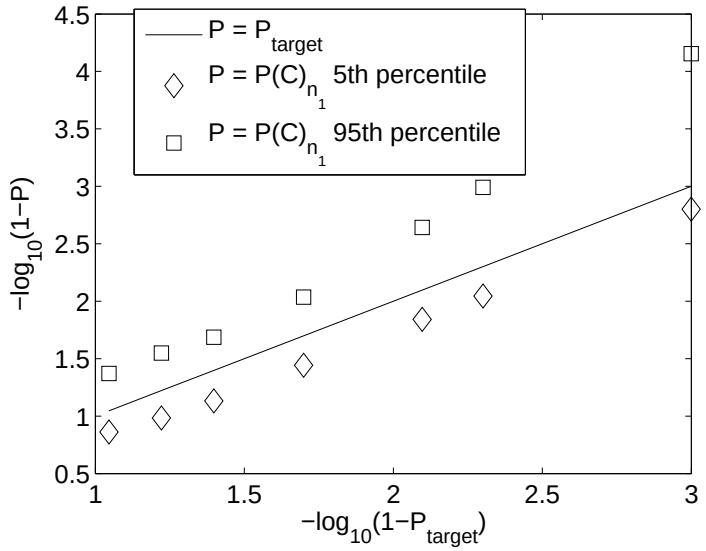

Figure 5.7: Simulation values for $\mathrm{P(C)}_{n_1}$.

results for n^* times r versus r. We demonstrate that for the case $\sigma/r = 1$, the value of n^*r is approximately constant (except for very small values of r, which correspond to unrealistically many nodes) as indicated by the roughly horizontal line. This behavior of n^*r versus r can be interpreted as follow: given constant small r and σ, the number of hops needed, n^*, is roughly proportional to the distance covered, d. When n^* is very large, there is an increased probability that one hop is much longer than the mean. This requires an increased margin $r - d/n^*$, causing n^*r to increase if r is very small.

Small r and fixed σ: Small r values indicate cheap low power sensors. It is of interest to study the trade off of number of sensors required versus their cost. In Fig. 5.9 we observe that n^*r increases as r decreases which indicates that the required number of sensors increases faster than r decreases. If a sensor cost function of r is available, results such as those of Fig. 5.9 could be used to optimize n.

In the next section, a simple but accurate approximation is proposed to obtain n^* when σ is small. Alternatively, it also can be used to derive required σ given the number of available sensors n, and the transmission radius r. This problem corresponds to an important problem in practice, that is, given the number of available nodes, and transmission radius r of each node, how much is the tolerable randomness in sensor placement that the network can still achieve required probability of connectivity.

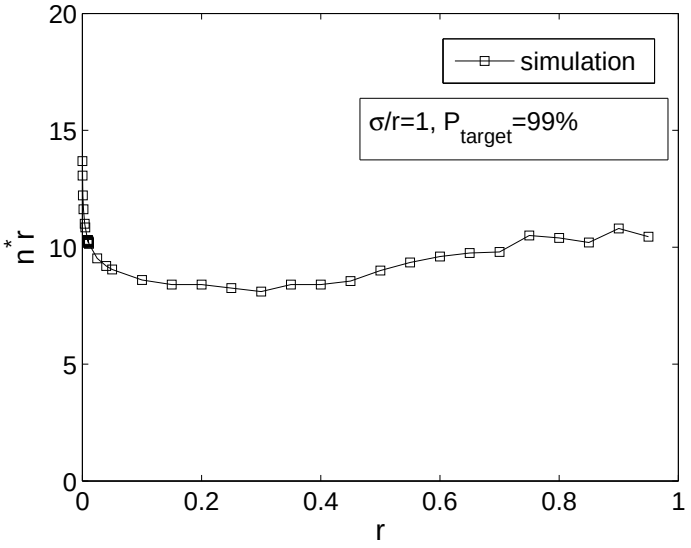

Figure 5.8: Behavior of n^*r versus r.

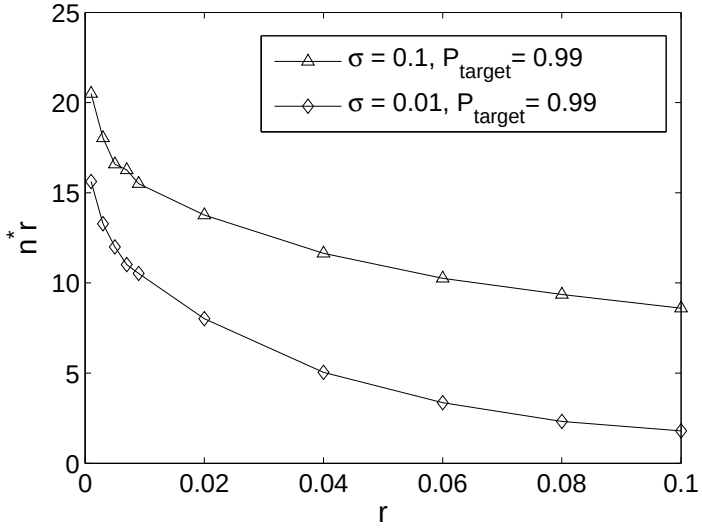

Figure 5.9: n^*r versus r under fixed σ.

5.5 Approximation for Small Perturbation of Node Positions

As mentioned before, even small σ leads to a large increment of n^*, compared with the n_{optimal}. We are interested in the relationship between the increment of σ, and the increment of the number of sensors, particularly, when σ is small compared with $d/(n+1)$.

We assume that all nodes do not cross over and hop lengths between adjacent nodes are independent with each other. This is because when σ is small compared with $d/(n+1)$, it is uncommon for nodes to be reordered, i.e., $x_i = x_{(i)}$, and distances between any adjacent two nodes are approximately independent.

5.5.1 A Simple Approximation for Connectivity Probability

We introduce a simple and straightforward approximation in this section to evaluate the probability of connectivity for small σ scenario.

The sufficient and necessary conditions for the network to be connected are:

$$\begin{cases} d \le r, \\ |x_{(i+1)} - x_{(i)}| \le r, \quad \text{for } i = 0, 1, ..., n. \end{cases} \quad \text{or}$$

The first condition means that the source destination pair is directly connected, and the second condition indicates that communication is conducted through a multi-hop fashion.

In this thesis, we assume $d > r$ to avoid the triviality. Under this assumption, intermediate relays are required. The network is connected if and only every pair of adjacent sensor nodes are connected, which is:

$$\mathrm{P}(\mathrm{C})_{n,r,\sigma} = \mathrm{P}\left(\bigcap_{i=0}^{n}\left(|x_{(i+1)} - x_{(i)}| \le r\right)\right) \tag{5.7}$$

In eq. (5.7), the values of $\left|x_{(i+1)} - x_{(i)}\right|$ and $\left|x_{(i+2)} - x_{(i+1)}\right|$ are dependent, for $i = 0, 1, ..., n$, because they have a common term $x_{(i+1)}$. However, in the scenario we are considering, i.e., $\sigma \ll d/(n+1)$, we assume that $\left|x_{(i+1)} - x_{(i)}\right|$ and $\left|x_{(i+2)} - x_{(i+1)}\right|$ are independent. We also assume that nodes do not cross over. According to these assumptions, eq. (5.7) reduces to

$$\begin{aligned} \mathrm{P}(\mathrm{C})_{n,r,\sigma} &= \mathrm{P}\left(\bigcap_{i=0}^{n}\left(|x_{i+1} - x_i| \le r\right)\right) \\ &= \prod_{i=0}^{n}\mathrm{P}\left(|x_{i+1} - x_i| \le r\right) \end{aligned} \tag{5.8}$$

It is easy to see that $x_{i+1} - x_i$ are Gaussian distributed since all x_i (except the positions of the source and destination nodes) are Gaussian random variables. The probability that the distance between two adjacent nodes is not longer than the transmission range r is given by

$$\begin{aligned} & \mathrm{P}(|x_{i+1} - x_i| \leq r) \\ = & \int_{-r}^{r} \frac{1}{2\sigma\sqrt{\pi}} \exp\left[-(y - \frac{1}{n+1})^2/4\sigma^2\right] dy, \qquad \text{for } i = 1, 2, ..., n-1, \end{aligned} \tag{5.9}$$

and

$$\mathrm{P}(|x_1| \leq r) = \int_{-r}^{r} \frac{1}{\sqrt{2\pi}\sigma} \exp\left[-(y - \frac{1}{n+1})^2/2\sigma^2\right] dy, \tag{5.10}$$

for the first hop, and

$$\mathrm{P}(|1 - x_n| \leq r) = \int_{-r}^{r} \frac{1}{\sqrt{2\pi}\sigma} \exp\left[-(y - \frac{1}{n+1})^2/2\sigma^2\right] dy, \tag{5.11}$$

for the last hop.

Combing (5.8), (5.9), (5.10) and (5.11) yields the following results:

$$\begin{aligned} \mathrm{P}(\mathrm{C})_{n,r,\sigma} = & \prod_{i=1}^{i=n-1} \int_{-r}^{r} \frac{1}{2\sigma\sqrt{\pi}} \exp\left[-(y_i - \frac{1}{n+1})^2/4\sigma^2\right] dy_i \\ & \times \int_{-r}^{r} \frac{1}{\sqrt{2\pi}\sigma} \exp\left[-(y - \frac{1}{n+1})^2/2\sigma^2\right] dy \\ & \times \int_{-r}^{r} \frac{1}{\sqrt{2\pi}\sigma} \exp\left[-(y - \frac{1}{n+1})^2/2\sigma^2\right] dy. \end{aligned} \tag{5.12}$$

Note that in eqs. (5.9) to (5.12), there is no parameter d, as it is scaled to 1. With eq. (5.12), we can numerically evaluate the probability of connectivity for a given network approximately when $\sigma \ll d/(n+1)$. We demonstrate validity of our approximation by conducting simulations.

5.5.2 Simulations and Numerical Results

To demonstrate the validity of our approach, we evaluate the probability of network connectivity through Monte Carlo simulations, and compare with the results obtained by eq. (5.12). Examples are demonstrated with following network parameters: $(r = 0.2, \sigma = 0.01)$, $(r = 0.2, \sigma = 0.05)$, $(r = 0.4, \sigma = 0.05)$, $(r = 0.4, \sigma = 0.08)$, and $(r = 0.4, \sigma = 0.15)$. Results are shown in Figs. 5.10 to 5.14.

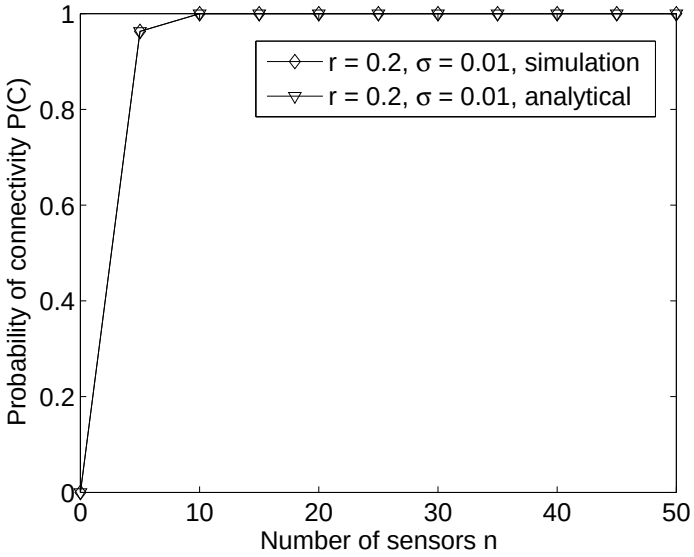

Figure 5.10: Comparison of connectivity probability, $r = 0.2$, $\sigma = 0.01$

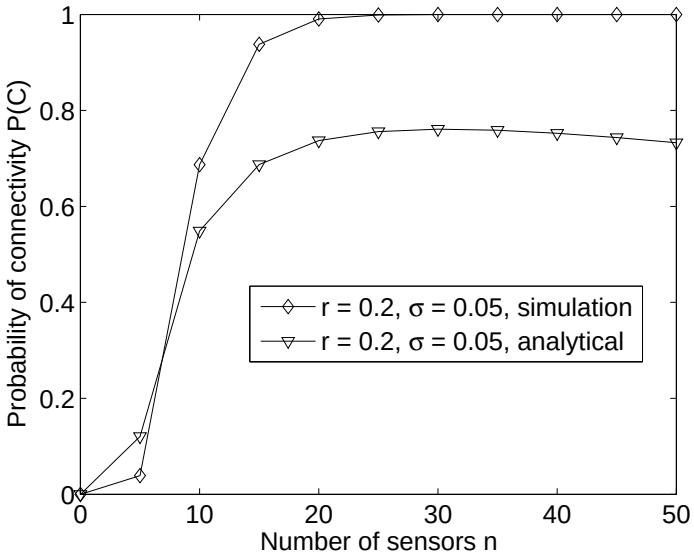

Figure 5.11: Comparison of connectivity probability, $r = 0.2$, $\sigma = 0.05$

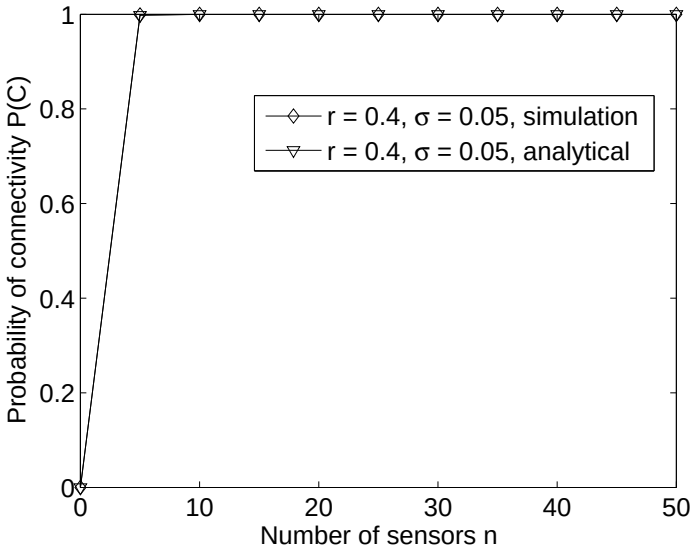

Figure 5.12: Comparison of connectivity probability, $r = 0.4$, $\sigma = 0.05$

We can see from these examples that when σ is small compared with $d/(n+1)$, eq. (5.12) can accurately predict the probability of connectivity, whereas large σ breaks the validity of this model. It is also shown that the decrease of connectivity probability caused by the increase of σ can be compensated by longer transmission radius r. In particular, as shown in Fig. 5.14, for large σ, eq. (5.12) does not yield a monotonic function. This is because large σ results in high randomness of nodes locations, which may lead to the crossover of node locations. Moreover, the assumption that the distances between adjacent nodes are independent is no longer valid.

These comparisons between simulation and analytical results show that our model is a good approximation to the probability of connectivity when σ is relative small compared to transmission range r and $d/(n+1)$. Although our model shows the validity for small σ, however, it only evaluates the connectivity probability for a given set of parameters but does not answer the question that how much perturbation on the node positions can be tolerated such that the network still provides required probability of connectivity with given number of nodes and transmission radius. In the next subsection, we propose another approximation which can answer this question.

5.5.3 Approximation to Compute Position Offset σ

Let p be the probability of an arbitrary pair of adjacent nodes being disconnected, hence $1-p$ denotes the probability that these two nodes are connected. When $\sigma \ll d/(n+1)$

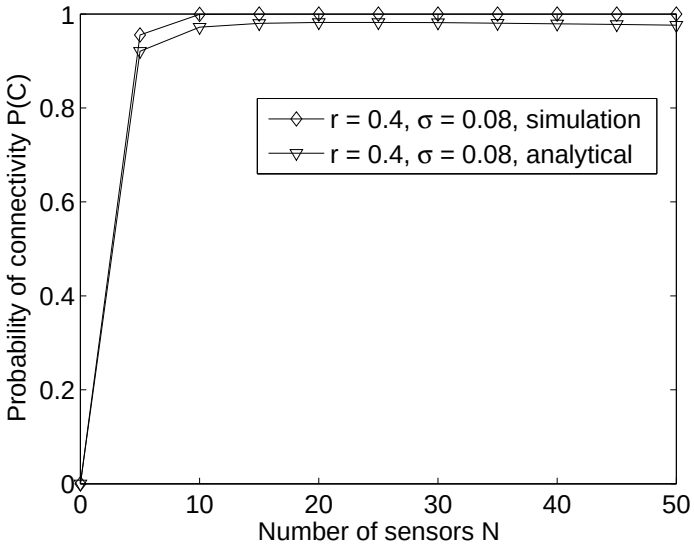

Figure 5.13: Comparison of connectivity probability, $r = 0.4$, $\sigma = 0.08$

and $\sigma \ll r$, p is small.

Since we approximate all the distances between adjacent nodes to be independent of each other, for n intermediate nodes in the network, we have $n-1$ independent distances (ignoring the edge effects). The network is connected only if all these $n-1$ distances are less than or equal to the transmission range r, whose probability is given by $1-p$. Therefore, the probability of connectivity is given by

$$\mathrm{P(C)} \approx (1-p)^{n-1} \tag{5.13}$$

By solving this equation, we can have

$$p \approx 1 - \exp\left[\log \mathrm{P(C)}/(n-1)\right] \tag{5.14}$$

Given n relays, and a required probability of connectivity $\mathrm{P_{target}}$, substitute it in eq. (5.14) for $\mathrm{P(C)}$, we can compute p. If we can manipulate the expression for p through the knowledge of node distribution, combining with eq. (5.14), we can evaluate the node position offset σ. Next we derive the expression for p in this case.

We assume that the left node of a pair of adjacent nodes is the i^{th} node. Let X be the random variable to represent its position, correspondingly $f_X(x)$ and $F_X(x)$ denote the pdf and CDF of X, respectively. Similarly, let random variable Y represent the position of the right node of the pair, denote the pdf and CDF of Y by $g_Y(y)$ and $G_Y(y)$, respectively.

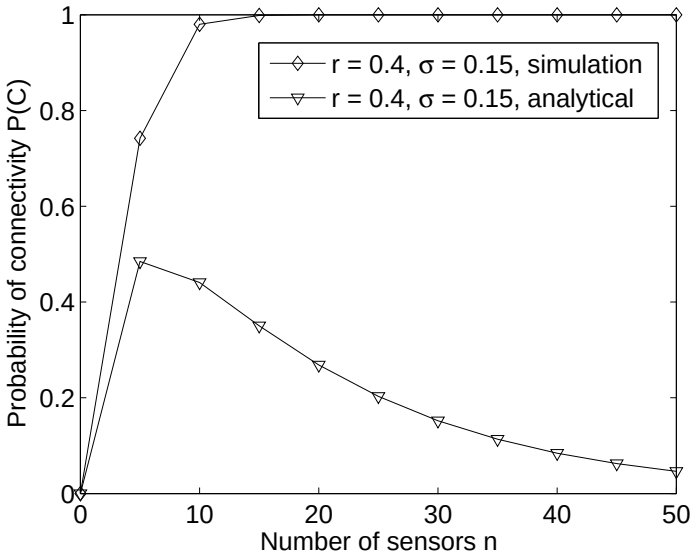

Figure 5.14: Comparison of connectivity probability, $r = 0.4$, $\sigma = 0.15$

Let $Z = Y - X$ be the distance between these two nodes. Denote the pdf and CDF of Z by $h_Z(z)$ and $H_Z(z)$. Let $R = -X$, and denote the pdf of R by $q_R(r)$. We have $q_R(r) = f_X(-r)$, hence $Z = Y - X = Y + R$, and $h_Z(z)$ is given by

$$\begin{aligned} h_Z(z) &= \int_{-\infty}^{\infty} g_Y(t) q_R(z-t) dt \\ &= \int_{-\infty}^{\infty} g_Y(t) f_X(t-z) dt \end{aligned} \tag{5.15}$$

Therefore,

$$\begin{aligned} p &= 1 - \int_{-\infty}^{1} \int_{-\infty}^{\infty} g_Y(t) f_X(t-z) dt dz \\ &= 1 - \int_{-\infty}^{\infty} \int_{-\infty}^{1} g_Y(t) f_X(t-z) dz dt \\ &= 1 - \int_{-\infty}^{\infty} F_X(t-1) g_Y(t) dt \end{aligned} \tag{5.16}$$

Equation (5.16) gives a general expression for p. Note that eq. (5.16) is valid for any distribution for X and Y.

For the case we are studying, X and Y follow Gaussian Distribution hence $f_X(x) = f(x)_{\mu_i,\sigma}$ and $f_Y(y) = f(y)_{\mu_{i+1},\sigma}$, where $f(x)_{\mu,\sigma}$ is given by

$$f(x)_{\mu,\sigma} = \frac{1}{\sqrt{2\pi}\sigma} \exp\left[-(x-\mu)^2/2\sigma^2\right] \tag{5.17}$$

In addition to eq. (5.16), we can also derive the pdf of Z via transform methods. Let $M_X(t)$ be the moment generating function of X. Accordingly,

$$M_X(t) = \exp\left[\mu_i t + (\sigma t)^2/2\right], \tag{5.18}$$

$$M_Y(t) = \exp\left[\mu_{i+1} t + (\sigma t)^2/2\right], \tag{5.19}$$

Therefore, the $M_Z(t) = M_Y(t)M_{-X}(t)$, which is given by

$$M_Z(t) = \exp\left[(\mu_{i+1} - \mu_i)t + (\sigma t)^2\right] \tag{5.20}$$

Notice that $\mu_{i+1} - \mu_i = 1/(n+1)$, we have $M_Z(t) = \exp\left[(1/(n+1))t + (\sigma t)^2\right]$. It means that Z is another Gaussian random variable with mean $\mu = 1/(n+1)$ and variance $2\sigma^2$. It has the CDF

$$F(z) = \frac{1}{2\sigma\sqrt{\pi}} \int_{-\infty}^{z} \exp\left[-(t - \frac{1}{n+1})^2/4\sigma^2\right] dt \tag{5.21}$$

which also gives the expression of p as

$$p = 1 - F(r). \tag{5.22}$$

From eq. (5.21) we know that if $\sigma \ll r - \frac{1}{n+1}$, $p = 1 - F(r)$ is close to zero, and the network is connected with high probability.

Combining eqs. (5.14) and (5.22), we can approximately derive some network design parameters such as the sensor placement variance parameter σ so that we need some certain amount more nodes than the amount when we place nodes on their optimal positions, while keeping a constant $\mathrm{P}_{\mathrm{target}}$.

To verify our approximation approach, we calculate p from (5.14) for given $\mathrm{P}_{\mathrm{target}}$ and n, solve σ from p, then do simulation to obtain the probability of connectivity. The probability is compared to the $\mathrm{P}_{\mathrm{target}}$. As the example shown in Fig. 5.15, the approximation gives very accurate results for small σ. In this example, n is arbitrarily chosen to be $n = 1.21 n_{\mathrm{optimal}}$.

As shown in Section 5.4.1, 5.4.4 and 5.5, for a wide range of n and σ, we provide solutions to evaluate the probability of connectivity, and to obtain the minimum number of nodes to achieve predefined network connectivity probability. We also propose a simple

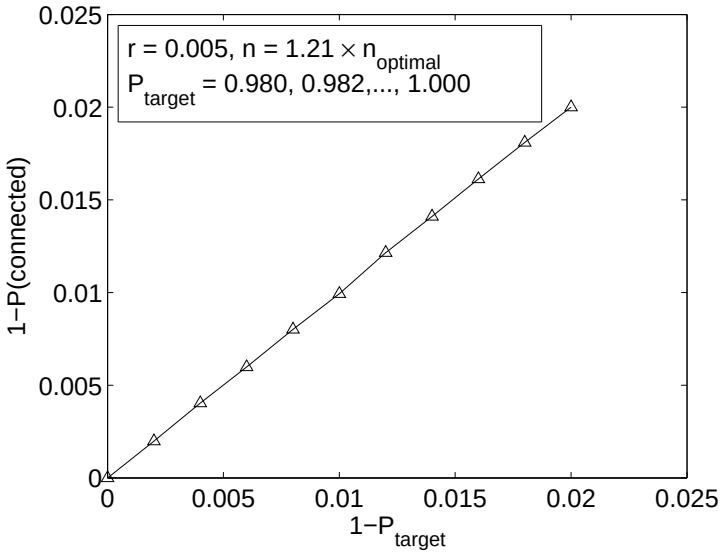

Figure 5.15: Simulation values for complementary $P(C)$ versus complementary P_{target} for small σ

but accurate approximation to compute the maximum allowable randomness of sensor placement given a certain number of nodes. The approach is accurate when the number of nodes is not very different from the number of nodes needed in deterministic sensor placement. This is equivalent to the situation where sensors are expensive, and so the placement needs to be carefully planned.

5.6 Networks with Laplacian Distributed Nodes

In this section, we study a network with all nodes distributed according to Laplace distributions (Double Exponential distributions) [128] with identical variance and equally spaced expectations. This network is similar to the one we have investigated, except all nodes are distributed according to Laplace distributions instead of Gaussian distributions. We want to study the impact of the distribution of node locations on the network connectivity. A similar empirical approach is adopted. Because the Laplace distribution has a much heavier tail than that of the Gaussian distribution, we consider a sensor network in which all nodes follow Laplace distributions in this section. The probability density function of Laplace distribution is

$$f(x) = \frac{1}{2\sigma} \exp\left[-\left|x-\mu\right|/\sigma\right], \tag{5.23}$$

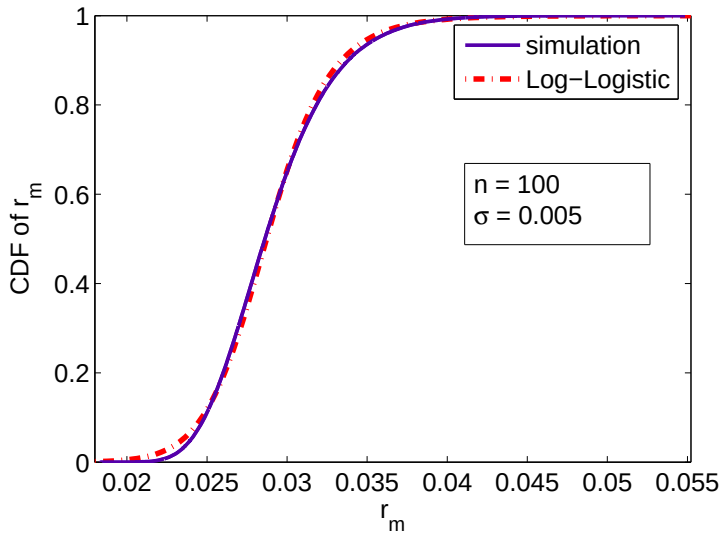

Figure 5.16: Curve fitting of CDF of r_m for a network with Laplacian distributed nodes.

in which μ is the mean, and σ is the standard deviation.

The sensor placement model is similar to the model shown in Fig. 5.1. However, locations of all the nodes follow Laplace distributions instead of Gaussian distributions. Using the same empirical approach described before, we can obtain an approximation of n^*, denoted by n_2, as follows.

Fitting the CDF of the maximum distance between physically consecutive nodes: We consider the same 988 pairs of parameters (n, σ) as used in Subsection 5.4.2. We conduct Monte Carlo simulation and generate empirical CDF of the maximum distance between physically consecutive nodes for each pair of (n, σ). As the example illustrated in Fig. 5.16, these CDFs are again well approximated by Log-Logistic distributions. The CDF of Log-logistic distribution was given by eq. (5.3).

For each pair of (n, σ), we can obtain a pair of parameters α and β after fitting.

Meta Fitting: Fitting α and β as functions of the parameters n and σ. However, β cannot be well expressed by a single function. Let the "piece xy" notation be the same as in section 5.4.3, in which $x = 0$ if $n < 200$ and $x = 1$ otherwise, and $y = 0$ if $\sigma < 0.1$ and $y = 1$ otherwise. Hence, we have β as a piecewise function.

When $n \geq 10$ and $\sigma \geq 0.005$, the surface of α and β can be well approximated by:

$$\alpha = a_1 + a_2 \log n + a_3 \sqrt{\sigma} \tag{5.24}$$

$$\beta = \begin{cases} b_{11} + b_{12}\sigma^{2.5} + b_{13}\sqrt{\sigma}\log\sigma, & \text{in pieces 00} \\ 1/(b_{21} + b_{22}(\log n)^2 + b_{23}\sqrt{\sigma}), & \text{in pieces 01} \\ 1/(b_{31} + b_{32}\sqrt{n} + b_{33}/\sqrt{\sigma}), & \text{in pieces 10} \\ 1/(b_{41} + b_{42}\log n + b_{43}\sigma\log\sigma), & \text{in pieces 11} \end{cases} \tag{5.25}$$

where a_i is listed in table 5.2 and b_{ij} are the element of matrix K given by:

Table 5.2: a_i

	i		
Parameters	1	2	3
a_i	0.10570042	-0.75547991	1.0780847

$$K = \begin{bmatrix} 0.019728 & 1.0062285 & -0.1301619 \\ 7.1305944 & 0.08837203 & -2.1444418 \\ 7.7860075 & 0.031850892 & 0.33342419 \\ 2.022401 & 1.0863066 & -1.0514925 \end{bmatrix}$$

From (5.24) and (5.25), we can compute α and β, and substitute them into (5.3), yielding

$$\mathrm{P}(r_m < r)_{n,\sigma} = \frac{1}{1 + \exp\left[-\frac{(\log r - \alpha(n,\sigma))}{\beta(n,\sigma)}\right]} \equiv f_1(n, r, \sigma). \tag{5.26}$$

For a pre-specified connectivity probability $\mathrm{P}_{\text{target}}$, the solution n_2 of $\mathrm{P}_{\text{target}} = f_1(n, r, \sigma)$ for n, with given r, σ, and $\mathrm{P}_{\text{target}}$, is an approximation of n^*.

5.6.1 Numerical and Simulation Results

To demonstrate the validity of our approach, we consider σ = 0.004, 0.008, ..., 0.04; r = 0.002, 0.008, 0.014,..., 0.038. For each pair of (r, σ), we compute n_2 by solving the equation $\mathrm{P}_{\text{target}} = f_1(n, r, \sigma)$ for n. We then conduct Monte Carlo simulation using the corresponding r and σ, for each n_2 obtained, to evaluate the probability of connectivity. We plot the 5th and 95th percentile for probability of connectivity in loglog scale graph Fig. 5.17. The probability of disconnect is set to 10^{-6} if there is no disconnection in 10^5 samples. It can be seen from Fig. 5.17 that our empirical approach can produce reasonable estimates for

n^*.

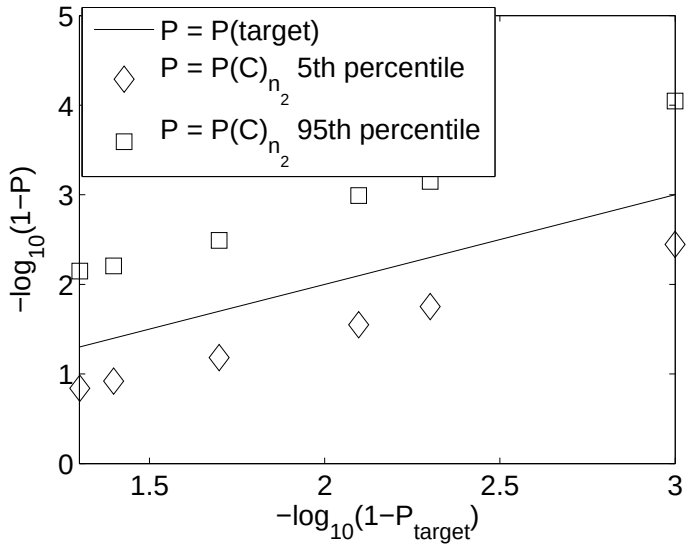

Figure 5.17: Simulation values for $\mathrm{P(C)}_{n_2}$.

As a comparison, Fig. 5.18 compares the numbers of nodes required, which are obtained from eq. (5.26) and simulations, respectively, when σ is small and $\mathrm{P}_{\mathrm{target}}$ is high. The results show good agreement. It is also indicated that even for small randomness in the positions of nodes, there is a large increment in the number of nodes needed compared with the number of nodes needed when all the nodes are placed in their optimized locations, which is consistent with the situations that all nodes are Gaussian distributed.

In order to compare the impacts of different distributions of nodes on the connectivity of networks, we conduct simulations to obtain n^*, for networks with nodes distributed according to both Gaussian and Laplace distributions. We compare the n^* obtained for these two different scenarios, when other system parameters are the same, i.e., transmission range r and standard deviation σ are the same. We show examples in Fig. 5.19, in which n^* are obtained for networks with $r = 0.05$ and 0.1, while the target probability of connectivity are set to 98% and 99%.

We can observe an interesting result. If the standard deviation is identical for both Gaussian and Laplace distribution, the number of Gaussian distributed nodes required is less than those for Laplace distributions when σ is small, while we need more Gaussian distributed nodes than Laplace distributed nodes as σ becomes large. This phenomenon can be interpreted as follows. When σ is small, to get a disconnect network, the positions of some nodes need to be far away from the mean, which is more likely to happen

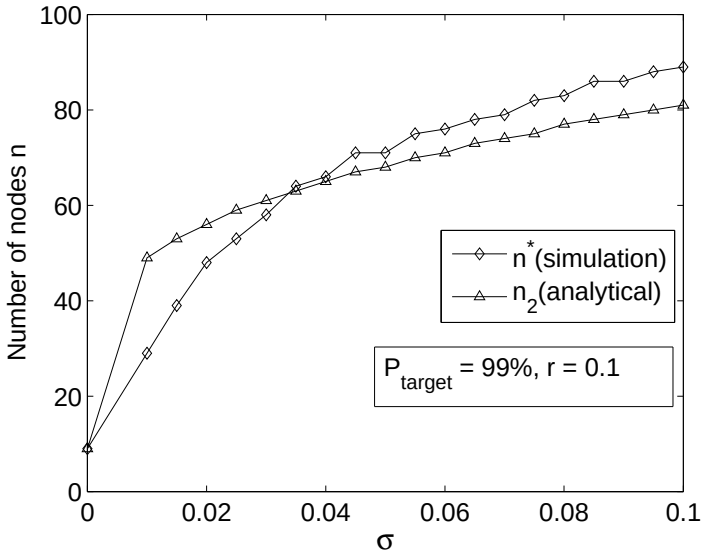

Figure 5.18: Analytical and simulation results for n^*.

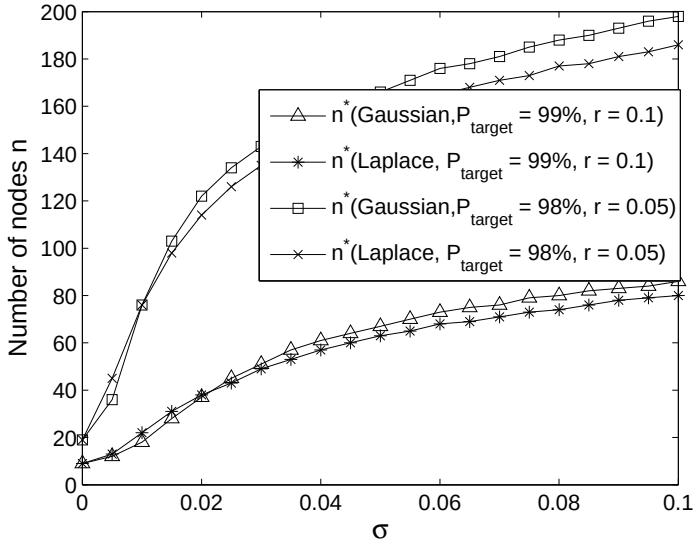

Figure 5.19: Comparison for simulation results of n^* for Gaussian distributed and Laplace distributed sensors.

for Laplace distribution as it has a heavier tail than Gaussian distribution has. When σ is large, the typical events account for the major part of disconnection. As the Laplace distribution is more concentrated on the mean, we need more nodes for Gaussian distribution. We also notice that for the same network design parameters, the number for Lapalcian distributed nodes is quite close to the number of Gaussian distributed nodes needed. Therefore, we conjecture that as long as the distributions that nodes followed are symmetric about the mean, the number of sensors needed to maintain certain probability of connectivity is not very sensitive to the distributions.

5.7 A Network Design Algorithm

Even though the empirical analysis can produce an approximation n_1 (or n_2) of n^*, it cannot guarantee that the approximation is conservative, i.e., the n_1 may be less than the n^* even they are very close. A design approach that can provide conservative estimation of n^* is thus expected. In this section, we propose an algorithm, intended to provide a conservative design.

Estimating n^* through the proposed empirical approach may not achieve the design objective of having the network connected with probability $\mathrm{P}_{\text{target}}$ since it is possible to underestimate n^* with grave consequences. One way to be more conservative is to approximate n^* by estimating $\hat{n}$ defined as the minimum number of nodes required to achieve a connectivity probability of $\hat{\mathrm{P}}$ such that $\mathrm{P}_{\text{target}} \leq \hat{\mathrm{P}} \leq 1$ using the above empirical procedure, which gives another value n_c. The $\hat{n}$ is the solution of optimization problem (5.1) with $\mathrm{P}_{\text{target}} = \hat{\mathrm{P}}$, and n_c is the solution of equation $f(n, r, \sigma) = \hat{\mathrm{P}}$ for n. Unfortunately, this may not be sufficient as shown by the following example. Consider the most conservative case of $\hat{\mathrm{P}} = 1$. If $\sigma = 0$ then $\mathrm{P}(\mathrm{C}|n = n^* = n_{\text{optimal}}) = 1$, but also $\mathrm{P}(\mathrm{C}|n = n^* - 1) = 0$. Thus, underestimating n^* by as little as one, yields a very low connectivity probability. Therefore, in order to find a conservative estimate of n^*, we choose $\hat{\mathrm{P}} > \mathrm{P}_{\text{target}}$, we estimate $\hat{n}$ and add safety margin which considers the error in estimating $\hat{n}$. This is summarized as follows.

Proposition 5.7.1. *Let $\hat{n}$ and n_c take the meaning as previously defined, and define $\eta = (\hat{n}/n_c) - 1$ be the fitting error. Let $\bar{\eta}$ be such that*

$$\mathrm{P}(\eta \leq \bar{\eta}) > \mathrm{P}_{\text{target}}/\hat{\mathrm{P}}. \tag{5.27}$$

Let $n_d = n_c(1+\bar{\eta})$. *Then*

$$\mathrm{P}(\mathrm{C}|n = n_d) \geq \mathrm{P}_{\text{target}}. \tag{5.28}$$

Proof.

$$\begin{aligned} \mathrm{P}(n_d \geq \hat{n}) &= \mathrm{P}\left(n_c(1+\bar{\eta}) \geq \hat{n}\right) \\ &= \mathrm{P}\left((1+\bar{\eta}) \geq (1+\eta)\right) \\ &= \mathrm{P}(\bar{\eta} \geq \eta). \end{aligned} \tag{5.29}$$

By the Law of Total Probability:

$$\begin{aligned} \mathrm{P}(\mathrm{C}|n = n_d) &\geq \mathrm{P}(\mathrm{C}|n = n_d \geq \hat{n})\mathrm{P}(n_d \geq \hat{n}) \\ &\geq \hat{\mathrm{P}}\,\mathrm{P}(n_d \geq \hat{n}). \end{aligned} \tag{5.30}$$

Therefore,

$$\begin{aligned} \mathrm{P}(\mathrm{C}|n = n_d) &\geq \hat{\mathrm{P}}\mathrm{P}(\bar{\eta} \geq \eta) \\ &\geq \mathrm{P}_{\text{target}}. \end{aligned} \tag{5.31}$$

□

The empirical distribution of η, for a given $\hat{\mathrm{P}}$ and many σ, n_c, and r values can then be calculated. This is shown for $\hat{\mathrm{P}} = 0.95, 0.99$ and 0.9995 in Fig. 5.20 for the scenario that all nodes are Gaussian distributed. Note that the empirical CDF of η is affected by the sampling scheme of σ and r selected by the network designer. Figure 5.20 is for $\sigma = 0.004, 0.0044, ..., 0.04$ and $r = 0.002, 0.0024, ..., 0.036$.

Combining (5.27), (5.29) and (5.30), a network containing n_d sensors is connected with probability at least $\mathrm{P}_{\text{target}}$. The algorithm can be summarized as Algorithm 3.

To illustrate our approach, we consider σ = 0.004, 0.008,..., 0.04; r = 0.002, 0.008, 0.014,..., 0.038. The intervals representing the range between the 5th percentile and the 95th percentile for $\mathrm{P}_{\text{target}} = 0.91, 0.94, 0.96, 0.98, 0.992, 0.995, 0.998$ are plotted in Fig. 5.21. We compare both the $\mathrm{P}(\mathrm{C})_{n_1}$ and $\mathrm{P}(\mathrm{C})_{n_d}$ via log scale. All the $\mathrm{P}(\mathrm{C})_{n_d}$ values are above $\mathrm{P}_{\text{target}}$, as we expected. We set $\mathrm{P}(\mathrm{C}) = 1 - 10^{-6}$ if there is no disconnection in 10^5 samples.

However, even though the examples show that our design approach can provide satisfactory performance, it still can not guarantee the n_d we obtained is conservative, be-

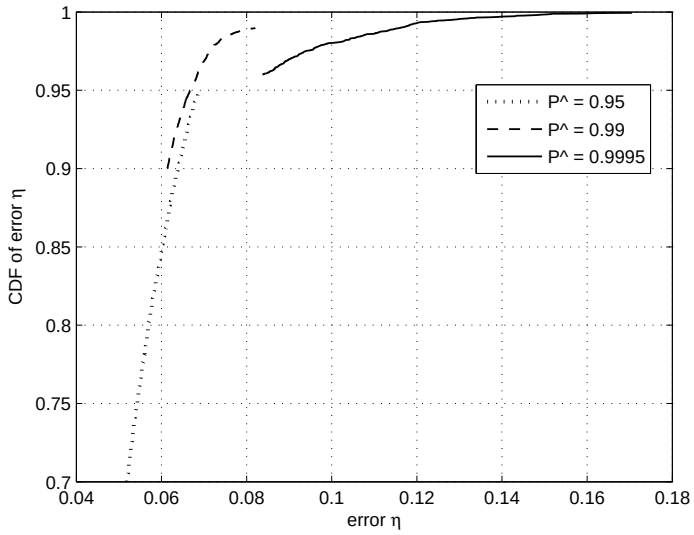

Figure 5.20: CDF of η.

Algorithm 3 Conservative Network Design Algorithm

Input: Nodes position spread data sheets such as shown in Fig. 5.20.
Output: A conservative estimate n_d of n^*.
1: $\hat{\mathrm{P}} = 0.95$, if $\mathrm{P}_{\mathrm{target}} < 0.95$, $\hat{\mathrm{P}} = 0.99$ if $\mathrm{P}_{\mathrm{target}} < 0.99$, $\hat{\mathrm{P}} = 0.9995$ otherwise.
2: Read the value of $\bar{\eta}$ from data sheets such Figure 5.20.
3: Calculate σ = location spread$/d$.
4: Solve $f(n, r, \sigma) = \hat{\mathrm{P}}$ for n, denote as n_c, where f is defined in (5.6).
5: Approximate n^* by $n_d = n_c(1 + \bar{\eta})$.
6: **return** n_d.

cause this approach depends on the sample scheme we used to produce the Fig. 5.20. In another word, it depends on how accurately that we can model the real CDF of error by the empirical CDF of error.

5.8 Conclusion

In this chapter, we have investigated the probability of connectivity for a 1-D network, in which all the nodes are randomly placed with equally spaced mean and i.i.d. variances σ^2. The positions of all the nodes follow double sided distributions that are symmetric about the mean.

By using an empirical approach, which is widely applied in different fields of science and engineering, we have obtained formulae to evaluate the probability of connectivity for a network given σ, number of nodes n, and node transmission range r. With those for-

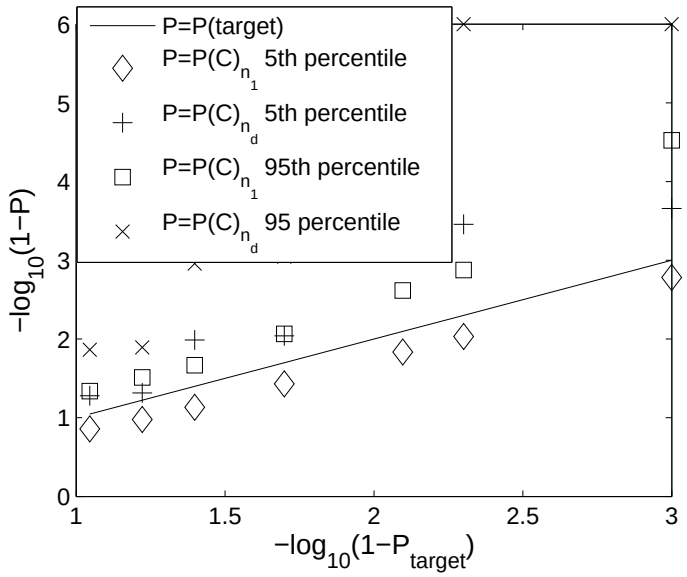

Figure 5.21: Simulation values for $P(C)_{n_1}$ and $P(C)_{n_d}$ versus P_{target}

mulae, we can numerically estimate the minimum number of nodes required to achieve a certain probability of connectivity, if network design parameters, such as σ and r are pre-specified. For the extreme cases in which the number of nodes required is very small, or the network is nearly deterministic, our empirical approach cannot be applied. However, we can obtain the necessary number of nodes needed easily by simulation if this number is small. Moreover, we have provided simple approximations to achieve the same goal when σ is small, and these approximations can accurately predict the probability of connectivity, as well as evaluate the required node placement accuracy to achieve network design targets.

We have studied networks in which all the nodes follow Gaussian distributions and Laplace distributions, through the empirical approach we proposed. Our studies have suggested that as long as the distribution that all sensor nodes followed is double sided and symmetric about the mean, the number of nodes required to maintain a pre-specified probability of connectivity is not very sensitive to the distribution, if all other network design parameters are the same. As our empirical approach does not provide a conservative estimate of the necessary number of nodes needed, the results it predicted may not be able to provide required probability of connectivity. Therefore, we have proposed an algorithm, aiming to provide a conservative estimate of the necessary number of nodes required to maintain the required probability of connectivity.

Chapter 6

Background for Passive Optical Networks

Motivated by the continuous demands for cheaper and faster broadband access solutions, we study Passive Optical Networks (PONs). In particular, we propose a generic planning approach for greenfield PON deployment in the second part of this thesis.

6.1 Introduction

With the ever-increasing user bandwidth demands for broadband services and the advances in backbone networks, copper and wireless access networks remain a bottleneck between end users and long haul backbones.

Current access networks can be classified into wireless, copper, and fibre access networks, according to the transmission media they use. Typical wireless technologies include WiMAX [5] [79], WiFi [141], and conventional Cellular systems [143], which can provide broadband access with low cost and much flexibility. The major limitations of wireless access are the low bandwidth and the short transmission range, due to the shared broadcasting wireless channel, and the dispersal, as well as the attenuation of the signal.

Copper access networks, based on DSL and Cable modem techniques, are currently the most widely deployed access networks. Compared to wireless access schemes, in general, copper based wired networks can provide higher bandwidth and longer transmission range. However, the typical bandwidth and transmission distances offered by copper access networks are still not satisfactory, e.g., even contemporary ADSL2+ standard [124] can only support up to 24 Mbps data rate over up to $23,000$ feet distance. Therefore, copper access technologies suffer similar drawbacks as their wireless counterparts.

In contrast to wireless and copper access technologies, fibre technology is an emerging promising option that can provide broadband access services through fibre to the home (FTTH), curb (FTTC), and business (FTTB) systems (generically abbreviated as

FTTx). Fibre access networks are grooming due to their virtually unlimited fibre transmission capacity. It can cater to the increasing bandwidth demands required by various bandwidth-intensive applications such as high-definition television (HDTV), Video-on-Demand (VoD), peer-to-peer and video conferencing.

Fibre-based optical access networks can be deployed as point-to-point (dedicated) or shared architectures, according to the utilization scheme of the transmission medium, i.e., fibre. Point-to-point architectures deploy a separate fibre between the central office (CO) and each subscriber. This makes them too costly, and they are generally considered an unattractive option. In contrast, with shared architectures each subscriber uses a separate fibre to connect to a network concentrator (e.g., switch, router), and the network concentrator connects to the CO using a single shared fibre. Thus shared architectures are in general much cheaper than dedicated architectures. As one of the shared fibre architectures, Passive Optical Network (PON), is widely considered a promising technique for the implementation of FTTx [69] [137].

In addition to providing FTTx solutions, PONs can also serve as backhaul architectures for the interconnection between wireless based stations, which potentially realize the future-proof fixed mobile convergence [202].

In this thesis, we use mathematical optimization models to formulate the optimal deployment problem of greenfield PON systems, aiming to minimize the total deployment cost, subject to the physical layer constraints of PON systems. Moreover, due to the high computational complexity of the optimization model, we develop efficient heuristics for suboptimal solutions. The approach is efficient to plan large network scenarios with hundreds of ONUs.

This chapter provides a background for passive optical networks, discusses existing major challenges, hence motivates our research in the optimal planning of PONs. In Section 6.2, we give an introduction to PON technology. Section 6.3 elaborates the issues of medium access control (MAC) and bandwidth allocation. The last section reviews existing optimization models for PONs and general networks, and positions our research topic.

6.2 Passive Optical Networks

Passive Optical Network technology is an emerging technique, which provides low cost point-to-multipoints fibre access to local subscribers. The term "passive" is due to the lack of active components that require electrical power, within the transmission paths. PONs provide simple optical fibre infrastructure without requiring power supply outside the operators plants [137], hence significantly reduce the operational and maintenance expenditure.

Several topologies can be implemented for PONs, including tree, tree-and-branch, ring, and bus [137]. Among all these topologies, trees are the most popular, due to its simplicity and ease of management. Figure 6.1 shows an example of PONs with the tree topology. However, trees suffer the intrinsic drawback of the single point failure. For example, a single break point on the trunk fibre can make the whole network out of function. It should be noted that this problem is due to the tree topology rather than the PON techniques. The Ring topology can be helpful to improve the reliability, with increasing cost.

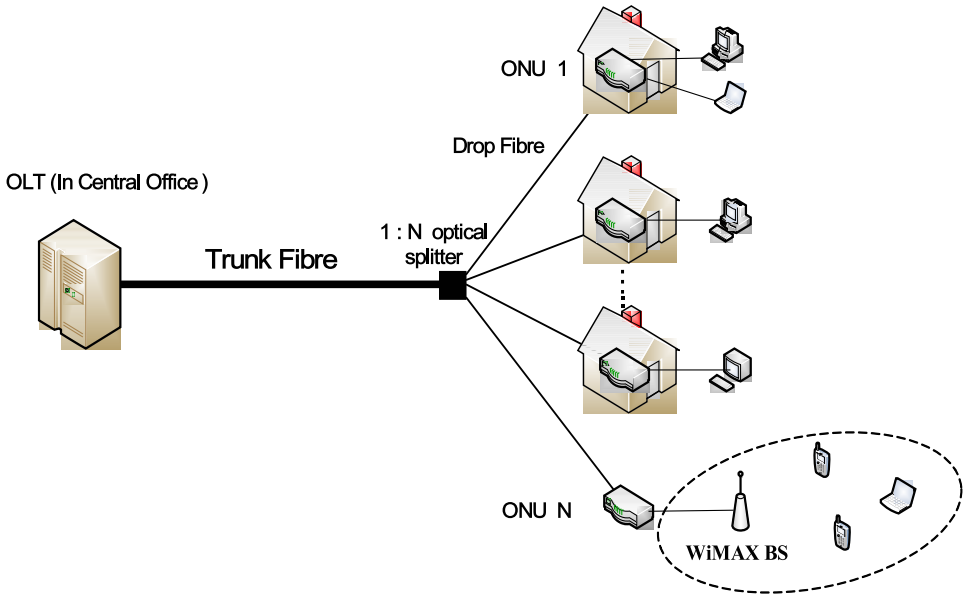

Figure 6.1: An example of PONs with the tree topology.

Typically, a PON comprises three types of components, including (i) an optical line terminal (OLT), which is located in a local exchange (Central Office), (ii) some passive optical splitters that duplicate optical signals by dividing signal power evenly to multiple output interfaces [82], and (iii) a number of optical network units (ONUs), each for a

service subscriber. With the tree topology, a single trunk or feeder fibre connects the OLT to a single splitter, while multiple drop fibres connect the splitter to ONUs, one for each. If the splitter has a maximal split ratio of $1 : N$, then the PON can support up to N drop fibres. In ring or bus topologies, there exist several splitters, one for each ONU. Compared to conventional access techniques, PONs have several advantages, including high bandwidth, long coverage, low cost, and transparent upgrade capability. The last merit is because optical splitters are not sensitive to the PON data rate, hence an upgrade of systems only requires an upgrade of the electronic devices in the central offices and the customer premises.

Today there are two primary types of standardized passive optical network technologies, Ethernet Passive Optical Networks (EPONs) [115] [137], and Gigabit-capable Passive Optical Networks (GPONs) [120] [121]. EPON is standardized by IEEE, and is a category of networks based on the Ethernet technique. It benefits from the huge market of Ethernet devices. An EPON combines the low-cost Ethernet equipment and fibre infrastructure, and transmits Ethernet data frames directly. It can provide 1 Gbps capacity in both upstream and downstream directions, and cover a distance of up to 20 km and support 20 km maximal differential distance [1]. In addition, current Ethernet techniques such as prioritization and virtual LAN tagging provide support for Quality of Service (QoS). These techniques enable EPONs to transmit data, voice and video traffic efficiently in an integrated network. In contrast, GPON evolves from the ATM PON (APON/BPON) technique [119], and is standardized by ITU-T under work of the Full-Service Access Network (FSAN) group [120] [121] [122] [123]. Compared to EPONs, a GPON can support higher data rate, up to 2.488 Gbps for both downstream and upstream. It can cover a longer distance, up to 60 km, and support a differential distance of up to 20 km.

Besides the two standardized PON techniques, PONs for the next generation are also being developed. Research has been done to extend the transmission distance and upgrade the network capacity, as these two features are essential to all types of access networks. In order to support users in rural areas who are far away from a central office, Gupta *et al.* [90] propose to extend the maximal transmission distance of a PON from standardized 20 km or 60 km, to 100 km. In terms of the bandwidth, a new generation

[1] The *coverage distance* of a PON is defined as the maximal transmission distance between an OLT and an ONU. The *Maximal differential distance* is the maximal distance difference between different ONUs from a central OLT within a common PON.

of PON techniques are being developed to increase the transmission capacity by either shortening the time duration of each data bit or increasing the number of parallel transmission channels. IEEE 10 Gbps EPON standards are being developed, and the EPON transmission capacity is upgraded from 1 Gbps to 10 Gbps [116]. A few GPON enhancements are also in progress to extend GPON to support 10 Gbps downstream data rate [69]. Driven by the idea of exploiting multiple channels, Gupta *et al.* [90] apply Wavelength Division Multiplexing (WDM) concept to increase PON transmission capacity by several times. Note that the transmission capacity of a PON is not likely to affect the cost minimized planning, if we assume that all subscribers accept whatever capacity is assigned by the operators. However, other system parameters, such as the maximal transmission and maximal differential distances do affect the planning, as these two parameters are constraints that should be satisfied when minimize the total deployment cost.

Existing implementations of PONs can be found in some Asian countries, where FTTH systems are widely deployed. For example, in Japan, NTT had more than 2.8 million FTTH users in March 2005, and expected to reach 30 million fibre access users by 2010 [203]. The original systems used by NTT were BPONs, but are now evolving towards EPONs.

In order to successfully design and deploy PON systems, there are several issues that should be addressed, including hardware related issues (e.g., transceiver design), security issues, service requirements, multiple access and bandwidth allocation, and optimized planning. Multiple access and bandwidth allocation in the upstream direction is important for the efficient utilization of bandwidth, whereas it is not a problem for downstream traffic since that is broadcast to all ONUs. As a result, the differential distance constraint in PON standards is introduced to improve the efficiency of multiple access and bandwidth allocation schemes. Hence the MAC layer issues indirectly affect the cost minimized planning of PONs. We review MAC and bandwidth allocation for PONs in the next section, followed by a section discussing existing models for optimal network planning. We do not provide details for hardware, security, and services issues.

6.3 Multiple Access and Bandwidth Allocation

Channel allocation or medium access control is an important issue in PONs, since the feeder fibre is shared by all the ONUs. In the downstream direction, owing to the broad-

casting nature of the PON system, there is no collision. But for upstream, all ONUs need to be coordinated to transmit data.

An explicit transmission scheduling scheme is preferred in PONs because contention-based random access is difficult to implement. In general, communication stations need to be able to detect collisions, if they are applying contention-based random access such as carrier sense multiple access/collision detection (CSMA/CD). However, due to the directional properties of optical splitters, ONUs cannot detect collisions occurring on the OLT side directly. Therefore, CSMA/CD cannot be directly used for PONs. Some extensions of CSMA/CD have been proposed to resolve this problem. Desai *et al.* [59] propose an optical loopback technique to efficiently exploit CSMA/CD for the access control in WDM PONs. Chae *et al.* [42] apply the similar idea to EPONs for a 155 Mb/s line rate. Centralized control of OLT can also help to realize the collision awareness on the ONU side. If the OLT informs ONUs the collision by broadcasting a special signal, all the ONUs know the occurrence of the packet collapse. With this central control function of the OLT, a PON can apply contention-based random access schemes. Nonetheless, this centralized mechanism results in low efficiency in long reach networks, and is less tolerable for voice and video traffic. In addition, contention-based MAC cannot guarantee bandwidth to each ONU, and the implementation is costly. Another possible solution for data collision is to apply the WDM concept, which enables each ONU to operate at a separate wavelength, thereby avoiding data collisions by using dedicated wavelength for different ONUs. However, the implementation of this idea is also cost prohibitive, as it requires a tunable receiver, or an array of receivers, each for a wavelength, at the OLT side. Moreover, ONUs should be equipped with different transmitters, which is also not cost-effective. Therefore, time-sharing scheduling is considered a more attractive solution to manage the channel allocation. It can avoid data collision with only one wavelength and a single transceiver in each ONU.

In general, scheduling can be classified into TDMA and polling, which represent static and dynamic time sharing mechanisms, respectively. In a static TDMA scheme, each ONU is allocated a fixed time slot, by using a common time reference that provides synchronization. ONUs need to buffer data until their time slots arrive. They can only transmit in their own time slots, and ONUs transmit idles if they have nothing to send when their time slots arrive. The main drawback of static TDMA is that it may suffer from low overall channel utilization. To resolve this problem, dynamic time sharing has been

proposed. In dynamic time sharing, bandwidth are allocated dynamically, according to the state information collected from all ONUs. Among all the dynamic time sharing schemes, polling has been widely applied. One standardized protocol on which many other polling algorithms are based is multipoint control protocol (MPCP). It is specified by the IEEE 802.3ah standard [115]. MPCP aims to provide primitives for any particular bandwidth allocation and transmission scheduling algorithms. A simple but inefficient polling scheme is the poll-and-stop polling, in which the OLT polls all ONUs in a round-robin fashion, while the polling of each ONU only starts after receiving reports from the previous ONU. To improve poll-and-stop, Kramer *et al.* [136] propose interleaved polling, in which polling for current ONU can be performed even if the OLT does not receive the response from the previous ONU. Other polling algorithms include [42] and [151]. Zheng *et al.* [232] give a brief overview of MAC and bandwidth allocation related issues for EPONs. By utilizing QoS related features such as traffic priority and service level agreements, other scheduling schemes are also available [137].

6.4 Optimized Design of PONs

As PONs aim to provide high bandwidth with low cost, numerous techniques have been developed to reduce the overall cost of PONs. These techniques mainly focus on the PON architectures refinement [229] and component costs reduction. However, optimal design and planning is also important for cost-effective PON deployment.

The costs of land trenching and laying fibres are expensive. These costs generally dominate the overall cost of the system deployment. Therefore, reduction of the total trenching distance for laying fibres can effectively reduce the PON deployment cost (we do not consider obstacles, and assume that a straight connection can be made between two arbitrary points, hence it is the greenfield PON planning we are investigating.). Nonetheless, little research has been conducted in cost-minimized design and planning for PON deployment. Only very recently, Hajduczenia *et al.* [96] tried to optimize the PON deployment based on optical power budget requirements and deployment cost. Algorithms are proposed to minimize the total deployment cost of a PON. This study however only considers several small special application scenarios, and the discussion is limited to a single PON. Therefore, more generalized and systematic approaches are required for practical deployment with hundreds of Optical Network Units (ONUs), in

which trenching, fibre cable, network components costs are considered simultaneously. The focuses include the formation of PONs and the determination of splitter position for each PON.

There also exists other work that applies optimization models to planning of PONs, but with different objectives rather than minimizing the deployment cost. They only focus on optimizing certain special performance metrics. For example, Sarkar *et al.* [198] study the optimal placement of ONUs for an optical-wireless hybrid access network, such that the average distance between all mobile users to an ONU is minimized, if each ONU is associated with a wireless base station that provides network services to mobile users.

It should be noted that the optimal network planning problem is not unique to PONs. Similar issues (e.g., the optimal choices of locations for network concentrators) arise in any distribution networks. The early studies of this problem can date back to 1960's. Hakimi studied the optimal placement of a single [98] and multiple [99] switching centres for communication networks in 1964 and 1965, respectively, in which the optimum is defined in the sense that the sum of connection distances is minimal.

Existing models for the optimal design of traditional networks can be categorized into uncapacitated, capacitated, and dynamic models. In the uncapacitated models, each network concentrator is assumed to have capacity to serve unlimited terminals. This type of models are over-simplified. Literature discussing this type of models include Krarup and Pruzan [138], Labbé *et al.* [140], and Mateus *et al.* [157]. To model the problem more practically, capacitated concentrator models are introduced, in which all concentrators have limited capacities. This type of models are studied by Amiri [12], Barcelo and Casanovas [19], Klincewicz and Luss [134], Lee [142], and Mirzaian [162], etc. The last type of models are dynamic models, which take future expansion of user demands into account. Models in this category include Balakrishnan *et al.* [18], Chardaire *et al.* [46], and Shulman [204]. However, all three types of models do not consider networks subject to constraints such as maximal differential distance, as PONs, and only few work (see Amiri [12] and Lee [142]) considers multitype concentrators.

In the investigations of the optimal network design problem, the following subproblems are often of interest (i) the number of concentrators needed, (ii) the location of each concentrator, (iii) the connection relationship, between terminals and concentrators, under different optimization objectives. However, though these subproblems can be identified, there are no general models and algorithms to solve all of them simultaneously.

In this thesis, we study the cost minimum planning for greenfield PON deployment. We propose a general mathematical model for the problem, and develop efficient heuristics to obtain sub-optimal solutions. In addition, we evaluate the impacts of PON system constraints, such as maximal split ratio, maximal PON transmission distance, and maximal PON differential distance, on the overall cost of PON deployment. Note that the usage of our algorithms are not limited to the optimal network design for PONs. With minor modifications, they can also be applied to the optimal network design and planning for more general networks.

Chapter 7

Cost Minimization Planning for Greenfield Passive Optical Networks

In this chapter, we investigate the optimal deployment of Passive Optical Networks. In particular, we aim to minimize the total deployment cost.

7.1 Introduction

With the emergence of various bandwidth-intensive services such as HDTV, VoD, peer-to-peer and video conferencing applications, there is an increasing bandwidth demand on broadband access. To meet this demand, the access networks are evolving from the traditional DSL and Cable techniques to a new generation of fibre-based access techniques. Fibres are permeating from the curb (FTTC), through the building (FTTB) and the node (FTTN), eventually to the home (FTTH) [69] [136]. Today there are two major types of passive optical access networks, i.e., Ethernet Passive Optical Network (EPON) [115] [136], and Gigabit-capable Passive Optical Network (GPON) [120] [121]. EPON is a type of networks based on the Ethernet technique, which benefit from the huge market of Ethernet devices. An EPON can provide 1 Gb/s capacity in both upstream and downstream directions, and cover a distance of up to 20 km as well as support 20 km differential distance. In contrast, GPON is a standard evolved from ATM PON (APON) technique. A GPON can support higher bandwidth, up to 2.5 Gb/s, in both upstream and downstream directions. It can cover a longer distance, up to 60 km, and support a differential distance of up to 20 km.

The research community has carried out much research for passive optical network, mainly focusing on the following aspects. First, many investigations are dedicated to efficient bandwidth allocation and QoS support, including Assi [13], Foh [74], and Kramer [136], as bandwidth allocation in the upstream direction in both EPON and GPON is always one of the most challenging issues. A range of efficient scheduling and bandwidth

allocation strategies have been developed and evaluated. Second, transmission distance and capacity are also essential to passive optical networks. In order to support users in rural areas who are far away from a central office, Gupta *et al.* [90] propose to extend the maximal transmission distance of a PON from standardized 20 km or 60 km, to up to 100 km. Also, to provide even higher bandwidth, a new generation of PON techniques is being developed to increase the transmission capacity by either shortening the time duration of each data bit or increasing the number of parallel transmission channels, as described in Chapter 6.

On the other hand, optimal design and planning for PON systems is also important to cost-effective PON deployment. As the cost of land trenching and laying fibres is expensive, which generally dominates the overall cost of the whole deployment, minimizing the total trenching distance for laying fibres is often regarded as a key optimization objective for PON deployment. Nonetheless, little research has focused on this aspect. Only very recently, Hajduczenia [96] tries to minimize the total PON network deployment cost. This study however only considers several small special application scenarios. More generalized approaches are thus required for practical deployment with hundreds of Optical Network Units (ONUs).

In this chapter, we consider a generic approach for greenfield PON system deployment, which is capable of planning a large network scenario with hundreds of ONUs. We formulate the research problem for the PON network design and planning and develop mathematical optimization models for the problem. Due to the high computational complexity of the optimization model, we also propose efficient heuristics for sub-optimal solutions. Extensive simulation studies indicate that the proposed approaches are very efficient compared to a benchmark sectoring approach. In addition, we also evaluate the impacts of PON system constraints, such as maximal optical split ratio, maximal PON transmission distance, and maximal PON differential distance, on the overall cost of PON deployment.

The rest of the chapter is structured as follows. In Section 7.2, we elaborate on the PON network deployment problem and develop a mathematical optimization model for the problem. We introduce a benchmark sectoring approach and an efficient heuristic, called Recursive Association and Relocation Algorithm (RARA) in Section 7.3. We also improve the performance of RARA by combining it with the Minimum Spanning Tree (MST) approach to exploit the benefit of cable conduit sharing among multiple fibre links.

In Section 7.4 and 7.5, we conduct simulation studies to evaluate the performance of the proposed approaches and gain insights into the factors that affect costs of PON deployment. We conclude the chapter in Section 7.6.

7.2 Problem Definition and Mathematical Optimization Model

7.2.1 Problem Definition

Fig. 7.1 shows an example of PON network planning and deployment. Given a dispersed set of locations, with one ONU at each location, and a central office, from which passive optical networks are deployed to connect to the ONUs, our objective for PON network deployment is to minimize its total cost. This total cost is composed of various subcosts, including (i) the system cost of PON, such as the costs of Optical Line Terminals (OLT), and optical splitters, (ii) the labour cost for trenching and laying fibres, and (iii) the cost of fibre cables. In general, among all these costs, the labour cost of trenching and laying fibres is the most expensive, which overwhelms all the other costs in the whole deployment. Thus, in the PON network deployment, minimizing the total distance of trenching and laying fibres is generally a key objective for the optimization.

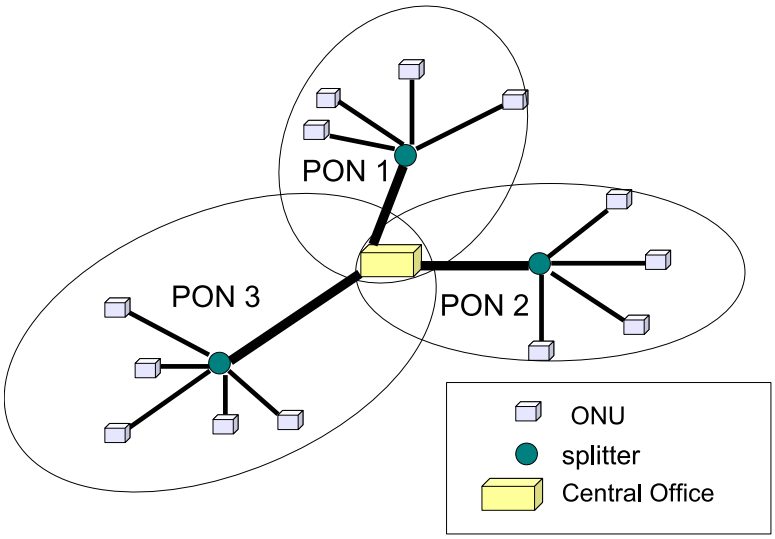

Figure 7.1: Illustration of PON networks.

The optimization problem needs to consider several PON systems constraints, including (i) maximal transmission distance, (ii) maximal differential distance, and (iii) optical split ratio. Typically, the optical split ratio ranges from 1:4, 1:8, 1:16, 1:32, 1:64, to up to 1:128. A 1:n optical splitter means that up to n ONUs can be connected to the splitter.

In addition to the above system constraints, we may also consider other geographic constraints, such as road maps, high mountains, and private properties, which may make the solutions obtained by RARA infeasible. However, in the current study we do not consider these constraints by assuming a greenfield type of network design and planning, in which the trenching distance between to points are the Euclidean distance between them, and we also assume no existing deployment. Moreover, solutions obtained by RARA can be used for two purposes even taking these constraints into account (i) they can serve as lower bounds and be useful for comparisons and (ii) they can be modified to turned to be feasible solutions. For example, if a fibre link of an optimization solution is required to cross a private property, which is however not accessible, we may make a local bypass to get around the property.

7.2.2 Mathematical Optimization Model

We develop a mathematical model for the optimization problem, which is as follows.

- Sets:
  - **S**: index set of splitters. The cardinality of **S** limits the maximal number of splitters allowed for the whole deployment. For example, if we have 500 ONUs, then the total number of splitters will never exceed 500. This is because each ONU can only connect to a single splitter, and thus the total number of splitters never exceeds the total number of ONUs; otherwise, there are unnecessary spare splitters, which are not cost-optimal.
  - $\mathbf{T}_s$: set of splitter types, which is based on the split ratios. The splitter types can range from 1:4, 1:8, 1:16, 1:32, 1:64, to up to 1:128 according to the PON standards.
  - **U**: index set of ONUs. Each ONU corresponds to a geographic position in the Euclidean plane.
- Parameters:
  - x_0, y_0: position coordinates of the central office (CO).
  - x_i^o, y_i^o: position coordinates of the i^{th} ONU, $i \in \mathbf{U}$.
  - Δ: a large value that is required by the Integer Linear Programming, which is set to be 10^5 in our study.

- T_k: the total number of outlet ports of the k^{th} type of splitter. For example, a 1:8 splitter has eight outlet ports.
- α: the cost factor or weight of the OLT.
- β_i: the cost factor or weight of each outlet port of the i^{th} types of splitter. For simplicity, we assume that the cost of each outlet port of each type of splitters in the set $\mathbf{T}_s$ is identical.
- γ: the cost factor or weight of trenching and laying fibres (per kilometer).
- θ: the cost factor or weight of fibre cables (per kilometer).
- $l_{\max}^{\text{total}}$: the maximal transmission distance of a PON between an OLT and an ONU, which is in general less than 100 km.
- $l_{\max}^{\text{diff}}$: the maximal differential distance between different ONUs within the same PON network, which is in general less than 20 km.

- Decision Variables:
  - x_i^s, y_i^s: the position coordinates of i^{th} splitter, $i \in \mathbf{S}$.
  - Φ_i: the usage indicator function of the i^{th} splitter. It takes the value of one if the splitter is used; otherwise, zero.
  - Ψ_i^j: the connection or association indicator function between the j^{th} ONU and the i^{th} splitter. It takes the value of one if the ONU is connected to the splitter; otherwise, zero.
  - π_i^k: the splitter type indicator function of the i^{th} splitter. It takes the value of one if the splitter is the k^{th} type; otherwise, zero.
  - l_i^s: the distance from the i^{th} splitter to the central OLT.
  - l_i^j: the distance from the j^{th} ONU to the i^{th} splitter.
  - $l_i^{\max}$: the maximal distance from an ONU to the OLT in the i^{th} PON, $i \in \mathbf{S}$. Each PON corresponds to a splitter.
  - $l_i^{\min}$: the minimal distance from an ONU to the OLT in the i^{th} PON.
  - τ_i, ζ_i^j: auxilliary binary variables for the "if and then" conditions in the optimization model.

- The objective is to minimize the total cost of PON deployment that interconnects all the ONUs to the central OLTs, subject to the PON system constraints including maximal transmission distance, maximal differential distance, and optical split ratio.

  Objective:

  minimize

$$\alpha\sum_{i\in\mathbf{S}}\Phi_i+\beta\sum_{i\in\mathbf{S}}\sum_{k\in\mathbf{T}_s}\Phi_i T_k\pi_i^k+(\gamma+\theta)\left(\sum_{i\in\mathbf{S}}\Phi_i l_i^s+\sum_{i\in\mathbf{S}}\sum_{j\in\mathbf{U}}\Psi_i^j l_i^j\right). \tag{7.1}$$

- Subject to:

$$\sum_{i\in\mathbf{S}}\Psi_i^j=1,\forall j\in\mathbf{U}; \tag{7.2}$$

$$\Delta\cdot\Phi_i\geq\sum_{j\in\mathbf{U}}\Psi_i^j,\forall i\in\mathbf{S}; \tag{7.3}$$

$$\sum_{j\in\mathbf{U}}\Psi_i^j\leq\sum_{k\in\mathbf{T}_s}T_k\cdot\pi_i^k,\forall i\in\mathbf{S}; \tag{7.4}$$

$$\sum_{k\in\mathbf{T}_s}\pi_i^k-1\leq\Delta\cdot\tau_i,\forall i\in\mathbf{S}; \tag{7.5}$$

$$1-\sum_{k\in\mathbf{T}_s}\pi_i^k\leq\Delta\cdot\tau_i,\forall i\in\mathbf{S}; \tag{7.6}$$

$$\Phi_i\leq\Delta\cdot(1-\tau_i),\forall i\in\mathbf{S}; \tag{7.7}$$

$$l_i^s=\sqrt{\left(x_i^s-x_0\right)^2+\left(y_i^s-y_0\right)^2},\forall i\in\mathbf{S}; \tag{7.8}$$

$$l_i^j=\sqrt{\left(x_i^s-x_j^o\right)^2+\left(y_i^s-y_j^o\right)^2},\forall i\in\mathbf{S},j\in\mathbf{U}; \tag{7.9}$$

$$\left(l_i^s+l_i^j\right)-l_i^{\max}\leq\Delta\cdot\zeta_i^j,\forall i\in\mathbf{S},j\in\mathbf{U}; \tag{7.10}$$

$$l_i^{\min}-\left(l_i^s+l_i^j\right)\leq\Delta\cdot\zeta_i^j,\forall i\in\mathbf{S},j\in\mathbf{U}; \tag{7.11}$$

$$\Psi_i^j\leq\Delta\cdot\left(1-\zeta_i^j\right),\forall i\in\mathbf{S},j\in\mathbf{U}; \tag{7.12}$$

$$l_i^{\max}\leq l_{max}^{\text{total}},\forall i\in\mathbf{S}; \tag{7.13}$$

$$l_i^{\max}-l_i^{\min}\leq l_{\max}^{\text{diff}},\forall i\in\mathbf{S}. \tag{7.14}$$

In this model, the total cost is made up of three parts. The first part is the cost of OLTs, as each splitter corresponds to a PON, which requires an OLT. The second part is the cost of splitters, and the last part includes the cost for trenching and laying fibres and the cost of fibre cables.

Constraint (7.2) says that each ONU must connect to a splitter. Constraint (7.3) determines whether the i^{th} splitter should be deployed, which depends on whether there are any ONUs connected to the splitter. If there are any, the splitter must be deployed; otherwise, not deployed. Constraint (7.4) selects a splitter type, which ensures that the splitter has sufficient outlet ports to accommodate all the ONUs connected to it.

Constraints (7.5)-(7.7) ensure an *if-then* condition. If the i^{th} splitter is selected, there must be only one splitter type associated with the splitter. More specifically, if $\Phi_i = 1$ (i.e., the i^{th} splitter is selected), then $\tau_i = 0$ must hold, which further leads to $\sum_{k \in \mathbf{T}_s} \pi_i^k = 1$ due to (7.5) and (7.6) (i.e., there is a single splitter type for the i^{th} splitter). Constraint (7.8) computes the distance from a splitter to the central OLT. Constraint (7.9) computes the distance from a splitter to an ONU. These two constraints are nonlinear.

Constraints (7.10)-(7.12) find the maximal distance and the minimum distance between an ONU and an OLT respectively within each PON. The constraints are also based on an *if-then* condition. If $\Psi_i^j = 1$ (i.e., the j^{th} ONU belongs to the i^{th} PON or splitter), then $\zeta_i^j = 0$ must hold, which thus derives constraints (7.10) and (7.11) into $l_i^s + l_i^j \leq l_i^{\max}$ and $l_i^{\min} \leq l_i^s + l_i^j$, respectively.

Constraint (7.13) ensures that the maximal transmission distance of a PON is not exceeded. Constraint (7.14) ensures that the maximal differential distance between different ONUs within the same PON network is satisfied.

7.2.3 Discussion

This model is difficult to solve. Even a simplified version is proved to be NP-hard [159]. It can be divided into three subproblems, they are (i) determining the total number of required PONs (i.e., splitters), (ii) associating ONUs to splitters, which is termed *ONU-splitter association* subproblem, i.e., clustering ONUs into groups that connect to common splitters, and (iii) relocating the positions of the splitters that achieve the optimal cost, which is called *relocation* subproblem.

In the first subproblem, the total number of required PONs or splitters cannot be determined in advance. The only way to evaluate the required number of PONs or splitters

that minimizes the total cost is to enumerate all possible partition patterns of ONUs and then determine the optimal splitter location for each ONU cluster. By exhausting all the possibilities, we can determine an optimal number of splitters. However, the computation complexity of this brute-force search increases factorially with the total number of ONUs, which is prohibitive for a large number of ONUs.

The ONU-splitter association subproblem, i.e., subproblem (ii), attempts to find an optimal association between ONUs and splitters, providing that the locations of the splitters are given. This subproblem can be proved to be NP-complete, which means that the problem is intractable for a large planning scenario. Thus, for sub-optimal solutions, we propose a heuristic subroutine to solve this subproblem. In this subproblem, the variables x_i^s, y_i^s, Φ_i, l_i^s and l_i^j all become given parameters. With given l_i^s and l_i^j, the nonlinear constraints (7.8) and (7.9) are consequently eliminated and the whole optimization model is thus degenerated into an Mix Integer Linear Programming (MILP) model, which can be solved optimally for medium size scenarios. In this study we will use this MILP optimization model to verify the effectiveness of our allocation heuristic.

The third subproblem focuses on determining splitter locations for each PON such that the total fibre length, which is the sum of the fibre lengths from each ONU to the OLT, is minimum. This relocation problem is well-known as Fermat-Weber point problem (FWPP) [53], which is a nonlinear optimization problem and whose objective function is convex, but not everywhere differentiable [139]. Several algorithms are available to solve the subproblem. One of them is Weiszfeld algorithm [53] [139]. We adopted this algorithm as a subroutine in our subsequent heuristic. Detailed description of Weiszfeld algorithm is given in Appendix C.

The above three subproblems entangle with each other. For the optimal solution to the whole problem, they need to be considered jointly, which however leads the whole optimization problem to be even more intractable. Thus, an efficient heuristic is required to solve this optimization problem.

Indeed, this optimization problem relates to the well-studied classical problem, called Multifacility Location-Allocation Problem (MLAP), which is introduced by Cooper [55] in the context of Operations Research. MLAP aims to select the positions of m distributed warehouses, such that the total cost (usually represented by the Euclidean distance) to serve a set of n given service centres is minimized, if each service centre is served by one and only one distributed warehouse. This problem also known as *p-median* or multi-

Weber problem. Basically, to explicitly solve this problem, one needs to solve $S(n, m)$ groups of equations, where $S(n, m)$ is the Stirling number of the second kind. In fact, this problem turned out to be NP-hard by [159].

Several heuristic algorithms were proposed to solve MLAP. Cooper [56] proposed Sequential Location Allocation (SLA) algorithm, which consists of alternating between an allocation phase and a location phase. In allocation phase, the set of existing facilities are partitioned into m groups, and facilities in same group will be served by same distributed warehouse. The Fermat-Weber problem is then solved for each group of facilities separately after finishing the allocation step. These two procedures are alternatively continued until no further improvement can be achieved. Note that the results of allocation step are kept if and only if the allocation can provide a better (less) cost value than the cost value obtained in location step of the previous iteration. For other algorithms, see [56] [63] [145] [150], and references therein.

Despite the similarity, the optimal PON deployment problem does show major differences from the classical MLAP problem in several aspects. First, the fibre deployment problem is subject to the maximal transmission distance and maximal differential distance of a PON, while in the MLAP problem, there are no such corresponding constraints. Second, in the fibre deployment problem, the number of splitters is not known in advance, which it is a part of the solution to be determined, while the number of required distributed warehouses is given and fixed in MLAP. Finally, the splitter capacity is limited in the fibre deployment problem, while the classical MLAP problem allows warehouses to serve any number of service centres.

7.3 Heuristic Algorithms

We proposed two heuristics to solve the above PON deployment problem. One is based on an intuitive sectoring approach, which functions as a benchmark for performance comparison, and the second is called Recursive Association and Relocation Algorithm (RARA), which employs a recursive process to keep on calling ONU-splitter association and splitter relocation subroutines until an optimal (at least locally minimal) solution is achieved.

7.3.1 The Sectoring Algorithm

We first propose an intuitive sectoring algorithm. Like cutting a cake, the sectoring algorithm partitions all the ONUs into equal-size groups according to their geometric positions. The group size is equal to the maximal optical split ratio[1]. ONUs in the same group form a PON. After finishing the partitioning, Weiszfeld algorithm [53] [139] is subsequently applied to find the optimal splitter position for each PON. Finally, all the ONUs in the same group connect to the common splitter.

Fig. 7.2 illustrates an example of the above grouping process. Given a dispersed set of ONUs and a maximal optical split ratio 1:4. We start from the positive direction of the vertical axis, and rotate the radius line in the clockwise direction for ONU grouping. A radius line is drawn when four ONUs are included in the current section. The rotation goes on until all the ONUs are grouped. Note that the starting point can be arbitrarily selected. If the number of ONUs is not integer multiple of splitter capacity, there is one group with number of ONUs equals to $\mod(n, m)$, as shown in the example, there is a group with three ONUs. After the partition, the position of splitter for each PON needs to be computed by Weiszfeld algorithm. For dense networks, radially partitioning the network may not be able to efficiently reduce the cost. However, the sectoring algorithm can also be modified to partition the network arbitrary, but systematically, according to some certain criteria.

7.3.2 Recursive Association and Relocation Algorithm (RARA)

Recursive Association and Relocation Algorithm (RARA) is extended from Cooper's algorithm [56], which has been used to solve MLAP in logistics studies. The flowchart of RARA is illustrated in Fig. 7.3.

The left column implements an outer loop, which can be divided into several steps. Step 1 randomly generates an initial set of splitters and their locations. The cardinality of the initial splitter set S, s, ranges from a minimum value, $S_{\min}$, to a maximal value, $S_{\max}$, in which $S_{\min}$ equals the number of necessary splitters to connect all the $|\mathbf{U}|$ ONUs, i.e., $S_{\min} = \lceil |\mathbf{U}|/n \rceil$, where 1:$n$ is the maximal allowed split ratio, and $S_{\max}$ is set to be the total number of ONUs, $|\mathbf{U}|$. To avoid falling into a local minimum, for each value of s, we

[1]Note that in the algorithm, if the total number of ONUs is not an integer multiple of the split ratio, the number of ONUs in the last group is less than the split ratio.

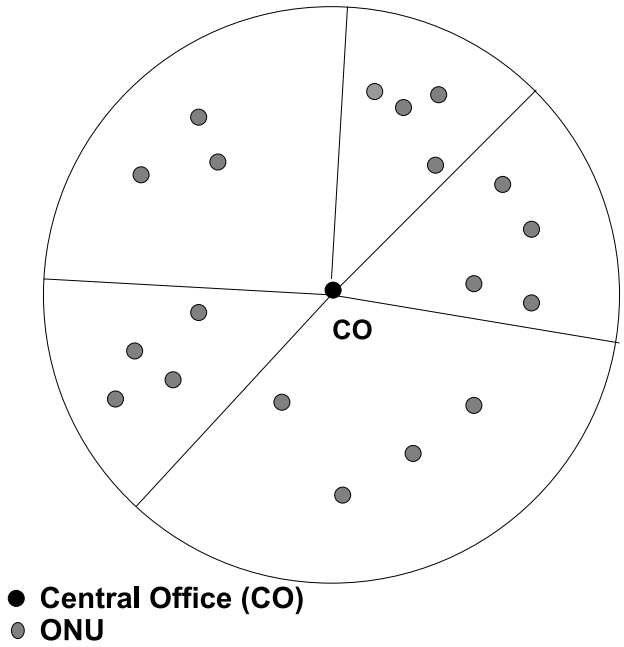

Figure 7.2: An example of the sectoring approach.

regenerate different initial splitter sets (splitter coordinates). As shown in the left column in Fig. 7.3, the algorithm runs this regeneration process N times, which is counted by an iteration counter i.

Step 2 validates whether this initial set of splitters are eligible to meet all the PON system constraints, such as the maximal transmission distance, maximal differential distance, and maximal optical split ratio, if this set of splitters are used to connect all the ONUs. If this initial set of splitters are valid, then the algorithm calls a recursive process, i.e., Step 3, to find the best set of splitters and their locations based on the initial set of splitters. The middle column in Fig. 7.3 shows the detail of the recursive (searching) process. Specifically, the process first calls an "ONU-splitter association and splitter relocation" step (i.e., Step 4), which is termed A/R step.

The detail of the A/R step is further shown in the right column of Fig. 7.3. The A/R step finds a set of valid splitters and their corresponding locations through a convergence process, i.e., loop **a**. If the new solution at the convergence performs better than a previously-recorded best solution, Step 5 is executed to update the best known solution. In most cases, loop **a** can converge within a few iterations. However, sometimes it may fail to converge after a predefined number R of iterations. If that occurs, a Simulated Annealing (SA)-like process (i.e., Step 6) is called to finalize a (good) solution.

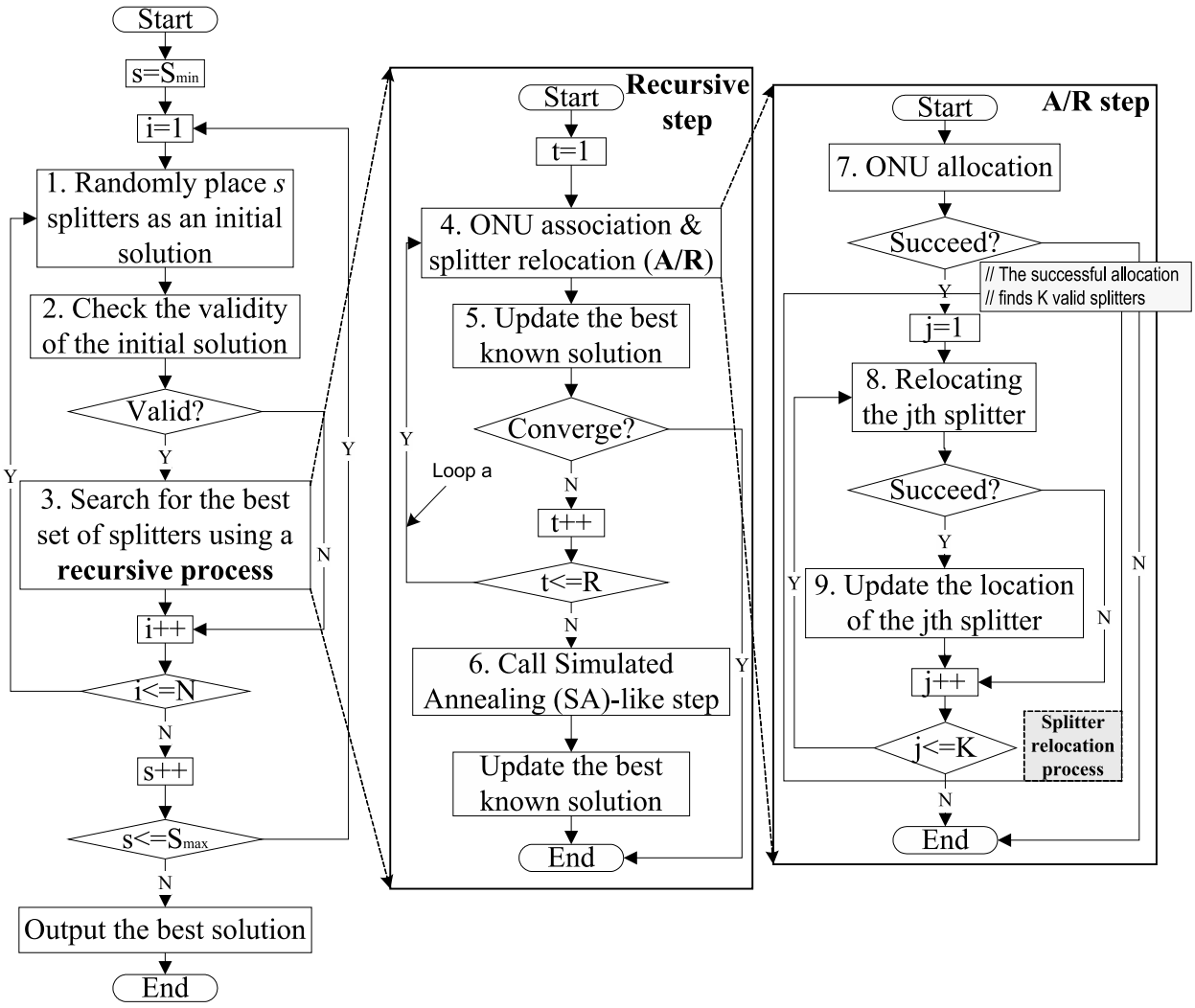

Figure 7.3: Flowchart of RARA.

Next, we describe the key components and subroutines in the RARA heuristic.

ONU-Splitter Association

The ONU-splitter association step is important to the whole heuristic to find an optimal association between ONUs and splitters, subject to the PON system constraints. Given the location of each splitter, it is possible to employ the aforementioned Mixed Integer Linear Programming (MILP) model to find optimal solutions. The MILP model essentially carries out an efficient exhaustive search. However, the association problem itself is NP-complete, which is intractable for a large size planning scenario. Thus, in the RARA algorithm we employed a heuristic subroutine to determine the association.

In the association heuristic, initially, all the ONUs are unconnected to any splitter. Since the positions of all the splitters and ONUs are known, distance between an arbitrary pair of ONU-splitter is also known. Specifically, the association process first finds a pair of ONU and splitter, which has the shortest distance among all the ONU-splitter pairs. Then, three PON system constraints including the maximal optical split ratio, maximal transmission distance, and maximal differential distance, are verified for the selected ONU-splitter association. If the association is found to be valid, then keep it and move on to the next pair of ONU and splitter that has the shortest distance among all the remaining unconnected ONUs, and the same verification process is carried out. Such a process is repeated until all the ONUs find their associated splitters.

The pseudo-code of the allocation algorithm is shown in Algorithm 4. We adopt the same notation as defined in the Section 7.2. The input of the algorithm is the set of ONUs, **U**, the set of splitters, **S**, and a $|\mathbf{U}| \times |\mathbf{S}|$ matrix **D**, whose (i, j) entry, **D**(i, j) is the distance between i^{th} splitter and j^{th} ONU. We denote $|\mathbf{U}|$ and $|\mathbf{S}|$ as the number of ONUs and splitters, respectively. **U** and **S** also denote the coordinates of ONUs and splitters. The algorithm returns an $|\mathbf{U}| \times |\mathbf{S}|$ matrix, called **Mapping**, indicating the connection relationship between splitters and ONUs, which is initialized as an all zero matrix. $\mathbf{Mapping}(i, j)$ is one if j^{th} ONU is connected to the i^{th} splitter.

The most time consuming operations of the algorithm is finding the splitter-ONU pair, which has the smallest distance value, among all the available splitter-ONU pairs. This operation requires $|\mathbf{U}||\mathbf{S}|$ comparisons. As $|\mathbf{S}|$ is bounded by $|\mathbf{U}|$. This operation is bounded by $O(|\mathbf{U}|^2)$. The operations of examining the system constraints of PON can be done in constant time, hence with time complexity $O(1)$. As the algorithm stops if and

Algorithm 4 Association Algorithm

Input: Set of ONUs, **U**; set of splitters, **S**; capacity of each splitter, **n**.
distance matrix: **D**
Output: Matrix of connection relationship: Mapping

```
1: Mapping ←0    %Mapping is an |U| × |S| matrix
2: N ← |P|
3: (splitter_i, ONU_j) ← argmin_{i,j}(D(i, j))
4: while N > 0 and D ≠ Ø do
5:     if |C_{splitter_i}| < n %C is the number of ONUs connected to the M_{index_i}th splitter
       then
6:         if D(splitter_i, ONU_j)+distance(splitter_i, 0) < constraint_t then
7:             if max_{j∈C_{splitter_i}}(splitter_i, j)-min_{j∈C_{splitter_i}}(splitter_i, j) < constraint_s % all
               the constraints are satisfied; then
8:                 D ← D\D(:, ONU_j)
9:                 Mapping(splitter_i, ONU_j) ← 1;
10:                C_{splitter_i} ← C_{splitter_i} ∪ U_{ONU_j};
11:                N ← N - 1
12:                (splitter_i, ONU_j) ← argmin_{i,j}(D(i, j))
13:            else
14:                D ← D \ D(splitter_i, ONU_j)
15:                (splitter_i, ONU_j) ← argmin_{i,j}(D(i, j))
16:        else
17:            D ← D \ D(splitter_i, ONU_j)
18:            (splitter_i, ONU_j) ← argmin_{i,j}(D(i, j))
19:    else
20:        D ← D \ D(splitter_i, :)
21:        (splitter_i, ONU_j) ← argmin_{i,j}(D(i, j))
22: return Mapping
```

only if all the ONUs have been examined, the above procedure needs to be perform for at least $|\mathbf{U}|$ times, and at most $|\mathbf{U}|^2$, yielding the time complexity of the allocation algorithm to be at least $O(|\mathbf{U}|^3)$, and $O(|\mathbf{U}|^4)$ at the worst case. Though this algorithm is with polynomial time complexity, it is still not very efficient for large value of $|\mathbf{U}|$, as its order is at least 3. The intrinsic nature of NP-completeness spawns this high order polynomial complexity. Therefore, we need to improve this allocation algorithm to reduce the time complexity.

Improvement of the Association Heuristic

In Algorithm 4, the distance between ONUs and splitters are store in an adjacency matrix. The complexity of finding the minimum in such an adjacency matrix is $O(|\mathbf{U}||\mathbf{S}|)$. Therefore, the worst case time complexity to finish the allocation is $O((|\mathbf{U}||\mathbf{S}|)^2)$. As the maximum $|\mathbf{S}|$ is bounded by a linear function of $|\mathbf{U}|$, the complexity is $O(|\mathbf{U}|^4)$, which is

not very efficient for large $|\mathbf{U}|$.

To improve this algorithm, a "Calendar" data structure [34] is employed to store the pairs of ONUs and splitters. A Calender is essentially a set of linked lists. In order to construct a calender, There is an array with k elements to store the header pointers of each linked list. Each splitter-ONU pair is represented as a node, which is attached to different linked lists of the Calender, according to the distance values. When a new splitter-ONU pair is connect to a linked list, it is inserted according to ascending order. Therefore, after finishing the construction of the Calender, elements in each linked list are sorted. If the value of k is a carefully selected large enough value, every linked list contains few elements, or a single element in the best case. Therefore, we only need to $O(1)$ operation to access the smallest distance of the splitter-ONU pair.

For Calender data structure, the most time is consumed in its construction. However, using similar idea as generating discrete uniform random numbers by using continuous uniform random number, we can directly place elements to their corresponding linked lists in the calender when we construct it. For example, if the maximal possible distance between splitters and ONUs is 1000, regardless the unit, we can let $k = 1000$, and the ith linked list stores all the splitter-ONU pairs that have distance within interval $[i-1, i]$. Therefore, if there exists a splitter-ONU pair whose distance is 888.8, this pair will be put into the 889th linked list. Hence with carefully selected k such that each linked list only contains a few elements(the best situation is 1), when we do the allocation, we only need to examine the calender in one round, which gives the time complexity $O(k)$. As k is often proportional to $|\mathbf{U}||\mathbf{S}|$, the time complexity is reduced to $O(|\mathbf{U}|^2)$, achieving an order of 2 improvement.

The above ONU association step eventually divides all the ONUs into several groups, each of which is connected to a common splitter. Based on these groups, we can further optimize the location of the splitter (i.e., Step 8) by employing Weiszfeld algorithm, which determines the Fermat-Weber point, i.e., geometric median, for a polygon with a group of ONUs and an OLT as vertices. Note that the Fermat-Weber point ensures the shortest fibre distance to connect this group of ONUs to the OLT among all possible locations in an Euclidean plane. Thus, if the new location of the splitter satisfies all the PON system constraints, Step 9 will record the new location for the splitter as a better solution.

Splitter relocation

The above ONU-splitter association step divides the whole group of ONUs into several small groups with each corresponding to a PON. Based on these ONU groups, the next step is to find the best location of optical splitter for each PON. The problem is essentially to find a Fermat-Weber point for a polygon with a group of ONUs and an OLT as vertices [53]. We extended traditional Weszfeld algorithm (see Appendix C) to realize such a splitter location. In particular, when applying Weszfeld algorithm, we need to ensure that the output satisfied the constraints of PON system. The output of the relocation process is the best location of the splitter.

Simulated Annealing (SA)-like Subroutine

There is a key loop (i.e., loop **a** in the middle column of Fig. 7.3) in the RARA algorithm. The loop stops whenever a solution to a set of splitters converges. However, the loop may fail to converge occasionally, and enter a deadlock between two or even more local minimum solutions. Under these circumstances, we need to find a way to resolve the deadlock. For this purpose, we proposed a Simulated Annealing-like subroutine in the RARA algorithm.

Specifically, when a deadlock occurs, the SA-like subroutine is called to repeat the A/R step. The subroutine stores two variables. One is the best solution during the whole Simulated Annealing process, and the other is the current solution. In each iteration, if the new found solution is better than the current best one, then the new solution substitutes for the current best one, as well as the current solution; otherwise, a random number between the interval of $[0, 1]$ is generated and compared with a temperature function, which is updated in each iteration. The new solution is also accepted as current solution if the random number is less than the value of the temperature function. The subroutine stops when the temperature function is less than a predefined small threshold.

7.3.3 Maximal Sharing of Cable Conduit

In RARA, an important assumption is that an independent cable conduit is built for each fibre link between an ONU and a splitter. However, it is possible to further tune down the deployment cost by allowing a fibre link to traverse the cable conduits that have been built for other fibre links, which is called *sharing of cable conduits*.

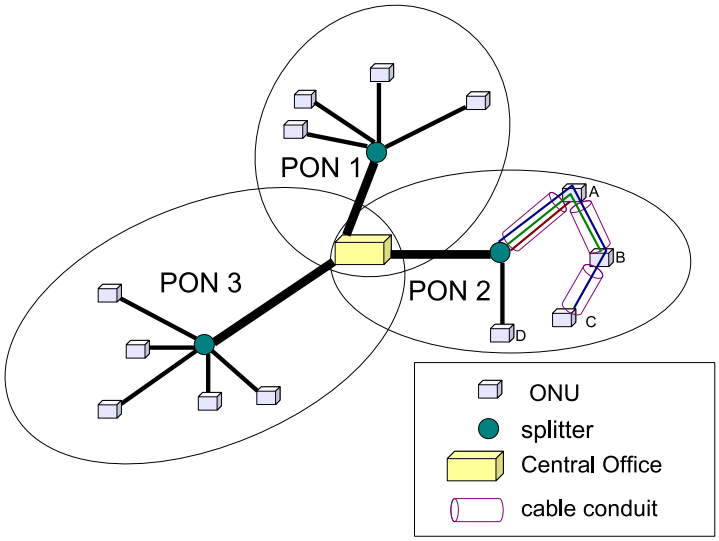

Figure 7.4: Concept of cable conduit sharing in PON networks.

As shown in Fig. 7.4, there are three PONs in the deployed system. We take PON 2 as an example to illustrate the concept of cable conduit sharing. Rather than building a cable conduit directly for the fibre links between the splitter and ONUs B and C respectively, we may build a cable conduit from A to B and from B to C, and then use the consecutive conduits from the splitter to A and from A to B to lay fibres for the link between the splitter and B. Similarly, we can use the consecutive conduits from the splitter to A, from A to B, and from B to C, to lay fibres for the link between the splitter and C. By doing this, the trenching cost for laying fibres can be significantly reduced, compared to independent trenching for each ONU-splitter link.

To exploit the potential cost-reduction through conduit sharing, we develop an enhanced algorithm subsequent to the design obtained by RARA. Specifically, for each PON, the algorithm employs the Minimum Spanning Tree (MST) concept to consider each of the locations, including the splitter and each of the ONUs, as a vertex. An extended MST algorithm, similar to Prim's algorithm [174], is then applied to find a constrained minimum spanning tree that connects all the locations. Note that different from the pure minimum spanning tree algorithm, here we need to ensure the PON system meets all the constraints, such as maximal transmission distance, when finding the minimum spanning tree.

7.4 Simulation Conditions and Test Scenarios

To evaluate the efficiency of the proposed approaches, we conduct extensive simulation studies. The following conditions are assumed during the simulations. As a starting point, the total number of splitter sets, N, is initially set to be 500, i.e., for a given number of splitters, we generate 500 instances. The available split ratios are 1:4, 1:8, 1:16, 1:32, and 1:64. A maximal split ratio constrains how large a PON can be deployed in the planning. Therefore, it is 1:64. For example, if the maximal split ratio is 1:32, up to 32 ONUs can be connected to a single PON, i.e., no more than 32 ONUs can be connected to the splitter in that PON. However, such a maximal split ratio does not require us to use the maximal-size splitter constantly. For example, if there are only 11 ONUs connected to a PON, then a smaller splitter with a ratio of 1:16, instead of 1:32, can be used for cost saving. The following cost factors are assumed for the planning: the cost of trenching and laying fibre is \$16,000/km, the cost of fibre cables is \$4,000/km, the cost of each OLT is \$2,500, and the cost of each splitter port is \$100.

Three PON network planning scenarios are studied, including (i) a circle with a 16 km radius, (ii) an annulus with a 16 km inner circle radius and a 50 km outer circle radius, and (iii) a circle with a 50 km radius. Within each of the areas, we assume that all ONUs are randomly distributed.

In scenario (i), we studied the cases with different numbers of ONUs ranging from 100 to 500 OUNs with 100 OUNs for each increment. Note that when making an increment of ONUs, the locations of the existing ONUs are not changed. In addition to the existing ONUs, the new ONUs are just randomly added and uniformly distributed. The EPON system standard is applied for this scenario, which is subject to the system constraints of 20 km the maximal transmission distance and 20 km the maximal differential distance.

In scenario (ii), we considered the cases with the numbers of ONUs ranging from 300 to 700 also with increments of 100 ONUs. In this scenario the system constraints of GPON are applied, which are subject to 60 km the maximal transmission distance and 20 km the maximal differential distance.

Finally, the numbers of ONUs in scenario (iii) ranges from 600 to 1000 also with increments of 100 ONUs. The locations of the ONUs in scenario (iii) are actually the combinations of the previous two scenarios. We combined the case of 300 ONUs of scenario (i) with all the cases ranging from 300 to 700 ONUs of scenario (ii) to form all the cases of

scenario (iii). For example, when considering the case of 700 ONUs in scenario (iii), those 700 ONUs is a combination of the case of 300 ONUs of scenario (i) and the case of 400 ONUs of scenario (ii). Also, for scenario (iii), the system constraints of GPON is applied, which are subject to 60 km the maximal transmission distance and 20 km the maximal differential distance.

7.5 Results and Analyses

7.5.1 Comparison of Different Approaches

In this section, we compare the performance of different planning approaches. Fig. 7.5 shows an example about how the total cost changes with the total number of ONUs for scenario (i). The shown example has the maximal split ratio 1:16. We can see that the RARA approach can achieve a much better performance, i.e., lower cost, than the benchmark sectoring approach. Moreover, RARA is shown to be more efficient with the increase of the total number of ONUs. Also, comparing the results of cable conduit sharing and non-sharing (i.e., with MST and without MST in the legends), we can see that cable conduit sharing can help to significantly reduce the cost of PON deployment. The cost reduction increases with the increase of the total number of ONUs. We also conducted simulation studies for other values of the maximal split ratios, and obtained similar results. Fig. 7.8 shows the performance comparison between different approaches for the scenario (i) with the maximal split ratio 1:32. Similar results are observed.

To highlight the significance of the RARA and the cable conduit sharing efforts, we also compare two extreme cases, i.e., the sectoring approach without cable conduit sharing, and the RARA approach with cable conduit sharing. it can be found that the RARA approach and the effort of cable conduit sharing can jointly bring about 50% cost reduction for a network design scenario with 500 ONUs.

Figs. 7.6 and 7.7 show similar results for the different planning approaches, under the annulus scenario, i.e., scenario (ii), and the larger circular scenario, i.e., scenario (iii), respectively. Specifically, the sectoring approach without MST performs worst, and the RARA approach with MST but without PON system constraints (i.e., allowing any maximal transmission distance and maximal differential distance) performs best.

An interesting result for the annulus scenario is that the Sectoring+MST approach outperforms the RARA+MST approach. This is because the sectoring approach does not con-

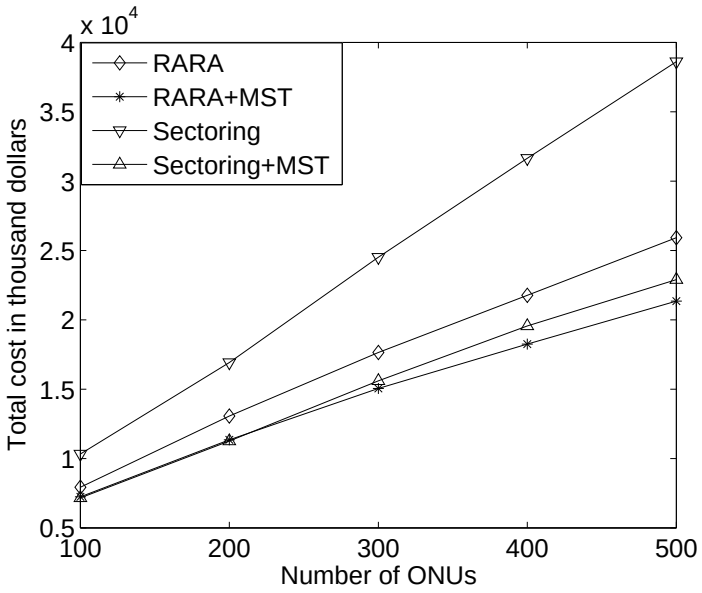

Figure 7.5: Total cost vs. number of ONUs, circular scenario, radius = 16 km, split ratio = 1:16.

sider the PON system constraints, including maximal transmission distance and maximal differential distance, while the RARA approach always takes these type of constraints into account. To evaluate the effectiveness of the RARA approach, we also report the results of RARA+MST without considering the system constraints of maximal transmission distance and maximal differential distance, i.e., RARA+MST (unconstrained), which significantly outperforms the approach of Sectoring+MST, as shown by the examples in Figs. 7.6 and 7.7.

For PON systems with other values of maximal split ratio (1:4, 1:8, 1:32, and 1:64), similar results are observed, as the example shown in Figs. 7.8 to 7.10, which show the comparison of total costs between different planning approaches, for the maximal split ratio of 1:32.

7.5.2 Impact of the ONU Density

The ONU density has great impact on the average cost per user. Figure 7.12 shows how the average cost per user changes with the number of ONUs for the network scenario with radius = 16 km, and maximal split ratio = 1:16 and 1:64, as examples. Since we keep the network area to be constant, an increase of ONU number corresponds to an increase of ONU density. It is clear from the graph that the average cost per user reduces as the number of ONUs increases, which is equivalent to that the average cost per user

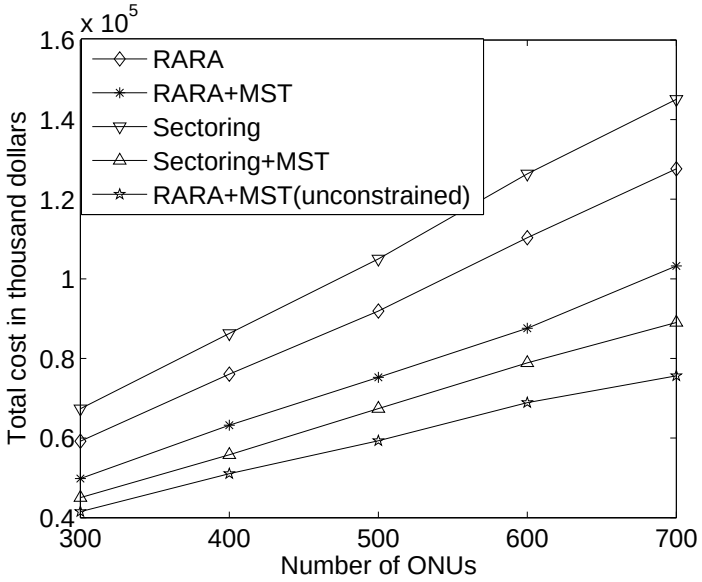

Figure 7.6: Total cost vs. number of ONUs, annulus scenario, split ratio = 1:16.

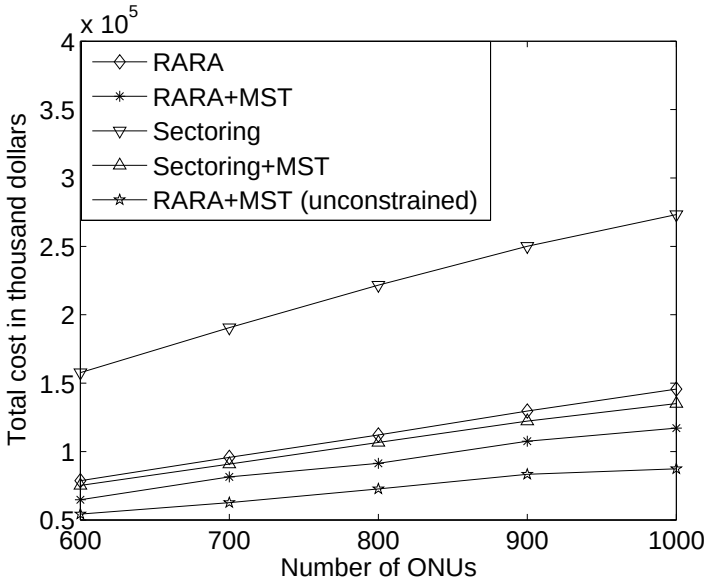

Figure 7.7: Total cost vs. number of ONUs, circular scenario, radius = 50 km, split ratio = 1:16.

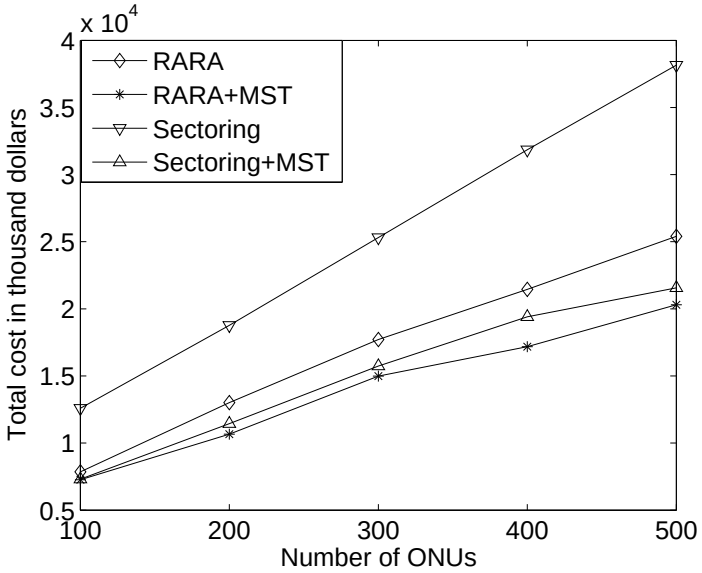

Figure 7.8: Total cost vs. number of ONUs, circular scenario, radius = 16 km, split ratio = 1:32.

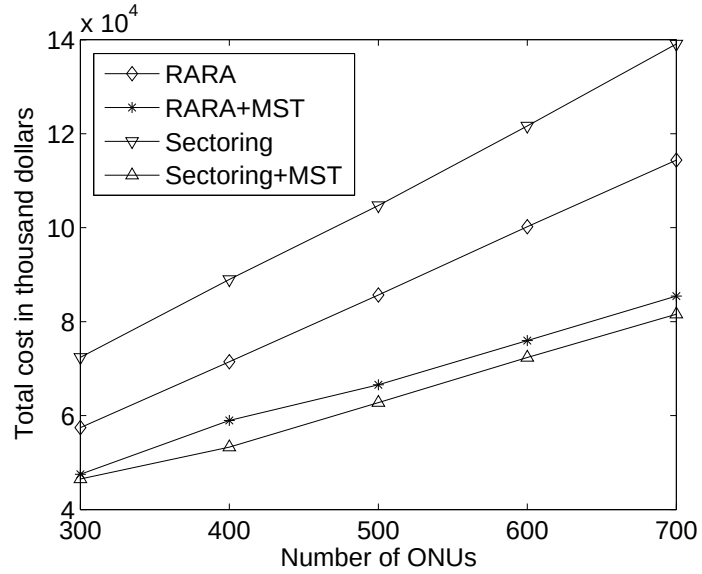

Figure 7.9: Total cost vs. number of ONUs, annular scenario, split ratio = 1:32.

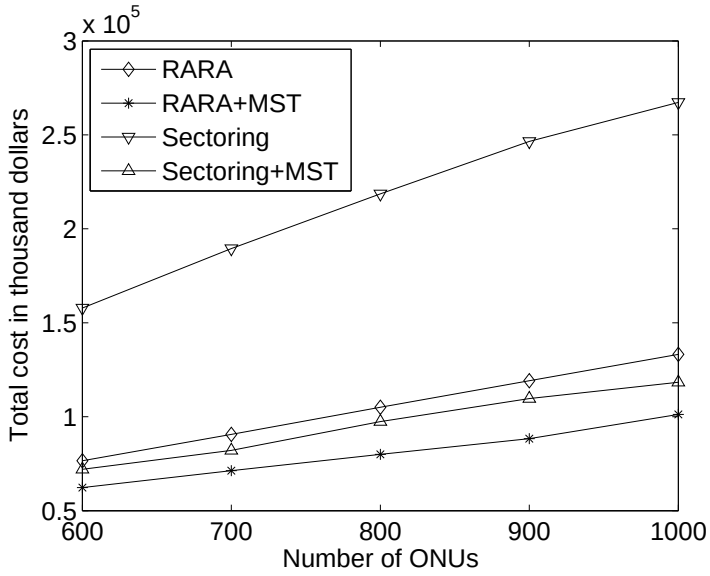

Figure 7.10: Total cost vs. number of ONUs, circular scenario, radius = 50 km, split ratio = 1:32.

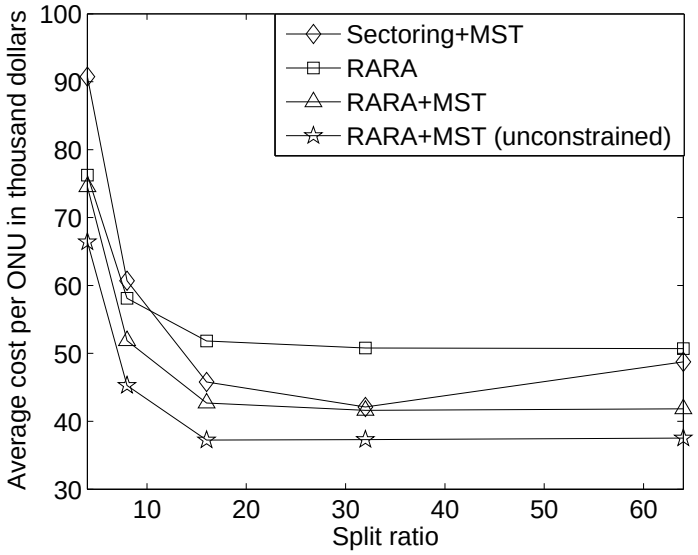

Figure 7.11: Average cost per user vs. split ratio, circular scenario, radius = 16 km, number of ONUs = 500.

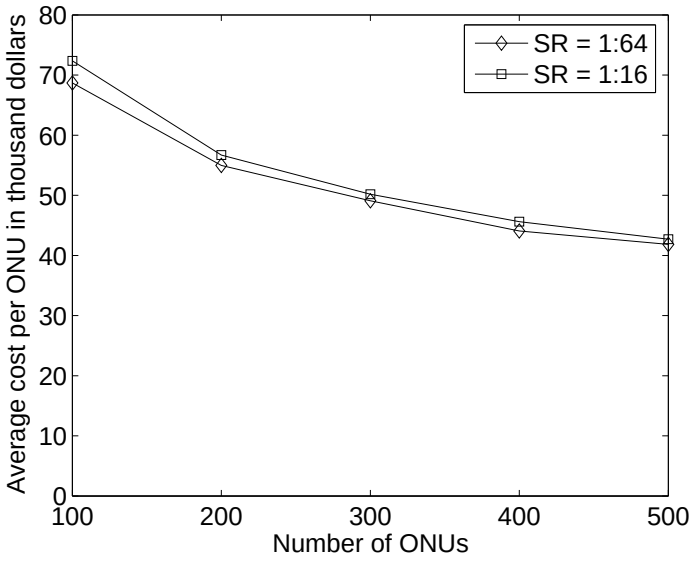

Figure 7.12: Average cost per user vs. number of ONUs, circular scenario, radius = 16 km, maximal split ratio = 1:16, and 1:64.

decreases with the increase of the ONU density.

This cost reduction brought by the high user density is because of the efficient exploitation of the single feeder fibre and the conduit sharing of the drop fibres. This result has suggested that the deployment of PON systems as a solution to provide Internet access to subscribers in urban areas is efficient.

7.5.3 Impact of Maximal Optical Split Ratio

Maximal optical split ratio is an important system parameter that affects the deployment cost of PONs. Figures 7.11 and 7.13 show how the average PON deployment cost per user changes with different maximal optical split ratios under the smaller circular scenario, i.e., scenario (i), and the annulus scenario, i.e., scenario (ii). As shown in Fig. 7.11, in addition to the similar performance ranks of the curves as reported in Section 7.5.1, we can see that the average cost per user decreases with the increase of the maximal optical split ratio. This is because a larger optical split ratio enables a single splitter to accommodate more ONUs, thereby more efficiently share the feeder fibre from the central OLT to the splitter.

On the other hand, it is interesting to see that there is a saturating trend with the increase of the maximal split ratio. When the maximal split ratio is small, the increase of the split ratio can significantly reduce the deployment cost per user, e.g., up to 40% from a

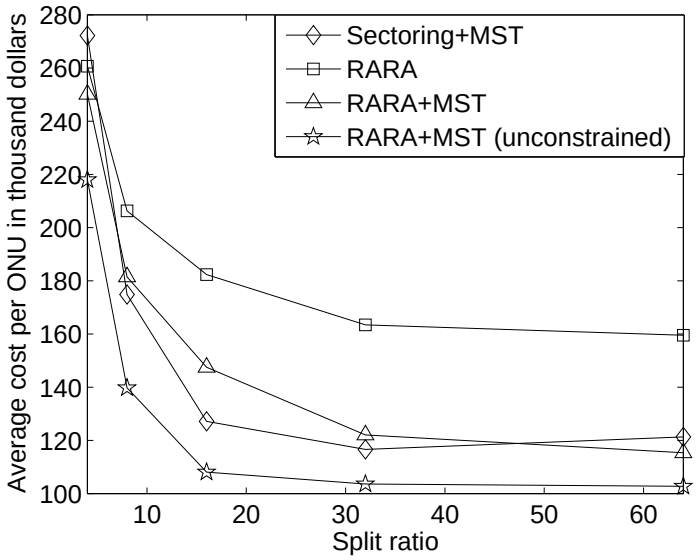

Figure 7.13: Average cost per user vs. split ratio, annulus scenario, number of ONUs = 700.

ratio of 1:4 to a ratio of 1:16. However, if the split ratio has reached a certain level, a further increase does not bring much reduction to the deployment cost. As shown in Fig. 7.11, the cost reduction from the split ratio of 1:16 to 1:32 is very marginal. Similar observations can be found for the annulus scenario as shown in Fig. 7.13, in which the cost per user decreases with the increase of split ratio, until it approaches a saturation split ratio of 1:32. This phenomenon can be explained as follows. In order to exploit the benefits of splitters with large value of maximal split ratio, more ONUs need to be connected to those splitters. However, these ONUs may be geographically far away from each other, which counteracts the cost reduction brought by the large split ratio. Therefore, the total deployment cost cannot be further reduced once the maximal split ratio reaches a certain level. It should be noted that the saturating threshold value changes with the density of ONUs.

7.5.4 Impact of Maximal PON Transmission Distance

The maximal transmission distance of a PON is another important system constraint that affects the total deployment cost. To evaluate the impact, the following test conditions are assumed. We consider the smaller circular scenario with radius = 16 km. There are 400 ONUs i.i.d. uniformly distributed within the circle. We only show results for maximal optical split ratios 1:4, 1:16, and 1:64. However, for other maximal split ratio, i.e., 1:8 and

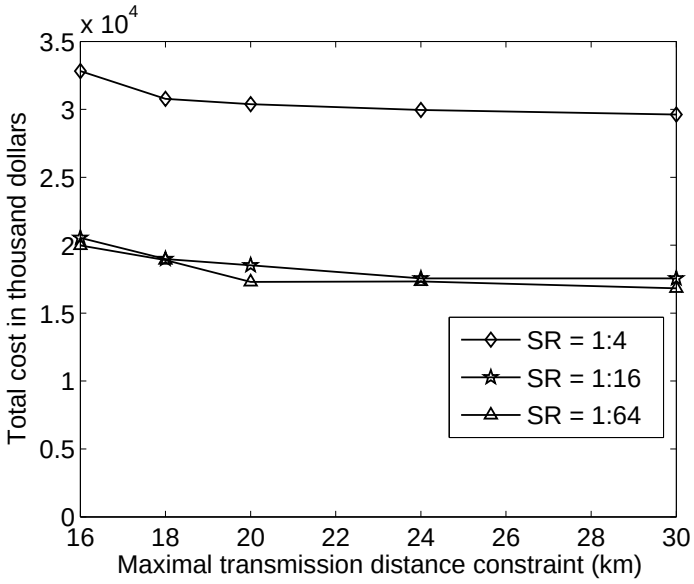

Figure 7.14: Total cost vs. maximal PON transmission distance, circular scenario, radius = 16 km, ONU number = 400.

1:32, results are similar. The maximal differential distance is 20 km. Finally, the maximal PON transmission distances are configured to change among 16, 18, 20, 24, and 30 km.

Fig. 7.14 shows how the total PON deployment cost changes with the increase of the PON maximal transmission distance under the RARA approach with cable conduit sharing. It is not surprising to see that the total cost decreases with the increase of the maximal transmission distance, as a longer maximal transmission distance provides more flexibility and optimization opportunities for the design. It is interesting to see that there is also a saturating trend, which shows a marginal total cost reduction after the maximal transmission distance has been extended to a certain range is very small. Specifically, for the current design scenario, such a saturation distance is around 20 km, which implies that after 20 km, a further increase of maximal transmission distance cannot bring much reduction in the total cost. This is because in order to be benefited from the longer maximal transmission range, the system needs to have longer distance between the OLT and ONUs. However, this long range communication is not desirable as it will incur more cost.

7.5.5 Impact of Maximal Differential Distance

The maximal differential distance of a PON can also influence the total deployment cost. To evaluate this effect, we again designed the test scenarios as follows. We consider the

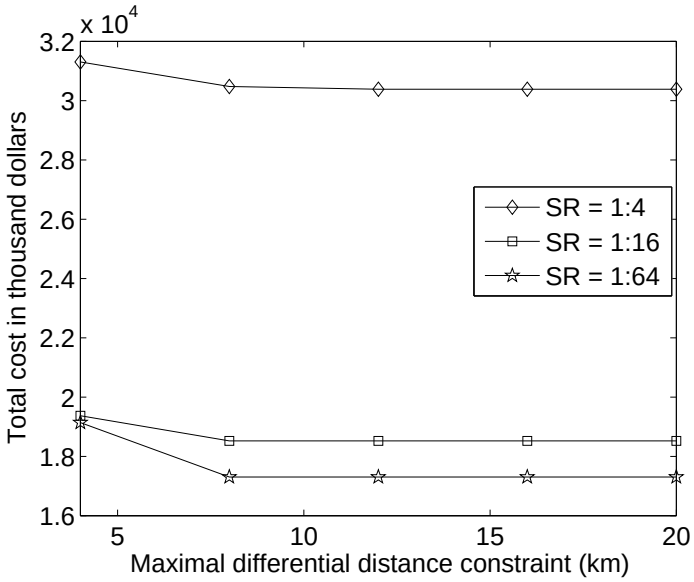

Figure 7.15: Total cost vs. maximal differential distance, circular scenario, radius = 16 km, ONU number = 400.

smaller circle scenario, i.e., scenario (i), with 400 ONUs i.i.d. uniformly distributed. The maximal transmission distance is set to be 20 km. The maximal differential distance is assumed to range from 4 km to 20 km with 4 km increment.

Fig. 7.15 shows examples of total deployment costs change with the increase of maximal differential distance under the RARA+MST approach, with the maximal split ratios 1:4, 1:16, and 1:64. It can be found out that although the increase of maximal differential distance can bring some reduction to the total deployment cost, the reduction is marginal. The result thus implies that the total PON deployment cost seems less sensitive to the change of the maximal differential distance than the change of the maximal transmission distance. This is because only nodes in the close vicinity of a splitter are expected to connect to that splitter, in order to reduce cost. This results in small differential distances in a single PON. Therefore, large values of maximal differential distance may not be necessary.

7.5.6 Effectiveness of ONU-Splitter Association Algorithm

In the RARA approach, there is an important step that associates ONUs to splitters for a given specific set of splitters. For this association, in addition to the heuristic subroutine as proposed in RARA, it is also possible to employ the MILP model described in Section 7.2 (ignoring constraints (7.8) and (7.9)) to find an optimal solution for a medium-

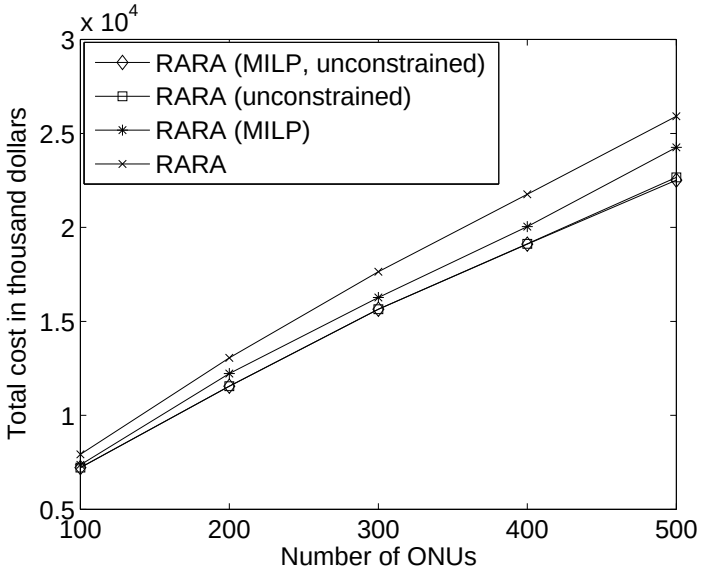

Figure 7.16: Comparison of the ONU-splitter association algorithm in RARA and the MILP model for the circular planning scenario with radius = 16 km, split ratio = 1:16.

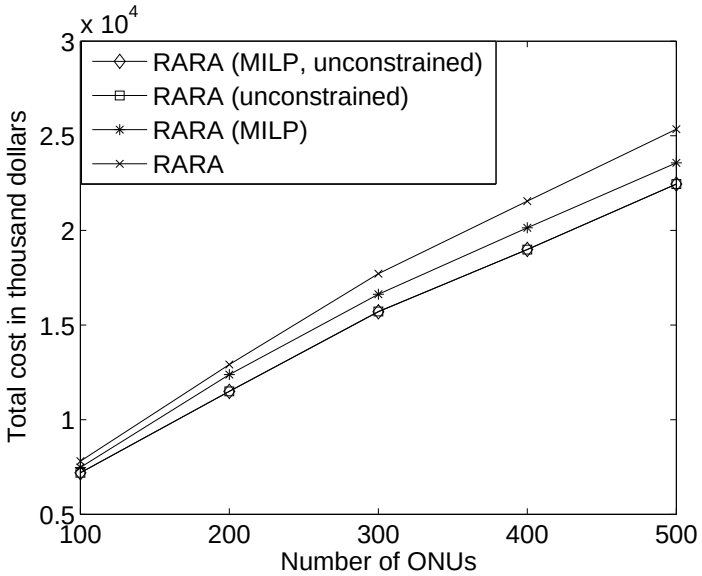

Figure 7.17: Comparison of the ONU-splitter association algorithm in RARA and the MILP model for the circular planning scenario with radius = 16 km, split ratio = 1:64.

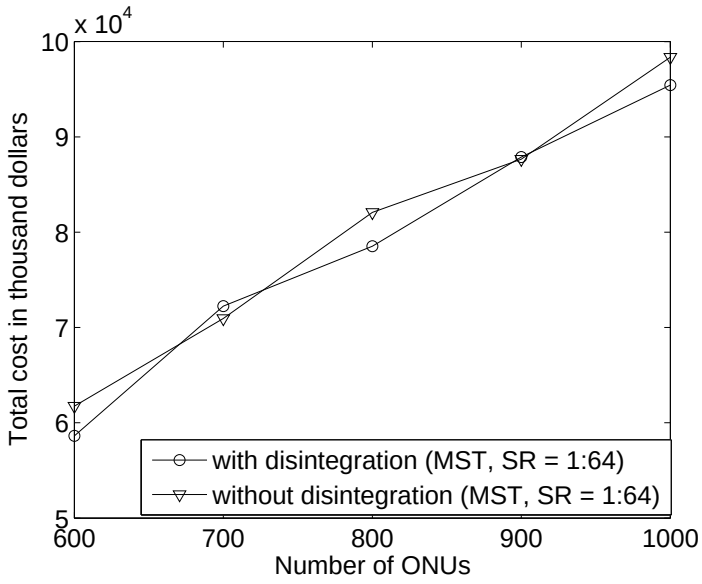

Figure 7.18: Total cost of the planning with disintegration and without disintegration, SR: split ratio

size planning scenario, e.g., with up to hundreds of ONUs. This posterior MILP optimization, termed RARA+MILP, is carried out after the RARA heuristic has found a list of splitters and the association relationship between the ONUs and the splitters. To solve the MILP optimization model, we have employed the commercial software package AMPL/CPLEX in the study. The smaller circular scenario, i.e., scenario (i), is considered for the evaluation, and only the cases with the total number of ONUs no greater than 500 are studied. In addition, the maximal optical split ratio is assumed to be 1:64.

Figures 7.16 and 7.17 compare the total costs of the two design approaches, i.e., RARA vs. RARA with the posterior MILP optimization (RARA+MILP), for maximal split ratio 1:16 and 1:64, as examples. It is found out that without considering the PON system constraints including maximal transmission distance and maximal differential distance, the RARA algorithm can achieve almost the same performance as that of RARA+MILP. Their relative performance difference is less than one percent. Moreover, when the PON system constraints are considered, the RARA algorithm still performs very well, close to that of RARA+MILP. Their relative difference is consistently less than ten percent. These results thus verify that the ONU-splitter association algorithm used in RARA is very efficient, which can achieve good solutions, close to the optimal results obtained by the MILP optimization.

Table 7.1: Comparison of computation times (hours) of the apporaches with disintegration and without disintegration

	Computation time (hours)				
Optical split ratio	1 : 4	1 : 8	1 : 16	1 : 32	1 : 64
With disintegration	4.93	6.16	7.06	7.93	8
Without disintegration	23.33	31.05	32.77	37.17	34.21

7.5.7 Disintegrating Large PON Planning Scenarios

RARA+MST is efficient and fast for scenarios containing only several hundreds of ONUs. However, for a very large-scale planning scenario with thousands or several thousands of ONUs, to obtain good solutions, the computation time of RARA+MST is significantly increased. To shorten the computation time, one effective way is to divide a large planning scenario into several smaller parts. For example, we need to plan for a large circular area containing 1400 ONUs. We may divide this large area into two parts, including one smaller circular area with 700 ONUs and one outer annulus area with the remaining 700 ONUs. Then we can apply the approaches proposed in this study to solve the two smaller scenarios and then sum them up to find a final solution to the large circular scenario. By doing this, we expect that the computation time can be significantly reduced, while the overall design performance is not significantly degraded, compared to the design without such disintegration.

In our study, scenario (iii) is essentially made up of the combinations of the cases of the smaller circular area, i.e., scenario (i), and the cases of the outer annulus, i.e., scenario (ii). Thus, to evaluate the effectiveness of the proposed disintegration method, we compare the solutions to scenario (iii) with the sums of the solutions to scenarios (i) and (ii).

Under the RARA+MST approach, Fig. 7.18 compares the total costs of the planning without disintegration, i.e., scenario (iii), and the planning with disintegration, i.e., the sum of scenarios (i) and (ii). We can see that the results without disintegration and with disintegration are very close, while the latter requires much shorter computation times. As shown by the example in Table 7.1, which are the computational time consumed for the 600 ONU cases, the approach with disintegration requires only 20% computational time of that required by the approach without disintegration. These results therefore show that the disintegration method can efficiently plan for large-size PON deployment without scarifying planning performance.

7.6 Conclusion

We have presented an algorithm to plan greenfield PON networks to minimize their total deployment cost. A mathematical optimization model has been developed, which is intractable due to its nonlinearity and NP-hard feature. We have proposed an efficient heuristic algorithm RARA to find sub-optimal solutions to the problem. Due to the dominant cost of trenching and laying fibres, we have also exploited the benefit of cable conduit sharing among different fibre links to further reduce the deployment cost. The simulation studies indicated that the RARA approach is efficient to significantly reduce PON deployment cost compared to the benchmark sectoring approach. The simulation studies also showed that the effort of cable conduit sharing can bring up to 20% cost saving compared to the pure RARA approach. Our studies have also revealed that high user density can reduce the average cost per user, which suggested that PON is efficient to provide network services in metro areas.

We have investigated the effects of various PON system constraints, including the maximal optical split ratio, maximal transmission distance, and maximal differential distance. The results showed that there are saturating trends for the PON deployment cost with the increase of the three system parameters. Moreover, compared to the maximal differential distance constraint, the maximal transmission distance showed a stronger impact on the total deployment cost.

The efficiency of the ONU-splitter association subroutine in RARA was also evaluated, compared to the optimal MILP approach. It was found out that the proposed association heuristic is efficient to perform closely to that of the MILP approach.

Finally, to shorten the computation time for a large planning scenario, we have presented an approach to disintegrate a large size planning scenario into several small scenarios. It was observed that the disintegration effort can significantly reduce computation time for the planning while no significant performance is sacrificed.

As a future research direction, since a Steiner tree in general has less total distance compared to a spanning tree, we could replace the MST algorithm in the conduit sharing procedure by a minimum Steiner tree algorithm, which may further reduce the total deployment cost.

Chapter 8

Concluding Remarks

8.1 Summary and Conclusion

Throughout this thesis, we have discussed a series of important optimization problems for the design, planning, and deployment of wireless sensor networks and passive optical networks. We have focused on the optimal resource placement in such networks with the aims of saving overall system deployment and operational costs, and improving system performance through these optimizations. In particular, we have investigated three problems: minimum sized virtual backbones in WSNs, minimum sized WSNs, and minimum cost greenfield PON planning. We briefly summarize the research conducted in this thesis as follows.

- In Chapter 3, we have numerically evaluated the expectation and the distribution of the cardinality of the minimum sized virtual backbone for one-dimensional dense random WSNs through the estimation of the margin between the ideal hop length and the actual hop length of each hop.

  As shown in Chapter 3, the cardinality of the minimum sized virtual backbone, which is the hop count in one-dimensional scenario for greedy routing, can be well approximated by $\frac{d-2/\lambda}{r-1/\lambda} - \frac{1}{2}$, in which d is the network length and r is the sensor transmission range. The approximation has been shown to be asymptotically accurate. This result greatly simplifies the computation of minimum sized backbone in dense 1-D networks.

- In Chapter 4, we have developed an algorithm and its distributed version to approximate the MCDS by a dominating set for two-dimensional dense random WSNs. We have also proposed a numerical approach to compute the expectation of the cardinality of the minimum sized virtual backbone.

  As shown in Chapter 4, the algorithms we proposed to approximate the MCDS are

efficient and scalable. The underlying principle of the algorithms is the evaluation of the optimal spacing between adjacent relays in the virtual backbone based on an extension of the asymptotic optimal results. This approach has shown that the asymptotic results applied to infinite networks can be well adopted by more practical finite dense networks with appropriate modifications. The dominating set found by our algorithm can help to simplify the network operations such as broadcasting, and reduce the network energy consumption.

In addition, the expected cardinality of the minimum sized virtual backbone through our numerical approach is a useful benchmark for the evaluation of existing routing algorithms and MCDS construction algorithms.

- In Chapter 5, we have investigated a one-dimensional random WSN with positions of all the nodes following non-i.i.d. distributions with equally spaced expectations and i.i.d. perturbations. The network scenario we studied represents the situation that all the nodes are randomly distributed with some control scheme on their positions, which is more practical, compared to previous network models which assumed all nodes are deployed with a purely random manner.

  An empirical approach has been developed to estimate the minimum number of sensors needed to maintain the network connectivity. We have solved extreme cases which are not covered by the empirical approach by analytical approaches. We have also proposed an algorithm aiming to provide conservative design of WSNs.

  Through the comparison of networks with different node distributions, we have observed that the number of nodes required to maintain the network connectivity is not very sensitive to the distributions, if those distributions are double sided distributions, which are symmetrical with respect to their means.

- In Chapter 7, we have presented a framework to minimize the total PON deployment cost for the optimal design and planning of greenfield PON systems. Practically, the framework has considered different PON system constraints, such as maximal transmission distance, maximal differential distance, and maximal split ratio simultaneously. This problem is NP-hard.

  A heuristic algorithm, called RARA, has been developed to solve the problem. The algorithm has also exploited the cable conduit sharing concept to further reduce

the deployment cost. For the deployment of large scale PON systems, a hierarchical scheme has been proposed, which can efficiently reduce the computational complexity while maintains a reasonable performance level.

The case studies have shown that cable conduit sharing can significantly reduce the PON system deployment cost compared to the situation without cable conduit sharing. In addition, our research has indicated that higher user density can benefit the cost reduction. This advantage come from the efficient exploitation of the single feeder fibre and the conduit sharing of the drop fibres, which is a result of the high density subscribers. This result has suggested that the deployment of PON systems as a solution to provide Internet access to subscribers in urban areas is efficient.

8.2 Key Contributions

The research in this thesis has aimed to provide optimal design and planning for various networks, hence enabled the thesis to be valuable to network operators and designers.

In particular, we have proposed a new network model, which is more realistic if we consider the practical network deployment schemes. Thus our network model provides a new tool for studies of sensor network behaviours. In addition, our new algorithm to approximate the MCDS, and the numerical approach to compute its cardinality, can find potential applications in routing protocol design and performance evaluation. Therefore, our results about the MCDS in sensor networks serve as powerful tools for protocol designer and researchers who study the performance of layer three protocols. Moreover, as the two-dimensional MCDS problem is NP-hard, our approaches, which evaluated the MCDS cardinality probabilistically, suggest an important direction, which may be able to quantitatively evaluate computationally intractable problems.

The optimization framework and heuristic algorithm presented in Chapter 7 have provided valuable tools to guide and evaluate network planning and provisioning. The algorithm efficiently provides network design guidance that greatly reduces the total network deployment cost. All the system level constraints of PON were considered in the framework, which makes the algorithm a practical solution kit for network operators. Using our algorithm, the case studies have quantified the decrease in cost per user as user density increases, which could be useful guidance for PON system planning.

8.3 Discussion and Future Research

The research presented in this thesis has focused on placing network resources optimally in wireless sensor networks and passive optical networks through optimization models. Many important observations have been made which are related to the general disciplines of the planning, deployment, and performance evaluation of such networks. We list the ones that we believe are the most important ones, and discuss some potential directions for future research.

Firstly, the probability modelling is an important tool in the study of sensor networks. This is primarily because of the intrinsic randomness embedded in such networks. The randomness has its roots in the network deployment approaches which we considered, as well as the wireless communication channels, which are left as future work. Note that the random wireless channels also introduce models other than the unit disk graph, which was used in this thesis. This randomness in the sensor networks brings difficulties and challenges to investigation of the systems. Therefore, probability modelling is critical to model such a network. However, important results can be derived despite this randomness. For example, although the MCDS problem is NP-hard, for a dense random network, we can estimate its cardinality and approximate the MCDS by exploiting the randomness and high density of nodes. However, the high density results in a large amount of sensors in the network, which imposes challenges to the simulation. Therefore, there is a demand for new techniques and algorithms for fast simulations.

Secondly, in our study of sensor network connectivity, it is clear to us that empirical approaches including curve fitting can provide useful tools to investigate sensor networks, particularly from an engineering problem solving perspective. More research can be initiated using fitting with fewer functions to get better insight.

As pointed out by Li [146], nonlinear optimization serves as a fundamental tool for wireless sensor networks, especially in the studies of resource allocation problems. Indeed, nonlinear optimization also plays an important role in the system level modelling for general communication architectures, including wireless and wired systems. It can be used to find the optimal parameters with which the system can be tuned to either provide better performance or reduce the deployment and operation costs. However, the optimization models formulated are often intractable due to the system complexity, or the non-convexity of the objectives, constraints, and feasible set. Therefore, heuristics

and approximations are required to obtained suboptimal solutions. The example of the former is the algorithm proposed in Chapter 7, and the relaxation of N_1 in Chapter 4 serves an example for the latter case. With these heuristics and approximations, although we may not be able to obtain the optimal results, we can have good sub-optimal solutions which still provide insights to the systems. Nonetheless, by applying heuristics and approximations, we have to cautiously consider the tradeoff between the computation accuracy and the computational complexity. It is in general desirable to obtain accurate results with less consumption of computational resources.

For the optimal PON planning problem, we have not considered the existence of any obstacles, whereas geographical constraints to deploy fibres may exist for practical situations. Therefore, it is important to generalize our framework to consider scenarios that have obstacles which block the fibres to be placed.

Bearing these points in mind, we propose some future research directions that are natural extensions to the work presented in this thesis.

- As we have used simple unit disk model to approximate the sensor transmission range for WSNs, our research results did not capture the random fluctuations of the wireless channels. We could extend our work by applying a more practical model, which reflects the randomness embedded in the wireless medium, for the transmission range.

- It will be interesting to find out the hop count of communications between random node pairs when they are using the virtual backbone constructed by our algorithms in the two-dimensional MCDS problem. The results can be used to evaluate the efficiency of our algorithm and indicate further improvement directions.

- As mentioned in Chapter 4, we could improve our algorithm by explicitly considering the connectivity. During the nominal dominator selection stage, we select a set of nodes to be candidate nodes for each nominal relay. Finally, the nominal relay will be selected from each candidate set by considering the connectivity.

- Since one of the purposes to construct an MCDS in a WSN is to save energy, one possible future direction is extending our algorithm proposed in Chapter 4 by introducing another parameter that indicates the energy level of each node. The selection of relays need to consider the remaining energy of each node. With this

new parameter, we can enable our algorithms to be energy-aware. If we relax the constraint that the entire network area needs to be contacted by some relays, we can modify our algorithms to generate different dominating sets at different time to incorporate the load balancing problem.

- For the optimal PON deployment problem, this thesis has solely considered greenfield network planning. Therefore, for the cases of PON deployment in city area, our approach does not work properly. This is because we need to consider more geographic constraints. For example, if there are several blocks of buildings in the city area, and fibre deployment is not allowed to cross the buildings. Thus fibre cables need to align with the streets, which prevents us from using the RALA algorithm. To resolve this problem, one possibility would be to extend our model and algorithm to consider the L_1 norm (Manhattan distances) rather than the Euclidean distances used in this thesis.

Together with results obtained in this thesis, solutions of these potential future research problems can serve tools for network design, planning, and performance evaluation, which can benefit both network operators and research community in networking areas.

Appendix A

Analysis of $E[N_1]$ and $E[N_3]$

In this appendix, we give a more accurate evaluation of $E[N_1]$ than that in Section 4.4.2.

A.0.1 Derivation of $E[N_1]$

For a $d \times d$ network, given r_o, with $\mathbf{H}$ and Δ_1 defined as in Section 4.4, also define another modification factor Δ_2, which stands for the additional nodes in even number rows compared to odd number rows. Hence N_1 is given by

$$N_1 = \left\lceil \frac{d - r_o/\sqrt{2}}{r_o} \right\rceil \times \mathbf{H} + \Delta_1 + \Delta_2. \tag{A.1}$$

where $\lceil x \rceil$ is the smallest integer that is no smaller than x. Equation (A.1) can be explained as follows. The first term in eq. (A.1) represents the number of nodes in odd rows, rounded it up to an integer, as the number of nominal positions is always integer. By the similar reason, we can also round up $\mathbf{H}$, that is

$$\mathbf{H} = \begin{cases} \left\lceil \frac{d-r_o/\sqrt{2}}{(\frac{\sqrt{3}}{2}+1)r_o} \right\rceil + 1, \text{if } (d - r_o/\sqrt{2}) - (\left\lceil \frac{d-r_o/\sqrt{2}}{(\frac{\sqrt{3}}{2}+1)r_o} \right\rceil - 1)(\frac{\sqrt{3}}{2}+1)r_o > r_o \\ \left\lceil \frac{d-r_o/\sqrt{2}}{(\frac{\sqrt{3}}{2}+1)r_o} \right\rceil, \text{otherwise.} \end{cases} \tag{A.2}$$

As the distance between adjacent horizontal strip is $(\frac{\sqrt{3}}{2}+1)r_o$, we should have at least $\left\lceil \frac{d-r_o/\sqrt{2}}{(\frac{\sqrt{3}}{2}+1)r_o} \right\rceil$ rows. The first condition in eq. (A.2), which is given as $(d - r_o/\sqrt{2}) - (\left\lceil \frac{d-r_o/\sqrt{2}}{(\frac{\sqrt{3}}{2}+1)r_o} \right\rceil - 1)(\frac{\sqrt{3}}{2}+1)r_o > r_o$, states that when the distance between the $\left\lceil \frac{d-r_o/\sqrt{2}}{(\frac{\sqrt{3}}{2}+1)r_o} \right\rceil^{\text{th}}$ row and the bottom edge of the network is larger than r_o but smaller than $(\frac{\sqrt{3}}{2}+1)r_o$, we need one extra row of nominal nodes to ensure that nodes close to bottom edge of network can be connected by nominal relays. If the distance is less than or equal to r_o, we do not need that additional row, which is described in the second condition in eq. (A.2).

The quantities Δ_1 and Δ_2 are given by

$$\Delta_1 = \begin{cases} \mathbf{H}-1, & \text{if } \mathbf{H} = \left\lceil \frac{d-r_o/\sqrt{2}}{(\frac{\sqrt{3}}{2}+1)r_o} \right\rceil \\ \mathbf{H}-2, & \text{otherwise} \end{cases} \tag{A.3}$$

and

$$\Delta_2 = \begin{cases} \left\lfloor \frac{\mathbf{H}}{2} \right\rfloor, & \text{if } \left\lceil \frac{d-r_o/2\sqrt{2}}{r_o} \right\rceil > \left\lceil \frac{d-r_o/\sqrt{2}}{r_o} \right\rceil \\ 0, & \text{otherwise} \end{cases} \tag{A.4}$$

respectively.

Equation (A.3) is basically the same as that in eq. (4.5).To explain Δ_2, note that the number of nodes in even rows may be different from that in odd rows, we need a modification factor. If we need an additional node in each even row, we need $[\mathbf{H}/\mathbf{2}]$ additional nodes to cover the right edge of the network.

We shall derive N_3 in next subsection.

A.0.2 Evaluation of N_3

The quantity N_3 is a function of d and r_o. For some large d,

$$\begin{aligned} N_3 &\approx N_1 - \left\lceil \frac{d-r_o/\sqrt{2}}{r_o} \right\rceil - \mathbf{H} - \Delta_1 - \Delta_2 \\ &= \left\lceil \frac{d-r_o/\sqrt{2}}{r_o} \right\rceil (\mathbf{H}-1) - \mathbf{H}. \end{aligned} \tag{A.5}$$

which means that for each node in the network, except those nodes in the last row, in the vertical rib, and those nodes in the first column, there exists a three node pattern. For each three node pattern, we probably need an extra relay node there.

Appendix B

Probability Density Function of $\Delta\mathbf{a}$

This section derives the pdf of $\Delta\mathbf{a}$, which is given by $\Delta\mathbf{a} = -(\cos\theta(R_1 \sin\alpha + R_2 \sin\beta) + R_3 \sin\gamma)$. The pdf common to R_1, R_2 and R_3 is given by eq. (4.14), while $\sin\alpha$, $\sin\beta$ and $\sin\gamma$ are also i.i.d. RV's, since α, β and γ are i.i.d. uniform RV's in $(0, 2\pi]$.

The common pdf of $\sin\alpha$, $\sin\beta$ and $\sin\gamma$ is given by eq. (4.18). We denote the product of R_1 and $\sin\alpha$ as Z, i.e., $Z = R_1 \sin\alpha$, and its pdf as f_Z. Therefore, $R_2 \sin\beta$ and $R_3 \sin\gamma$ also follow the same pdf f_Z. We firstly derive the pdf of Z.

B.1 Probability Density of Product of RV's Z

$Z = R\sin\alpha$, it is the product of two RV's. To obtain the distribution of Z, we apply Rohatgi's well-known result [189], which says that for continuous RV's X and Y, and given their joint pdf $f_{X,Y}$, define another RV $V = XY$, the pdf of V, f_V is given by

$$f_V(v) = \int_{-\infty}^{\infty} f_{X,Y}(x, \frac{v}{x}) \frac{1}{|x|} \mathrm{d}x. \tag{B.1}$$

Note that R and $\sin\alpha$ are independent, eq. (B.1), (4.18) and (4.14) yield the pdf of Z

$$f_Z(z) = \int_{-1}^{1} \frac{1}{\pi\sqrt{1-t^2}} \cdot 2\lambda\pi \left(\frac{z}{t}\right) \exp\left(-\lambda \left(\frac{z}{t}\right)^2 \pi\right) \frac{1}{|t|} \mathrm{d}t. \tag{B.2}$$

Therefore, we have the pdf of $\Delta\mathbf{a} = -(\cos\theta(R_1 \sin\alpha + R_2 \sin\beta) + R_3 \sin\gamma)$ as

$$f_{\Delta\mathbf{a}}(h) = \int_{-\infty}^{\infty} \frac{1}{|\cos\theta|} \int_{-\infty}^{\infty} f_Z(x_1) f_Z(\frac{x}{\cos\theta} - x_1) \mathrm{d}x_1 f_Z(-h - x) \mathrm{d}x. \tag{B.3}$$

This formula can be explained as follows. As $R_1 \sin\alpha$ and $R_2 \sin\beta$ are i.i.d RV's, the pdf of their sum is the convolution of their pdf's. This sum times the $\frac{1}{|\cos\theta|}$ stands for a scaled version of $R_1 \sin\alpha + R_2 \sin\beta$. It can be shown that $-R_3 \sin\gamma$ has identical distribution with $R_1 \sin\alpha$, thus pdf of $\Delta\mathbf{a}$ is the convolution of a scaled version of $R_1 \sin\alpha + R_2 \sin\beta$ and $R_3 \sin\gamma$, yields the (B.3).

Substitute eq. (B.2) into eq. (B.3), we have

$$\begin{aligned} f(h) &= \int_{-\infty}^{\infty} \frac{1}{|\cos(\theta)|} \int_{-\infty}^{\infty} \int_{-1}^{1} \frac{1}{\pi\sqrt{1-t^2}} \cdot 2\lambda\pi \left(\frac{x_1}{t}\right) \exp\left(-\lambda \left(\frac{x_1}{t}\right)^2 \pi\right) \frac{1}{|t|} \mathrm{d}t \\ &\quad \times \int_{-1}^{1} \frac{1}{\pi\sqrt{1-t^2}} \cdot 2\lambda\pi \left(\frac{x/\cos\theta - x_1}{t}\right) \exp\left(-\lambda \left(\frac{x/\cos\theta - x_1}{t}\right)^2 \pi\right) \frac{1}{|t|} \mathrm{d}t\mathrm{d}x_1 \\ &\quad \times \int_{-1}^{1} \frac{1}{\pi\sqrt{1-t^2}} \cdot 2\lambda\pi \left(\frac{-h-x}{t}\right) \exp\left(-\lambda \left(\frac{-h-x}{t}\right)^2 \pi\right) \frac{1}{|t|} \mathrm{d}t\mathrm{d}x. \end{aligned} \tag{B.4}$$

Appendix C

Weiszfeld Algorithm

Weiszfeld algorithm is an iterative re-weight least square method, which computes the position of geometric median, also known as Fermat-Weber point, for a convex polygon. Though the complexity of Fermat-Weber problem itself is not known [53], Weiszfeld algorithm is proved to be efficient in practice, especially for a small-scale problem. The algorithm is proved to be convergent in linear time. The pesudo-code of Weiszfeld algorithm is given below

Algorithm 5 Weiszfeld Algorithm [53]

Input: Set of ONUs **U**;

1: **for** $i = 1$ to $|\mathbf{U}|$ **do**
2: **if** $\| \sum_{\vec{v} \in \mathbf{U} \setminus \vec{v}_i} \frac{\vec{v} - \vec{v}_i}{\|\vec{v} - \vec{v}_i\|} \| \leq 1$ **then**
3: **return** $\vec{v}_i$
4: Select initial solution x_0 inside the convex hull form by **U**.
5: **repeat**
6: $\vec{x}_{k+1} = \sum_{\vec{v} \in \mathbf{U}} \frac{\vec{v}}{\|\vec{v} - \vec{x}_k\|} / \sum_{\vec{v} \in \mathbf{U}} \frac{1}{\|\vec{v} - \vec{x}_k\|}$
7: **until** $\|\vec{x}_k - \vec{x}_{k+1}\| \leq \epsilon$
8: **return** $\vec{x}_{k+1}$

In the algorithm, $|\mathbf{U}|$ stands for the cardinality of set **U**. $\vec{v}$ corresponds to an ONU in **U**, which is a two dimension vector embedding the coordinates of the ONU. The **for** loop (i.e., lines 1-3) is a procedure to check whether the Fermat-Weber point coincides with any of the ONU positions. The procedure of the **repeat-until** loop (i.e., lines 5-7) is an iterative step to find the Fermat-Weber point, providing that the point does not coincide with any of the ONU positions. The subscript k of $\vec{x}_k$ is an iteration counter.

Bibliography

[1] IMote2. http://www.xbow.com/Products/Product_pdf_files/Wireless_pdf/Imote2_Datasheet.pdf. Accessed in Feb, 2008.

[2] Inc. Crossbow Technology. http://www.xbow.com/Support/Support_pdf_files/MTS-MDA_Series_Users_Manual.pdf. Accessed in Feb, 2008.

[3] KEYENCE America. http://www.keyence.com/products/sensors.html. Accessed in Jan, 2008.

[4] J. Abate and W. Whitt. Numerical Inversion of Laplace Transforms of Probability Distributions. *ORSA Journal on Computing*, 7(1):36–43, 1995.

[5] Z. Abichar, Y. Peng, and J. M. Chang. WiMAX: the Emergence of Wireless Broadband. *IT Professional*, 8(4):44–48, July-Aug. 2006.

[6] C. Adjih, P. Jacquet, and L. Viennot. Computing Connected Dominated Sets with Multipoint Relays. *Ad Hoc & Sensor Networks*, 1:27–39, May 2005.

[7] I. F. Akyildiz, W. Su, Y. Sankarasubramaniam, and E. Cayirci. A Survey on Sensor Networks. *IEEE Communications Magazine*, 40:102–114, Aug 2002.

[8] I. F. Akyildiz, W. Su, Y. Sankarasubramaniam, and E. Cayirci. Wireless Sensor Networks: a Survey. *Computer Networks*, 38:393–422, 2002.

[9] K. M. Alzoubi, P. J. Wan, and O. Frieder. Distributed Heuristics for Connected Dominating Sets in Wireless Ad Hoc Networks. *Journal of Communications and Networks*, 4(1):15–19, March 2002.

[10] K. M. Alzoubi, P. J. Wan, and O. Frieder. Message Optimal Connected Dominating Sets in Mobile Ad Hoc Networks. In *Proc. 3rd ACM International Symposium of Mobile Ad Hoc Networks and Computing (MobiHoc'02)*, pages 157–164, Lausanne, Switzerland, June 2002.

[11] G. Amato, S. Chessa, F. Conforti, A. Macerata, and C. Marchesi. Health Care Monitoring of Mobile Patients. *ERCIM News*, (60):69–70, Jan. 2005.

[12] A. Amiri. Solution Procedures for the Service System Design Problem. *Computers and Operations Research*, 24(1):49–60, Jan. 1997.

[13] C. M. Assi, Y. Ye, S. Dixit, and M. A. Ali. Dynamic Bandwidth Allocation for Quality-of-Service over Ethernet PONs. *IEEE Journal on Selected Areas in Communications*, 3(9):1467–1477, Nov. 2003.

[14] F. Atay, I. Stojmenovic, and H. Yanikomeroglu. Generating Random Graphs for the Simulation of Wireless Ad Hoc, Actuator, Sensor, and Internet Networks. *Pervasive and Mobile Computing*, 4(5):597–615, Oct. 2008.

[15] T. L. Austin, R. E. Fagen, W. F. Penney, and J. Riordan. The Number of Components in Random Linear Graphs. *Ann. Math. Statist.*, 30:747–754, 1959.

[16] X. Bai, K. Santosh, X. Dong, Z. Yun, and H. L. Ten. Deploying Wireless Sensors to Achieve Both Coverage and Connectivity. In *Proc. 7th ACM International Symposium on Mobile Ad Hoc Networking and Computing (MobiHoc'06)*, May 2006.

[17] X. Bai, D. Xuan, Z. Yun, T. H. Lai, and W. Jia. Complete Optimal Deployment Patterns for Full-Coverage and k-Connectivity ($k \leq 6$) Wireless Sensor Networks. In *Proc. 9th ACM International Symposium on Mobile Ad Hoc Networking and Computing (MobiHoc'08)*, pages 401–410, Hong Kong, May 2008.

[18] A. Balakrishnan, T. L. Magnanti, and R. T. Wong. A Decomposition Algorithm for Local Access Telecommunications Network Expansion Planning. *Operations Research*, 43(1):58–76, Jan.-Feb. 1995.

[19] J. Barcelo and J. Casanovas. A Heuristic Lagrangian Algorithm for the Capacitated Plant Location Problem. *European Journal of Operations Research*, 15:212–226, 1984.

[20] C. Bettstetter. On the Connectivity of Wireless Multihop Networks with Homogeneous and Inhomogeneous Range Assignment. In *Proc. 56th IEEE Vehicular Technology Conference (VTC 2002, Fall)*, volume 3, pages 1706–1710, 2002.

[21] C. Bettstetter. On the Minimum Node Degree and Connectivity of a Wireless Multihop Network. In *Proc. 3rd ACM International Symposium on Mobile Ad Hoc Networking and Computing (MobiHoc'02)*, pages 80–91, 2002.

[22] C. Bettstetter. Topology Properties of Ad hoc Networks with Random Waypoint Mobility. *ACM SIGMOBILE Mobile Computing and Communications Review*, 7(3):50–52, July 2003.

[23] C. Bettstetter and C. Hartmann. Connectivity of Wireless Multihop Networks in a Shadow Fading Environment. *Wireless Networks*, 11(5):571–579, Sep. 2005.

[24] C. Bettstetter and O. Krause. On Border Effects in Modeling and Simulation of Wireless Ad Hoc Networks. In *Proc. IEEE International Conference on Mobile and Wireless Communication Networks (MWCN)*, Recife, Brazil, Aug. 2001.

[25] C. Bettstetter and J. Zangl. How to Achieve a Connected Ad Hoc Network with Homogeneous Range Assignment: An Analytical Study with Consideration of Border Effects. In *Proc. IEEE International Conference on Mobile and Wireless Communication Networks (MWCN)*, pages 125–129, Stockholm, Sweden, Sep. 2002.

[26] E. S. Biagioni and G. Sasaki. Wireless Sensor Placement for Reliable and Efficient Data Collection. In *Proc. 36th Annual Hawaii International Conference on System Sciences*, Jan. 2003.

[27] D. M. Blough, M. Leoncini, G. Resta, and P. Santi. The K-Neigh Protocol for Symmetric Topology Control in Ad Hoc Networks. In *Proc. 4th ACM International Symposium on Mobile Ad Hoc Networking and Computing (MobiHoc'03)*, pages 141–152, Annapolis, Maryland, USA., 2003.

[28] D. M. Blough, G. Resta, and P. Santi. A Statistical Analysis of the Long-run Node Spatial Distribution in Mobile Ad Hoc Networks. *Wireless Networks*, 10(5):543–554, 2004.

[29] B. Bollobás. *Random Graphs*. Cambridge University Press, 2nd edition, 2001.

[30] L. Booth, J. Bruck, M. Cook, and M. Franceschetti. Ad Hoc Wireless Networks with Noisy Links. In *Proc. 2003 IEEE International Symposium on Information Theory*, 29 June-4 July 2003.

[31] L. Booth, J. Bruck, M. Cook, and M. Franceschetti. Covering Algorithms, Continuum Percolation and the Geometry of Wireless Networks. *Annals of Applied Probability*, 13(2):722–731, 2003.

[32] S. R. Broadbent. Discussion on Symposium on Monte Carlo Methods. *Journal of the Royal Statistical Society: Series B*, 16(68):61–75, 1954.

[33] S. R. Broadbent and J. M. Hammersley. Percolation Processes, I. Crystals and Mazes. *Proceedings Of The Cambridge Philosophical Society*, 53:629–641, 1957.

[34] R. Brown. Calendar Queues: A Fast 0(1) Priority Queue Implementation for the Simulation Event Set Problem. *Communications of the ACM*, 31(10):1220–1227, Oct. 1988.

[35] J. Burrell, T. Brooke, and R. Beckwith. Wineyard Computing: Sensor Networks in Agricultural Production. *IEEE Pervasive Computing*, 3(1):38–45, 2004.

[36] S. Butenko, X. Cheng, D. Z. Du, and P. M. Pardalos. On the Construction of Virtual Backbone for Ad Hoc Wireless Networks. In S. Butenko, R. Murphey, and P. M. Pardalos, editors, *Cooperative Control: Models, Applications and Algorithms*, pages 43–54. Kluwer Academic Publishers, 2003.

[37] S. Butenko, X. Cheng, C. Oliveira, and P. M. Pardalos. A New Heuristic for the Minimum Connected Dominating Set Problem on Ad Hoc Wireless Networks. In S. Butenko, R. Murphey, and P. M. Pardalos, editors, *Recent Developments in Cooperative Contral and Optimization*, chapter 4, pages 61 – 73. Kluwer Academic Publishers, 2004.

[38] M. Cadei, X. Cheng, and D. Z. Du. Connected Domination in Ad Hoc Wireless Networks. In *Proc. 6th International Conference on Computer Science and Informatics*, 2002.

[39] R. Cardell-Oliver, K. Smettem, M. Kranz, and K. Mayer. A Reactive Soil Moisture Sensor Network: Design and Field Evaluation. *International Journal of Distributed Sensor Networks*, 1(2):149–162, 2005.

[40] J. Cartigny, D. Simplot, and I. Stojmenovic. Localized Minimum-Energy Broadcasting in Ad-Hoc Networks. In *Proc. 22nd Annual Joint Conference of the IEEE Computer*

and Communications Societies (INFOCOM'03), volume 3, pages 2210–2217, San Francisco, USA., March-April 2003.

[41] A. Cerpa, J. Elson, D. Estrin, L. Girod, M. Hamilton, and J. Zhao. Habitat Monitoring: Application Driver for Wireless Communications Technology. In *Proc. ACM. SIGCOMM.*, San Jose, Costa Rica, April 2001.

[42] C. J. Chae, E. Wong, and R. S. Tucker. Optical CSMA/CD Media Access Scheme for Ethernet over Passive Optical Network. *IEEE Photonics Technology Letters*, 14(5):711–713, 2002.

[43] K. Chakrabarty, S. S. Iyengar, H. Qi, and E. Cho. Grid Coverage for Surveillance and Target Location in Distributed Sensor Networks. *IEEE Transactions on Computers*, 51(12):1448–1453, Dec. 2002.

[44] S. C. Chapra and R. P. Canale. *Numerical Methods for Engineers With Programming and Software Applications*. McGraw-Hill, 3rd edition, 1998.

[45] T. W. Charbonneau and Jr. Gass, J. H. Connectivity Analysis for a Tactical Radio Network. In *Proc. IEEE Military Communications Conference on Communications for Network-Centric Operations: Creating the Information Force*, volume 1, pages 595–599, Oct 2001.

[46] P. Chardaire, A. Sutter, and M. C. Costa. Solving the Dynamic Facility Location Problem. *Networks*, 28(2):117–124, 1996.

[47] D. Chen, D. Z. Du, X. D. Hu, G. Lin, L. Wang, and G. Xue. Approximations for Steiner Trees with Minimum Number of Steiner Points. *Journal of Global Optimization*, 18:17–33, 2000.

[48] X. Chen and J. Shen. Reducing Connected Dominating Set Size with Multipoint Relays in Ad Hoc Wireless Networks. In *Proc. 7th International Symposium on Parallel Architectures, Algorithms and Networks (ISPAN'04)*, pages 539–543, May 2004.

[49] X. Cheng, D. Z. Du, L. Wang, and B. Xu. Relay Sensor Placement in Wireless Sensor Networks. *Wireless Networks*, 14(3):347–355, June 2008.

[50] Y. C. Cheng and T. G. Robertazzi. Critical Connectivity Phenomena in Multihop Radio Models. *IEEE Transactions on Communications*, 37:770–777, July 1989.

[51] I. Chlamtac and A. Faragó. A New Approach to the Design and Analysis of peer-to-peer Mobile Networks. *ACM Wireless Networks*, 5(3):149–156, May 1999.

[52] C. Y. Chong and S. P. Kumar. Sensor Networks: Evolution, Opportunities, and Challenges. *Proceedings of the IEEE*, 91(8):1247–1256, Aug. 2003.

[53] D. Cieslik. *Steiner Minimal Trees*. Kluwer Academic Publishers, 1998.

[54] B. N. Clark, C. J. Colbourn, and D. S. Johnson. Unit Disk Graphs. *Discrete Mathematics*, 86:165–177, 1990.

[55] L. Cooper. Location-Allocation Problems. *Operations Research*, 11(3):331–343, 1963.

[56] L. Cooper. Heuristic Methods for Location-Allocation Problems. *SIAM Review*, 6(1):37–53, 1964.

[57] Y. Cui, K. Xu, J. Wu, and Z. Yu. An Internet Routing Emulation System: Research and Development. In *Proc. 2003 International Conference on Communications Technology (ICCT'03)*, volume 1, pages 495–499, 2003.

[58] B. Das and V. Bharghavan. Routing in Ad-Hoc Networks Using Minimum Connected Dominating Sets. In *Proc. 1997 IEEE International Conference on Communication (ICC'97)*, pages 376–380, 1997.

[59] B. N. Desai, N. J. Frigo, A. Smiljanic, K. C. Reichmann, P. P. Iannone, and R. S. Roman. An Optical Implementation of a Packet-based (Ethernet) MAC in a WDM Passive Optical Network Overlay. In *Proceedings of Optical Fiber Communication Conference and Exhibit (OFC '01)*, volume 3, pages WN5–1 – WN5–3, 2001.

[60] M. Desai and D. Manjunath. On the Connectivity in Finite Ad Hoc Networks. *IEEE Communications Letters*, 6(10):437–439, 2002.

[61] S. S. Dhillon and K. Chakrabarty. Sensor Placement for Effective Coverage and Surveillance in Distributed Sensor Networks. In *Proc. IEEE Wireless Communications and Networking (WCNC'03)*, volume 3, pages 1609–1614, March 2003.

[62] R. Diestel. *Graph Theory*. Springer-Verlag Heidelberg, electronic edition, 2005.

[63] S.-H. Doong, C.-C. Lai, and C.-H.. Wu. Genetic Subgradient Method for Solving Location-Allocation Problems. *Applied Soft Computing*, 7:373–386, 2007.

[64] O. Dousse, F. Baccelli, and P. Thiran. Impact of Interferences on Connectivity in Ad Hoc Networks. *IEEE/ACM Transactions on Networking (TON)*, 13(2):425–436, 2005.

[65] O. Dousse, M. Franceschetti, and P. Thiran. Information Theoretic Bounds on the Throughput Scaling of Wireless Relay Networks. In *Proc. 24th Annual Joint Conference of the IEEE Computer and Communications Societies (INFOCOM'05)*, volume 4, pages 2670–2678, Miami, USA., March 2005.

[66] O. Dousse and P. Thiran. Connectivity vs Capacity in Dense Ad Hoc Networks. In *Proc. 23rd Annual Joint Conference of the IEEE Computer and Communications Societies (INFOCOM'04)*, volume 1, pages –486, March 2004.

[67] O. Dousse, P. Thiran, and M. Hasler. Connectivity in Ad-Hoc and Hybrid Networks. In *Proc. 21st Annual Joint Conference of the IEEE Computer and Communications Societies (INFOCOM'02)*, volume 2, pages 1079–1088, June 2002.

[68] L. J. Dowell and M. L. Bruno. Connectivity of Random Graphs and Mobile Networks: Validation of Monte Carlo Simulation Results. In *Proc. 2001 ACM Symposium on Applied Computing (SAC '01)*, pages 77–81, Las Vegas, Nevada, USA., March 2001.

[69] F. Effenberger, D. C. Calix, G. Kramer, R. Li, M. Oron, and T. Pfeiffer. An Introduction to PON Technologies. *IEEE Communications Magazine*, 45(3):s17–s25, 2007.

[70] J. Elson and D. Estrin. Sensor Networks: A Bridge to the Physical World. In C. S. Raghavendra, K. M. Sivalingam, and T. Znati, editors, *Wireless Sensor Networks*, pages 51–69. Springer, 2004.

[71] P. Erdős and A. Rényi. On Random Graphs. *Publications Mathematical*, 6:290–297, 1959.

[72] P. Erdős and A. Rényi. On the Evolution of Random Graphs. *Publ. Math. Inst. Hungarian Acad. Sci.*, 5:17–61, 1960.

[73] W. Feller. *An Introduction to Probability Theory and Its Applications*, volume 2. John Wiley & Sons, Inc, 2nd edition, 1971.

[74] C. H. Foh, L. Andrew, E. Wong, and M. Zukerman. FULL-RCMA: a High Utilization EPON. *IEEE Journal on Selected Areas in Communications*, 22(8):1514–1524, 2004.

[75] C. H. Foh and B. S. Lee. A Closed Form Network Connectivity Formula for One-Dimensional MANETs. In *Proc. 2004 IEEE International Conference on Communications (ICC'04)*, volume 6, pages 3739–3742, June 2004.

[76] C. H. Foh, G. Liu, B. S. Lee, B. C. Seet, K. J. Wong, and C. P. Fu. Network Connectivity of One-Dimensional MANETs with Random Waypoint Movement. *IEEE Communications Letters*, 9:31–33, Jan. 2005.

[77] G. W. Ford and G. E. Uhlenbeck. Combinatorial Problems in the Theory of Graphs. IV. *Porc. Natn. Acad. Sci. U.S.A.*, 43(1):163–167, Jan. 1957.

[78] M. R. Garey and D. S. Johnson. *Computers and Intractability: A Guide to the Theory of NP-Completeness*. W. H. Freeman, San Francisco, 1979.

[79] A. Ghosh, D. R. Wolter, J. G. Andrews, and R. Chen. Broadband Wireless Access with WiMAX/802.16: current Performance Benchmarks and Future Potential. *IEEE Communications Magazine*, 43(2):129–136, Feb. 2005.

[80] E. N. Gilbert. Random Graphs. *Ann. Math. Statist.*, 30:1141–1144, 1959.

[81] E. N. Gilbert. Random Plane Networks. *SIAM J.*, 9(4):533–543, Dec. 1961.

[82] A. Girard. *FTTx PON Technology and Testing*. Expertise Reaching Out, 2005.

[83] C. Gkantsidis, M. Mihail, and E. Zegura. The Markov Chain Simulation Method for Generating Connected Power Law Random Graphs. In *Proc. 5th SIAM Workshop on Algorithm Engineering and Experiments (ALENEX)*, Jan. 2003.

[84] H. Gonzólez-Banos. A Randomized Art-Gallery Algorithm for Sensor Placement. In *Proc.7th Annual Symposium on Computational Geometry*, pages 232–240, Medford, Massachusetts, USA., 2001.

[85] A. D. Gore. Comments on "On the Connectivity in Finite Ad Hoc Networks". *IEEE Communications Letters*, 10(2):88–90, 2006.

[86] A. D. Gore. Correction to "Comments on 'On the Connectivity in Finite Ad Hoc Networks'". *IEEE Communications Letters*, 10(5):359, 2006.

[87] R. L. Graham, D. E. Knuth, and O. Patashnik. *Concrete Mathematics: A Foundation for Computer Science*. Pearson Education, 2nd edition, 2002.

[88] G. Grimmett. *Percolation*. Springer, 2nd edition, June 1999.

[89] S. Guha and S. Khuller. Approximation Algorithms for Connected Dominating Sets. *Algorithmica*, 20(4):374 – 387, 1998.

[90] G. C. Gupta, M. Kashima, H. Iwamura, H. Tamai, T. Ushikubo, and T. Kamijoh. Over 100km Bidirectional, Multi-channels COF-PON without Optical Amplifier. In *PDP51, OFC 2006*.

[91] P. Gupta and P. R. Kumar. Critical Power for Asymptotic Connectivity in Wireless Networks. *Stochastic Analysis, Control, Optimization and Applications: A Volume in Honor of W.H. Fleming*, pages 1106–1110, 1998.

[92] P. Gupta and P. R. Kumar. The Capacity of Wireless Networks. *IEEE Transactions on Information Theory*, 46(2):388–404, March 2000.

[93] M. Haenggi. The Impact of Power Amplifier Characteristics of Routing in Random Wireless Networks. In *Proc. IEEE Global Telecommunications Conference (GLOBECOM'03)*, volume 1, pages 513–517, San Francisco, CA, USA., Dec. 2003.

[94] M. Haenggi. Opportunities and Challenges in Wireless Sensor Networks. In M. Ilyas and I. Mahgoub, editors, *Handbook of Sensor Networks: Compact Wireless and Wired Sensing Systems*, pages 1.1–1.14. CRC Press, 2004.

[95] M. Haenggi and D. Puccinelli. Routing in Ad Hoc Networks: A Case for Long Hops. *IEEE Communications Magazine*, 43(10):93 – 101, Oct. 2005.

[96] M. Hajduczenia, B. Lakic, H. J. A. Da Silva, and P. P. Monteiro. Optimized Passive Optical Network Deployment. *Journal of Optical Networking*, 6(9):1079–1103, 2007.

[97] B. Hajek. Adaptive Transmission Strategies and Routing in Mobile Radio Networks. In *Proc. Conference on Information Sciences and Systems*, pages 372–378, March 1983.

[98] S. L. Hakimi. Optimum Locations of Switching Centers and the Absolute Centers and Medians of a Graph. *Operations Research*, 12(3):450–459, 1964.

[99] S. L. Hakimi. Optimum Distribution of Switching Centers in a Communication Network and Some Related Graph Theoretic Problems. *Operations Research*, 13(3):462–475, 1965.

[100] P. Hall. On Continuum Percolation. *Annals of Probability*, 13(4):1250–1266, 1985.

[101] J. M. Hammersley. Percolation Processes, II. The Connective Constant. *Proceedings Of The Cambridge Philosophical Society*, 53:642–645, 1957.

[102] B. Hao, J. Tang, and G. Xue. Fault-Tolerant Relay Node Placement in Wireless Sensor Networks: Formulation and Approximation. In *Proc. IEEE Workshop on High Performance Switching and Routing (HPSR'04)*, pages 246–250, 2004.

[103] J. W. Harris and H. Stocker. *Handbook of Mathematics and Computational Science*. Springer-Verlag, New York, 1998.

[104] M. Hatler. *Wireless Sensor Networks: Mass Market Opportunities*. ON World, Inc., San Diego, CA., 2004.

[105] C. Hedrick. Routing Information Protocol. Internet Request for Comments RFC 1058, 1998.

[106] W. Heinzelman, A. Chandrakasan, and H. Balakrishnan. Energy-efficient Communication Protocol for Wireless Microsensor Networks. In *Proc. Hawaii International Conference on Systems Science*, volume 2, Jan. 2000.

[107] C. Ho, K. Obraczka, G. Tsudik, and K. Viswanath. Flooding for Reliable Multicast in Multi-Hop Ad Hoc Networks. In *Proc. International Workshop on Discrete Algorithms and Methods for Mobile Computing and Communications (DIALM)*, pages 64–71, 1999.

[108] T. Hou and V. Li. Performance Analysis of Routing Strategies in Multihop Packet Radio Network. In *Proc. 1984 IEEE Global Communications Conference (GLOBECOM'84)*, volume 1, pages 487–492, Atlanta, GA, Nov 1984.

[109] T. Hou and V. Li. Transmission Range Control in Multihop Packet Radio Networks. *IEEE Transactions on Communications*, 34(1):38–44, Jan. 1986.

[110] T. T. Hsieh. Using Sensor Networks for Highway and Traffic Applications. *IEEE Potentials*, 23(2):13–16, April-May 2004.

[111] S. Hussain and A. W. Matin. Hierarchical Cluster-based Routing in Wireless Sensor Networks. In *Proc. International Conference on Information Processing in Sensor Networks (IPSN'06)*, Nashville, TN, USA, 2006.

[112] IEEE. *IEEE Standard for Wireless LAN Medium Access Control (MAC) and Physical Layer (PHY) Specifications*, 1999.

[113] IEEE. *IEEE Standard for Information technology - Telecommunications and information exchange between systems - Local and metropolitan area networks - Specific requirements Part 15.3: Wireless Medium Access Control (MAC) and Physical Layer (PHY) Specifications for High Rate Wireless Personal Area Networks (WPANs) Amendment 1: MAC Sublayer*, 2005.

[114] IEEE. *IEEE Standard for Information Technology - Telecommunications and information exchange between systems - Local and metropolitan area networks - specific requirement Part 15.4: Wireless Medium Access Control (MAC) and Physical Layer (PHY) Specifications for Low-Rate Wireless Personal Area Networks (WPANs)*, 2007.

[115] IEEE 802.3ah. Ethernet in the First Mile. June 2004.

[116] IEEE 802.3av. 10Gb/s Ethernet Passive Optical Network. 2006.

[117] Y. M. Ioannides. Random Graphs and Social Networks: An Economics Perspective. http://ase.tufts.edu/econ/papers/200518.pdf. Accessed April, 2008.

[118] M. Ishizuka and M. Aida. Performance Study of Node Placement in Sensor Networks. In *Proc. 24th International Conference on Distributed Computing Systems Workshops*, pages 598–603, March 2004.

[119] ITU-T G.983, SG 15. Broadband Passive Optical Network.

[120] ITU-T G.984.1, SG 15. Gigabit-capable Passive Optical Networks (G-PON): General Characteristics, March 2003.

[121] ITU-T G.984.2, SG 15. Gigabit-capable Passive Optical Networks (g-pon): Physical Media Dependent (PMD) Layer Specification, March 2003.

[122] ITU-T G.984.3, SG 15. Gigabit-capable Passive Optical Networks (G-PON): Transmission Convergence Layer Specification, June 2005.

[123] ITU-T G.984.4, SG 15. Gigabit-capable Passive Optical Networks (G-PON): Transmission Convergence Layer Specification, July 2005.

[124] ITU-T G.992.5. Asymmetric Digital SubscriberLine (ADSL) Transceivers - Extended bandwidth ADSL2 (ADSL2+), Jan. 2003.

[125] R. Iyengar, K. Kar, and S. Banerjee. Low-coordination Topologies for Redundancy in Sensor Networks. In *Proc. 6th ACM International Symposium on Mobile Ad Hoc Networking and Computing (MobiHoc'05)*, pages 332–342, USA, May 2005.

[126] M. Jiang, J. Li, and Y. Tay. Cluster Based Routing Protocol (CBRP) Functional Specification. In *IETF draft-ietf-manet-cbrp-spec-01*, March 1999.

[127] D. B. Johnson and D. A. Maltz. Dynamic Source Routing in Ad Hoc Wireless Networks. *Mobile Computing*, 353:153–181, 1996.

[128] N. L. Johnson, S. Kotz, and N. Balakrishnan. *Continuous Univariate Distributions*. John Wiley & Sons, Inc, 1995.

[129] A. Kashyap, S. Khuller, and M. Shayman. Relay Placement for Higher Order Connectivity in Wireless Sensor Networks. In *Proc. 25th IEEE International Conference on Computer Communications (INFOCOM'06)*, pages 1–12, Barcelona, Spain, 2006.

[130] R. Kershner. The Number of Circles Covering a Set. *American Journal of Mathematics*, 61(3):665 – 671, 1939.

[131] S. U. Khan. Approximate Optimal Sensor Placements in Grid Sensor Fields. In *Proc. IEEE 65th Vehicular Technology Conference 2007, VTC2007-Spring*, pages 248–251, Dublin, April 2007.

[132] B. Kim, J. Yang, D. Zhou, and M. T. Sun. Energy-aware Connected Dominating Set Construction in Mobile Ad Hoc Networks. In *Proc. 14th International Conference on Computer Communications and Networks*, pages 229 – 234, Oct. 2005.

[133] L. Kleinrock and J. Silvester. Optimum Transmission Radii for Packet Radio Networks or Why Six is a Magic Number. In *Proc. National Telecommunications Conference*, Birmingham, Ala., Dec. 1978.

[134] J. G. Klincewicz and H. Luss. A Lagrangian Relaxation Heuristic for Capacitated Facility Location with Single source Constraints. *Journal of Operational Research Society*, 37(5):495–500, May 1986.

[135] S. Kotz and L. J. Norman. Encyclopedia of Statistical Sciences. volume 5. John Wiley & Sons, New York, 1985.

[136] G. Kramer, B. Mukherjee, and G. Pesavento. IPACT: a Dynamic Protocol for an Ethernet PON (EPON). *IEEE Communications Magazine*, 40(2):74–80, 2002.

[137] G. Kramer and G. Pesavento. Ethernet Passive Optical Network (EPON): Building a Next-Generation Optical Access Network. *IEEE Communications Magazine*, 40(2):66–73, Feb. 2002.

[138] J. Krarup and P. M. Pruzan. The Simple Plant Location Problem: Survey and Synthesis. *European Journal of Operations Research*, 12(1):36–81, Jan. 1983.

[139] H. W. Kuhn and R. E. Kuenne. An Efficient Algorithm for the Numerical Solution of the Generalized Weber Problem in Spatial Economics. *Journal of Regional Science*, 4(2):21–33, 1962.

[140] M. Labbé, D. Peeters, and J. F. Thisse. Location on Networks. In M. O. Ball, T. L. Magnanti, C. L. Monma, and G. L. Nemhauser, editors, *Network Routing, Handbooks in Operations Research and Management Sciences*, volume 8. NorthHolland, Amsterdam.

[141] J. LaRocca and R. LaRocca. *802.11 Demystified*. McGraw-Hill, 2002.

[142] C. Y. Lee. An Algorithm for the Design of Multitype Concentrator Networks. *Journal of Operational Research Society*, 44(5):471–482, May 1993.

[143] W. C. Y. Lee. *Mobile Cellular Telecommunications Systems*. McGraw-Hill Book Company, 1989.

[144] M. Leoncini, G. Resta, and P. Santi. Analysis of a Wireless Sensor Dropping Problem in Wide-area Environmental Monitoring. In *Proc. 4th International Symposium on Information Processing in Sensor Networks*, pages 239–245, April 2005.

[145] Y. Levin and A. Ben-Israel. A Heuristic Method for Large Scale Multifacility Location Problems. *Computers and Operations Research*, 31(2):257–272, Feb. 2004.

[146] C. Li. *Topics in Resource Allocation in Wireless Sensor Networks*. PhD thesis, The University of Melbourne, 2008.

[147] F. Y. S. Lin and P. L. Chiu. A Near-Optimal Sensor Placement Algorithm to Achieve Complete Coverage/Discrimination in Sensor Networks. *IEEE Communications Letters*, 9(1):43–45, Jan. 2005.

[148] G. Lin and G. Xue. Steiner Tree Problem with Minimum Number of Steiner Points and Bounded Edge-Length. *Information Processing Letters*, 69:53–57, 1999.

[149] E. L. Lloyd and G. Xue. Relay Node Placement in Wireless Sensor Networks. *IEEE Transactions on Comoputers*, 56(1):134–138, Jan. 2007.

[150] R. F. Love and H. Juel. Properties and Solution Methods for Large Location-Allocation Problems. *The Journal of the Operational Research Society*, 33(5):443–452, May 1982.

[151] M. Ma, Y. Zhu, and T.H. Cheng. A Bandwidth Guaranteed Polling MAC Protocol for Ethernet Passive Optical Networks. In *Proc. 22nd Annual Joint Conference of the IEEE Computer and Communications Societies (INFOCOM'03)*, volume 1, pages 22–31, March-April 2003.

[152] A. Mainwaring, J. Polastre, R. Szewczyk, D. Culler, and J. Anderson. Wireless Sensor Network for Habitat Monitoring. In *Proc. 1st ACM International Workshop on Wireless Sensor Networks and Applications (WSNA'02)*, pages 88–97, Atlanta, Georgia., 2002.

[153] A. Manjeshwar and D. Agrawal. TEEN: A Routing Protocol for Enhanced Efficiency in Wireless Sensor Networks. In *Proc. 15st International Symposium on Parallel and Distributed Processing*, pages 2009–2015, San Francisco, CA, USA, April 2001.

[154] A. Manjeshwar and D. Agrawal. APTEEN: A Hybrid Protocol for Efficient Routing and Comprehensive Information Retrieval in WSNs. In *Proc. 2nd International Parallel and Distributed Computing Issues in Wireless Networks and Mobile Computing*, pages 195–202, Ft. Lauderdale, FL, USA, April 2002.

[155] M. V. Marathe, H. Breu, H. B. Hunt III, S. S. Ravi, and D. J. Rosenkrantz. Simple Heuristics for Unit Disk Graphs. *Networks*, 25:59–68, 1995.

[156] J. K. Martinez, J. K. Hart, and R. Ong. Environmental Sensor Networks. *Computer*, 37(8):50–56, Aug. 2004.

[157] G. R. Mateus, F. R. B. Cruz, and H. P. L. Luna. An Algorithm for Hierarchical Network Design. *Location Science*, 2(3):149–164, Oct. 1994.

[158] R. Meester and R. Roy. *Continuum Percolation*. Cambridge University Press, Cambridge, U.K., 1996.

[159] N. Megiddo and K. J. Supowit. On the Complexity of some Common Geometric Location Problems. *SIAM Journal of Computing*, 13(1):182–196, 1984.

[160] M. V. Menshikov. Coincidence of Critical Points in Percolation Problems. *Soviet Math. Dokl.*, 24:856–859, 1986.

[161] L. E. Miller. Distribution of Link Distances in a Wireless Network. *Journal of Research of the National Institute of Standards and Technology*, 106(2):401–412, March-April 2001.

[162] A. Mirzaian. Lagrangian Relaxation for the Star-Star Concentrator Location Problem: Approximation Algorithm and Bounds. *Networks*, 15(1):1–20, 1985.

[163] S. Misra, S. D. Hong, G. Xue, and J. Tang. Constrained Relay Node Placement in Wireless Sensor Networks to Meet Connectivity and Survivability Requirements. In *Proc. IEEE 27th Conference on Computer Communications (INFOCOM'08)*, pages 281–285, April 2008.

[164] J. Moy. OSPF Version 2. Internet Request For Comments RFC 1247, 1991.

[165] C. Siva Ram Murthy and B. S. Manoj. *Ad Hoc Wireless Networks: Architectures and Protocols*. Prentice Hall, 2004.

[166] M. Nekovee. Sensor Networks on the Road: the Promises and Challenges of Vehicular Ad Hoc Networks and Vehicular Grids. In *Proc. Workshop on Ubiquitous Computing and e-Research*, Edinburgh,UK, May 2005.

[167] M. E. J. Newman, D. J. Watts, and S. H. Strogatz. Random Graph Models of Social Networks. *Proceedings of the National Academy of Sciences of the United States of America*, 99(Suppl. 1):2566–2572, Feb. 2002.

[168] J. Ni and S. Chandler. Connectivity Properties of a Random Radio Network. *Proceedings of the IEE Communications*, 141(4):289–296, Aug. 1994.

[169] S-Y. Ni, Y-C. Tseng, Y-S. Chen, and J-P. Sheu. The Broadcast Storm Problem in a Mobile Ad Hoc Network. In *Proc. 5th Annual ACM/IEEE International Conference on Mobile Computing and Networking (MobiCom'99)*, pages 151–162, Seattle, Washington, USA., 1999.

[170] J. O'Rourke. *Art Gallery Theorems and Algorithms*. Oxford University Press, Inc., New York, NY, USA., 1987.

[171] L. Ou, Y. A. Şekercioğlu, and N. Mani. A Survey of Multipoint Relay Based Broadcast Schemes in Wireless Ad Hoc Networks. *IEEE Communications Surveys and Tutorials*, 8(4):30–46, 2006.

[172] L. Ou, Y. A. Sekercioglu, and N. Mani. A Low-cost Flooding Algorithm for Wireless Sensor Networks. In *Proc. 2007 Wireless Communications and Networking Conference (WCNC'07)*, March 2007.

[173] J. Pan, Y. T. Hou, L. Cai, Y. Shi, and S. X. Shen. Topology control for Wireless Sensor Networks. In *Proc. 9th Annual International Conference on Mobile Computing and Networking (MobiCom'03)*, pages 286–299, San Diego, CA, USA., 2003.

[174] C. H. Papadimitriou and K. Steiglitz. *Combinatorial Optimization: Algorithms and Complexity*. Prentice-Hall, 1982.

[175] A. Papoulis. *Probability, Random Variables, and Stochastic Processes*. Electrical & Electronic Engineering Series. McGraw-Hill, 3rd, international edition, 1991. pp.97.

[176] M. D. Penrose. On k-Connectivity for a Geometric Random Graph. *Random Structures and Algorithms*, 15(2):145–164, Sep. 1999.

[177] M. D. Penrose. *Random Geometric Graphs*. Oxford University Press, USA, July 2003.

[178] C. E. Perkins and E. M. Royer. Ad Hoc On-Demand Distance Vector Routing. In *Proc. IEEE Workshop on Mobile Computing Systems and Applications*, pages 90 – 100, Feb 1999.

[179] T. K. Philips, S. S. Panwar, and A. N. Tantawi. Connectivity Properties of a Packet Radio Network Model. *IEEE Transactions on Information Theory*, 35:1044–1047, Sep. 1989.

[180] P. Piret. On the Connectivity of Radio Networks. *IEEE Transactions on Information Theory*, 37(5):1490–1492, 1991.

[181] G. J. Pottie and W. J. Kaiser. Wireless Integrated Network Sensors. *Communications of the ACM*, 43(5):51–58, May 2000.

[182] R. Prasad. *CDMA for Wireless Personal Communications*. The Artech House Mobile Communications Series. Artech House, 1996.

[183] A. Qayyum, L. Viennot, and A. Laouiti. Multipoint Relaying for Flooding Broadcast Messages in Mobile Wireless Networks. In *Proc. 35th Hawaii International Conference on System Sciences*, pages 3866–3875, Jan. 2002.

[184] S. Quintanilla, S. Torquato, and R. M. Ziff. Efficient Measurement of the Percolation Threshold for Fully Penetrable Discs. *Journal of Physics A: Mathematical and General*, 33(42):L399–L407, Oct 2000.

[185] V. Raghunathan, C. Schurgers, S. Park, and M. B. Srivastava. Energy Efficient Design of Wireless Sensor Nodes. In C. S. Raghavendra, K. M. Sivalingam, and T. Znati, editors, *Wireless Sensor Networks*, pages 51–69. Springer, 2004.

[186] T. S. Rappaport. *Wireless Communications Principles and Practice*. Pearson Education, 2nd edition, 2004.

[187] L. G. Roberts. Extensions of Packet Communication Technology to a Hand Held Personal Terminal. In *Proc. Spring Joint Computer Conference, AFIPS*, pages 295–298, 1972.

[188] V. Rodoplu and T. H. Meng. Minimum Energy Mobile Wireless Networks. *IEEE Journal on Selected Areas in Communications*, 17(8):1333–1344, 1999.

[189] V. K. Rohatgi. *An Introduction to Probability Theory and Mathematical Statistics*. Wiley, New Youk, 1976.

[190] S. M. Ross. *Introduction to Probability Models*. Academic Press, 8th edition, 2002.

[191] M. Sanchez, P. Manzoni, and Z. J. Haas. Determination of Critical Transmitting Ranges in Ad Hoc Networks. In *Proc. Multiaccess, Mobility and Teletraffic for Wireless Communications Conference*, 1999.

[192] L. A. Sanchis. Experimental Analysis of Heuristic Algorithms for the Dominating Set Problem. *Algorithmica*, 33:3–18, Feb. 2002.

[193] P. Santi. The Critical Transmitting Range for Connectivity in Mobile Ad Hoc Networks. *IEEE Transactions on Mobile Computing*, 4(3):310–317, May 2005.

[194] P. Santi. *Topology Control in Wireless Ad Hoc and Sensor Networks*. John Wiley and Sons, Chichester, UK., July 2005.

[195] P. Santi and D. M. Blough. An Evaluation of Connectivity in Mobile Wireless Ad Hoc Networks. In *Proc. 2002 International Conference on Dependable Systems and Networks (DSN'02)*, pages 89–98, June 2002.

[196] P. Santi and D. M. Blough. The Critical Transmitting Range for Connectivity in Sparse Wireless Ad Hoc Networks. *IEEE Transactions on Mobile Computing*, 2(1):1–15, 2003.

[197] P. Santi, D. M. Blough, and F. Vainstein. A Probabilistic Analysis for the Range Assignment Problem in Ad Hoc Networks. In *Proc. 2nd ACM International Symposium on Mobile Ad Hoc Networking and Computing (MobiHoc'01)*, pages 212–220, 2001.

[198] S. Sarkar, B. Mukherjee, and S. Dixit. Optimum Placement of Multiple Optical Network Units (ONUs) in Optical-Wireless Hybrid Access Networks. In *Proc. Optical Fiber Communication Conference (OFC'06)*, March 2006.

[199] Z. M. Saul and V. Filkov. Exploring Biological Network Structure Using Exponential Random Graph Models. *Bioinformatics*, 2007. Number: btm370v1-7.

[200] L. Schwiebert, S. K. S. Gupta, and J. Weinmann. Research Challenges in Wireless Networks of Biomedical Sensors. In *Proc. 7th Annual International Conference on Mobile Computing and Networking (MobiCom'01)*, pages 151–165, Rome, Italy., 2001.

[201] G. A. F. Seber and C. J. Wild. *Nonlinear Regression*. Wiley Series in Probability and Mathematical Statistics. John Wiley & Sons, 1989.

[202] G. Shen, R. S. Tucker, and C. J. Chae. Fixed Mobile Convergence Architectures for Broadband Access: Integration of EPON and WiMAX. *IEEE Communications Magazine*, 45(8):44–50, Aug. 2007.

[203] H. Shinohara. Broadband Access in Japan: Rapidly Growing FTTH Market. *IEEE Communications Magazine*, 43(9):72–78, Sep. 2005.

[204] A. Shulman. An Algorithm for Solving Dynamic Capacitated Plant Location Problems with Discrete Expensian Sizes. *Operations Research*, 39:423–436, 1991.

[205] R. Sivakumar, P. Sinha, and V. Bharghavan. CEDAR: a core-extraction distributed ad hoc routing protocol. *IEEE Journal on Selected Areas in Communications*, 17(8):1454–1465, Aug. 1999.

[206] B. Sklar. *Digital Communications Fundamentals and Applications*. Pearson Education, 2nd edition, 2002.

[207] K. Sohraby, D. Minoli, and T. Znati. *Wireless Sensor Networks: Technology, Protocols and Applications*. John Wiley & Sons, Inc., 2007.

[208] A. Srinivas and E. Modiano. Joint Node Placement and Assignment for Throughput Optimization in Mobile Backbone Networks. In *Proc. IEEE 27th Conference on Computer Communications (INFOCOM'08)*, pages 1130–1138, April 2008.

[209] I. Stojmenovic and X. Lin. GEDIR: Loop-free Location based Routing in Wireless Networks. In *Proc. IASTED International Conference on Parallel and Distributed Computing and Systems*, pages 1025–1028, Boston, USA, Nov. 1999.

[210] H. Takagi and L. Kleinrock. Optimal Transmission Ranges for Randomly Distributed Packet Radio Terminals. *IEEE Transactions on Communications*, 32(3):246–257, March 1984.

[211] A. Tang, C. Florens, and S. H. Low. An Empirical Study on the Connectivity of Ad Hoc Networks. In *Proc. 2003 Aerospace Conference*, 2003.

[212] J. Tang, B. Hao, and A. Sen. Relay Node Placement in Large Scale Wireless Sensor Networks. *Computer Communications*, 29:490–501, 2006.

[213] M. Tubaishat and S. Madria. Sensor Networks: an Overview. *IEEE Potentials*, 22:20–23, April-May 2003.

[214] P. J. Wan and C. W. Yi. Asymptotic Critical Transmission Radius and Critical Neighbor Number for k-Connectivity in Wireless Ad Hoc Networks. In *Proc. 5th ACM*

International Symposium on Mobile Ad Hoc Networking and Computing (MobiHoc'04), pages 1–8, Roppongi Hills, Tokyo, Japan, 2004.

[215] X. Wang, G. Xing, Y. Zhang, C. Lu, R. Pless, and C. Gill. Integrated Coverage and Connectivity Configuration in Wireless Sensor Networks. In *Proc. 1st International Conference on Embedded Networked Sensor Systems (SenSys'03)*, pages 28–39, Los Angeles, California, USA, Nov. 2003.

[216] Y. Wang, W. Wang, and X. Y. Li. Distributed Low-cost Backbone Formation for Wireless Ad Hoc Networks. In *Proc. 6th ACM International Symposium on Mobile Ad Hoc Networking and Computing (MobiHoc'05)*, pages 2–13, Urbana-Champaign, IL, USA, 2005.

[217] Y. C. Wang, C. C. Hu, and Y. C. Tseng. Efficient Deployment Algorithms for Ensuring Coverage and Connectivity of Wireless Sensor Networks. In *Proc. 1st International Conference on Wireless Internet*, pages 114–121, July 2005.

[218] E. C. Whitman. Sosus: The "secret weapon" of undersea surveillance. *Undersea Warfare*, 7(2), 2005.

[219] W. L. Winston. *Operations Research, Applications and Algorithms*. Thomson Brooks/Cole, 4th edition, 2004.

[220] J. Wu. Extended Dominating-Set-Based Routing in Ad Hoc Wireless Networks with Unidirectional Links. *IEEE Transactions on Parallel and Distributed Systems*, 13(9):866–881, Sep. 2002.

[221] J. Wu. An Enhanced Approach to determine a small Forward Node Set Based on Multipoint Relays. In *Proc. 2003 IEEE 58th Vehicular Technology Conference (VTC 2003-Fall)*, volume 4, pages 2774– 2777, Orlando, Florida, USA., Oct. 2003.

[222] J. Wu, M. Gao, and I. Stojmenovic. On Calculating Power-Aware Connected Dominating Sets for Efficient Routing in Ad Hoc Wireless Networks. In *Proc. 2001 International Conference of Parallel Processing (ICPP'01)*, pages 346–356, 2001.

[223] J. Wu and H. Li. On Calculating Connected Dominating Set for Efficient Routing in Ad Hoc Wireless Networks. In *Proc. 3rd International Workshop on Discrete Algorithms and Methods for Mible Computing and Communications*, pages 7–14, Aug. 1999.

[224] J. Wu, W. Lou, and F. Dai. Extended Multipoint Relays to Determine Connected Dominating Sets in MANETs. *IEEE Transactions on Computers*, 55(3):334–347, March 2006.

[225] L. Xin and R. Srikant. An Information-Theoretic View of Connectivity in Wireless Sensor Networks. In *Proc. 1st Annual IEEE Communications Society Conference on Sensor and Ad Hoc Communications and Networks*, pages 508–516, Oct. 2004.

[226] N. Xu. A Survey of Sensor Network Applications. http://courses.cs.tamu.edu/rabi/cpsc689/resources/sensor%20nw-survey.pdf. Accessed in Feb, 2008.

[227] N. Xu, S. Rangwala, K. K. Chintalapudi, D. Ganesan, A. Broad, R. Govindan, and D. Estrin. A Wireless Sensor Network for Structural Monitoring. In *Proc. 2nd International Conference on Embedded Networked Sensor Systems (Sensys'04)*, pages 13–24, Baltimore, Maryland, USA., Nov. 2004.

[228] F. Xue and P. R. Kumar. The Number of Neighbors Needed for Connectivity of Wireless Networks. *Wireless Networks*, 10(2):169–181, March 2004.

[229] A. D. Yablon and R. T. Bise. Low-loss High-strength Microstructured Fiber Fusion Splices using grin Fiber Lenses. *IEEE Photonics Technology Letters*, 17:118–120, 2005.

[230] H. Zhang and J. C. Hou. Maintaining Sensing Coverage and Connectivity in Large Sensor Networks. *Ad Hoc and Sensor Wireless Networks*, 1:89–124, March 2005.

[231] W. Zhang, G. Xue, and S. Misra. Fault-Tolerant Relay Node Placement in Wireless Sensor Networks: Problems and Algorithms. In *Proc. 26th IEEE International Conference on Computer Communications (INFOCOM'07)*, pages 1649–1657, May 2007.

[232] J. Zheng and H. T. Mouftah. Media Access Control for Ethernet Passive Optical Networks: an Overview. *IEEE Communications Magazine*, 43(2):145–150, 2005.

[233] Q. Zheng, X. Hong, and S. Ray. Recent Advances in Mobility Modeling for Mobile Ad Hoc Network Research. In *Proc. 42nd Annual Southeast Regional Conference*, 2004.

[234] M. Zorzi and S. Pupolin. Optimum Transmission Ranges in Multihop Packet Radio Networks in the Presence of Fading. *IEEE Transactions on Communications*, 43:2201–2205, July 1995.